Clarifying Multi-Component Polymerization Kinetics for Tailoring Properties of Acrylamide/Acrylic Acid Copolymers for Enhanced Oil Recovery

by

Marzieh Riahinezhad

A thesis
presented to the University of Waterloo
in fulfillment of the
thesis requirement for the degree of
Doctor of Philosophy
in
Chemical Engineering

Waterloo, Ontario, Canada, 2015

AUTHOR'S DECLARATION

I hereby declare that I am the sole author of this thesis. This is a true copy of the thesis, including any required final revisions, as accepted by my examiners.

I understand that my thesis may be made electronically available to the public.

Abstract

Among water-soluble polymers, copolymers of acrylamide (AAm) and acrylic acid (AAc) are probably the most common and widely used in practical applications. However, information on the kinetics of the AAm/AAc radical copolymerization is rather scarce. It is also clear, after reviewing the literature, that there is much debate about the details of reaction kinetics for this copolymerization.

Reactivity ratios for AAm/AAc copolymerization system exhibit considerable scatter in the published literature, and therefore, there was a need for more definitive values for these reactivity ratios. An appropriate methodology, based on the error-in-variables-model (EVM) framework along with a direct numerical integration (DNI) of the copolymer composition model, was applied in order to determine reliable reactivity ratios. The reliability of the results was confirmed with extensive and independent replication. Furthermore, via an EVM-based criterion for the design of experiments using mechanistic models, optimal feed compositions were calculated, and from these optimal reactivity ratios were re-estimated for the first time based on information from the full conversion range.

With respect to copolymerization kinetics, the polymerization medium is well known to play a significant role in terms of pH and ionic strength, because of the electrolyte nature of the monomers. The largely unstudied effect of ionic strength on monomer reactivity ratios and copolymerization rate was investigated in detail. Salt addition affects the nature of overall charges of the polyelectrolyte solution and diminishes the electrostatic repulsions between

reacting radicals. It was found that changing the ionic strength of the solution by incorporating salts affected not only the point estimates for the monomer reactivity ratios, but also the overall behavior of the copolymerization with respect to chain composition (which, in its turn, affects other important application properties). Experimental observations confirmed the observed trends in reactivity ratios and were explained in detail, probably for the first time.

A systematic study was also conducted to investigate and clarify the effect of polymerization recipe factors such as total monomer concentration, monomer feed fractions, and solution pH on copolymer microstructure. To study the effect of these factors, reliable reactivity ratios at constant ionic strength were estimated first. The trends in monomer conversion, copolymer composition, molecular weight, sequence length distribution and triad fractions were subsequently examined. Having a better understanding of kinetic profiles was needed in order to manipulate influential factors for tailoring AAm/AAc copolymer properties for the desired application.

The shear viscosity of the copolymer solution is extremely important in determining the performance properties of AAm/AAc copolymers. A series of copolymers with selected properties were prepared to study the effect of polymer concentration, copolymer composition, and salinity on the shear viscosity of the copolymer solutions. The results revealed the considerable effect of solution concentration and salinity on shear viscosity. Moreover, the behavior of the copolymer composition showed a maximum with respect to shear viscosity.

AAm/AAc copolymers are being used in a wide spectrum of applications, from which enhanced oil recovery (EOR) was the target application in this research study. This application was selected due to its continuously growing interest in both academia and industry for Canada.

AAm/AAc copolymer application performance is tied to copolymer properties, which in turn are related to the kinetics of the copolymerization. Therefore, the prior systematic study of copolymerization kinetics and copolymer properties provided us with the required understanding of possible influential factors in both recipe and operation conditions. Based on this knowledge, tailor-made AAm/AAc copolymers with the specific desirable properties were designed for EOR applications.

The copolymer performance was evaluated and compared with a commercially available copolymer of the same type. The results showed not only a noticeable improvement in the behavior of our tailor-made copolymers in improving mobility control and oil recovery efficiency, but also gave a perfect representation of how to go full circle from copolymerization kinetics (fundamental science) to the final desirable application properties (applied engineering phase).

Acknowledgements

First and foremost, I would like to express my deepest and sincere gratitude to my supervisor and mentor, Professor Alexander Penlidis, for all his expert guidance, support, and encouragement throughout my PhD research and his mentorship towards other aspects of my personal development. Words cannot express how grateful I am for all the countless hours of discussions (technical and non-technical) that we had and how much I learnt from him both in polymer science and engineering and life.

I would also like to express my deepest and sincere gratitude to my co-supervisor, Professor Neil McManus, for all his insightful support and guidance, throughout every single step of my PhD research.

I wish to express my appreciation to Prof. Laura Romero-Zeron, Department of Chemical Engineering, University of New Brunswick, for all her support, instructive input, and collaborative spirit towards this research project.

I wish to gratefully acknowledge financial support from the Natural Sciences and Engineering Research Council (NSERC) of Canada, and the Canada Research Chair (CRC) program.

Many thanks go to all my colleagues in our research group for all the support, encouragement, great memories, and their invaluable friendship.

Last, but not least, I would like to thank my family. I am in debt of their unconditional love, support, and confidence they always give me, even when we are thousands of kilometers away. I would never be the person I am today without them. And I wish to thank my husband for all his love and trust in me, and his enormous support.

Dedication

To my family, my endless source of support, inspiration, and love.

Table of Contents

List of Figures

List of Tables

Chapter 1. Introduction, Objectives, Motivation, and Thesis Outline

1.1 Introduction

Copolymers of acrylamide (AAm) and acrylic acid (AAc) are some of the most important types of water-soluble polymers, widely used in applications such as drag reduction agents, paper and textile formulation processing aids, and flocculants for waste water treatment.[1-3] Another important application of AAm/AAc copolymers is in enhanced oil recovery (EOR) and this subject has received renewed interest recently in both scientific and practical areas. EOR demands specific properties, namely high aqueous solution viscosity along with mechanical and thermal stability of the polymers used.[4-7] The application properties of copolymers are tied to their microstructure, therefore it is essential to have a clear understanding of the copolymerization kinetics, and the first step for that is having reliable values for copolymerization reactivity ratios.

Past work has shown that the kinetic behavior of AAm/AAc copolymerization is heavily dependent on the polymerization medium (such as polarity of the solvent, degree of ionization of monomers, pH and ionic strength), due to the electrolytic nature of the monomers, and that makes this system especially complicated. This is because the balance of all polymerization factors dictates the proportions of the various ion forms of the reactants

(monomers and macroradicals), with a subsequent bearing on the overall reaction.[8] This is probably one of the main reasons why the monomer reactivity ratios for this copolymerization are highly inconsistent in the literature.[9] The monomer reactivity ratios, well known indicators of monomer reactivity characteristics, are defined as ratios of the homo-propagation rate constant over the cross-propagation rate constant for each monomer.

As a result of varying pH, for example, different forms of monomer and polymer species for AAc and AAm (acrylic acid, acrylate anion, acrylamide, and protonated acrylamide) can be formed in aqueous media exhibiting different reactivities which, in turn, affect the polymerization kinetics of the system.[10] At low pH, the concentration of undissociated acid monomer is high and AAm is protonated. As pH increases, AAc becomes partially ionized, while AAm is neutral. At pH greater than 6.5, by adding sodium hydroxide, AAc is essentially converted to sodium acrylate monomer, which may exist as an ion pair or as dissociated sodium and AAc ions. Hence, the concentration of ions depends on the polymerization medium and therefore the ionic strength of the medium changes accordingly. However, information about the effect of ionic strength on reaction kinetics is rather scarce. It has been reported that by increasing ionic strength of the medium, the negative charges of the ions are screened, resulting in an increase of the reaction rate.[11]

In order to be able to use AAm/AAc copolymers for specific applications, a detailed knowledge of the factors controlling AAm/AAc copolymerization is required.[12] Modifying AAm/AAc copolymer properties (such as molecular weight, copolymer composition, and sequence length distribution) for use in EOR is a particularly popular target application.

Despite the longevity of this copolymer in general applications, there are still many unanswered questions regarding optimal recipes and reaction conditions needed to produce such copolymers with desirable properties for a target application. Therefore, it is required to establish a general framework to relate copolymerization kinetics to copolymer microstructure.

AAm-based polymers are the most-widely used polymers in EOR applications. They are water-soluble polymers with good mobility control that can improve the efficiency of oil recovery.[13] Moreover, they are cost-efficient and can be used in large scale tertiary oil production. However, despite the importance and popularity of this copolymer in polymer flooding, there are still several aspects related to copolymer properties that need improvement in order to eliminate issues associated with polymer flooding and increase the efficiency of oil recovery. As a result, one needs to understand the process of making these copolymers in order to modify and design them accordingly for EOR (polymer flooding) applications.

1.2 Objectives and motivation

This thesis aimed to design novel AAm/AAc copolymers for EOR applications. In order to achieve this goal, we applied a systematic approach with the following steps:

- The first step to understand AAm/AAc copolymerization is to know about monomer reactivity ratios. Our first target was to clarify the reactivity ratios for this system, as

reported values in the literature were highly inconsistent. In order to do this, we implemented the error-in-variables-model (EVM) framework along with a direct numerical integration (DNI) of the copolymerization composition model to estimate optimal reactivity ratios for AAm/AAc.

- The next step was to understand the main factors affecting the copolymerization of AAm/AAc. Among all factors, ionic strength is very important because of the polyelectrolyte nature of the system. Therefore, the effect of ionic strength on AAm/AAc copolymerization kinetics was studied separately, since there was no direct investigation in the literature to show clearly how this affects the system, especially with regards to the reactivity ratio values.

  Then, the effects of other important factors in copolymerization kinetics, like monomer concentration, pH, and monomer feed fractions, were studied. We aimed to identify these factor effects on polymerization rate, copolymer composition, reactivity ratios, molecular weight, sequence length distribution, and solution shear viscosity.

  At the end of this stage, we established a framework that related copolymerization kinetics to copolymer microstructure.

- The third stage was to design AAm/AAc copolymers based on the established framework. We thus synthesized different copolymers with desirable properties based on prior knowledge at selected copolymerization conditions. Then, copolymer properties, including copolymer composition, molecular weight, sequence length, solution viscosity, and rheological properties were determined in detail.

- The last stage was to investigate the actual performance of AAm/AAc copolymer in EOR applications. We conducted polymer flooding and heavy oil displacement tests in order to evaluate the flow behavior and efficiency of oil recovery for the designed copolymers. By having well-designed polymers, significant improvements in mobility control and efficiency of oil recovery can be gained, which was the main objective of this research. Therefore, this thesis went full circle from fundamental copolymerization kinetics to the final engineering application.

Figure 1-1 shows a summary of the above research objectives and stages.

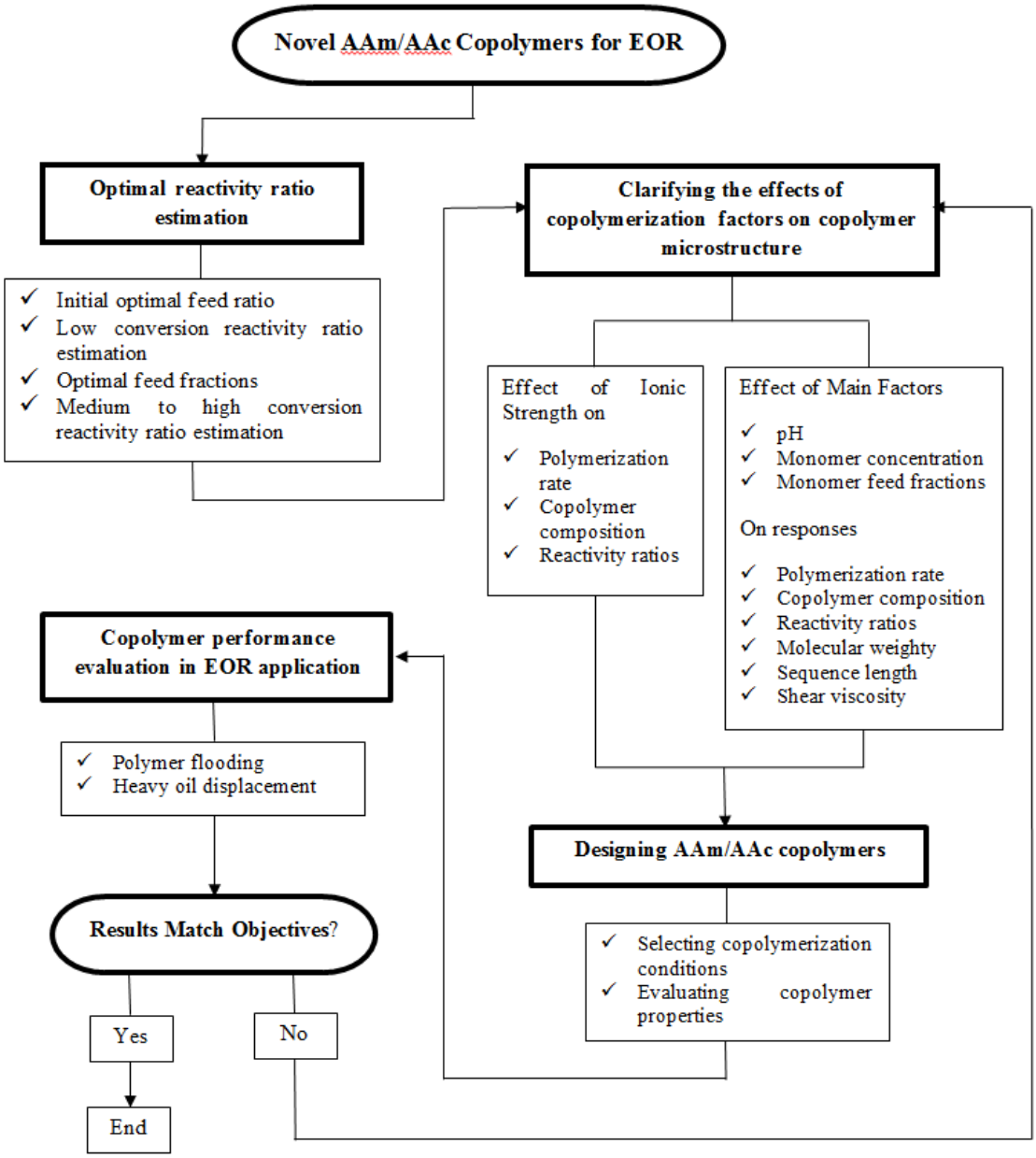

Figure 1-1: The overall research goal and stages

1.3 Thesis outline

The work in this thesis is presented in 8 chapters. Brief descriptions for the thesis chapters are given below:

Chapter 2 offers general background information about the different themes discussed throughout this thesis, ranging from basics in copolymerization kinetics all the way to the final EOR application

Chapter 3 presents a description of materials, and experimental methodologies used to polymerize and characterize AAm/AAc. The chapter ends with a description of the testing procedures in order to evaluate copolymer performance in EOR applications.

Chapter 4 estimates optimal reactivity ratios for AAm/AAc copolymerization by implementing EVM. This includes preliminary reactivity ratio estimation at low monomer conversion, locating optimal monomer feed compositions, conducting the polymerization to higher monomer conversions, and re-estimating reactivity ratios.

Chapter 5 concentrates on investigating the importance and effects of ionic strength on polymerization kinetics. The effects of having constant and variable (but controlled) levels of ionic strength on reactivity ratios, copolymer composition, and polymerization rate are discussed.

Chapter 6 presents the experimental design for investigating the effects of other important copolymerization factors on copolymer microstructure. These factors include total monomer concentration, monomer feed fractions, and solution pH. The responses studied and discussed

in detail are monomer conversion, copolymer composition, molecular weight, sequence length distribution, triad fractions, and solution viscosity.

Chapter 7 is the application chapter and is divided into two major sections. The first section rationalizes the design of copolymer properties for EOR applications by selecting operating conditions and recipe ingredients. The second section of this chapter includes studies performed to evaluate the application performance of AAm/AAc copolymers in EOR. Polymer flooding and heavy oil displacement tests were conducted in order to understand the flow behavior of the copolymers in porous media and determine mobility control and oil recovery efficiency. Finally, the performance of the tailor-made copolymers is compared with a commercially available reference polymer.

Chapter 8 presents the main thesis conclusions (for the overall thesis, as more specific concluding remarks are made at the end of each chapter), the main contributions of the work, and recommendations for future steps (short-term and longer-term).

Finally, five appendices at the end of the thesis complement the different thesis chapters.

Chapter 2. Literature Background

2.1 Water-soluble polymers

Water-soluble polymers can be classified into three main groups; natural polymers (e.g., polysaccharides and proteins), semi-synthetic polymers, including polymers which are not soluble in water but can be modified to become water-soluble (e.g., oxidized cellulose and starch acetates), and synthetic polymers, including polymers that can be produced by a variety of polymerization methods such as condensation, addition, free radical, and ring-opening polymerization.[1] Synthetic polymers, and among them copolymers of acrylamide (AAm) and acrylic acid (AAc), are the subject of this thesis. The standard chemical structures of the two monomers are shown in Figure 2-1.

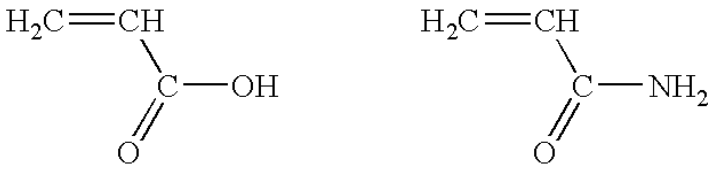

Figure 2-1: AAc and AAm monomer structures

Free radical polymerization is the main synthetic route to make such polymers because of its great versatility, simplicity, and compatibility with many functional groups, tolerance to impurities, and also possibility of using polar and non-polar polymerization media. Free radical copolymerization will be briefly described in Section 2.2.

2.2 Free radical copolymerization: Propagation step

Knowledge of the kinetics of free radical polymerization is a key aspect in polymer synthesis, because it relates not only to how fast a reaction will proceed, but also determines the microstructure of the polymer product (such as the molecular weight or the arrangement of the repeating units in a copolymer chain).

In copolymerization systems, the relative tendency of monomers to react with each other can simply be evaluated with the terminal model, which was developed by Mayo and Lewis.[14] According to the Mayo-Lewis model, there are four possible reactions for the overall propagation step (Equation 2-1):

$$M_{r,1}\cdot + M_1 \xrightarrow{k_{11}} M_{r+1,1}\cdot \qquad \textbf{(Equation 2-1)}$$

$$M_{r,1}\cdot + M_2 \xrightarrow{k_{12}} M_{r+1,2}\cdot$$

$$Mr_{,2}\cdot + M_1 \xrightarrow{k_{21}} M_{r+1,1}\cdot$$

$$M_{r,2}\cdot + M_2 \xrightarrow{k_{22}} M_{r+1,2}\cdot$$

where M_1 and M_2 represent monomer units, $M_{r,1}\cdot$ and $M_{r,2}\cdot$ denote radical chains of length r ending in monomer type i, and k_{11}, k_{12}, k_{21} and k_{22} are rate constants of the individual propagation reactions (ij, i=radical type, j=monomer type). The propagating radical with monomer type M_1 at the chain end (terminal unit) is involved in the first two reactions, while the propagating radical with M_2 as the terminal unit participates in the last two reactions. The monomer reactivity ratios (r_1 and r_2) are defined as the ratios of the rate constants of homo-propagation, k_{ii}, over the corresponding rate constants of cross-propagation, k_{ij} (Equation 2-2):

$$r_1 = \frac{k_{11}}{k_{12}} \qquad \textbf{Equation 2-2}$$

$$r_2 = \frac{k_{22}}{k_{21}}$$

2.3 Reactivity ratio determination

The Mayo-Lewis model[14] describes the instantaneous copolymer composition as a function of reactivity ratios and monomer feed composition and can be derived from the kinetic mechanism of copolymerization, Section 2.2 (see Equation 2-1):

$$F_1 = \frac{r_1 f_1^2 + f_1 f_2}{r_1 f_1^2 + 2 f_1 f_2 + r_2 f_2^2} \qquad \textbf{Equation 2-3}$$

F_1 is the instantaneous mole fraction of monomer 1 bound in the copolymer, whereas f_1 and f_2 are the respective mole fractions of unreacted monomer 1 and 2 in the feed.

The Mayo-Lewis model gives the instantaneous copolymer composition, and so it is only truly applicable in the low conversion polymerization region, where the instantaneous and cumulative composition values do not drift much. Equation 2-3 can be used to determine the reactivity ratios of the monomers from experiments using known feed compositions and measured copolymer compositions, for low conversion polymerizations (typically below 5%). Initial feed compositions can be directly determined from the initial concentration of reagents and the copolymer composition can be determined by different methods, such as elemental analysis, nuclear magnetic resonance (NMR), high performance liquid chromatography (HPLC), etc.

With respect to the AAm/AAc copolymer, there is much debate about the actual values of the reactivity ratios. A summary of the determined values of reactivity ratios for AAm/AAc copolymerization by several groups is given in Table 2-1. Since AAc may exist in the form of sodium acrylate monomer (NaAc) in the aqueous solution, depending on the experimental conditions, reactivity ratios for AAm/NaAc are also presented in Table 2-1.

Table 2-1: Reactivity ratios for AAm/AAc and AAm/NaAc radical copolymerization

Ref.	pH	r_{AAm}	r_{AAc} (r_{NaAc})	Evaluation method
AAm/AAc				
Ponratnam and Kapur [15]	2	0.25±0.36	0.92±0.82	Kelen–Tüdös
	4	0.57±0.067	0.32±0.046	
	6	0.85±0.62	0.33±0.20	
	8	0.12±0.004	0.63±0.004	
	9	0.95±0.21	0.30±0.21	
Paril et al. [16]	2	0.16±0.04	0.88±0.08	EVM
	3.6	1.46-1.94	2.06-2.40	
	5-6	1.88±0.17	0.80±0.07	
Rintoul and Wandrey [17]	1.8	0.54	1.48	Kelen–Tüdös
	2.7	0.69	1.34	
	3.6	0.82	1.28	
	4.4	1.27	0.91	
	5.3	1.83	0.51	
	6.2	2.50	0.39	
	7.8	2.95	0.42	
	8.8	3.05	0.42	
Cabaness et al. [10]	2.17	0.48±0.06	1.73±0.21	Intercepts
	3.77	0.56±0.09	0.56±0.09	
	4.25	0.67±0.04	0.45±0.03	
	4.73	0.95±0.03	0.42±0.02	
	6.25	1.32±0.12	0.35±0.03	
Shawki and Hamielec [18]	-	0.57±0.04	1.45±0.33	Non-linear least squares
Truong et al. [19]	2-2.5	0.50± 0.06	0.79±1.67	Kelen-Tüdös
Bourdais [20]	2	0.60±0.02	1.43±0.03	Approximate graphical technique
	5.2	1.10±0.05	0.35±0.03	
Chapiro et al. [21]	-	0.47	1.30	Fineman-Ross
Vinu and Madras [22]	Basic	3.76	0.28	Fineman-Ross &Kelen-Tüdös
AAm/NaAc				
Kurenkov et al. [23]	10	2.00±0.03	0.60±0.03	Fineman-Ross
		2.00±0.03	0.60±0.03	Kelen-Tüdös
	10 + 1% NaCl	1.40±0.03	0.90±0.03	Fineman-Ross
		1.50±0.03	0.80±0.03	Kelen-Tüdös
Plochocka and Wojnarowski [24]	7.1-7.2	0.94±0.03	0.30±0.03	Fineman-Ross

Comparing reactivity ratios of this copolymer under the same reaction conditions shows a large inconsistency in the values reported in the literature. There are four main reasons that account for such scattered and unreliable reactivity ratios for AAm/AAc copolymerization in the literature:

1. The first reason is the lack of independent replication in the literature. Inevitably, every polymerization experiment has some error in the reaction and characterization parts. Any technique to determine monomer conversion (NMR, gravimetry, HPLC, etc.) and copolymer composition (elemental analysis, NMR, potentiometry, etc.) suffers from analytical errors. Therefore, it is critically important to check the reliability of experimental data with independent replicates. Otherwise, the experimental errors propagate and there would be no knowledge of or control over the magnitude of error.
2. The second reason is related to the use of incorrect reactivity ratio estimation methods that do not consider the inherent non-linearity of the Mayo-Lewis equation. Examples of these methods are linear methods such as Kelen-Tudos or Fineman Ross. The Mayo-Lewis model is a non-linear model with respect to r_1 and r_2, and so the reactivity ratios are best determined using non-linear parameter estimation techniques. Basic non-linear parameter estimation is relatively simple these days using software packages; if linear techniques are used, then the basic least squares assumptions are violated for the problem of reactivity ratio estimation, where the most appropriate method is known to be the error-in-variables-model (EVM), as discussed in extensive detail in the literature by Reilly et al.[25], Dube et al.[26], and Polic et al.[27] The EVM method is appropriate for parameter estimation problems not only because it is non-linear, but also because

dependent and independent variables are no longer distinguishable, as it properly accounts for all sources of experimental uncertainty in system variables (i.e., feed and copolymer compositions). For the reactivity ratio estimation problem, using traditional nonlinear regression analysis (and even worse, linear parameter estimation techniques) results in biased and unreliable reactivity ratios. Nonetheless, these linear and nonlinear estimation techniques are still being used, populating the literature database of reactivity ratios with inconsistent and unreliable values for most copolymerization systems, including AAm/AAc.

3. The third reason for AAm/AAc reactivity ratio inconsistency in the literature is related to not considering the assumption inherent in the Mayo-Lewis model that the model is only truly applicable for low conversion polymerizations. At very low conversion levels, the instantaneous and cumulative copolymer composition values can be assumed to be the same. In order to determine reactivity ratios, the usual methodology is to carry out low conversion polymerizations for set feed compositions, and then measure the copolymer composition of the products. However, stopping the polymerization at low conversion can be difficult experimentally and leads to another source of potentially high error. Some polymerizations simply cannot be consistently controlled below, say, 5% conversion. Moreover, even in the low conversion regions, there can be considerable composition drift which will also result in uncertainty, as clearly shown by Shawki et al.[18] in 1979 for the system in question. For the medium and high conversion regions, the instantaneous Mayo-Lewis equation should be integrated either analytically (Mayer-Lowry model[28]) or numerically (direct numerical integration (DNI) model[29]). This has led

to more recent developments for estimating reactivity ratios using the direct numerical integration (DNI) procedure.[29] This methodology uses data from total monomer conversion levels and the respective cumulative copolymer compositions. This makes it applicable at all conversion levels (low, medium, and high) without introducing any restrictions. As such, the approach is far more practical than traditional methods using only low conversion composition data. This is mainly related to the fact that all the information regarding composition drift over the polymerization trajectory can be now included in the analysis and uncertainties regarding assumptions made when using low conversion data are avoided.

4. The last but not least source of error stems from the fact that for AAm/AAc copolymerization, the ionic strength of the mixture plays an important role and should be controlled during polymerization (this will be explained further in Section 2.4.3). The ionic strength of the solution determines the overall charges of the reactants, and as a result affects monomer reactivity characteristics (in essence, the monomer reactivity ratios). The importance of ionic strength in polymerization kinetics is not well understood and therefore is one of the reasons for high fluctuations in reported reactivity ratio values.

2.4 Copolymerization kinetics of AAm/AAc

2.4.1 Polyelectrolytic nature of the AAm/AAc copolymer

Polyelectrolytes are polymers with functional, covalently bound anionic or cationic groups that tend to dissociate in water and form polymer chains which for AAm/AAc polymers are

surrounded by negatively charged ions and protons or cations.[30] In other words, their dissociation in polar solvents leaves charges on the polar chains and also introduces counter-ions in the solution. Polar monomers like AAc have more complicated polymerization kinetics as compared to non-polar ones. AAc is a weak acid which dissociates in water and is considered as a poor proton donor.[1,15,31,32] It undergoes ionization through the following equilibrium with K_a as the acid dissociation constant:

$$HA + H_2O \leftrightarrow H_3O^+ + A^- \qquad \textbf{Equation 2-4}$$

The values of pK_a, reported as $-\log(K_a)$, for AAc and PAAc reported as 4.2 and 4.75, respectively. Indicating the degree of ionization in water is greater for AAc compared to PAAc (at constant pH). It should be mentioned that in this research, the ionization of AAc monomer is considered at the beginning of the polymerization for assessing ion contents.

At low pH, the concentration of undissociated acid monomer (HA) is high, while the concentration of the dissociated form (A^-) becomes progressively greater as pH increases. Moreover, HA is more reactive towards radical polymerization than A^-. In other words, dissociated acid monomer reacts at a much slower rate than the undissociated acid. Therefore, with such monomers, the overall polymerization rate is strongly dependent on the relative concentration of the undissociated form of monomer acid or the degree of ionization/dissociation (α), where α is a direct function of pH according to the Henderson-Hasselbach Equation 2-5:

$$pH \cong pK_a + log\frac{\propto}{1-\propto}$$ **Equation 2-5**

Therefore, the pH of a solution is related to the degree of ionization of the acid and the dissociation constant (K_a), and this degree of ionization of the ionizable groups has an influence on the rate of polymerization.

As a result of the electrostatic interactions between charges, polyelectrolytes possess some special characteristics. The repulsion between the negatively charged ions on a given chain makes the polymer chain stretch rather than attain the usual random coil structure. Conversely, in the presence of added positively charged ions, the negative charge is cancelled out and makes the polymer chain like a random coil. Addition of salts leads to ion pair formation and a reduction in repulsive forces between the dissociated monomer acid and the dissociated polymer acid radical (Equation 2-6):

$$R_{\circ}^{-} + Na^{+} \overset{K}{\leftrightarrow} RNa$$ **Equation 2-6**

In Equation 2-6, Na^+ is the sodium cation, $R_{\circ}^{-}$ is an anionic polymeric radical, RNa is the equivalent ion pair radical associated with Na^+, and K is the association/dissociation equilibrium constant. It should be mentioned that the suggested ion pair formation mechanism is definitely not clear.

For polyelectrolytes in good or theta solvents, the fraction of free counter-ions depends on the polymer concentration. In dilute solutions, most of the counter-ions stay free in the solution, while as the concentration increases, counter-ions start condensing on the polymer chains. This is due to the electrostatic attraction of counter-ions which are localized in the vicinity of the polymer chain. This phenomenon leads to weakening of the electrostatic interactions between the ionic groups in the chain and causes polymer chain shrinkage and a reduction in chain size. When additional counter-ions are present in the solution, there are effects from ion pairing and shielding of the anionic charge of acrylate by those other counter-ions. In aqueous salt solutions, the acrylate ion is surrounded by two layers, based on what Ikegami showed for the hydration and ion binding of AAc in the presence of salts (Figure 2-2).[33]

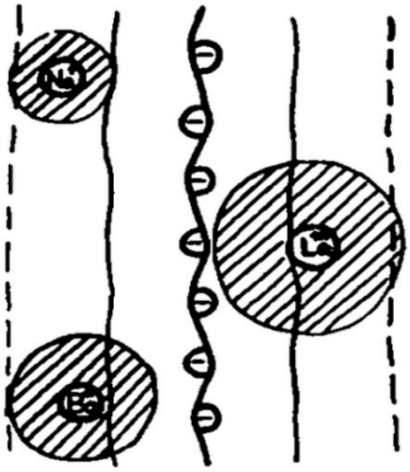

Figure 2-2: Schematic of hydration layer and cation binding for a polyion chain [33]

Referring to Figure 2-2, in the first layer, which is called "intrinsic hydration region," the acrylate ion is surrounded by water molecules. This is surrounded further by a second layer, where cations are localized by a condensation phenomenon (counter-ion binding), which is a feature of highly charged polyelectrolytes. So, one can visualize this as if the acrylate anion (either monomer or radical) is surrounded by other molecules and ions within two cylinders, where hydration with water molecules and ion binding with cations occur, respectively. During polymerization, the negative charges on the acrylate monomers and growing radicals cause electrostatic repulsions between them. These repulsions make reactive interactions less favorable. In relation to this, it has been claimed that the shielding of like charged anions by cations (e.g., from salts) decreases the degree of electrostatic repulsion between charged groups.[34,35] As a result of this shielding, ionic strength becomes an important factor for polymerizations involving ionic monomers.

Based on what has been said about ionization of AAc, the main complexity of AAm/AAc copolymerization lies in the polyelectrolyte nature of the copolymer and local placement of ionic monomer along the polymer chain. In other words, reactivities of monomers and radical species in copolymerzation are expected to change depending on the reaction medium, since monomers, radicals and the resulting polymer chains may be ionized to varying extents. Among various reaction conditions, pH, ionic strength, and monomer concentration of the media become important and affect the reaction kinetics. In the following sections, the effect of these factors on the kinetic behavior of AAm/AAc copolymerizations will be discussed.

2.4.2 Effect of pH

A review of reaction kinetics of polyelectrolyte systems reveals that the reactivity of the AAm/AAc radicals is significantly dependent on the charge characteristics of the monomers as well as their charge distribution, and pH is the key factor controlling that. In other words, for any copolymer with an anionic nature, it is well-known that pH can change the kinetics of the copolymerization.[16,17,36] At highly acidic pH (pH=2-3), AAc exists in non-ionized form, whereas from pH around 4 to basic pH values, AAc is mostly in the form of acrylate anion. The situation is opposite for AAm; at highly acidic pH, AAm is protonated, while at pH values from around 2 to high pH, AAm is in the neutral non-protonated form. Therefore, depending on pH, there are various monomer forms in the reaction mixture. As a result of this, controlling pH is important for determining reliable monomer reactivity ratios. It has been reported that the reactivity ratio of AAc tends to decrease by changing pH from highly acidic values to basic ones, because of higher prevalence of electrostatic repulsions between negatively charged ionized AAc monomer molecules and growing radicals. Similarly, there are electrostatic interactions between AAm monomer units and radicals at very low pH values, where AAm is protonated. Therefore, as pH increases from acidic to more basic values, the reactivity ratio of AAm increases.

Cabaness et al. were the pioneers in studying AAm/AAc copolymers and evaluated the effect of changing pH (in the range of 2.17-6.25) on reactivity ratios in this system.[10] Figure 2-3 shows the different forms of monomer and polymer species for AAc and AAm (acrylic acid, acrylate anion, acrylamide, and protonated acrylamide) as a result of varying pH.

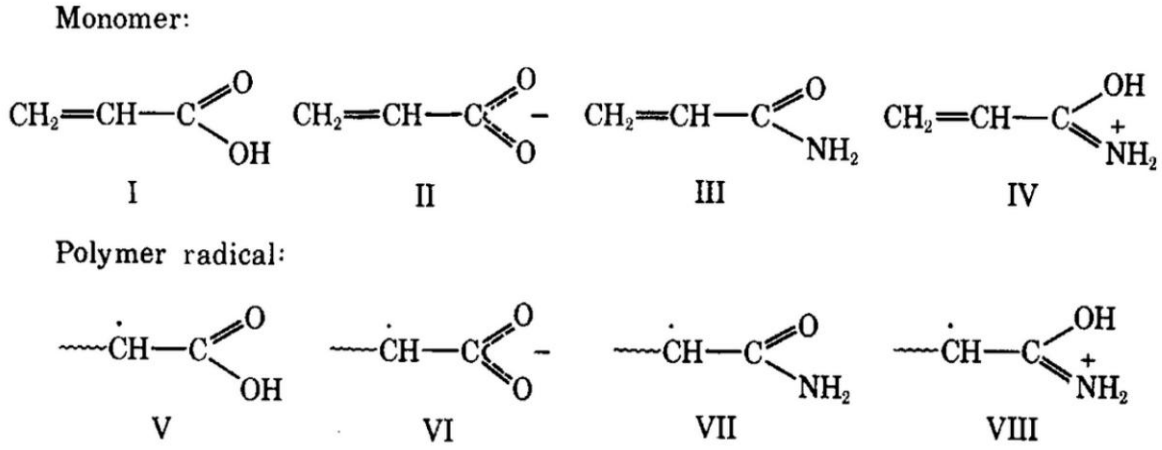

Figure 2-3: Various forms of AAc and AAm in reaction mixture [10]

By changing the pH of the medium, various forms of AAc, acrylate anion, AAm, and protonated AAm result (due to the dissociation of AAc and protonation of AAm), which affect the reactivity ratios and, as a result, alter the kinetics.

Table 2-2 shows the relationships between pH and the various monomer forms. An interesting fact is that the reaction of AAm/AAc can be considered as a terpolymerization at some pH values, since AAc has two interchangeable forms. To avoid ionization and subsequently terpolymerization, the polymerization should be carried out in a medium other than water, like methanol or benzene, but that would lead to complexities resulting from polymer solubility.[37]

Table 2-2: Relationship between pH and monomer forms [10]

pH < 2	Fully non-ionized AAc, and partially protonated AAm	Copolymerization
2 < pH < 6	Partially ionized AAc (AAc and acrylate anion) and AAm	Terpolymerization
pH > 6	Fully ionized AAc (acrylate anion) and AAm	Copolymerization

Besides AAc monomer units, AAc radical chain ends can also dissociate the proton and therefore have a separate degree of ionization. Since there is a difference between the dissociation ability of the AAc monomer units of the polymer and the monomer unit located at chain end (-AAc), one has to consider different degrees of ionization for them (α and α′, respectively). Rintoul et al. and Laćik et al. introduced a classification of the species in the polymerization system based on both pH and degree of ionization.[38,39] According to Table 2-3, five regions can be defined by the presence or absence of potentially reactive species.

Table 2-3: Reaction regions for AAc[38]

Region	**pH range**	**Ionization of AAc as**		**Occurrence of AAc**	**Polymerization type**
		Monomer α	**Polymer chain end α′**		
I.	pH < 2.2	0	0	AAc, -AAc	Copolymerization
II.	2.2 < pH < 3.8	0 < α < 1	0	AAc, A^-, -AAc	Terpolymerization
III.	3.8 < pH < 6.2	0 < α < 1	0 < α′ < 1	AAc, A^-, -AAc, -A^-	
IV.	6.2 < pH < 8.4	1	0 < α′ < 1	A^-, -AAc, -A^-	
V.	8.4 < pH	1	1	A^-, -A^-	Copolymerization

These various forms of monomers influence the reactivity of AAc and so the reactivity ratios change accordingly.

From Figure 2-4, three distinct regions can be observed.[17] The first region is the pH from 2 to 4, where r_1 (AAm) is smaller than r_2 (AAc). The second region is the crossover of both reactivity ratios at pH around 4.2, with r_1 and r_2 close to 1 (other values at the crossover pH have been reported as 3.6 and 3.77).[10] In the third region, r_1 becomes considerably larger than r_2 and then both r_1 and r_2 start to level off. At low pH (pH<2), there is an electrostatic repulsion between the positively charged propagating chain and the protonated AAm, and therefore the reactivity of macro-radicals towards AAm is less than that towards AAc ($k_{11}<k_{21}$) and therefore $r_1<1$. At the same time, it is speculated that for AAc, $k_{22}>k_{12}$ and, as a result, $r_2>1$, due to penultimate and ante-penultimate effects (which become important in the case of highly polar and ionizable polymers)[10]. As pH goes up, k_{12} and k_{22} decrease (more significant decrease for k_{22}) due to the electrostatic repulsion between ionized AAc and ionized macro-radical, while k_{11} is assumed to remain relatively constant. This results in a decrease of r_2 and an increase of r_1.

The curve shown in Figure 2-4 for the degree of ionization of AAc (right-hand-side axis) is consistent with the electrochemistry of the system.[17] At pH below 2, AAc is fully non-dissociated and at pH larger than 6, it is essentially fully dissociated and this is the reason why the degree of ionization curve shows constancy over both these regions. Between these two, there is an abrupt change in pH which indicates an equilibrium between ionized AAc

and AAc. The story is totally different for the AAm monomer and polymer chains, which are partially protonated at pH below 2 and then become fully neutral at higher pH.

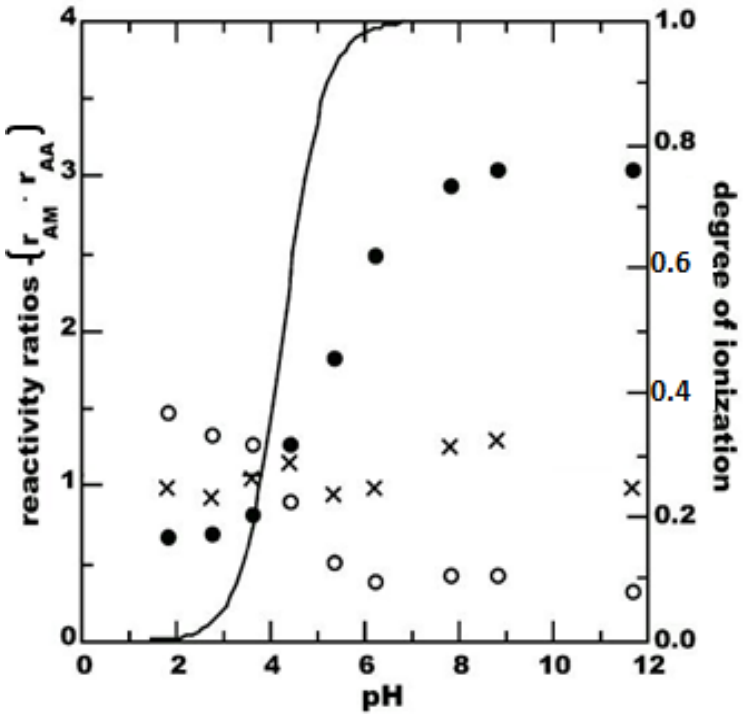

Figure 2-4: Reactivity ratios, r_{AM} (●) and r_{AA} (○), reactivity ratio product $r_{AM}.r_{AA}$ (×), and degree of ionization of AAc (curve) vs. pH [17]

The effect of changing pH on the reactivity ratios means there are changes in copolymer composition.[17] In other words, pH strongly changes the kinetics and, as a result, the copolymer composition (copolymer microstructure) is affected by pH. The effect of pH on copolymer composition can be seen in Figure 2-5.

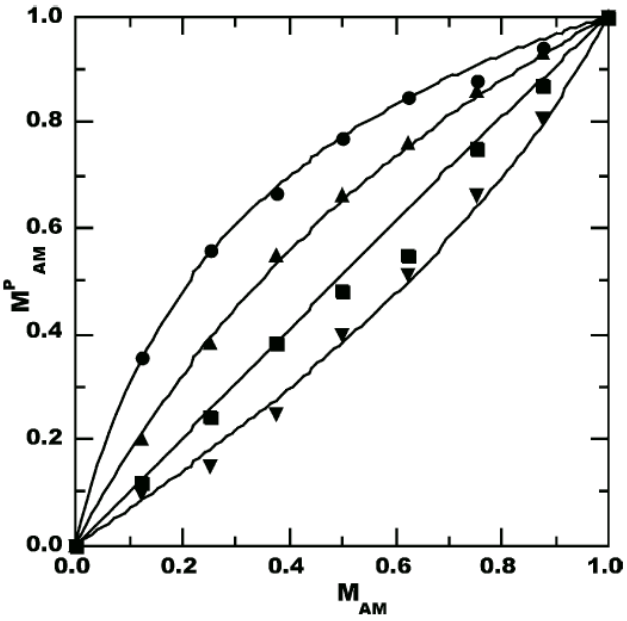

Figure 2-5: Copolymerization diagram of AAm fraction in copolymer (M^P_{AM}) vs. AAm fraction in monomer feed (M_{AM}). pH=1.8 (▼), 4.4 (■), 5.3 (▲), 12 (●) [17]

As indicated by Figure 2-5, copolymer composition is affected by pH, and by inference the degree of composition drift can also be influenced by the pH of the medium.[16] From Figure 2-6 (a), it can be inferred that AAm has a higher homo-propagation rate constant compared to cross-propagation and, therefore, its fraction in the polymer is greater than it is in the feed. In other words, r_1 (AAm) is larger than r_2 (AAc) at pH=5 and 12. At pH=2 (see Figure 2-6 (b)), the situation is different, since AAc is the more active monomer and so its instantaneous fraction in the feed mixture decreases faster during polymerization. As described before, it is the protonation of AAm at this pH which causes an electrostatic repulsion between the AAm monomer and its macro-radical.

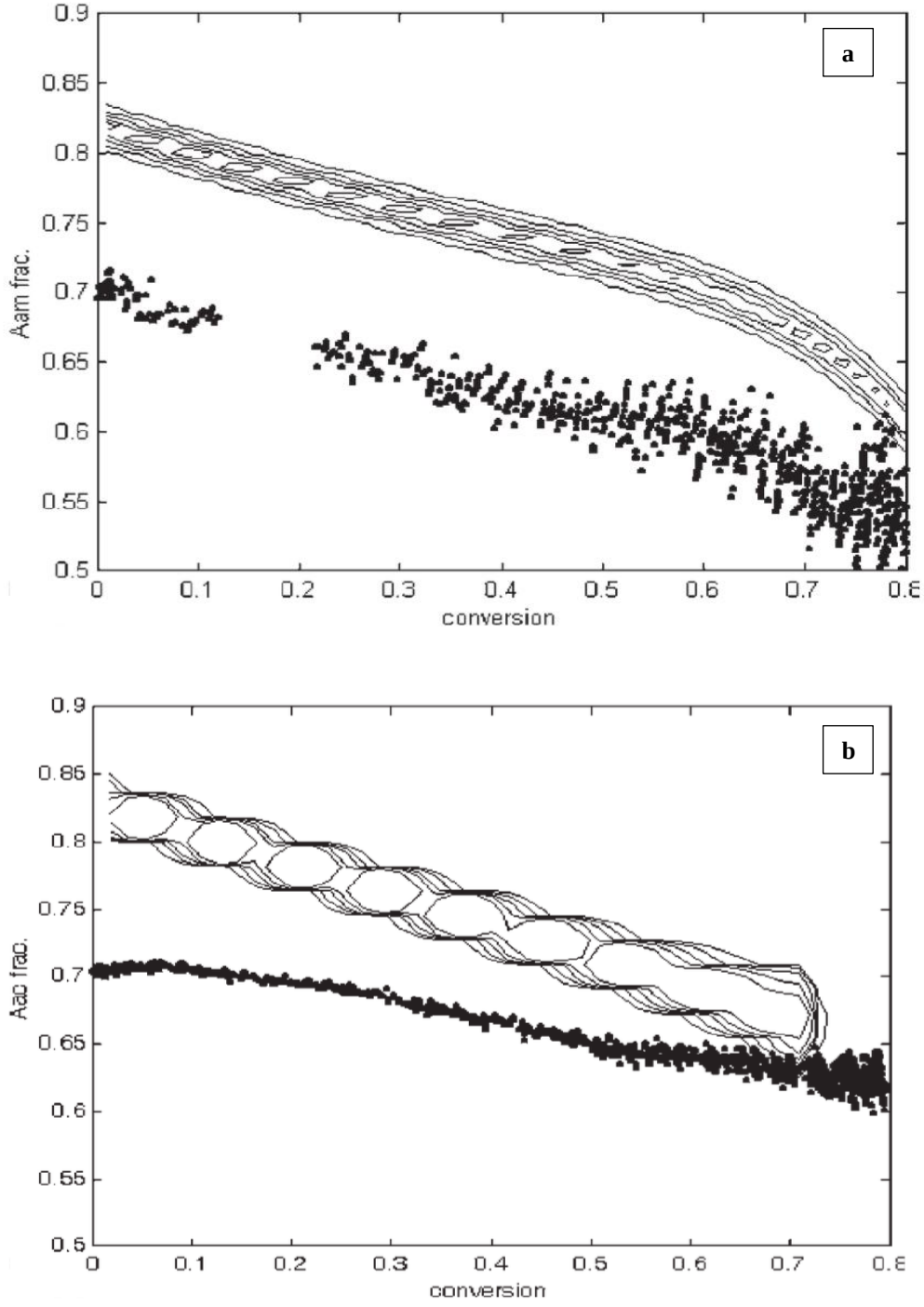

Figure 2-6: Composition drift curve for a) 70 % AAm content (fraction) at pH=5, b) 70 % AAc content (fraction) at pH=2. Dots are experimental values and contour lines are theoretical values [16]

2.4.3 Effect of ionic strength

The importance of the ionic strength and its effect on polymerization kinetics are rarely discussed in the polymerization literature. Ionic strength can be calculated by adding the product of concentrations times the square of charge of all ions present in the solution (Equation 2-7).

$$I = \frac{1}{2}\sum_{i=1}^{n} c_i z_i^2 \qquad \textbf{Equation 2-7}$$

where c_i is the molar concentration of ion i (mol/L), and z_i is the charge number of that ion. In the case of AAm/AAc copolymerization, the ions present are acrylate anions (depending on the degree of ionization) and additional counter-ions (e.g. salts) present in the solution. These counter-ions shield the negative charges on acrylate anions and reduce the electrostatic repulsion between like charged anions.[34,35]

It should be mentioned that not only does the ion charge number play a role in the ion shielding, but also the type of the cation, which affects the electrostatic attraction between anion and counter-ions. It has been shown that the reactivities of both AAm and AAc in the system are affected by the type of cation.[24,40] The effect of the nature of the dissolved ionic species on rate naturally extends into copolymerization.

Having made these introductory statements, it is important to understand how ionic strength acts as a controlling factor during copolymerization of AAm/AAc polyelectrolytes. Kabanov

et al. did pioneering work in this respect and proposed that ion pairing affects the reactivities of ionizable monomers.[41] They related an increase in polymerization rate, observed upon adding salts, to ion pairing between the growing radicals and the counter-ions from the added salt, which diminished the electrostatic repulsions between like charged species at the reaction site. Paril et al. also studied the effect of ionic strength on the rate for the AAm/AAc system at different AAc feed contents at pH around 3.6 (Figure 2-7).[11] At low ionic strength, they observed a reduction in the rate by introducing more AAc in the feed. They related this behavior to the stronger electrostatic repulsion upon increasing the AAc content, which made the polymerization slower. At high ionic strength, on the other hand, they could not observe any specific trend between AAc content and copolymerization rate. However, it should be mentioned that in their study there were two variables affecting the system, namely, the AAc mole fraction in the feed and the total monomer concentration. Hence, the total monomer concentration varied at constant ionic strength (both at low and high levels), which made it complicated to distinguish between the effects of these variables. Moreover, salt had been used in the carrier solvent, but not for maintaining ionic strength constant between runs.

The reactivity ratios of monomers and radical species in copolymerzation are also expected to change depending on the makeup of the reaction medium, since monomers, radicals and the resulting polymer chains may be ionized to varying extents. Ponratnam and Kapur observed an increase in reactivity ratios of AAc and AAm at pH=4 by adding NaCl.[15] They attributed this change to the partial neutralization of the ionic charges on the ionizable monomer, which caused in turn a faster addition of monomer units to the radicals. At pH=6, adding 1 M NaCl caused a slight decrease in r_{AAc} while the r_{AAm} remained constant. On the

other hand, Kurenkov et al. noticed that r_{AAc} and r_{AAm} increased and decreased, respectively, after adding NaCl to the reaction at pH=10.[23]

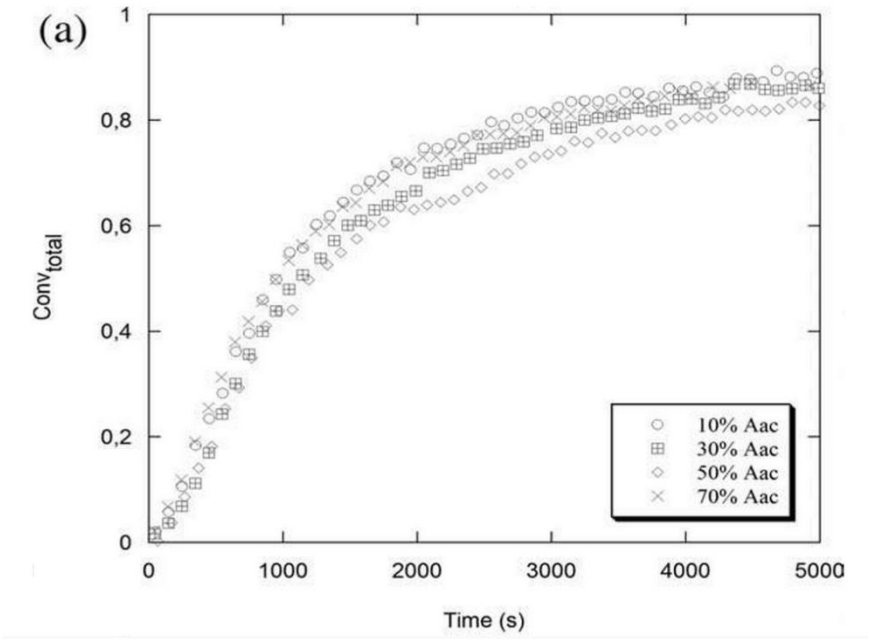

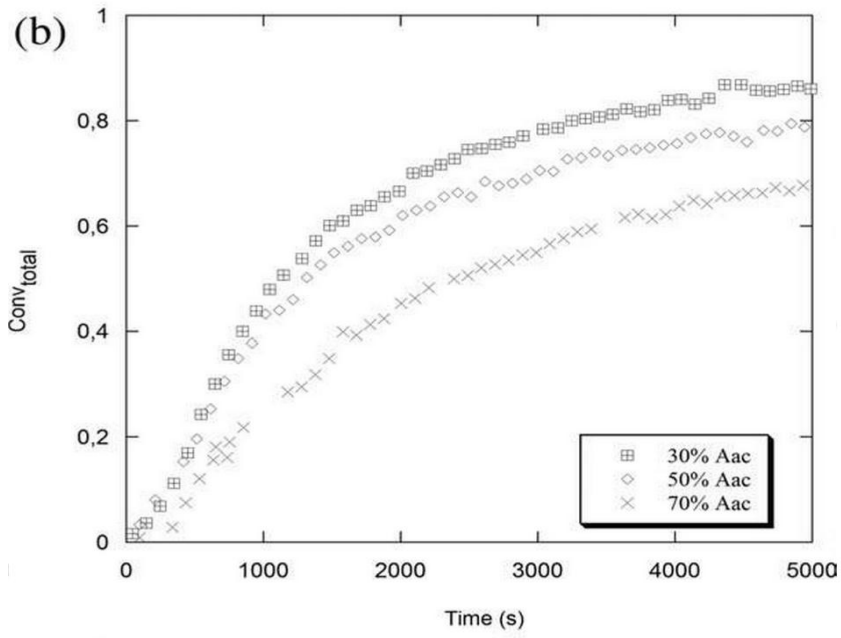

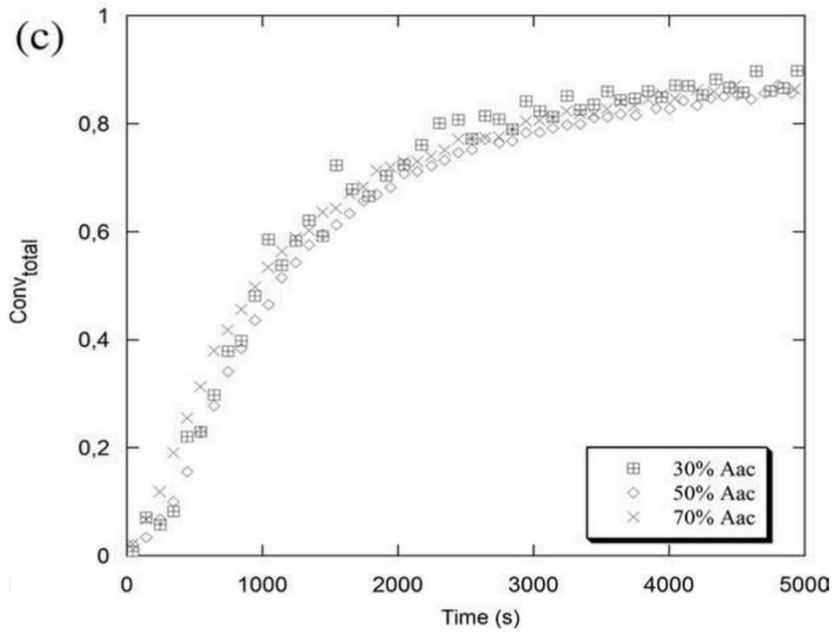

Figure 2-7: Conversion ($Conv_{total}$) vs. time for various AAc contents in AAm/AAc copolymerization at a) variable ionic strength, b) low ionic strength, c) high ionic strength [11]

Paril et al. observed an increase in both reactivity ratios of AAc and AAm at pH=3 but at higher ionic strength.[11] As mentioned before, this can also be caused by different total monomer concentrations in these studies, since the total monomer concentration varied as well. The effect of added salt is not unique to the AAm/AAc system. McCormick and Salazar examined the copolymerization of AAm and sodium 3-acrylamido-3-methylbutanoate (NaAMB) and found that the reactivity ratio of AAm decreased with adding 1 M salt solution to the copolymerization, whereas the reactivity ratio of the charged monomer (NaAMB) increased.[35]

2.4.4 Effect of monomer concentration

Total monomer concentration is another factor affecting the reaction kinetics, rarely studied in the literature. Rintoul and Wandrey observed a trend for monomer reactivity ratios with respect to monomer concentration.[17] They found an increase in the reactivity ratio of AAc (r_{AAc}) and a decrease in the reactivity ratio of AAm (r_{AAm}) by changing monomer concentration from 0.2 to 0.6 M at pH=12 (Figure 2-8). They justified this by the higher ionic strength and consequently more ion charge screening due to the higher monomer concentration. They concluded that a lower electrostatic repulsion of negative charges made the cross-propagation of AAm with AAc more probable and therefore reduced r_{AAm}. On the other hand, AAc was more likely to homo-propagate and therefore an increase in r_{AAc} was observed.

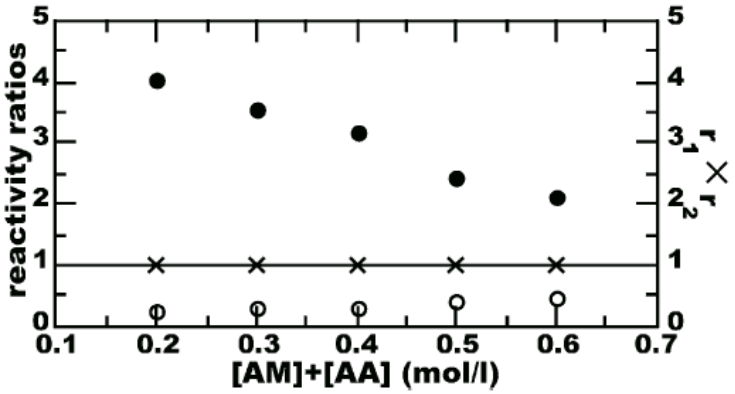

Figure 2-8: Reactivity ratio vs. total monomer concentration (r_{AAm} ●, r_{AAc} ○, ($r_1.r_2$) ×) [17]

In a more recent study, the effect of monomer concentration on AAm and non-ionized AAc copolymer was investigated.[42] It has been reported that increasing monomer concentration from 5 to 40 wt% increases the rate of monomer conversion.

2.4.5 Effect of other factors

The effect of the initiator concentration on the kinetics of the AAm/AAc copolymerization has also been investigated.[17] No significant effect on the reactivity ratios with a change in initiator concentration was found.

Solvent nature plays an important role in the copolymerization kinetics of the AAm/AAc system due to the high sensitivity of the monomers to the reaction medium. Besides water-phase polymerization, polymerization of AAc and AAm can also be conducted in organic solvents. It should be noted that some of these systems are heterogeneous as the polymers formed are insoluble in the reaction media and precipitate from the solvent. Chapiro et al. studied the effect of solvent type on the AAm/AAc copolymerization system.[21,43] Their results showed that the reactivity ratios strongly depend on the solvent type and the dielectric characteristics of the solvent, and therefore the copolymer composition varies significantly with the solvent nature. Table 2-4 cites reactivity ratios for AAc and AAm in different solvents.

Table 2-4: Effect of solvent type on reactivity ratios of AAm/AAc copolymer [21,43]

Solvent	Dielectric constant	r_1 (AAm)	r_2 (AAc)
Bulk monomer	_	0.60	0.57
Dioxane	2.2	1.02	0.35
Benzene	2.3	1.0	0.30
Acetic acid	6.15	0.55	0.75
Methanol	32.6	0.84	0.75
Dimethylformamide	36.7	0.52	1
Water	78.5	0.47	1.3

It should be noted that formation of AAm/AAc copolymer can also take place through hydrolysis of the amide group when there is an acid group in the immediate neighborhood or at extremely alkaline or acidic conditions or at high temperatures.[44] One should be aware of this possibility since during hydrolysis, amide groups are converted to carboxylate groups which affect the characterization test based on amide group. This kind of system is not within the scope of this research.

2.5 Copolymer structure

It is usually assumed that the AAm/AAc copolymer has a roughly uniform distribution of anionic charges along the chain.[45] The distribution of AAc units and subsequently anionic charges is very important with respect to polymer solution behavior and copolymer application performance properties. So, it is crucial to have more information about the

detailed microstructure of the copolymer. In copolymer systems, instantaneous (F_i) and cumulative (cum F_i) copolymer compositions (mole fractions of monomer i in the copolymer chains) are popular indicators of the microscopic instantaneous/cumulative composition of the copolymer chains. However, F_i and cum F_i alone cannot fully describe the arrangements of the two monomers along the polymer chain (distribution of sequences). It is well known that two copolymers with the same copolymer composition might have different copolymer structures (block, random or alternating). So, in order to have a better insight into the copolymer chain structure and monomer arrangements in the chain, the chain sequence distribution needs to be evaluated. Information about the sequence length distribution of AAm/AAc copolymers is very rare in the literature.[19,46,47]

Molecular weight of AAm/AAc copolymer also has an important impact on the solution viscosity and application performance. Considering enhanced oil recovery as a potential application, high molecular weight polymers are preferred; however, it has been reported that polymers with higher molecular weights are more sensitive towards shear degradation, have more retention in the oil reservoir (low propagation) and cause injectivity problems because of their large size.[45,48,49] On the other hand, as molecular weight of the polymer goes up, the viscosity of the polymer solution and, as a result, its effectiveness increases. Therefore, molecular weight of the polymer should be chosen carefully. A representative molecular weight for an AAm-based polymer used in polymer flooding is reported to be around 7-9 million.

Measuring the molecular weight of AAm/AAc copolymer is not straightforward. This is mainly because of the polyelectrolyte nature of the copolymer and the electrostatic interactions within the polymer that alter the size of polymer chains depending on the detailed nature of the solution with respect to pH and dissolved salts.[5,50] Normally, gel permeation chromatography (GPC) is the most reliable method for measuring polymer molecular weights. However, accurate characterization of high molecular weight polyelectrolytes with GPC is especially complicated, due to the polyelectrolyte nature of the copolymer that affects the mechanism of separation in the GPC columns. In the literature, molecular weights of AAm/AAc copolymer have mainly been determined by intrinsic viscometry or (much less frequently) by light scattering.[46,50-52]

2.6 Copolymer solution rheology

Aqueous solution viscosity of AAm/AAc copolymer is extremely important in understanding and predicting the copolymer application behavior. For example, in applications such as flocculation, drag reduction, or enhanced oil recovery, when the polymer is subjected to high shear stresses, degradation might happen and therefore knowing about the solution viscosity at different shear rates and shear stresses is necessary.

Shear viscosity of polyacrylamide and its degradation behavior have been studied by Abdel-Alim et al. using a high shear Couette viscometer.[6] They studied the shear degradation of polyacrylamide after exposing it to various shear stresses at different temperatures. Despite the fact that it was assumed that shear rate was the controlling factor, they concluded that

shear stress and viscosity of the polymer were more important than shear rate. At constant shear rate, by decreasing the temperature and increasing the polymer solution concentration, both shear stress and polymer viscosity increase, which results in more degradation and narrower molecular weight distribution.

Copolymer composition plays an important role in polymer solution behavior. Kulicke and Hörl observed a maximum in the intrinsic viscosity profile of AAm/NaAc copolymers with respect to copolymer composition (Figure 2-9).[53] By increasing the AAm percentage in the copolymer from zero to 35%, the intrinsic viscosity goes up. However, upon further increasing AAm in the copolymer composition, the intrinsic viscosity decreases. They also noticed a similar dependence on the AAm content for the radius of gyration behavior of the copolymer. The authors explained this maximum based on the polyelectrolyte character of the copolymer (electrostatic effects) and also non-ionic intermolecular hydrogen bonding.

The same maximum for AAm/AAc copolymer solutions was also reported by Myagchenkov et al.[54] Figure 2-10 shows viscosity number of AAm and NaAc copolymers with respect to degree of neutralization. As can be seen from the figure, near 70-80% degree of neutralization, there is a maximum for the viscosity number value because of the macroanion-counter ion interactions.

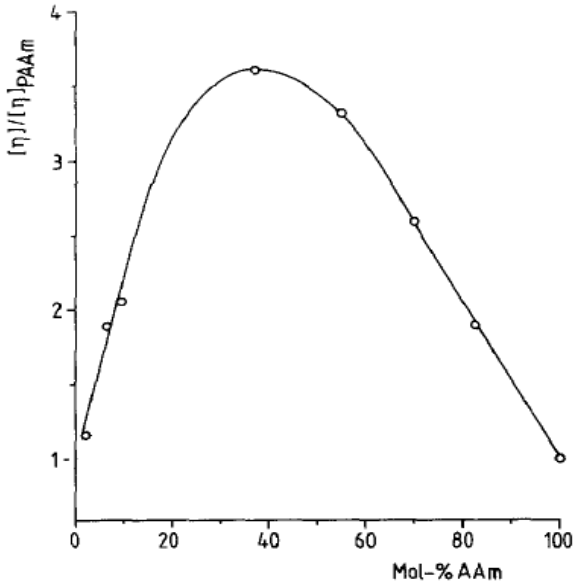

Figure 2-9: Intrinsic viscosities of AAm/NaAc copolymer and AAm homopolymer in 0.1 M Na_2SO_4 salt solution [53]

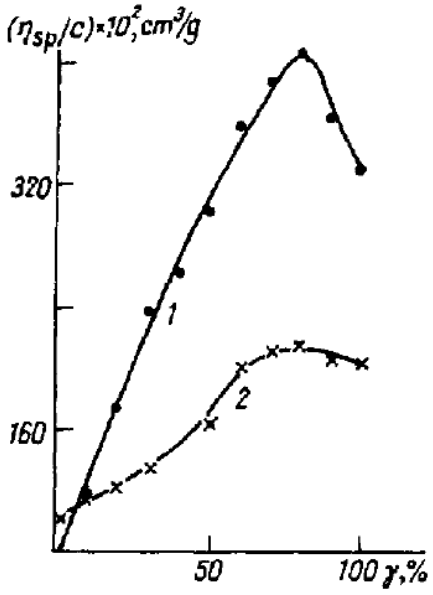

Figure 2-10: Viscosity number versus degree of neutralization γ, for copolymers of AAm/AAc at concentrations 0.001 wt% (1) and 0.004 wt% (2) [54]

Besides shear viscosity, intrinsic viscosity also varies with copolymer composition. Candau et al. studied the intrinsic viscosity of AAm/NaAc copolymer with respect to the NaAc content in the copolymer (Figure 2-11).[47] The figure shows a maximum in intrinsic viscosity of the solution around 40% mole content of NaAc. They explained it based again on electrostatic interactions and hydrogen bonding within the copolymer chains. At NaAc contents below 40%, because of cyclization between amide and carboxylate groups, chain stiffness and an increase in intrinsic viscosity happens. At NaAc content higher than 40%, the probability of intramolecular hydrogen bonding formation decreases (due to high electrostatic repulsions between the chains), and subsequently the intrinsic viscosity decreases.

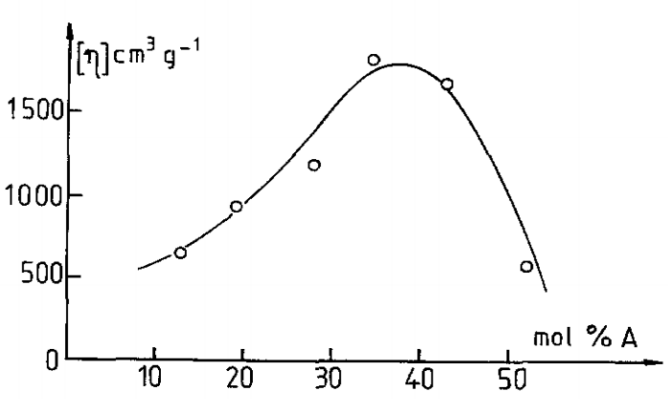

Figure 2-11: Intrinsic viscosity of AAm/NaAc copolymer as a function of NaAc content [47]

McCormick and Salazar reported a similar behavior for the copolymers of AAm and sodium 3-acrylamido-3-methylbutanoate (NaAMB).[35] They observed a maximum in the intrinsic viscosity of AAm/NaAMB copolymers with respect to copolymer composition. This

behavior was explained based on counter-ion condensation and decrease in molecular weight by having more NaAMB in the copolymer. Moreover, the copolymer composition at which the intrinsic viscosity is at a maximum depends on the hydrogen bonding (between the comonomers of the copolymer backbone) that makes the copolymer chain stiff.

Based on all these studies, it can be concluded that copolymer composition plays an important role in determining viscosity of the polymer solution. In other words, in order to achieve high shear viscosity, one should optimize the percentage of each monomer in the copolymer chain.

The effect of pH on electrostatic repulsion and, as a result, solution viscosity is important.[48] At high pH values, carboxylic groups exist in their ionized forms, while at low pH values, they are converted to their undissociated acid forms. Consequently, at low pH, there are lower levels of electrostatic repulsions between groups and less viscosity enhancement behavior. It has been reported that by decreasing the solution pH from 9.8 to 4, the viscosity of AAm-based copolymer solutions decreases by a factor of 4.

Solution viscosity of AAm/AAc copolymers with respect to polymer concentration has also been studied in the literature.[52,55,56] Solution shear viscosity of hydrolyzed polyacrylamide increases significantly with higher concentrations of solutions at a given temperature.[45,55,57]

The other important factor that affects the rheology of AAm/AAc copolymer is solution salinity.[5,58] Since the copolymer has a polyelectrolyte nature, any factor that influences the electrostatic interactions will change the solution and rheological properties as well. It has

been observed that adding salts (such as sodium chloride) into a polyelectrolyte solution screens the negative charges on the copolymer chain and, as a result, significantly reduces the polymer solution viscosity. Figure 2-12 shows how solution shear viscosity of hydrolyzed polyacrylamide, HPAM, changes with addition of salt.[55] By increasing salt concentration from 0 to 1 wt%, there is a noticeable decrease in solution viscosity, especially at low shear rates. After a critical salt concentration, the change in solution viscosity is negligible. This phenomenon is called "critical salinity" and occurs because of saturation in the screening effect of salt cations.

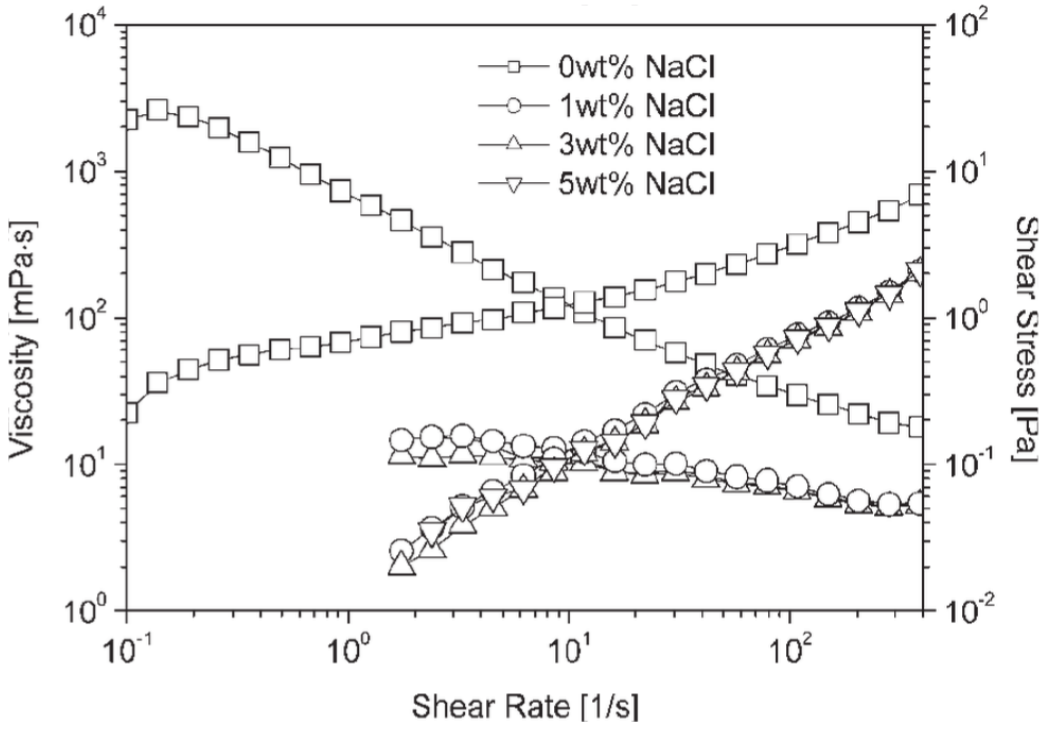

Figure 2-12: Shear viscosity and shear stress of HPAM versus shear rate with different salt concentrations at 1500 ppm concentration and 25 ºC [55]

2.7 Applications of AAm/AAc copolymers

Synthetic water-soluble polymers can improve the aqueous solution properties in relation to gelation, thickening, emulsification, and stabilization. Therefore, they find many uses as flocculants and coagulants (for waste water treatment), film-formers, binders and lubricants; enhanced oil recovery, oil field products and mineral processing; coatings, pulp and paper industry (improving paper's printing quality), water retention and treatment; and also biomedical, pharmaceutical and high value cosmetic products. [3,59]

Among various important applications for this copolymer, tailoring properties for enhanced oil recovery (EOR) is the target for this research and, as a result, it will be discussed in more detail in Section 2.7.1. Application of this copolymer as a flocculant for water treatment was also studied briefly in this research and therefore flocculation applications will be briefly overviewed in Section 2.7.2.

2.7.1 Enhanced oil recovery (EOR)

Enhanced oil recovery, which is also called improved oil recovery or tertiary oil recovery, encompasses the implementation of various techniques in order to increase the efficiency of oil extraction from oil fields. Among various EOR techniques, polymer flooding (which is also called polymer-augmented flooding) is well-recognized for its versatility and popularity and has been applied in many oil fields with a long commercial history and proven results. [45,60] Figure 2-13 shows a schematic of a typical EOR operation.

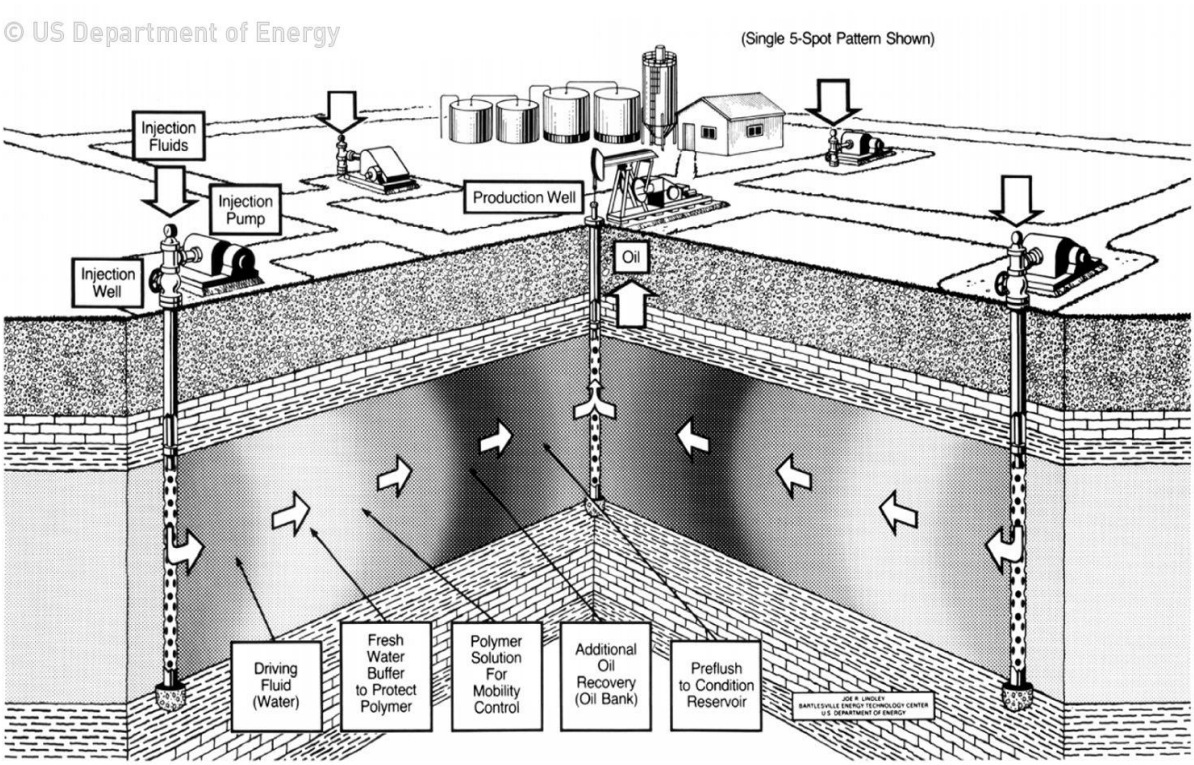

Figure 2-13: Schematic of polymer flooding [48]

The relative high oil prices compared to low cost of polymers, the ability to make polymers with super high viscosity or change their properties to increase their effectiveness and the impossibility to apply other EOR techniques in specific oil reservoirs has made polymer flooding the most promising EOR technique. To be more specific about the benefit of using polymer flooding, an example of polymer flooding in Saskatchewan, Canada is given.[48] The results of a study showed that by injecting 17% of the pore volume (which means 17% of the reservoir volume) of a polyacrylamide polymer solution (with concentration ranging from 1100 to 1500 ppm) increased the oil production from 410 BOPD (Barrels of Oil Per Day) to 1100 BOPD, which is quite significant.

There are two general types of water-soluble polymers that act as viscosity-enhancing polymers during polymer flooding: xanthan gum polymer (a biopolymer) and AAm-based polymer (synthetic polymer).[48] The chemical structure of xanthan is given in Figure 2-14.

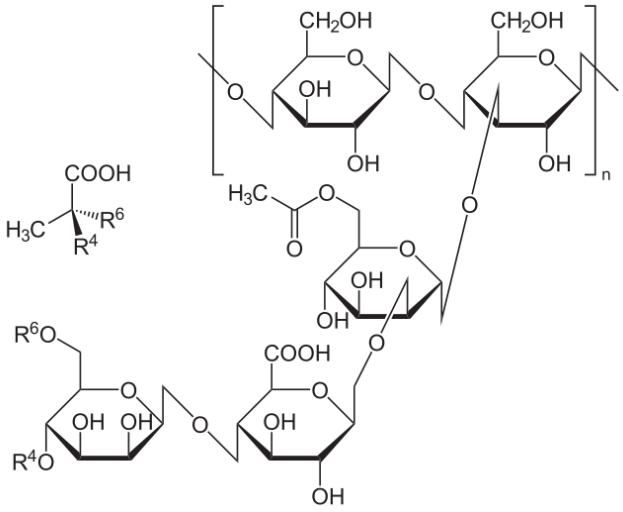

Figure 2-14: Xanthan chemical structure

Synthetic AAm-based polymers are more commonly used in commercial oil fields as compared to biopolymers, due to better price and higher inherent stability.[45,48] AAm-based polymers are highly flexible macromolecules with relatively chemically stable carbon-carbon bonds and an amide pendant group that makes the polymer soluble in water.

It is known that by addition of only small quantities of high molecular weight water-soluble polymers in water, the efficiency of oil recovery increases considerably.[61] In order to understand the role of polymers in oil recovery, it is necessary to define the mobility ratio (M) as Equation 2-8:

$$M = \frac{\lambda_w}{\lambda_o} = \frac{k_w/\mu_w}{k_o/\mu_o}$$ **Equation 2-8**

where λ, μ, and k are mobility, viscosity, and effective permeability, respectively. The subscript o represents oil (displaced fluid) and w refers to water (displacing liquid). Polymers help to decrease the mobility ratio by increasing the viscosity of water (thickening the aqueous phase) and reducing the effective permeability of the reservoir matrix rock and consequently water (pore blocking). Therefore, addition of polymers to the drilling fluids can enhance the oil recovery efficiency. In other words, the role of water-soluble polymers is to modify/control the viscosity of the injected water and to reduce the relative permeability of the rock formation to water. Therefore, the injected water propagates slowly through the reservoir, which makes it more efficient in displacing oil towards the production well. Otherwise, the injected water could flow very fast, which makes the water flooding process inefficient. There are several mechanisms responsible for reducing the permeability of water (k_w) by adding polymers. Among these mechanisms, polymer adsorption onto pore walls (layer formation) that selectively reduces the k_w (not k_o) has been considered as the dominant mechanism.

Dissolving water-soluble polymers in water diminishes water fingering and channeling effects, and as a result decreases the mobility ratio.[62] Without having high viscosity polymer solutions, large quantities of oil are left behind (due to the significant difference between

water and oil viscosities), and water fingering or water channeling takes places which causes a decline in oil recovery efficiency. This effect is schematically shown in Figure 2-15.

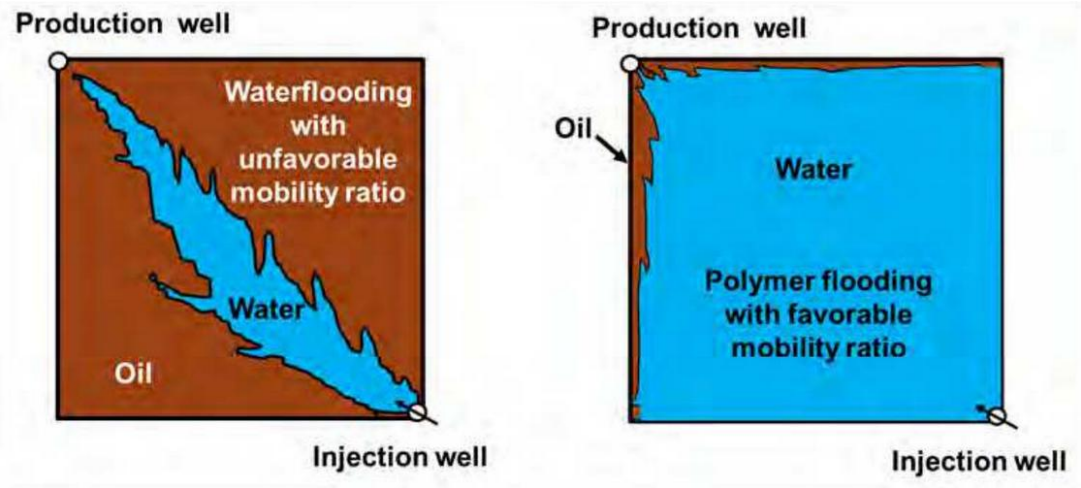

Figure 2-15: Water flooding (left) versus polymer flooding (right) [63]

Acrylamide homopolymers (including partially hydrolyzed acrylamide) and copolymers of AAm (such as AAm/AAc) make the largest contribution in oil recovery processes because of their availability and low cost.[1,60,64,65] AAm homopolymer is slightly positively charged in acidic pH medium and therefore it has a tendency to adsorb on reservoir porous media such as rocks and sands.[48] As a result, partially hydrolyzed AAm or AAm/AAc copolymer is usually favored over AAm homopolymer in order to increase the viscosity better and decrease the adsorption onto the rock surfaces. It should be mentioned that it is preferred for carboxylate groups in AAc to be in the sodium salt form for polymer flooding use. This is

because the thickening capability (increase in viscosity) of AAm/AAc copolymer in solution is highly related to the electrostatic nature of the copolymer.[45]

It should be noted that AAm homopolymers or copolymers suffer from lack of stability (chemical, thermal, mechanical, etc.) in oil reservoirs and so should be considered. They degrade at high flow rate (high degree of shear rate). An important factor that controls shear stability is macromolecule chain rigidity.[7] AAm homopolymer and copolymers behave as flexible coils and are very shear sensitive, while the presence of acrylate groups, coming for example from AAc incorporation, increases polymer shear resistance (since they increase chain rigidity). It is important to know that normal and elongational stresses are applied on the viscoelastic polymer solution in parallel to shear stresses in oil recovery applications.[4,66] So, in order to study the degradation behavior of the polymer solution completely, one should consider the effects of these stresses together.

Besides shear and elongation stability, the other important characteristic of the copolymer in most applications is thermal stability, since molecular properties and their resistance to thermal degradation are a key factor. In the case of AAm/sodium acrylate copolymers, it has been found that viscosity average molecular weight, $\overline{M_\eta}$, decreases over time with increasing temperature due to carbon-carbon bond rupture in the copolymer backbone. After meeting a critical temperature, $\overline{M_\eta}$ starts increasing with an increase in temperature, possibly due to intermolecular crosslinking of amide groups in the copolymer.[51,67] Besides thermal degradation at high temperatures, hydrolysis of AAm should be considered too. At high

temperature and/or acidic/basic conditions, there is a chance for AAm hydrolysis, which then affects the rheology and viscosity of the solution.[68]

Moreover, AAm homopolymers and copolymers precipitate in high salinity reservoirs.[61,69] Oilfields sometimes contain high concentration of dissolved salts and divalent ions which decreases the hydrodynamic volume of the polymer chains and affect their solution viscosity. As a result, AAm copolymers perform best when they are used in low salinity reservoir brines.[48] The reason is that in low salinity conditions, the polymer chains adopt an extended conformation which increases the solution viscosity more effectively. At high salinity conditions, on the other hand, the polymer chains coil up because of the shielding of the negative charges of acrylate anions by the cations of dissolved salts. Therefore, the viscosity enhancement effect is less at high salinity conditions. A schematic of the polymer chains in these two conditions is shown in Figure 2-16.

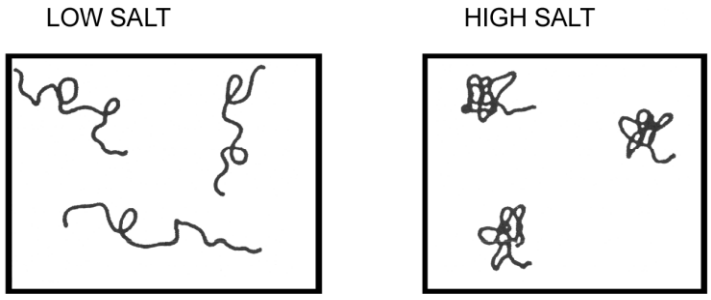

Figure 2-16: Effect of salinity conditions on polymer chain conformation [48]

Therefore, despite the fact that the AAm/AAc copolymer has the best mobility control characteristics as compared to other water-soluble polymers, it still suffers from some

important deficiencies as mentioned above. There are several ways to compensate for these issues. It has been suggested in the literature that introducing a third monomer to make terpolymers can improve the characteristics of the water-soluble polymer.[48,70] For example, the hydrogen of the amide group in AAm can be replaced by a methyl group to eliminate the chance of AAm hydrolysis and hence induce a reduction in solution viscosity.[70] Moreover, a large and more polar side group such as SO^-_3 can substitute small side groups to enhance stability of the polymer chains. The SO^-_3 groups also make the hydrogen bonding stronger compared to monomers with $–CO^-_2$ groups. As a result, it is expected that sodium-2-acrylamido-2-methyl propane sulfonate (AMPS) should increase the water solubility of the polymer. At the same time, due to the presence of the bulky group, polymer solution viscosity would be higher. In addition, AMPS shows higher stability compared to AAm/AAc copolymer at high temperatures (95 ºC) and in high salinity reservoirs.[48]

Another option is to add vinylpyrrolidone to make terpolymer that has superior properties compared to AAm/AAc copolymers.[48] Terpolymers of vinylpyrrolidone, acrylamide, and acrylate, have been reported to be candidate polymers for use in polymer flooding at high-temperature reservoirs with harsh environments. Certain vinylpyrrolidone polymers were reported to not precipitate from seawater after aging for six years at 250°F. The potential concerns regarding these terpolymers are their relatively high cost and low molecular weight as compared with more conventional acrylamide polymers.

Associative polymers are a recent category that has been developed to increase effective viscosity in oil reservoirs significantly.[45,71] This kind of polymer has both hydrophilic and

hydrophobic parts. The role of the hydrophobic part is to associate in water and increase the solution viscosity.

Some of the commercially available water-soluble AAm-based polymers for EOR are presented in Table 2-5.[45,72]

Table 2-5: AAm-based polymers for EOR applications [45,72]

Trade name	Polymer type	Characteristics
Aspiro^{TM} P 4201 (producer: BASF)	AAm/AAc copolymer	Cost efficient polymers for mild reservoir conditions
Aspiro^{TM} P 5411 X (producer: BASF)	Sulfonated polyacrylamide	For harsh reservoir conditions (temperature up to 95 ^{o}C)
Aspiro^{TM} P 6631 (producer: BASF)	Associated thickening polyacrylamide	For extreme salinity and hardness in reservoirs
Flopaam 3630S (producer: SNF)	AAm/AAc copolymer	For reservoirs with T< 80 ^{o}C and medium hardness
Flopaam AN125SH (producer: SNF)	Sulfonated polyacrylamide	For reservoirs with T< 95 ^{o}C and all salinities
Superpusher C319 (producer: SNF)	Associated polyacrylamide	High resistance factor un reservoir and medium hardness

To visualize the effect of polymer flooding, we can consider Figure 2-17. This figure shows the advantage of polymer flooding in a 2-layer porous media system, where the top layer has 11.2 times higher permeability compared to the bottom layer.[73] The polymer used in polymer flooding is xanthan which is a natural polymer (qualitatively it is expected that AAm/AAc

copolymers would behave similarly). The figure outlines the position of the polymer front in two layers at 5 different conditions. As can be seen from the figure, by increasing the polymer solution concentration (from 0 to 2000 ppm) and polymer solution viscosity (from 1 to 75 cp) the water displacement and sweep efficiency in the less-permeable layer increase noticeably.

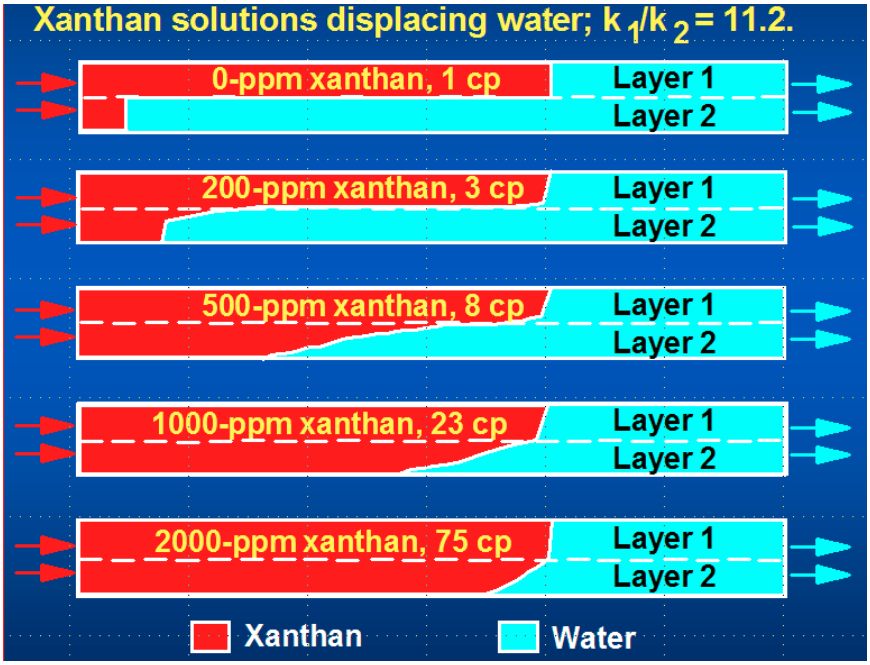

Figure 2-17: Polymer flooding in a 2-layer system [73]

In order to evaluate polymer solution performance in oil reservoirs, sand-pack flooding tests can be conducted that provide valuable information about the polymer solution behavior in porous media and the efficiency of oil recovery. These tests quantify two measures of the

solution flow performance, i.e., the resistance factor (RF) and the residual resistance factor (RRF), both useful indicators of the polymer flooding operation.

The resistance factor, RF, provides information about the effective viscosity or mobility control capability of the polymer solution in porous media relative to water. Hence, the higher the RF, the better the result of the polymer flooding operation will be.

The residual resistance factor, RRF, gives information about permeability reduction induced by polymer because of polymer adsorption onto solid surfaces (mostly physical adsorption as compared to chemisorption) or mechanical retention (because of the large size of the macromolecules). Polymer retention results in permeability reduction of the porous media, polymer propagation retardation, and potential injectivity issues in oil reservoirs. Hence, the lower the RRF, the better the polymer solution performance will be in EOR applications. It has been mentioned in the literature that the efficiency of oil recovery per gram of injected polymer is inversely related to the polymer retention.[48] Polymer retention is also related directly to the molecular weight of the polymer, the clay content of the reservoir, and the cationic charge of the polymer's pendant group.

Figure 2-18 shows a comparison of determined RF and RRF values (and, hence, trade-offs) among three types of polymers used in polymer flooding: xanthan gum, hydrolyzed polyacrylamide (HPAM), and hydrophobically modified acrylamide-based copolymer (HMSPAM).[74] RF results clearly suggest that HMSPAM has higher effective viscosity compared to HPAM and xanthan gum. This might be due to the viscoelastic properties and the high elasticity of this polymer (such details will be discussed more in this section and also

in Chapter 7). On the other hand, HMSPAM showed significantly higher RRF compared to the other polymer solutions, which is an indication of high permeability reduction and this can be an issue in oil field applications (injectivity problems).

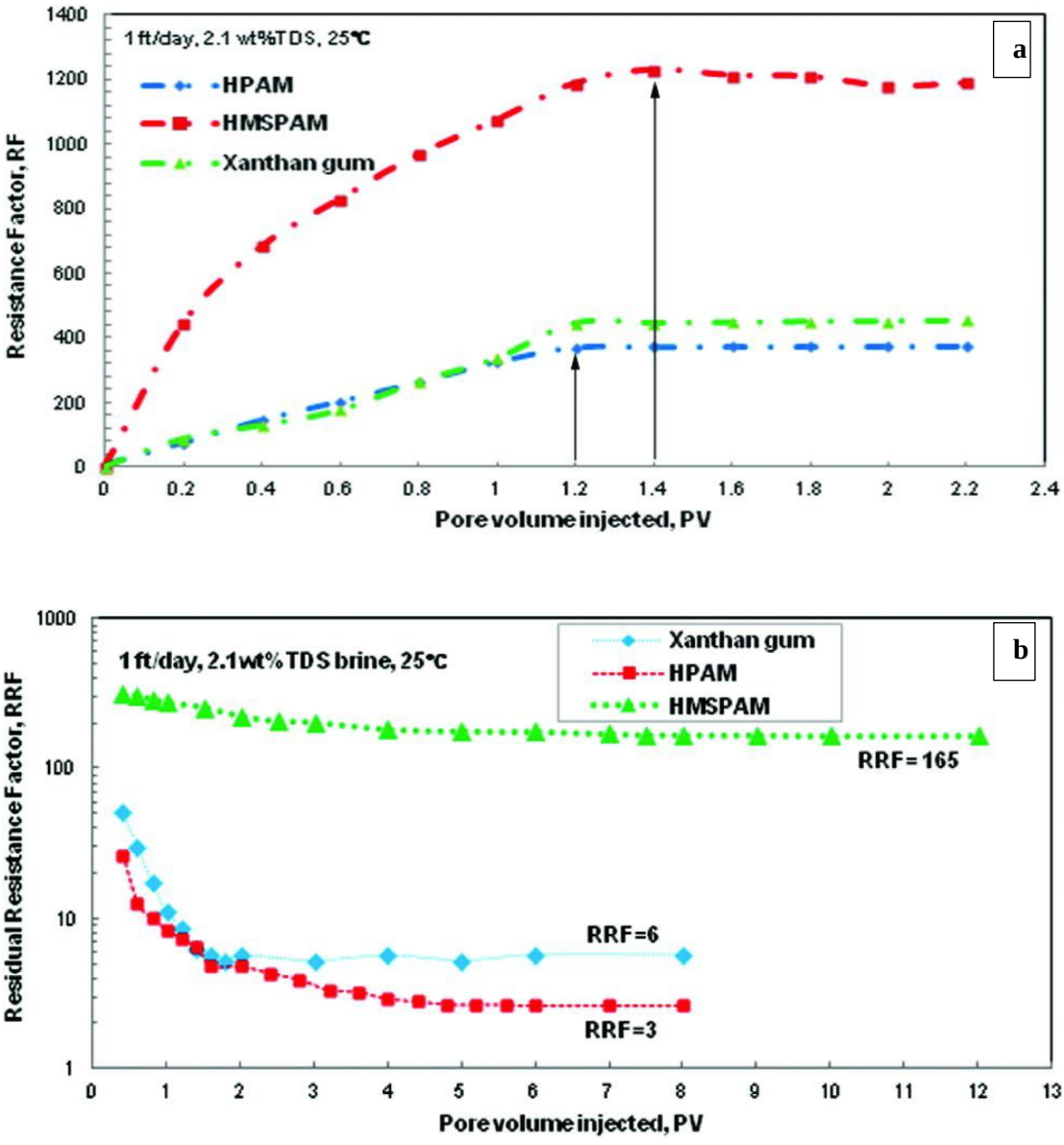

Figure 2-18: Flow behavior of polymer solutions: a) resistance factor (RF); b) residual resistance factor (RRF) versus pore volume of injected polymer solution [74]

The overall oil displacement efficiency in EOR is defined as microscopic and macroscopic displacement efficiency of fluids contacting the oil in the micro- and macro-scale, respectively.[62,63] Microscopic displacement efficiency deals with mobilizing oil at the pore scale, while macroscopic displacement efficiency refers to mobilization of oil in volumetric scale. In general, any macro- or micro-displacement that enhances oil sweep efficiency can improve the efficiency of oil production during polymer flooding. Figure 2-19 shows a schematic of microscopic and macroscopic displacements.

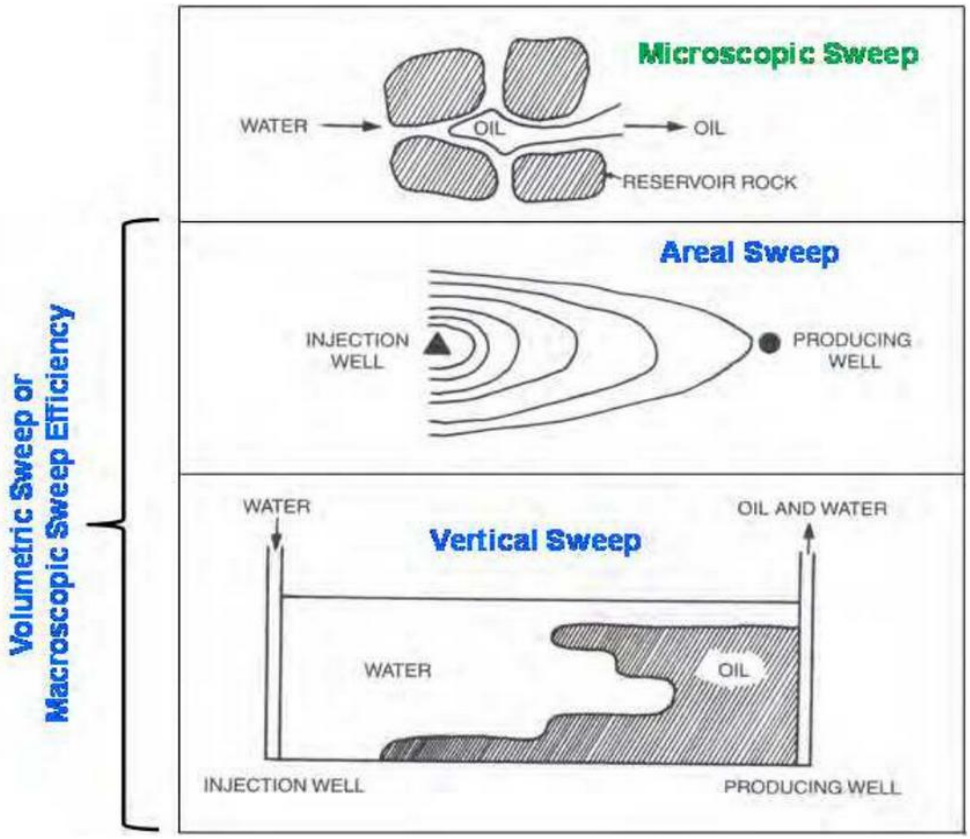

Figure 2-19: Schematic of microscopic and macroscopic displacements [63]

The results of cumulative oil recovery in heavy oil displacement tests for three kinds of polymers, xanthan gum, HPAM, and HMSPAM, are presented in Table 2-6.[75] The second column in Table 2-6 shows the amount of oil recovery as a result of water flooding. The results of water flooding are not economically justifiable, since only one third of oil could be displaced. The third and fourth columns present the amount of further oil recovery as a result of polymer flooding and total oil recovery, respectively. The results showed that xanthan gum had the highest oil recovery compared to the other polymers. The most commonly used polymer in EOR, HPAM, enhanced the oil recovery by 68.3% OOIP in total, which is the lowest compared to xanthan and HMSPAM.

Table 2-6: Oil recovery in heavy oil displacement test [75]

Polymer type	Water flooding oil recovery (% OOIP*)	Polymer flooding oil recovery (% OOIP*)	Total oil recovery (% OOIP*)
HPAM	34.7	33.6	68.3
HMSPAM	34.5	48.8	83.3
Xanthan gum	31.5	51.9	83.4

* OOIP stands for original oil in place

The viscoelastic properties of polymers are extremely important for efficient oil recovery and have been studied in the literature. It has been found that appropriate viscoelastic properties in polymer solutions give them an extra ability to impose a large force on oil droplets in reservoirs and pull them out of the porous media,[62,76,77] while non-polymeric fluids are not capable of pulling out the oil from a pore. This difference in behavior of polymeric and non-

polymeric fluids is shown in Figure 2-20. The figure shows that water and glycerin, both Newtonian fluids, are only capable of pushing the oil ahead but they cannot pull the oil out of the dead end. On the contrary, viscoelastic polymer is capable of both pushing and pulling out the oil at the same time, because of the elasticity properties. In other words, viscoelastic polymers can pull other materials both behind and beside them due to high molecular weight and chain entanglements.[76]

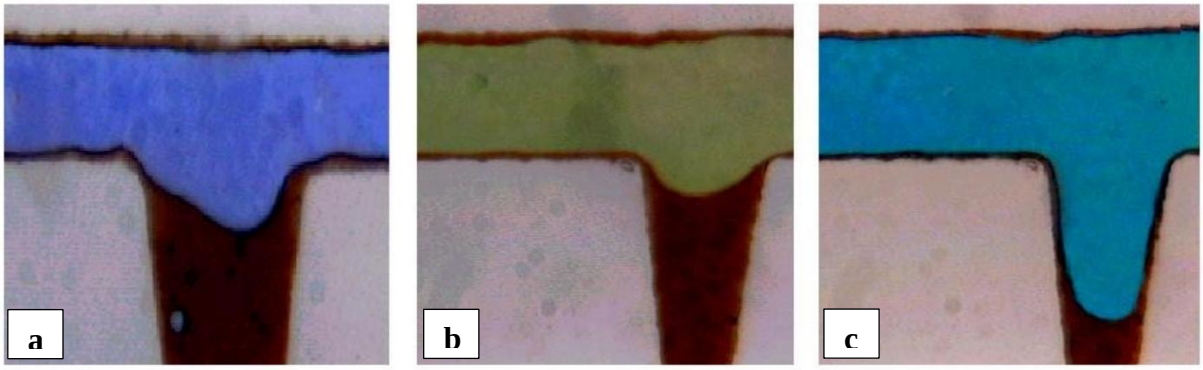

Figure 2-20: Oil displacement from "dead-end" pore flushed by a) water, b) glycerin, c) hydrolyzed polyacrylamide; darker color represents oil [76]

The amount of sweep efficiency is also related to the degree of polymer elasticity.[62] It has been found that viscoelastic polymers with higher elasticity showed higher efficiency in oil displacement. In a research study, the behavior of water and three polymers with different viscoelastic properties for removing the oil from a dead end pore was compared. The values of the storage (elastic) modulus over the loss (viscous) modulus ratio (G'/G") for the three polymer solutions were equal to 0.92, 1.75, and 2.72. The results showed that the polymer

with G'/G" ratio equal to 2.72 performed better in pulling the oil out of the dead end pore in oil reservoir compared to the other polymers due to its higher elasticity. On the other hand, water flooding made almost no change in the displacement of the residual oil in the dead end.

The standard polymer basis for EOR applications is the AAm/AAc copolymer and this copolymer has been in use for many years in polymer flooding. However, there are still many unanswered questions about optimizing the copolymer properties by controlling and exploiting copolymerization kinetics. Therefore, we studied this copolymer in more detail with a wider aim to clarify its behavior in polymer flooding. In general, in order to obtain the highest efficiency of oil recovery under critical reservoir conditions, it is necessary to have high shear viscosity and low polymer retention in permeable media and also improve the chemical (salt and hardness tolerance), mechanical (shear and elongation stresses) and thermal stability of AAm copolymers. In order to improve these factors, one should have a good and clear understanding of the copolymerization kinetics and resulting microstructures of the AAm copolymers (such as chain composition, molecular weight, etc.) to modify the copolymer properties for the target application. Therefore, our target was to study AAm/AAc copolymerization kinetics and establish a framework for structure-property relationships in order to tailor make this copolymer for improved polymer flooding application.

2.7.2 Flocculation

The growing need for pure water has led to research for materials that are able to remove suspended impurities.[2] These impurities are typically organic and inorganic colloids and

other partly soluble substances that can be removed by coagulation processes which purify the water and also decrease or diminish water turbidity. The role of flocculants is to remove suspended solids from a liquid by bringing together particles into larger aggregates and settling them. The operation is based on decreasing repulsive forces between suspended particles. Copolymers of AAm/AAc, for example, are of great interest among water-soluble polymers that are used as flocculants. Table 2-7 lists the characteristics of AAm and AAm copolymers which are used in flocculation applications (flocculation aids).

Table 2-7: Summary of acrylamide polymers for flocculation applications [2]

Chemical family	Trade name	Charge	Molecular weight	Maximum dosage in potable water (mg/L)	Form
Acrylamide homopolymer or copolymer	Magnafloc LT 7922 (BASF)	Low degree of cationic charge	Very high	1	Liquid
Anionic polyacrylamide	SuperFloc A-120 (Cytec industries Inc.)	Low degree of anionic charge	High	1	Powder
Cationic polyacrylamide	Hyperfloc CE 854 (Hychem Inc.)	High degree of cationic charge	Very high	0.5–20	Liquid

Figure 2-21 shows the effectiveness of Hyperfloc CE 854 (cationic polyacrylamide copolymer emulsion) in reducing water turbidity.[2] As seen from the figure, with a small amount of AAm copolymer, the turbidity of water can decrease significantly. Adding more copolymer causes an increase in turbidity, probably due to charge reversal of the particles.

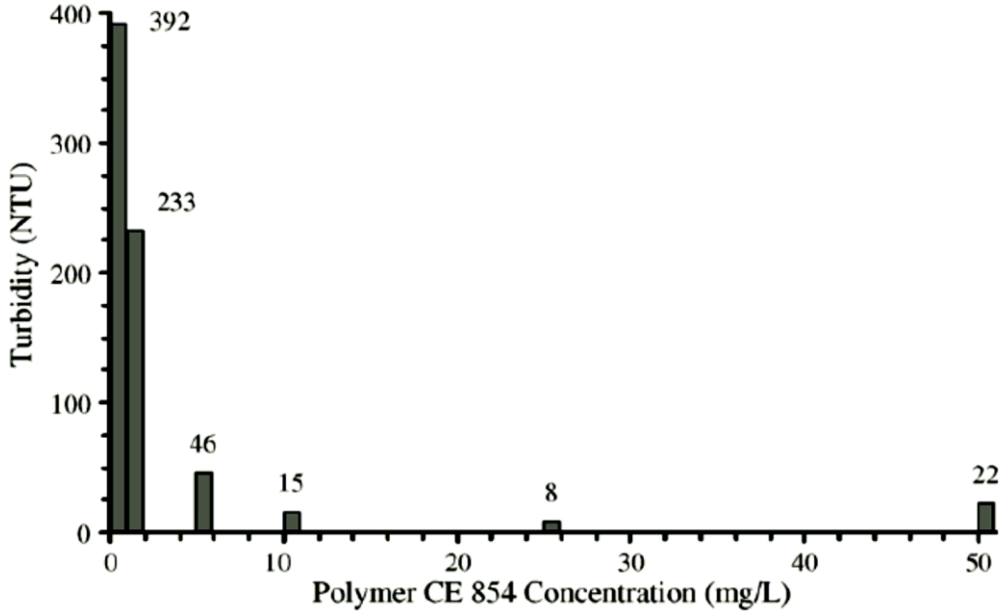

Figure 2-21: Turbidity vs. concentration dosage for AAm copolymer Hyperfloc CE 854 [2]

The flocculation ability of AAm/AAc copolymers was tested only as a side project of this thesis and the results are briefly presented in Appendix A.

Chapter 3. Experimental

3.1 Materials

Monomers (AAm, electrophoresis grade, purity ≥ 99%; AAc, purity 99%), initiator (4,4′-azo-bis-(4-cyano valeric acid)), inhibitor (hydroquinone), and sodium hydroxide were purchased from Sigma-Aldrich, Oakville, Canada.

Sodium nitrate (ACS grade), sodium phosphate (monobasic, monohydrate, HPLC grade), and sodium phosphate (dibasic, heptahydrate, ACS grade) were used to make buffer solutions. All were purchased from EMD Millipore, Etobicoke, Canada.

Water was Millipore quality (18 MΩ.cm) and methanol was ACS grade from VWR, Mississauga, Canada. Sodium chloride was also ACS grade from Merck, Kirkland, Canada. Nitrogen gas acquired from Praxair, Toronto, Canada (4.8 grade) was used for degassing of solutions. Deuterium oxide (D, purity 99.9%) was used for NMR solution preparation and was from Cambridge isotope laboratories, Massachusetts, USA.

Polyethylene oxide GPC standards were used for determining GPC detector constants and were purchased from Polymer Laboratories (Varian), Massachusetts, USA.

3.2 Polymerization

AAc was purified by vacuum distillation at 30 ^{o}C. This was essential since AAc is a reactive monomer that can be dimerized to diacrylic acid during storage.[78] Removal of diacrylic acid from AAc by distillation was confirmed by conducting ^{1}H NMR analysis before and after distillation.

Primary monomer stock solutions with a desired monomer concentration in water were prepared at the selected feed compositions with predetermined monomer molar ratios. Measured amounts of the solutions of AAm/AAc in water were titrated with sodium hydroxide and the pH adjusted to the specific value. Initiator (concentration at 0.004 M) and sodium chloride salt (to control ionic strength of the solution as will be discussed in Chapter 5) were added to the solutions and then the solutions were further diluted with high purity water to give the target total monomer concentrations.

The solution was then purged with nitrogen gas with a gas flow rate of 200 ml/min, while sitting in an ice bath, for about 2 hours. The gas flow rate was controlled with a mass flow controller (CCR Process Products). After degassing, the solution was transferred to 20 ml vials, fitted with crimped rubber seals, using the so-called cannula transfer method. Cannula transfer is an air-free technique for transferring a solution avoiding atmospheric contamination. The schematic of this method is shown in Figure 3-1. The cannula transfer method basically consists of two flasks; the donating flask (the stock solution) and receiving flask (here the polymerization vial). The donating flask is connected to a source of nitrogen. Nitrogen gas pressure pushes the fluid through the double tipped needle into the vial due to

the pressure difference between the two vessels. The flow rate of the solution can be controlled by adjusting the nitrogen pressure. The receiving flask (vial) is connected to an oil filled bubbler, which prevents air return to the vial and also acts as a vent to allow liquid flow and prevent overpressure.

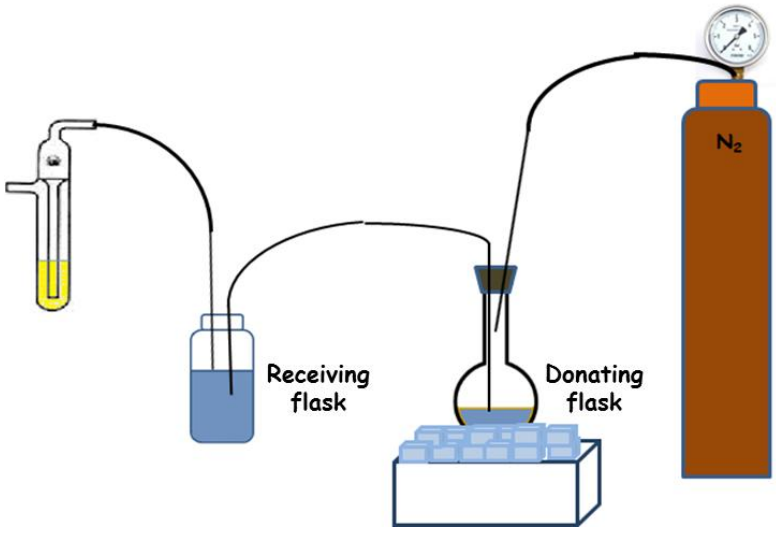

Figure 3-1: Schematic setup of cannula transfer

The vials were subsequently put in a temperature controlled water shaker bath (Grant, OLS200) at 40^{o}C and 100 rpm, and then removed at specific time intervals and chilled in an ice bath. A few drops of inhibitor solution were quickly syringed into the vial to stop any further polymerization. Polymer products were precipitated with a ten-fold excess of methanol to water, gravity filtered (paper filter grade number 41, Whatman), and dried in a vacuum oven at 50 ^{o}C until they reached constant weight.

3.3 Characterization

3.3.1 Monomer conversion

Precipitation and gravimetry were used to determine masses of copolymer products. Fractional monomer conversions were determined as polymer mass over initial monomer mass (Equation 3-1).

$$Conversion = \frac{mass\ of\ isolated\ polymer}{mass\ of\ initial\ monomer} \times 100$$ **Equation 3-1**

For systems containing partially or fully ionized AAc (sodium acrylate NaAc), the mass of NaAc monomer was considered as the reactant mass in conversion calculations. In other words, based on pH levels, various degrees of ionization existed for the AAc monomer (α=0.059, 0.863, and 0.998, for pH=3, 5, 7, respectively). Therefore, at each reaction condition, the mass of monomer was considered as a summation of AAm monomer and the combinations of the acrylate anion plus AAc monomer. A related sample calculation is shown in Appendix B.

It is worth mentioning that since various amounts of sodium hydroxide (to adjust pH) and sodium chloride (to control ionic strength level) were added to the reaction solution, it was important to consider the mass of sodium in the polymer product. The mass of sodium in the product was deduced from the polymer mass based on elemental analysis results. Not doing so would introduce error and bias the results considerably. This is something that is usually neglected in the literature, although it should be routinely considered and discussed. The

reliability of Na mass calculations was independently checked for selected samples using inductively coupled plasma (ICP) analysis (Prodigy Radial ICP-OES by Teledyne-Leeman).

3.3.2 Polymer molecular weight

Copolymer molecular weight was determined by gel permeation chromatography (GPC, PL-GPC 50, Agilent, with two columns, type PL aquagel-OH MIXED-H 8 μm, Agilent). The GPC set-up had refractive index (RI), dual-angle light scattering (LS 45 and 90 degrees) and viscometry detectors. The mobile phase was an aqueous solution of $NaNO_3$ (0.2 M) and NaH_2PO_4/Na_2HPO_4 (0.01 M), with total concentration of 0.01 M at pH=7. Polyethylene oxide standards of narrow molecular weight distribution were used for calibration and for determining the required detector constants. Commercial high molecular weight polyacrylamide (M_p=6.5E6, M_w=9E6, M_n=4.2E6) was also used as a standard to check the reliability of the molecular weights from GPC. The polymer solution concentration for GPC samples was about 0.5 mg/ml and the flow rate was set at 0.5 ml/min.

3.3.3 Copolymer composition

Elemental analysis (CHNS, Vario Micro Cube, Elementar) was used to measure the C, H, and N content of the samples and determine copolymer composition. Since water absorption by the polymer samples affects the H element percentage and, consequently, the other element percentages, the composition of the AAm/AAc copolymer was calculated based on the percentages of the C and N elements only.[79] A typical calculation is given in Appendix C.

The reliability of the copolymer composition calculations was independently checked for selected samples using nuclear magnetic resonance (^{13}C $^{1}\{H\}$NMR). ^{13}C NMR nuclear magnetic resonance was conducted on a Bruker AVANCE 300 NMR spectrometer operating at 75.5 MHz with inverse gated proton decoupling (30 degree pulse) using a pulse delay of 6 s. The NMR was run overnight at 60 ºC (around 6,000 scans). The copolymers were dissolved in a D_2O/buffer mixture to yield roughly a 6 wt% solution concentration (about 0.05 g of polymer in 0.8 ml of D_2O/buffer). The spectra were also used for determining microstructure (triad fractions) of the copolymer, as discussed in Chapter 6.

3.3.4 Copolymer rheology

A stress-controlled cone and plate rheometer (AR2000, TA instruments) was used to measure the shear viscosity of samples at room temperature. Cone and plate (ETC steel) with a 40 mm diameter and 1° angle were used for all shear viscosity tests.

A parallel plate rheometer (Bohlin Gemini HR Nano 150, Malvern Instruments Ltd., UK) was used for frequency sweep measurements at room temperature. The diameter of the plates was 60 mm and the gap between the plates was fixed at 1 mm.

3.4 EOR application

3.4.1 Polymer flooding tests

Polymer flooding tests at simulated reservoir conditions were conducted in order to evaluate the performance of AAm/AAc copolymers in EOR applications. A schematic of the polymer flooding set-up is shown in Figure 3-2.

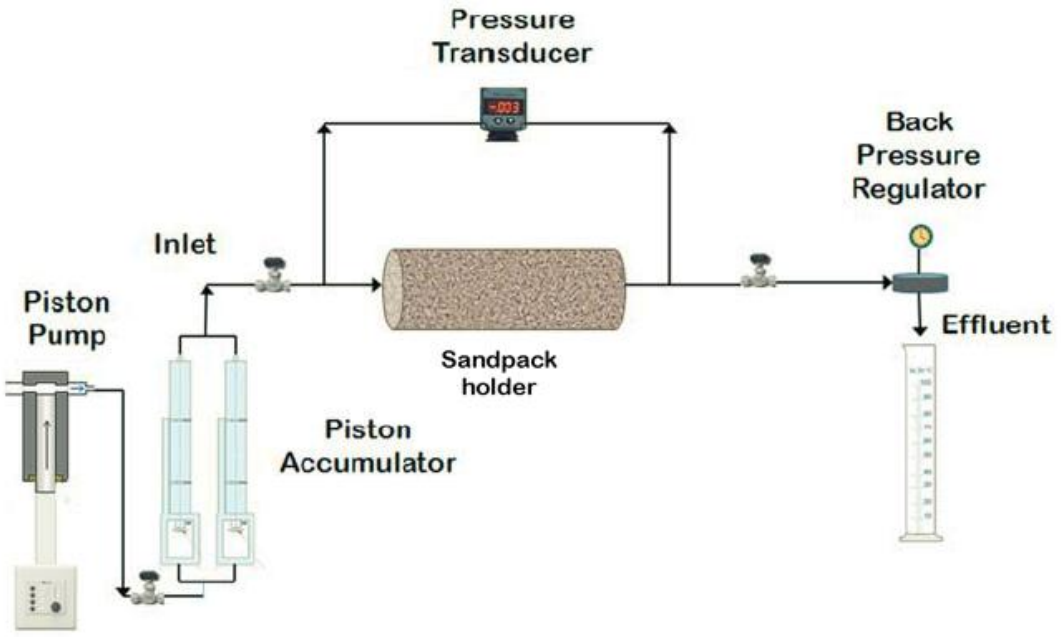

Figure 3-2: Sand-pack flood test set-up [80]

The heart of the set-up was the sand-pack with 46.1 cm length. The sand-pack was composed of sandstone with mineral composition of 74.3% quartz, 17.8% muscovite, and 7.9% sylvite. The sandstone had an average size ranging from 75 to 800 μm. The particle size distribution

for sandstone is shown in Figure 3-3. It can be seen that most of the sandstone had a size around 250 μm.

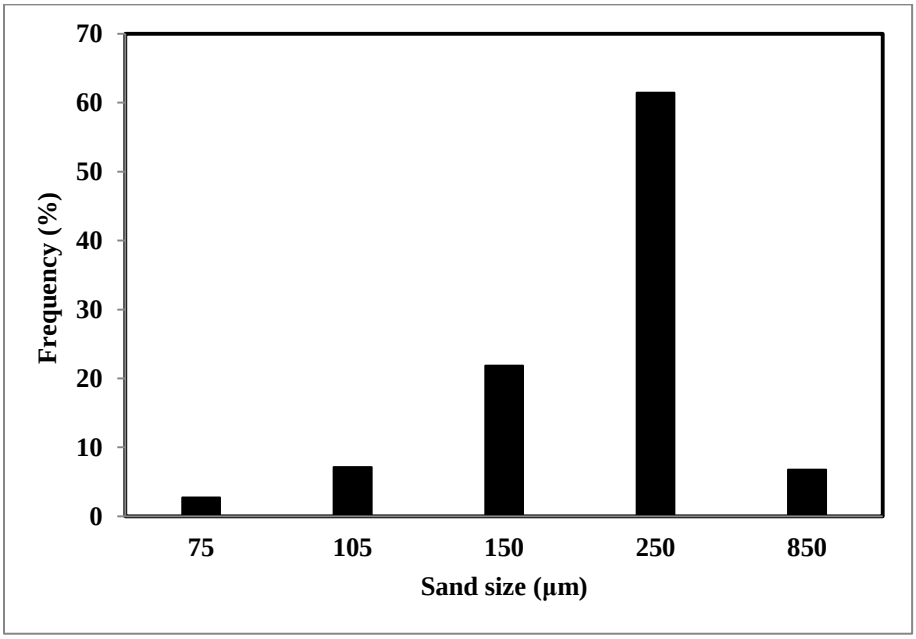

Figure 3-3: Particle size distribution of the sandstone in sand-pack tests

There were four pressure gauges along the sand-pack and two more before and after the sand-pack in order to monitor the pressure drop during the flooding test. The locations of the pressure gauges in the sand-pack are given in Table 3-1.

Table 3-1: Pressure gauges along the sand-pack

Pressure gauges	P1	P2	P3	P4	P5	P6
Length across the sand-pack (cm)	0	8	23	30.5	38.5	47

The pump injected the solutions at a specific flow rate to simulate an average linear velocity of 1 ft/day in real conditions at oil fields far from the injection port. The linear velocity of 1 ft/day can be translated to the volumetric flow rate of 0.259 cm^3/min using the sand-pack cross sectional area. The flow rate of effluent (output fluid) was also measured in order to compare with the adjusted inlet flow rate of the system. A considerable difference between inlet and outlet flow rates can be a sign of sand-pack clogging. Overburden pressure is a constant pressure that is applied on the sand-pack sleeve to simulate and mimic the pressure in oil reservoirs. The sand-pack characteristics are given in Table 3-2.

Table 3-2: Sand-pack characteristics

Property	Value
Length	46.1 cm
Diameter	3.95 cm
Cross sectional area	12.25 cm^2
Pump flow rate	0.26 ml/min
Overburden pressure	100-120 psi

The procedure for a typical polymer flooding test is as follows:

1. Sand-pack was packed with sandstone, pressurized with distilled water, and sealed. Then, vacuum was applied to the system in order to remove air and water.
2. Brine was introduced into the vacuumed sand-pack until the sand-pack was fully saturated. The volume of the brine that was taken by the vacuumed sand-pack is equivalent to the *pore volume* of the system. Then, the permeability of the sand-pack to

brine was experimentally determined by using Darcy's law. After permeability determination, the sand-pack was ready for polymer injection.

3. Polymer solution was injected into the sand-pack at constant flow rate until ΔP showed a constant value. Injection time, flow rate, and pressure readings were recorded.
4. Brine was injected again after the polymer flooding until ΔP across the sand-pack reached a constant value. Injection time, flow rate, and pressure readings were recorded.
5. The sand-pack was cleaned by injecting bleach solution (domestic household grade) in order to remove the polymer solution residue from the system. This process continued till the original permeability of the sand-pack was achieved.
6. At the end, distilled water and more brine were injected in order to wash out the bleach solution from the sand-pack, which was confirmed by constantly monitoring the pH of the produced brine.

The porosity of the sand-pack can be measured by dividing the pore volume (unoccupied volume in a porous media) to sand-pack volume (sleeve volume). The polymer solution concentration was fixed at 1 wt %. So, in all the tests 5 g of polymer was dissolved in 500 ml of synthetic brine. It is crucial to grind the polymer into fine powder before dissolving it in the brine and also add the powder gradually, since the viscosities of polymer solutions are very high (otherwise, homogeneous polymer solutions cannot be obtained). The synthetic brine that was used in the test had the composition based on real conditions in oil reservoirs in Alberta (Canada), according to Table 3-3. The brine pH was measured as 6.

The reference polymer that was used as baseline for the evaluation of the EOR application tests was Alcoflood 955, purchased from BASF, USA. This polymer was a AAm-based copolymer with high molecular weight and low anionicity under the category of water control polymers, which can form flowing gels with high viscosity in reservoirs.

Table 3-3: Composition of synthetic brine

Salt	**wt %**
NaCl	1.72
$MgCl_2$	0.09
$CaCl_2$	0.32
Na_2SO_4	0.01
Total dissolved solids	**2.14**

3.4.2 Heavy oil displacement tests

Heavy oil displacement tests were carried out using the same sand-pack set-up shown in Figure 3-2 and at reservoir conditions similar to the real conditions. The only difference in the sand-pack set-up was the overburden pressure which was set at 500 psi. The procedure for a typical heavy oil displacement test is as follows:

1. Sand-pack preparation (same as step 1 in polymer flooding test, Section 3.4.1).
2. Brine injection and pore volume, permeability, and porosity determination (same as step 2 in polymer flooding test, Section 3.4.1).

3. Heavy oil was injected into the sand-pack at constant flow rate (at a linear velocity of 1ft/day, same as for polymer flooding test) until no more brine was produced. Injection time, flow rate, pressure readings, volume of brine produced, and volume of oil produced were recorded. At the end of this stage, the oil and brine saturation in the sand-pack was calculated (oil and brine saturation calculations will be discussed in Chapter 7).
4. Brine was injected into the sand-pack at constant flow rate (at a linear velocity of 1 ft/day). The injection of brine continued until no more oil was produced. Injection time, flow rate, pressure readings, volume of brine produced, and volume of oil produced were recorded. At the end of this stage, the oil and brine saturation in the sand-pack was calculated.
5. One pore volume of polymer solution (1 wt% concentration) was injected into the sand-pack at constant flow rate (at a linear velocity of 1 ft/day). Injection time, flow rate, pressure readings, volume of brine produced, and volume of oil produced were recorded. At the end of this stage, the oil and brine saturation in the sand-pack was calculated.
6. Additional brine (around 3 PV) was injected into the sand-pack at constant flow rate. Injection time, flow rate, pressure readings, volume of brine produced, and volume of oil produced were recorded. At the end of this stage, the oil and brine saturation in the sand-pack was calculated.
7. Finally, oil recovery after each stage was calculated.

In order to measure the volume of oil and brine produced, the output fluid was collected from the sand-pack in a graduated cylinder and then was sealed and placed in a warm bath at a

temperature between 60-70 ºC for a few days in order to let phase separation between oil and brine happen. Then, the volume of each phase was recorded.

The viscosity of heavy crude oil used for the heavy oil displacement tests was 3 Pa.s at 25°C. The oil was provided by Husky Energy, Canada. The oil was diluted with 5 vol% condensate (provided by Corridor Resources Inc., Canada).

Chapter 4. Copolymerization Kinetics, Step 1: Comonomer Reactivity Ratios

4.1 Introduction

The purpose of this chapter is to clarify the estimation of reactivity ratios for the AAm/AAc copolymerization, since there are many inconsistencies with respect to its reported reactivity ratios (Table 2-1). To do so, one should start with the collection of reliable kinetic data containing independent replication, which is sorely missing in the previous literature studies. For the initial study, all polymerization runs were conducted at the same experimental conditions (i.e., pH, total monomer concentration, initiator type and concentration, temperature) and the only variable was feed composition. The pH of 7 was chosen in order to make sure that there were only ionized AAc (rather than partially ionized AAc) and AAm (rather than protonated AAm) in the system. The total monomer concentration was also moved to higher values compared to existing literature. The reason for increasing total monomer concentration was to have more relevance for actual production scales. The ionic strength was variable but known between runs (it depended on the fraction of AAc in solution), since we wanted to compare the reactivity ratios of the system with literature studies where the ionic strength was indeed varying. Then, independent replication confirmed the reliability of the estimated reactivity ratios. By having reliable reactivity ratios, one can gain equally reliable information about significant kinetic factors of the

copolymerization, which control microstructure chain properties, such as copolymer composition, sequence length and other related properties (to be addressed in later chapters). This will lead to better engineering protocols for controlling macrostructure and subsequent bulk properties of the copolymer.

4.2 Reactivity ratio estimation methodology

Our approach for estimating reactivity ratios is based on the error-in-variables-model (EVM) algorithm, proposed originally by Reilly et al.[25] This algorithm was specifically applied on the problem of estimating reactivity ratios for copolymerization systems by Dube et al.[26] and Polic et al.[27] and the latest methodology for using this algorithm and several key factors for its numerical implementation are highlighted in Kazemi et al.[81] The EVM methodology is a sequential and iterative procedure, which combines three main stages, briefly described in the sections that follow.

4.2.1 Parameter estimation

Essentially, the EVM method treats all the measurements ($\underline{x}_i$) as if they are coming from an unknown true value ($\underline{\xi}_i$) with a multiplicative error term ($\underline{\varepsilon}_i$). This relation is given by Equation 4-1, where $\underline{x}_i$ can represent any one of the measurements, such as initial feed composition (f_0), conversion (X_n), or cumulative copolymer composition ($\bar{F}$).

$$\underline{x_i} = \underline{\xi_i}\left(1 + \underline{\varepsilon_i}\right) \; where \; i = 1, 2, \ldots, n$$ **Equation 4-1**

The error vector is assumed to be normally distributed with mean of zero, and a non-singular variance-covariance matrix of $\underline{V}$, which may be known or unknown.[82] The relation between the true values of the variables and the estimated parameters is presented in general by a model that is given by Equation 4-2, where $\underline{\theta}^*$ is the vector of the true (yet unknown) parameter values to be estimated. The model that is used in our EVM procedure is the cumulative copolymer composition equation, which is explained in Section 4.2.3.

$$\underline{g}\left(\underline{\xi_i}, \underline{\theta^*}\right) = 0 \;\; where \; i = 1, 2, \ldots, n$$ **Equation 4-2**

The objective function for minimization in order to find the point estimates, $\underline{\hat{\theta}}$, is given by Equation 4-3, where r_i is the number of replicates at the i^{th} trial, $\underline{\bar{x}}_i$ is the average of the r_i measurements $\underline{x}_i$, and $\underline{\hat{\xi}}_i$ denotes estimates of the true values of the variables $\underline{\xi}_i$. The target parameters, in our case two reactivity ratios, can be found by implementing a Newton-type optimization algorithm, as explained in detail in Kazemi et al.[81]

$$\phi = \frac{1}{2}\sum_{i=1}^{n} r_i \left(\underline{\bar{x}_i} - \underline{\hat{\xi}_i}\right)' \underline{V}^{-1} \left(\underline{\bar{x}_i} - \underline{\hat{\xi}_i}\right)$$ **Equation 4-3**

4.2.2 Design of optimal experiments

Utilizing optimally designed experiments can improve the precision of parameter estimates. It is therefore desirable to add a design of experiments step to the reactivity ratio estimation routine in order to find highly precise parameter estimates. Since there are two reactivity ratios for estimation, there are two optimal feed compositions that should be determined, which are used for the optimal experimental trials. These optimal trials will hopefully maximize the information for the reactivity ratio estimation.

Design of experiments in the EVM context is implemented by maximizing the determinant of the information matrix (which is the approach used in D-optimal design for nonlinear regression analysis), as shown in Equation 4-4.[83] The constraints for this problem are the function (model) itself as well as lower and upper bounds of the experimentally feasible region, L and U, respectively.

$$Max_{\underline{\xi}} \left| \sum_{i=1}^{n} \underline{Z}_i' \left(\underline{B}_i \underline{V} \underline{B}_i' \right)^{-1} \underline{Z}_i \right| \qquad \textbf{Equation 4-4}$$

$$\text{subject to } \begin{cases} \underline{g}(\underline{\xi}_i, \underline{\theta}) = 0 \\ L \leq \underline{\xi}_i \leq U \end{cases}$$

$\underline{Z}_i$ is the vector of partial derivatives of the (model) function, $\underline{g}(\underline{\xi}_i, \underline{\theta})$, with respect to the parameters, and $\underline{B}_i$ is the vector of partial derivatives of the function, $\underline{g}(\underline{\xi}_i, \underline{\theta})$, with respect to the variables, given by Equation 4-5 and 4-6, respectively:

$$\underline{Z_i} = \left[\frac{\partial g(\underline{\xi_i}, \underline{\theta})}{\partial \theta_m}\right] m^{th} element$$ **Equation 4-5**

$$\underline{B_i} = \left[\frac{\partial g\left(\underline{\xi_i}, \underline{\theta}\right)}{\partial\left(\underline{\xi_i}\right)}\right]$$ **Equation 4-6**

4.2.3 Full conversion experimentation

As mentioned earlier, since the development of the Mayo-Lewis (ML) model (Equation 2-3), monomer reactivity ratios have been generally determined at low conversion levels using the instantaneous model, owing to the assumption that the composition drift in the monomer feed and copolymer composition is negligible at low conversion levels. However, many copolymerizations will inevitably show composition drift as the degree of conversion increases, and thus, the measured copolymer composition, which is in actual fact the cumulative composition, cannot be assumed to be the same as the instantaneous composition. In order to avoid the related error propagation problems, we have employed a direct numerical integration (DNI) approach, which is based on cumulative copolymer composition models and can be applied over the whole conversion trajectory.[29] The basis of the numerical integration is the model that relates cumulative copolymer composition ($\overline{F_1}$) to the mole fraction of unreacted monomer (f_1) in the polymerizing mixture and molar conversion, X_n, as shown in Equation 4-7:

$$\overline{F_1} = \frac{f_{10} - f_1(1 - X_n)}{X_n}$$ **Equation 4-7**

As the polymerization proceeds with time, X_n changes, and f_1, the mole fraction of unreacted monomer in the polymerizing mixture, is evaluated by the differential copolymer composition equation, given by Equation 4-8, where the value of F_1 is given by the Mayo-Lewis equation:

$$\frac{df_1}{dX_n} = \frac{f_1 - F_1}{1 - X_n} \qquad \textbf{Equation 4-8}$$

Using the DNI approach allows experiments to be run up to high conversion and captures the complete process information for estimating reactivity ratios. Based on the two optimal feed compositions (a result from the design of experiments, Section 4.2.2), experimental data on copolymer composition should be collected at different conversion levels such as 5%, 10%, …, 60%, and 70% (higher conversion, if possible). All these data points, in terms of their initial feed compositions, conversion values, and the corresponding cumulative copolymer compositions are analyzed with the DNI approach. The reactivity ratio (point) estimates are commonly reported along with their corresponding joint confidence region (JCR) that reflects their level of uncertainty.[29]

4.3 Results and discussion

To start the reactivity ratio estimation from scratch, and in order to be able to compare with the new optimal design of experiments via EVM, the Tidwell-Mortimer criterion[84] was employed for the initial design of experiments, as shown in Equation 4-9.

$$(f_1')_0 \cong \frac{r_2}{2+r_2} \qquad \textbf{Equation 4-9}$$

$$(f_1'')_0 \cong \frac{2}{2+r_1}$$

In Equation 4-9, $(f_1')_0$ and $(f_1'')_0$ represent initial feed mole fractions for monomer 1 (AAm), at which to run the initial copolymerization experiments that will yield the experimental data for subsequent parameter estimation. Initial guesses for r_1 and r_2 are needed for Equation 4-9, and these were obtained from Rintoul and Wandrey[17] for a similar pH, as r_1(AAm)=2.5 and r_2(AAc)=0.39. The Rintoul and Wandrey[17] values for the reactivity ratios of AAm/AAc (M_1/M_2) are considered the best estimates currently available in the literature. Using Equation 4-9, the calculated mole fractions (based on Tidwell-Mortimer[84]) for the initial experimental feeds were f_{0AAm}=0.16 and 0.44. A third feed was added to the design at f_{0AAm} = 0.7, to enable obtaining supporting copolymer composition data at higher AAm levels (despite the fact that having the third feed is not necessary for reactivity ratio estimation).

The full conversion-time trajectories for AAm/AAc copolymerization at three feed compositions are shown in Figure 4-1.

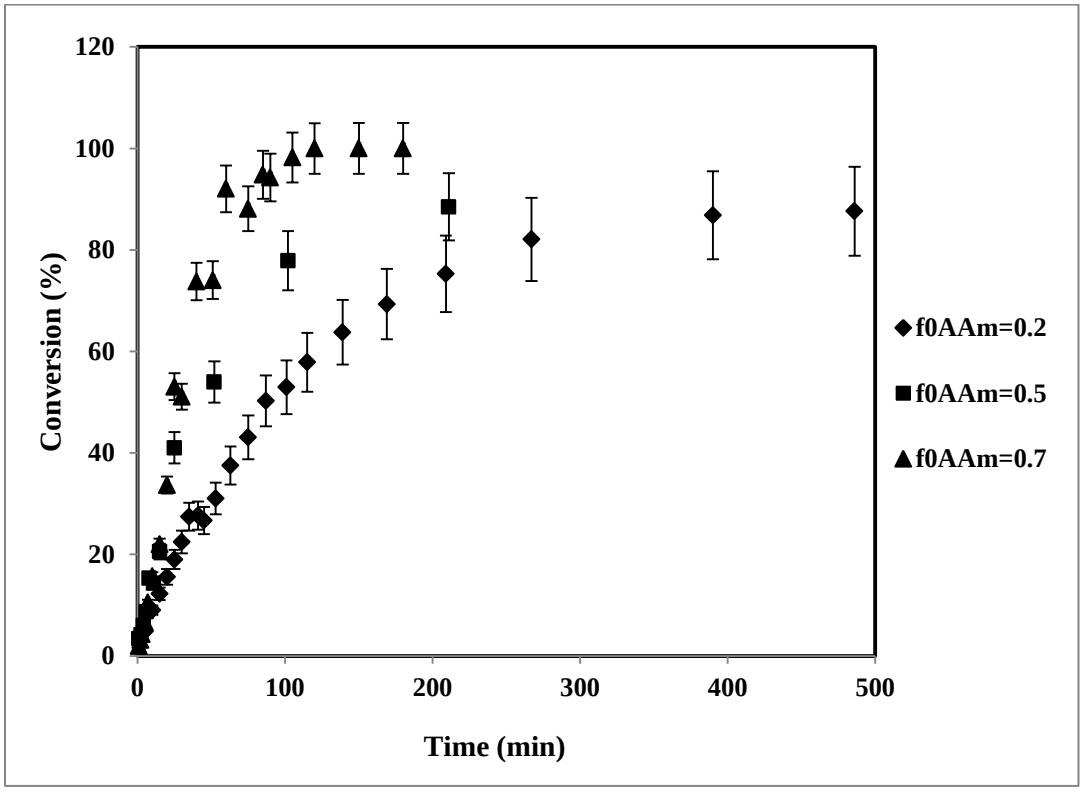

Figure 4-1: Conversion vs. time (with independent replicates) for AAm/AAc polymerization at three feed compositions

The error bars represent the standard deviation among three independent replications conducted at each feed composition. As the level of AAm in the feed increases, there is an increase in the polymerization rate (the opposite, of course, with respect to AAc). As the proportion of AAc increases (considering that the AAc is fully ionized at this pH), the electrostatic repulsions between ionized AAc monomers and anionically charged radicals become significant. This reduces the AAc homo-propagation rate and, overall, the total polymerization rate. This general trend is in agreement with recent results from Paril et al.[11] collected under variable but low ionic strength levels.

In order to demonstrate our points better, we followed a multi-step sequential process to determine reactivity ratios which will be explained in the following subsections.

4.3.1 Preliminary reactivity ratio estimation

In the first step, low conversion data and the ML model were used for parameter estimation. The data set used (cumulative copolymer composition determined by elemental analysis and the corresponding conversion at three feed compositions) is presented in Table 4-1.

The reliability of elemental analysis results was randomly checked with a ^{13}C NMR test. A typical ^{13}C NMR spectrum of the AAm/AAc copolymer is shown in Figure 4-2. Resolution enhancement was applied for the peaks and is shown in the middle of the Figure 4-2. The three distinct sets of signals from the different carbon atoms can be distinguished in ^{13}C NMR based on their polarity. The chemical shifts of the carbonyl resonances corresponding to AAc and AAm are 182.98 ppm and 180.18 ppm, respectively. For the methine carbon region, AAc (45.37 ppm) can be distinguished from AAm (42.86 ppm). The overlap of methylene peaks from AAm and AAc makes copolymer composition determination difficult with these signals. Based on the areas under the carbonyl resonance peaks, the cumulative copolymer composition of AAm was determined to be equal to 0.69. This is in good agreement with the elemental analysis result (cumulative copolymer composition of 0.66) for the copolymerization at $f_{0AAm} = 0.5$ and a conversion level of 9.89% (see Table 4-1).

Table 4-1: Low conversion cumulative copolymer composition data at three feed compositions

f_{0AAm}=0.2	
Conversion (wt%)	**Cum F_{AAm}**
0.71	0.43
1.82	0.41
2.05	0.40
2.17	0.41
3.66	0.44
3.82	0.40
4.11	0.39
4.89	0.39
5.26	0.41
6.10	0.41
f_{0AAm}=0.5	
Conversion (wt%)	**Cum F_{AAm}**
0.73	0.74
0.75	0.75
1.94	0.68
2.58	0.66
2.42	0.67
6.96	0.68
7.74	0.67
6.96	0.63
9.85	0.62
9.89	0.66
f_{0AAm}=0.7	
Conversion (wt%)	**Cum F_{AAm}**
1.05	0.75
1.49	0.79
1.88	0.77
1.88	0.80
2.89	0.73
3.99	0.81
5.64	0.74
6.04	0.78
6.10	0.74
9.11	0.77

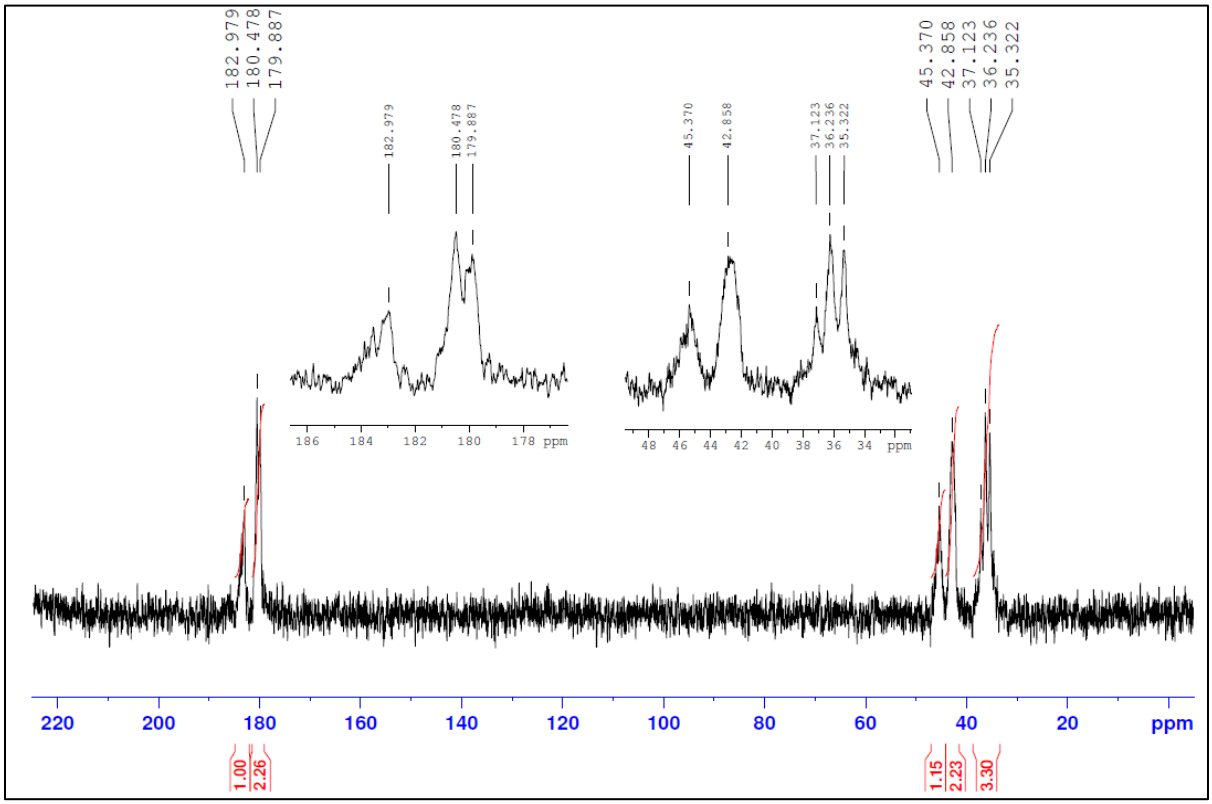

Figure 4-2: ^{13}C NMR spectrum for AAm/AAc copolymer; f_{0AAm}=0.5; polymer concentration in D_2O/buffer =7.4 wt%, T=60 ^{o}C.

Due to poor signal to noise ratio, well-distinct peaks could not be obtained for all samples used for NMR testing. It was found that preparing concentrated and, at the same time, homogeneous and bubble-free samples, was extremely difficult due to the high viscosity of the solution (because of the high molecular weight of the polymers). Therefore, despite typical efforts to try and improve resolution (i.e., higher number of scans, longer time, and higher temperature), only selected samples gave usable spectra for quantitative analysis.

^{1}H NMR is not particularly useful for AAc/AAm copolymer composition analysis as there are no protons that give unique diagnostic signals for either monomer. Figure 4-3 shows the ^{1}H NMR spectrum for a sample AAm/AAc copolymer. As can be seen from Figure 4-3, the signals in the range of 1-2.5 ppm from methylene and methine protons cannot be separated based on the monomer type. The other peaks from NH_2 show low intensity and so integrals are not reliable for fixing the amide level.

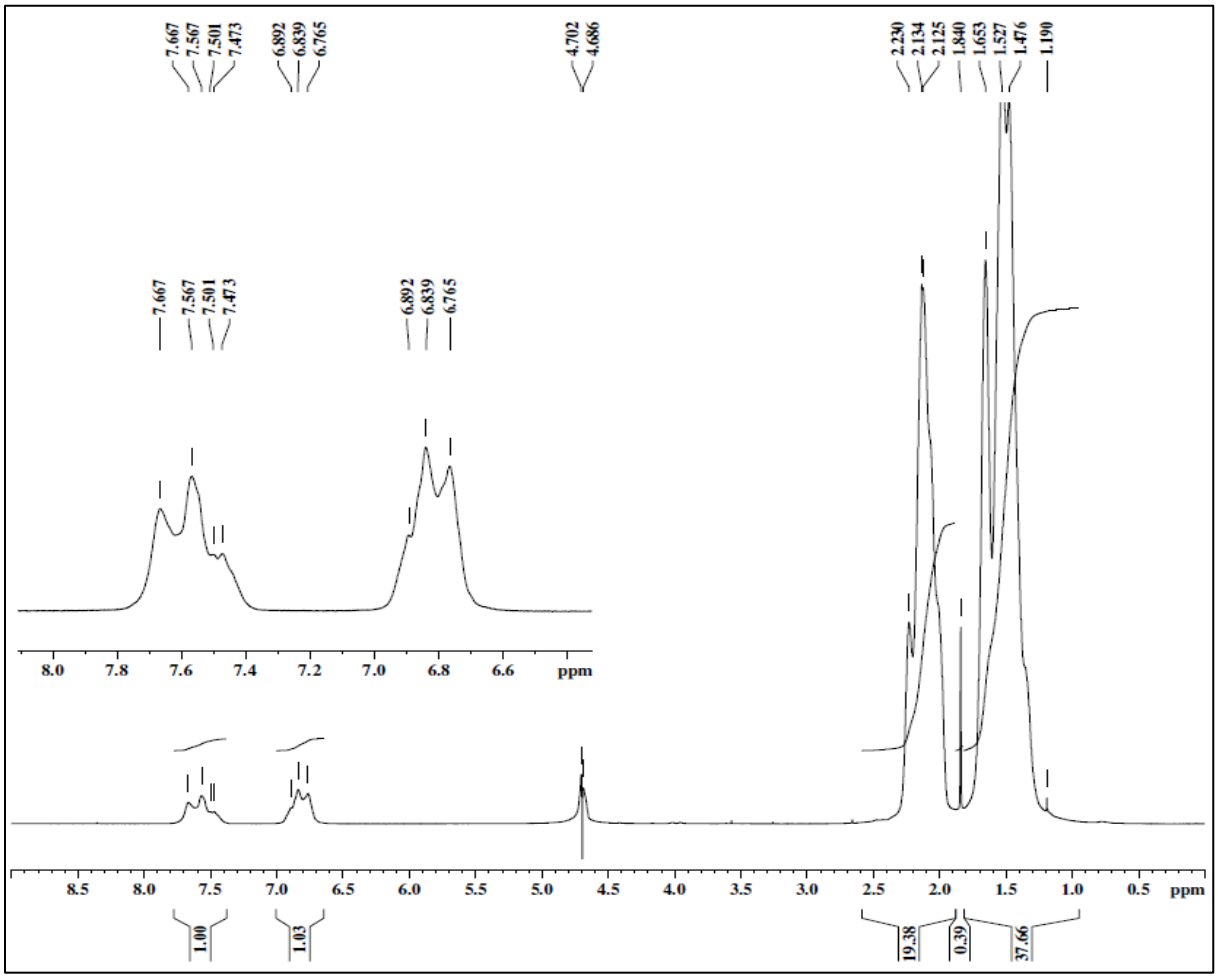

Figure 4-3: ^{1}H NMR spectrum for AAm/AAc copolymer; f_{0AAm}=0.5; polymer concentration in D_2O/buffer =6.8 wt%, room temperature

Figure 4-4 shows point estimates (parameter estimates) along with 95% joint confidence regions (JCR) corresponding to several estimation cases. A JCR is a measure of the uncertainty surrounding the corresponding point estimates. A smaller (area) JCR shows a smaller variance (variability) and, hence, more reliable point estimates (since a smaller variance corresponds to more informative data).

Using EVM (as explained in Section 4.2.1), but applied to low conversion data with the ML model, one obtains the picture depicted in Figure 4-4 by the dashed curve as "preliminary ML". For the next estimation case, the DNI procedure was applied to the low conversion data (with ML) of Table 4-1. In Figure 4-4, this resulted in the dotted line designated as "preliminary DNI". The two JCRs for "preliminary ML" and "preliminary DNI" are relatively similar. In addition, the values of the corresponding point estimates (▲ for "preliminary ML" vs. ■ for "preliminary DNI") are about the same.

For the third and fourth estimation cases, the low conversion data of Table 4-1 were independently replicated three times and subsequently used for parameter estimation, depicted now by the JCR curves of Figure 4-4 as "replicated preliminary ML" and "replicated preliminary DNI".

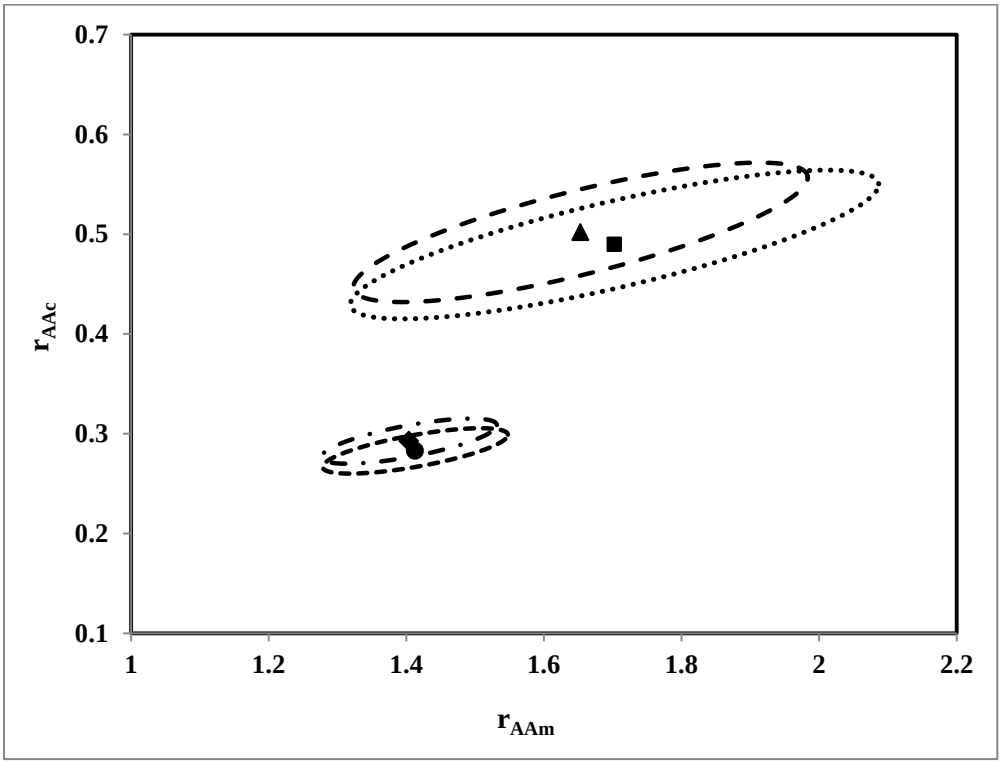

Figure 4-4: JCRs for the ML & DNI models for AAm/AAc copolymerization at low conversion. (- - - , ▲)"preliminary ML"; (…, ■) "preliminary DNI"; (- . - . - , ♦) "replicated preliminary ML"; and (--- ,●) "replicated preliminary DNI"

Several remarks can now be made on the patterns observed in Figure 4-4:

1. There are no large differences within the estimation cases "preliminary" (i.e., no replicates) and "replicated preliminary" with respect to ML and DNI models. This is "as expected", since both the ML and DNI models (note: both under the EVM context) are handling data sets with the same information content. Since the conversion levels are low, the DNI procedure does not see any significant benefits over the ML approach.

2. Both replicated cases exhibit much smaller JCRs (hence, smaller variance). This is again "as expected" and shows the tremendous benefits of independent replication (alas, only after replications are conducted).
3. Because of the smaller JCRs for "replicated" versus "preliminary", the corresponding point estimates are much more reliable (i.e., more reliable parameter estimates).
4. The reactivity ratio estimates have shifted from "preliminary" values of about r_{AAm}=1.68 and r_{AAc}=0.49, to the "replicated preliminary" values of about r_{AAm}=1.41 and r_{AAc}=0.29. In both cases, the estimated reactivity ratios indicate that the AAm radical is more reactive towards the AAm monomer than the AAc monomer (faster homo-propagation compared to cross-propagation) and, therefore, r_{AAm} is greater than 1. On the other hand, r_{AAc} is less than 1, which indicates the lower reactivity of the AAc radical towards itself compared to AAm (slower homo-propagation compared to cross-propagation). The general observation that r_{AAm} is greater than 1 and r_{AAc} is less than 1 at pH around 7 is in agreement with other reported reactivity ratios in the copolymerization literature, however, the values of Figure 4-4 are significantly different from the values cited in Table 2-1.

4.3.2 Optimal design of experiments and full conversion experimentation

In step 2 of the estimation procedure, the previously estimated reactivity ratios were used from the "replicated preliminary DNI" procedure (from step 1 in Section 4.3.1). These values were r_{AAm}=1.41 and r_{AAc}=0.28. Based on these values and using the equations of Section 4.2.2, we conducted model-based optimal design of experiments using an optimal EVM

design criterion[83], which has been found to be superior to the usual Tidwell-Mortimer D-optimal design.[84] (Of course, in most cases in the literature, no design whatsoever is used, with arbitrary chosen feed mole fractions leading to biased results; for more details, see Kazemi et al.[83]). The EVM optimal design criterion suggested two optimal feed mole fractions of f_{0AAm}=0.1 and f_{0AAm}=0.46, at which new experiments were run, again independently replicated three times. The conversion versus time results over the full conversion range (low to high levels), are shown in Figure 4-5.

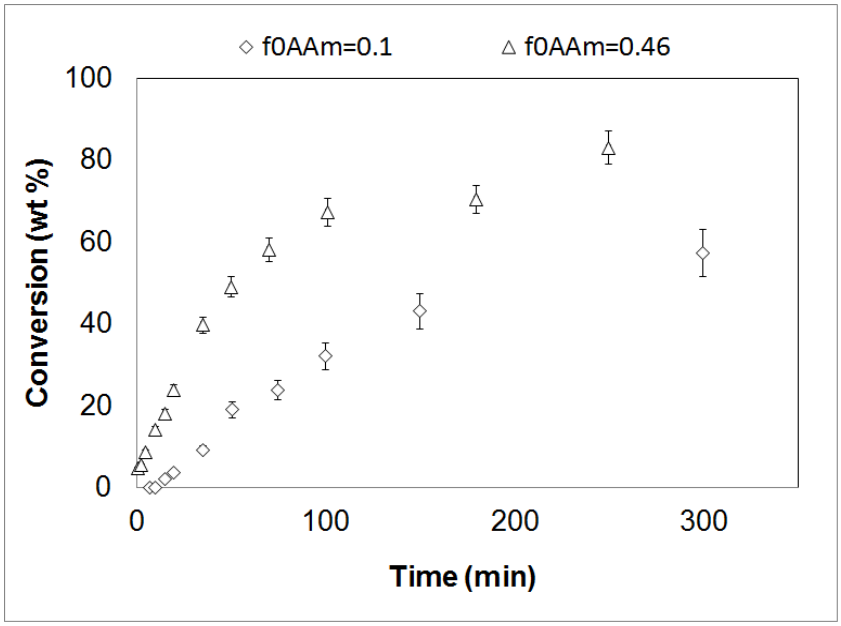

Figure 4-5: Conversion vs. time (with independent replicates) for AAm/AAc polymerization at optimal feed compositions

The corresponding values of cumulative copolymer composition, Cum F_{AAm} (as the mole fraction of AAm bound in the copolymer) with respect to conversion for these optimal feed compositions are cited in Table 4-2.

Table 4-2: Cumulative copolymer composition versus conversion at optimal feed compositions

Feed composition			
f_{0AAm}=0.1		f_{0AAm}=0.46	
Conversion (wt%)	Cum F_{AAm}	Conversion (wt%)	Cum F_{AAm}
2.03	0.27	4.58	0.64
3.58	0.27	5.55	0.62
4.85	0.26	6.71	0.62
9.09	0.25	8.67	0.62
9.12	0.25	10.11	0.62
11.83	0.24	14.09	0.61
16.69	0.24	14.42	0.64
18.99	0.24	18.07	0.62
21.85	0.23	22.60	0.58
23.75	0.23	22.89	0.61
32.13	0.22	23.79	0.61
32.01	0.22	37.50	0.61
32.08	0.21	39.64	0.58
43.04	0.20	40.29	0.59
46.51	0.19	49.02	0.57
49.86	0.18	55.17	0.57
57.26	0.17	56.49	0.59
63.98	0.16	58.08	0.58
65.69	0.15	67.19	0.56
87.49	0.12	65.91	0.57
		70.38	0.54
		83.07	0.53

4.3.3 Optimal reactivity ratio estimation

Using the data from these optimal feed mole fractions from the EVM design criterion, and employing the DNI approach (for more details see Kazemi et al.[29]), results shown in Figure 4-6 were obtained.

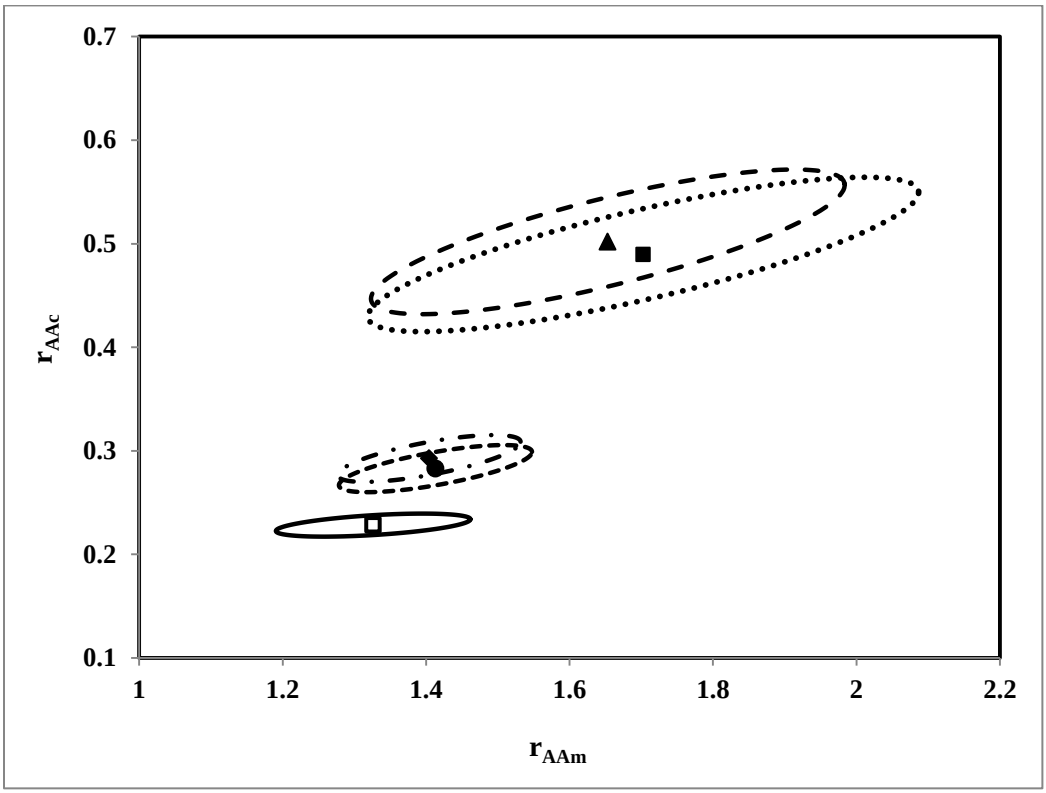

Figure 4-6: Comparison of JCRs for the ML & DNI approaches; (- - - , ▲)"preliminary ML"; (…, ■) "preliminary DNI"; (- . - . - , ♦) "replicated preliminary ML"; (--- ,●) "replicated preliminary DNI"; (__ , □) optimal DNI

Figure 4-6 gives the overall summary and an interesting visual progression of the JCR trends, from "preliminary" to "replicated preliminary" and, finally, to the optimal JCRs. One can see

the improvement as one moves from step 1 to step 3 of the estimation. The final optimal values of the reactivity ratios are r_{AAm}=1.33 and r_{AAc}=0.23. A noteworthy remark here is with respect to the shape of the final (optimal) JCR: the JCR is almost parallel to the x-axis, indicating almost no correlation between the parameters, which is another, rather implicit, benefit of using statistically designed experiments.

Figure 4-7 puts the new estimation results and the currently best literature results by Rintoul and Wandrey[17] in perspective.

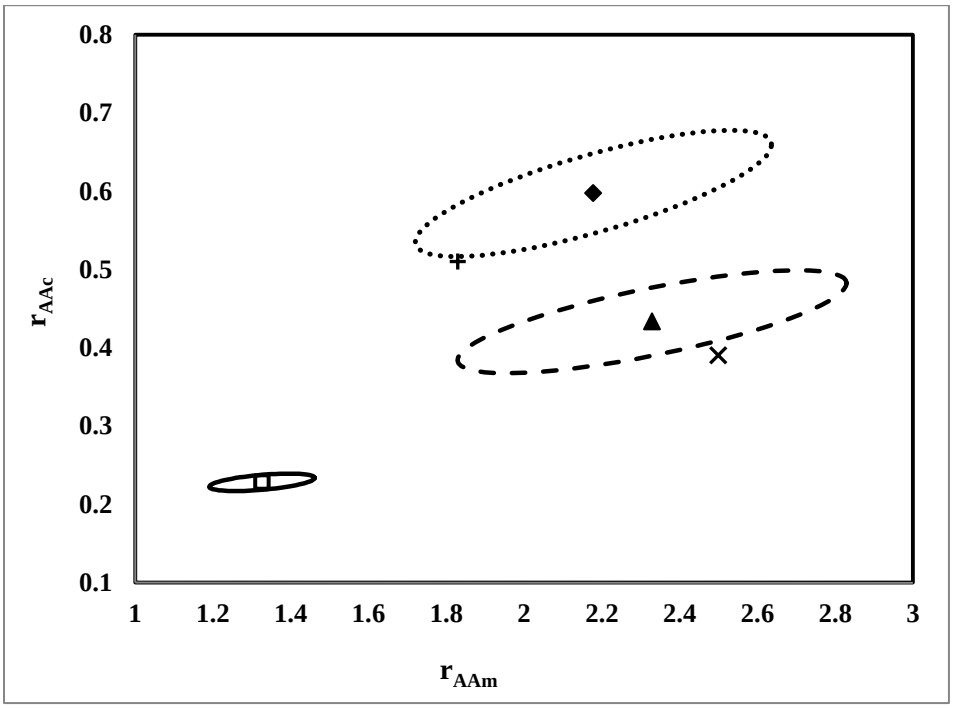

Figure 4-7: Comparison of reactivity ratios and JCRs; (__ ,□) optimal DNI; (… , ♦) DNI estimation based on Rintoul and Wandrey[17] data at pH=5.3; (+)reported reactivity ratios by Rintoul and Wandrey at pH= 5.3; (--- ,▲) DNI estimation based on Rintoul and Wandrey data at pH=6.2; (X) reported reactivity ratios by Rintoul and Wandrey at pH=6.2.

The reactivity ratios reported by this group were used as initial estimates in this work, as discussed earlier. The solid curve is the optimal JCR from Figure 4-6. The dotted curve is the JCR based on reported cumulative copolymer composition data from Rintoul and Wandrey at pH=5.3. The dashed curve is the JCR from approximate cumulative copolymer composition data extracted from Rintoul and Wandrey[17] at pH=6.2. Despite the fact that very similar reaction conditions were used in their work (albeit a different initiator and a lower total monomer concentration), the calculated JCRs do not contain the reported point estimates of reactivity ratios (see + and × located almost at the borderline or slightly outside of the calculated JCRs). This likely stems from the fact that Rintoul and Wandrey[17] used an incorrect (yet widely used) estimation technique, the Kelen–Tüdös method, in addition to having unknown magnitudes of experimental errors (maybe inevitable in such a complex system, but compounded due to lack of independent replication).

It is not then very surprising, after this critical comparison, that there are so many discrepancies and contradictions with respect to reactivity ratios for the AAm/AAc system in the literature. First, variable induction times (which become more important at low conversion levels) and inconsistent experimental techniques during data collection would easily account for considerable error propagation in the final calculated results. In addition, independent replication is almost non-existent in the literature, which compounds the magnitude of the error. Last, but not least, the situation becomes even more complicated due to wide employment of inappropriate estimation methods for finding reactivity ratios.

4.4 Concluding remarks

The AAm/AAc copolymerization is a complex system in terms of reactivity ratio determination. It has been shown in this chapter that for the purpose of reactivity ratio estimation, it is very important to design experiments, so that the parameter estimation is based on an informative data set and moreover, it is critical to check the reliability of the data with independent replicates. For a system as complex as AAm/AAc copolymerization this is especially true. The reactivity ratios for AAm/AAc, at pH=7, were estimated at low, medium, and high conversions by applying optimal statistical design of experiments and two approaches were eventually contrasted, namely, the commonly employed Mayo-Lewis method, and the improved DNI procedure with optimally designed experiments. Optimal reactivity ratio values for the conditions chosen are r_{AAm}=1.33 and r_{AAc}=0.23.

Chapter 5. Copolymerization Kinetics, Step 2: Polyelectrolyte Characteristics and Ionic Strength

5.1 Introduction

A review of the relevant literature has revealed that, despite the importance of controlling the ionic strength, there is no systematic study of the effect of ionic strength on the reaction kinetics of AAm/AAc copolymerization. In addition, as explained in the Section 2.4.3, in the few existing studies, the experimental observations are rather contradictory (both on polymerization kinetics and monomer reactivity ratios) with respect to the effects of this factor.

Chapter 4 targeted the case where the ionic strength was variable (but known) for a specific pH for the different copolymerization runs, in order to be able to compare the estimated reactivity ratios of the system with literature values. The scope of this chapter is to study the effect of ionic strength on the kinetics of AAm/AAc copolymerizations at a chosen pH (pH=7). In doing so, the experimental conditions for pH, temperature, total monomer concentration, and initiator concentration were the same for all the experiments. This level of control over these factors allowed us to investigate the effect of ionic strength, without any interactions with other factors interfering into the picture. The ionic strength was varied by changing the proportion of AAc in the feed composition and also by adding NaCl into the reaction solution. First, the system was studied at constant ionic strength by incorporating

salt in the reaction recipe. Subsequently, the effect of having variable but controlled ionic strength on the copolymerization system was studied. To our knowledge, there have been no other attempts so far to clarify the effect of ionic strength as a single factor on the copolymerization kinetics of AAm/AAc (with AAc in the form of NaAc).

5.2 Ionic strength experimental design

The AAm mole fractions in the feed solutions were f_{0AAm}=0.1 and 0.46. These feed mole fractions were determined as optimal values (for the specific reaction conditions) for reactivity ratio estimation based on an optimal design criterion as described in Chapter 4. A summary of the experimental details in the copolymerization runs is given in Table 5-1. Each run was independently replicated at least once.

Table 5-1: Experimental runs of AAm/AAc copolymerization at various f_{0AAm} and ionic strength

Run #	f_{0AAm} [a]	Ionic strength (M)	NaCl (M)
1	0.1	0.898	0
2	0.1	1.078	0.181
3	0.1	1.437	0.539
4	0.46	0.538	0
5	0.46	0.898	0.359
6	0.46	1.078	0.539
7	0.46	1.258	0.719
8	0.46	1.437	0.898

[a] f_{0AAm}: initial mole fraction of AAm in the feed

In all the experiments all of the other factors except ionic strength (including pH and therefore degree of ionization of AAc, total monomer concentration (1 M), initiator concentration, and temperature) were kept constant. Otherwise one cannot distinguish the effect of ionic strength from the other factors. Ionic strength was variable between runs based on different AAc mole fractions in the feed or different levels of added NaCl salt.

5.3 Results and discussion

5.3.1 Constant ionic strength

In Chapter 4, reactivity ratios for AAm/AAc at pH = 7 and total monomer concentration of 1 M were determined, while ionic strength was allowed to vary between runs based on the fraction of AAc in the feed composition. In other words, since the two comonomer feeds (f_{0AAm}= 0.1 and f_{0AAm}= 0.46) used for reactivity ratio estimation had different levels of neutralized AAc, ionic strength was not constant for the different feeds (Runs # 1 and 4 in Table 5-1). A varying ionic strength level represents the typical case in the literature. Most (if not all) of the reported reactivity ratio values in the literature have been calculated based on a "floating" ionic strength. The broader study reported herein was undertaken to examine effects on estimated reactivity ratios caused by varying ionic strength, at the same pH level, by adding various amounts of NaCl to the copolymerization solutions. But first the reactivity ratio estimation at constant ionic strength will be considered.

Based on the ionic strength data presented in Table 5-1, NaCl was added to the solution at f_{0AAm}=0.46 with a concentration equal to 0.359 M, in order to bring its ionic strength level

from 0.538 (Run # 4) to 0.898 (Run # 5), so that runs 1 and 5 had the same ionic strength. Then, copolymerizations were conducted at the conditions outlined over the whole conversion range and cumulative copolymer compositions were determined. Figure 5-1 shows the cumulative copolymer composition of AAm, cum F_{AAm}, determined by elemental analysis versus conversion for f_{0AAm}=0.46 at two ionic strength levels (with independent replicates). It can be seen that incorporating 0.359 M of NaCl leads to a slight decrease in the cumulative AAm copolymer composition, and hence a slight increase in AAc incorporation.

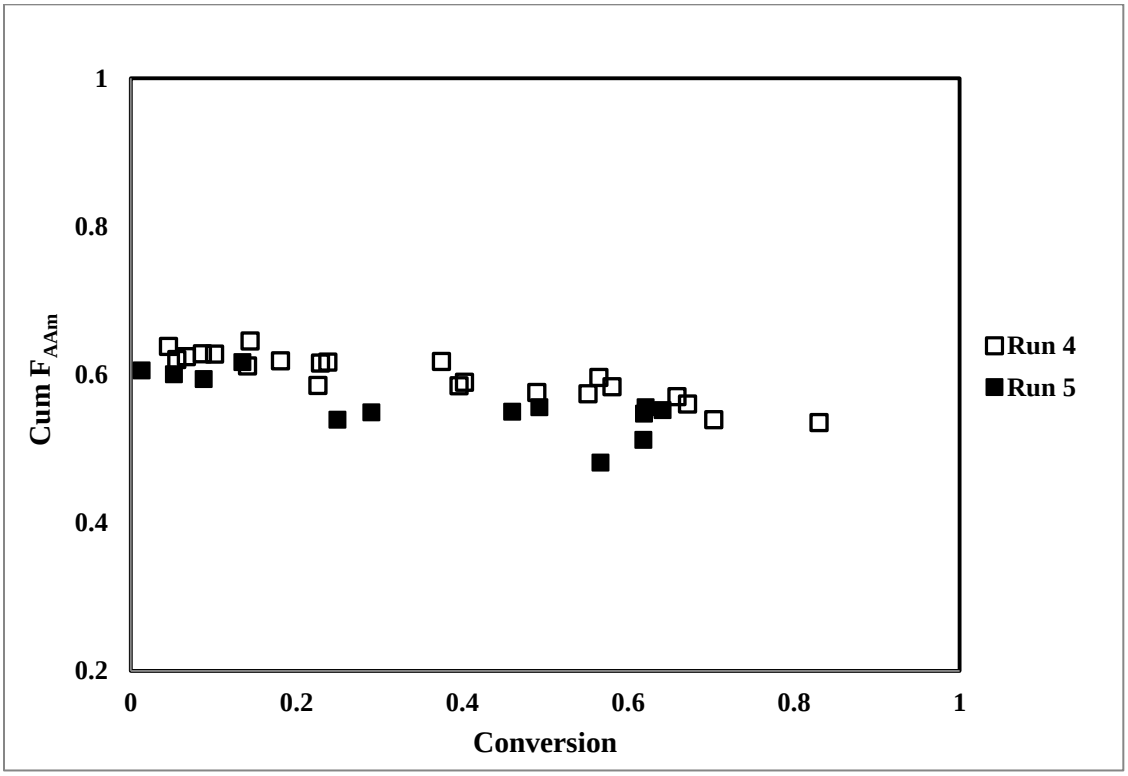

Figure 5-1: Cumulative copolymer composition of AAm versus conversion for f_{0AAm}= 0.46

Based on the cumulative copolymer compositions (cum F_{AAm}) and conversion results from Figure 5-1, reactivity ratios were estimated for runs 1 and 4 (variable ionic strength) and runs 1 and 5 (constant ionic strength). Figure 5-2 shows both point estimates for these reactivity ratios and the corresponding 95% joint confidence regions (JCRs). The reactivity ratio estimation was done based on the EVM algorithm and DNI approach (in order to estimate the parameters over the whole conversion trajectory), which were explained in detail in Chapter 4. JCRs in Figure 5-2 act as measures of the uncertainty (variability) related to the parameter estimates. As it was explained in Chapter 4, a larger JCR denotes a higher variance and therefore higher variability in the system. Figure 5-2 makes several points. The error levels for the two sets of runs are almost identical (JCRs have about the same area), which is an indirect confirmation of the consistency of the experimental procedures and data collection. The JCRs demonstrate almost no covariance (no correlation) between the estimates (otherwise the obtained ellipses would be more inclined, with a positive or negative slope), which is another good feature of the estimation. Finally, one can see that the reactivity ratio value for r_{AAc} has remained almost the same, while that for r_{AAm} has shifted to lower values (from a point estimate of 1.33 to 1.06), when ionic strength stayed constant at a higher level (0.898). Of course, one could argue that the observed drop in the r_{AAm} value might be due to experimental error, i.e., an experimental artifact. Therefore, the experiments were replicated independently and the validity of the trend was confirmed. In order to check the consistency of the trend of the ionic strength effect on r_{AAm}, and also confirm the fact that the observed drop in r_{AAm} is due to a mechanistic reason (effect of salt addition), the investigation was continued at higher salt levels.

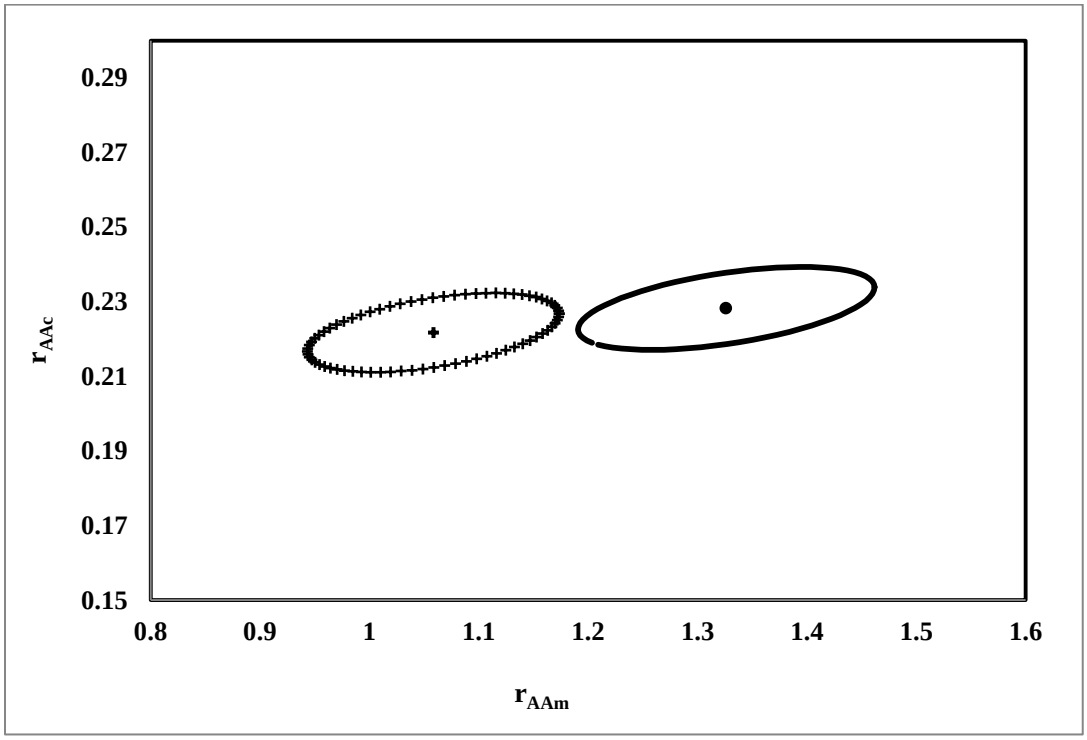

Figure 5-2: Reactivity ratios at variable and constant ionic strength, (●,—) Runs (1, 4); (+,+++) Runs (1, 5)

5.3.2 Controlled but variable ionic strength

The previous results showed that changes in ionic strength (while maintaining other polymerization factors constant), affect the reactivity ratio of AAm, through the change in cumulative copolymer composition at f_{0AAm} = 0.46. In order to check if this effect on copolymerization kinetics extends to higher ionic strength, more runs were conducted with progressively higher levels of sodium chloride, namely, 0.539, 0.719, and 0.898 M, added to the f_{0AAm}=0.46 solution (runs 6, 7, and 8 of Table 5-1). In these experiments, the ionic strength was not constant between the two feed composition levels (i.e., f_{0AAm}=0.1 and 0.46)

that were used for reactivity ratio estimation. However, the ionic strength value was known (controlled) in order to examine the effect of changing ionic strength on the cumulative F_{AAm} and estimated reactivity ratios. The collected copolymer composition and conversion results were used to estimate reactivity ratios for the runs and the final outcomes of the analysis are shown in Figure 5-3.

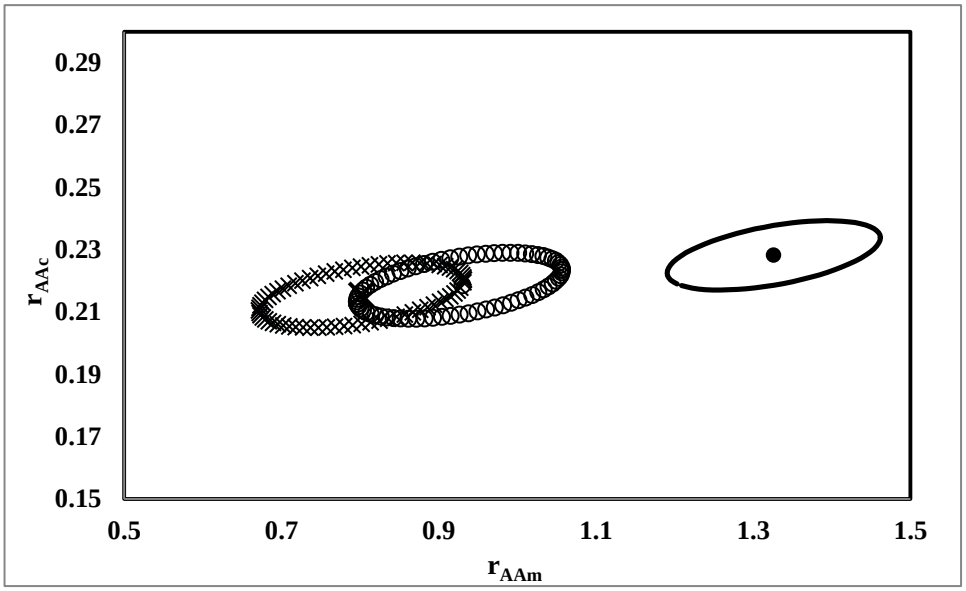

Figure 5-3: Reactivity ratio point estimates and JCRs for different ionic strength levels in AAm/NaAc copolymerization. From right to left JCR: (●,—) Runs (1, 4); (○,○○○) Runs (1, 6); (×,×××) Runs (1, 8)

The JCR for runs (1, 7) overlapped with that of runs (1, 6) and so it is not included in the Figure 5-3. In addition, the JCR for runs (1, 5) was omitted, since it was shown earlier in Figure 5-2. Table 5-2 presents a summary of the point estimates of the reactivity ratios.

Table 5-2 Reactivity ratios for copolymerization at f_{0AAm}=0.46 at various ionic strength levels

Run #	r_{AAm}	r_{AAc}
(1, 4)	1.326	0.228
(1, 5)	1.058	0.222
(1, 6)	0.926	0.218
(1, 7)	0.912	0.217
(1, 8)	0.802	0.215

It can thus be concluded from Figure 5-3 that by adding more sodium chloride to the f_{0AAm}=0.46 reaction solution, r_{AAc} remained almost unchanged, whereas r_{AAm} decreased significantly. Furthermore, this confirmed the trend observed in Figure 5-2.

Regarding the shift in the reactivity ratio values of AAm ($r_{AAm}=r_1=k_{11}/k_{12}$), the AAm homo-propagation rate constant, k_{11}, is likely insensitive to the addition of salt, since the AAm homo-propagation reaction depends only on the AAm monomer and its radical, which are both uncharged at pH=7. Hence, the drop in the r_{AAm} value must be due to changes (increases) in the value of the cross-propagation rate constant, k_{12} (AAm radical with AAc monomer). This term must have increased significantly upon adding more salt to the reaction solution. To explain this, there must be changes in the nature of the overall charges of the polyelectrolyte chains. It is expected that without adding salt, the polyelectrolyte chains containing acrylate anions are more extended because of charge-charge repulsion between anionically charged groups along the chain, as is normal for polyelectrolyte solutions.[85] In addition, there is a relatively low degree of shielding between the negative charges of the

anionic acrylate repeat units in the copolymer chains and the free acrylate monomer. In the case with no added NaCl, with respect to runs (1, 4), there is a greater chance of repulsive interactions between unshielded negative charges, which makes the overall chance of reactive interactions for AAm lower. Hence, with added salt, the opposite will happen, and the cross-propagation rate constant will have the tendency to increase, thus causing a decrease in r_{AAm}.

Incorporating simple electrolytes (such as salts) to the aqueous solution makes the polymer chains contract to denser random coil structures, since the repulsion interactions between acrylate groups are diminished.[85] In other words, in polyelectrolye solutions containing salt, the random coil structure of the copolymer chain is adopted because of the negative charge shielding of the acrylate anions by salt cations. This ion pairing increases the chance of the cross-propagation reaction because the degree of repulsion is diminished between the radical chain and the monomer, which makes the interaction of a growing radical ending in AAm radical with acrylate monomer more probable.

The most interesting observation from Figure 5-3 and Table 5-2 was that initially r_{AAm} was greater than unity and r_{AAc} below unity, whereas after exceeding a specific amount of salt (and hence ionic strength level) in copolymerization at f_{0AAm}=0.46, both reactivity ratios became less than unity. This represents a significant change in copolymerization behavior, as the system now, with both reactivity ratios below unity, is exhibiting potential azeotropic behavior. To confirm the reliability of the estimated reactivity ratios and the azeotropic

behavior, the reactivity ratios for these runs were employed and the feed composition corresponding to the azeotropic point was calculated by Equation 5-1.

$$F_1 = f_1 = \frac{1-r_2}{2-r_1-r_2} = 0.85$$ **Equation 5-1**

Based on the azeotropic runs of Table 5-2, the suggested mole fraction for AAm in the feed was in the range of 0.79-0.89, so the average value of 0.85 was considered. Therefore, a copolymerization was conducted at f_{0AAm}=0.85 with 1.288 M added salt in order to achieve the same ionic strength as that for run (1, 8). The collected conversion data and cumulative copolymer composition are presented in Table 5-3.

Table 5-3: Cumulative copolymer composition versus conversion for f_{0AAm}=0.85

Conversion (wt %)	Cum F_{AAm}
5.785	0.894
6.009	0.904
6.007	0.891
6.724	0.878
12.069	0.892
16.042	0.876
19.949	0.885
41.466	0.874
42.675	0.869
64.759	0.867
95.667	0.863

The copolymer composition results confirmed the reliability of the reactivity ratios, since the values of cum F_{AAm} are close to f_{0AAm} and remained almost constant (within experimental error).

In order to check the effect of ionic strength on the other optimal feed composition, f_{0AAm}=0.1, experiments were run at two levels of added NaCl, namely, 0.181 and 0.539 M (runs 2 and 3 of Table 5-1) in order to obtain the same ionic strength as runs 6 and 8, respectively. Cumulative copolymer composition of AAm versus conversion data for these two salt levels (runs 2 and 3 of Table 5-1) were obtained and the results are compared to those for the polymerization without adding salt (run 1 of Table 5-1) in Figure 5-4.

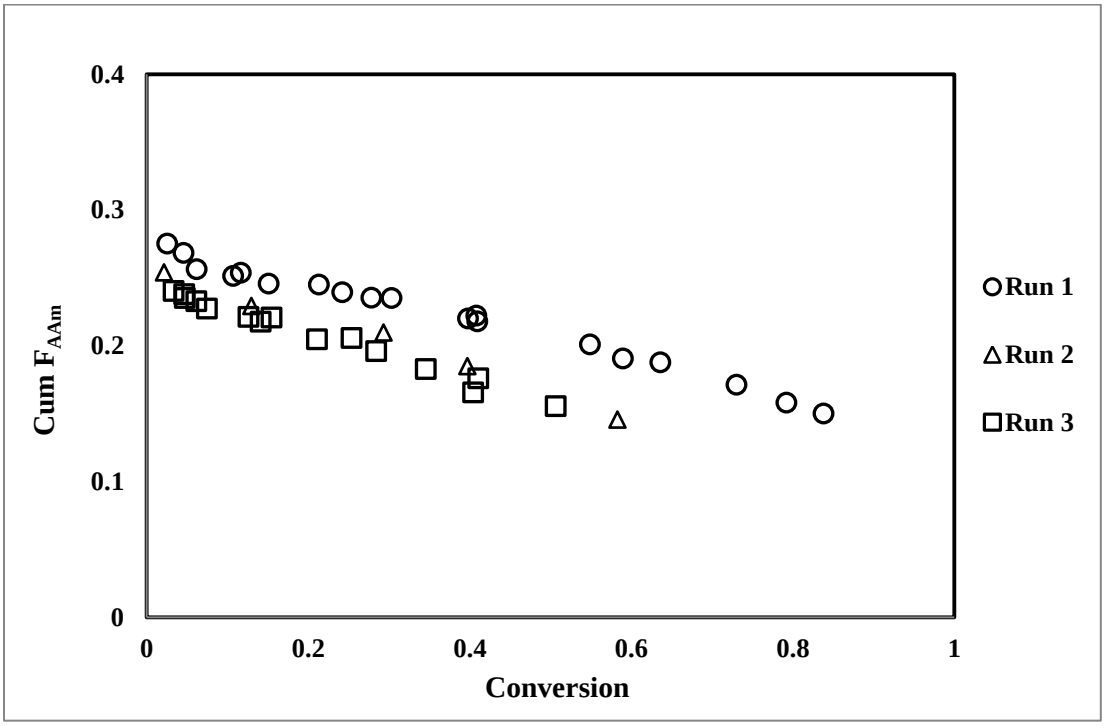

Figure 5-4: Cumulative copolymer composition versus conversion for AAm/AAc at f_{0AAm}=0.1

As can be inferred from the plot, the added salt in the copolymerizations with f_{0AAm}=0.1 resulted in lower levels of incorporation of AAm in the copolymer. This again suggests that incorporating salt and, consequently increasing ionic strength, shields the negative charge interactions of acrylate anions and makes the system electrostatically more stable, which results in the presence of more AAc (less AAm) units in the copolymer chain. This trend agrees well with what was seen for the experiments with f_{0AAm} = 0.46. It is also in agreement with trends of copolymer composition versus concentration of added salts described by McCormick and Salazar for copolymerization of AAm and sodium 3-acrylamido-3-methylbutanoate.[35]

Using the copolymer composition and conversion results, reactivity ratios were estimated for runs (2, 6) and (3, 8) of Table 5-1, which had the same ionic strength between two feed compositions (i.e., between f_{0AAm}=0.1 and 0.46). Point estimates and JCRs for the reactivity ratios of these runs are compared in Figure 5-5 with runs (1, 4), where there was no salt addition in the copolymerization. Table 5-4 also cites the point estimates of Figure 5-5.

Considering Figure 5-5 and Table 5-4 reveals that adding more salt to the solutions with higher AAc content in the feed, f_{0AAm}=0.1, had more of an effect on the reactivity ratio of AAc compared to the runs at lower AAc content, f_{0AAm}=0.46. This was expected since AAc addition was the preferred reaction, and so shielding by adding salt facilitated the homo-propagation of AAc relative to cross-propagation and therefore increased r_{AAc}. The decrease in r_{AAm} with salt addition is also consistent with earlier discussion.

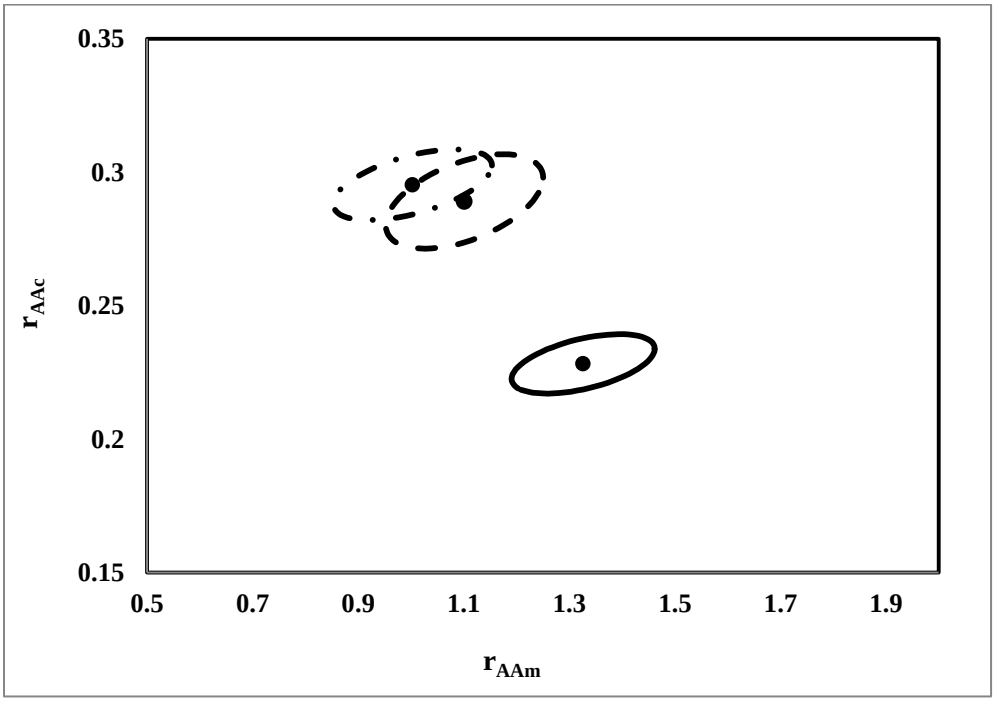

Figure 5-5: Reactivity ratio point estimates and JCRs. (●,—) Runs (1, 4); (●,- - -) Runs (2, 6); (●,- . -. -) Runs (3, 8)

Table 5-4: Reactivity ratios for copolymerizations with varied salt concentration at f_{0AAm}=0.1.

Run #	r_{AAm}	r_{Ac}
(1, 4)	1.326	0.228
(2,6)	1.101	0.289
(3,8)	1.003	0.295

5.3.3 Effect of ionic strength on copolymerization rate

Besides the effect of ionic strength on the monomer reactivity ratios, it has been observed that having different salt amounts in the aqueous solution, changes the overall copolymerization rate.[11,86] Figure 5-6 shows monomer conversion versus reaction time profiles for the two cases with low and high ionic strength at f_{0AAm}=0.46 (runs 5 & 8). It can be seen from this figure that a higher salt level (0.898 M NaCl compared to 0.359 M) in the polyelectrolyte solution, made the copolymerization reaction faster, pointing again towards the shielding effect of salt and less repulsion interactions between reacting species.

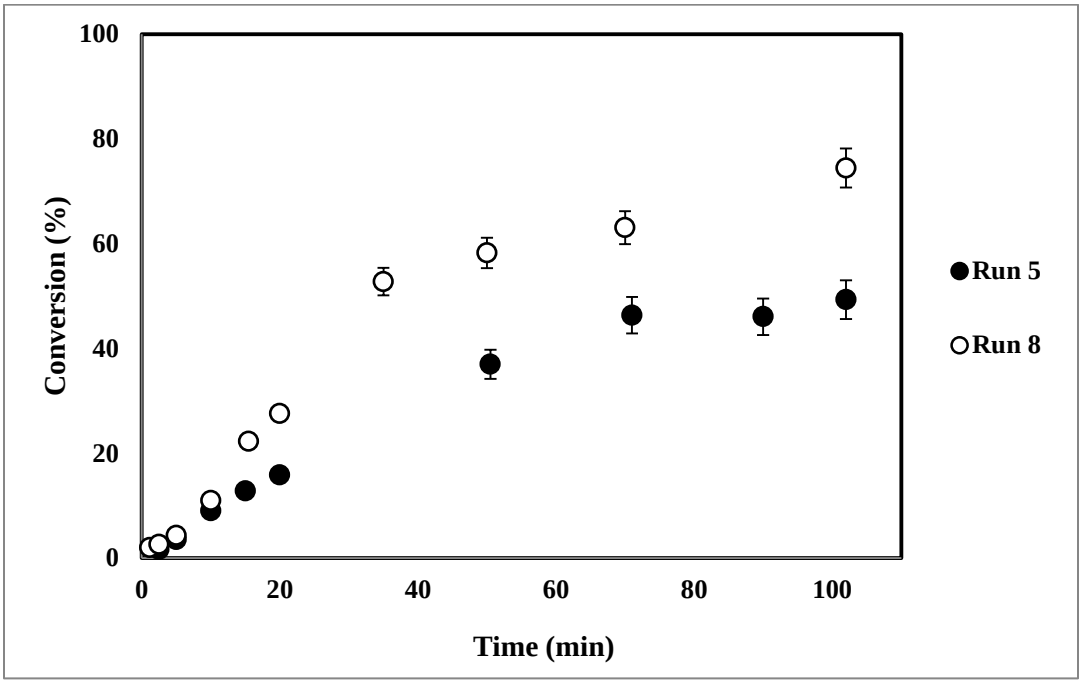

Figure 5-6: Conversion versus time profiles for copolymerizations at f_{0AAm}=0.46

If ionic strength is constant, though, having higher AAc content in the feed composition is expected to cause a reduction in the overall copolymerization rate. Figure 5-7 compares the copolymerization rates of the runs with the same ionic strength but different feed compositions (runs 3 and 8 of Table 5-1). In addition, an extra copolymerization run was conducted at f_{0AAm}=0.85 with 1.288 M salt in order to reach the same ionic strength as runs 3 and 8. Considering these rates at the same experimental conditions, including pH and ionic strength, it is again observed that the rate for runs with higher AAc is slower, due to the electrostatic repulsion between negatively charged reacting species. Effectively, Figure 5-6 and Figure 5-7 represent a corroboration of the results and trends observed earlier.

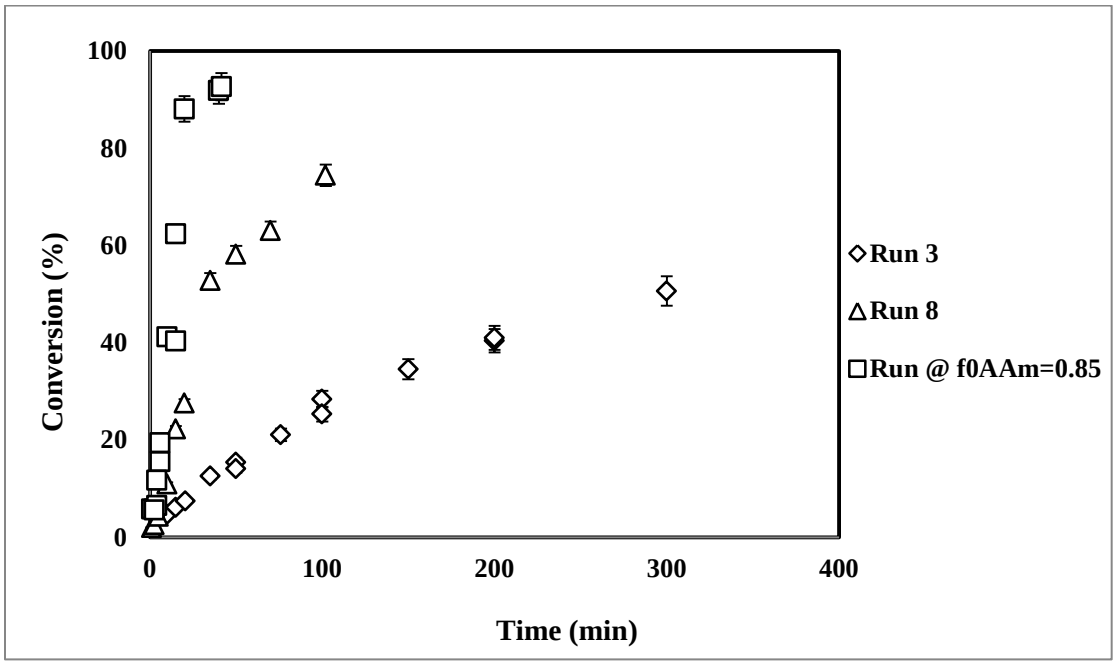

Figure 5-7: Conversion versus time profiles for AAm/NaAc copolymerization at constant ionic strength, 1.437 M

5.4 Concluding remarks

The largely unstudied effect of ionic strength on monomer reactivity ratios and overall polymerization rate of the polyelectrolyte AAm/AAc (AAc in the form of sodium acrylate, NaAc) copolymer system was investigated experimentally. It has been shown that at various feed compositions, incorporating salt in the reaction solution, affects the monomer reactivity ratios as well as the copolymerization rate, by decreasing the electrostatic repulsions between the charged ions. It has also been shown that depending on the initial feed composition of the solution, the effect of ionic strength on reactivity ratios is different. By adding sodium chloride to the polymerization solution with initial feed composition of f_{0AAm}=0.46, r_{AAc} remains almost unchanged, whereas r_{AAm} decreases significantly, with a shift into a system with reactivity ratios that have an azeotropic copolymerization feed composition. However, at copolymerizations with more AAc in the feed, f_{0AAm}=0.1, the effect on the reactivity ratio of AAc is more obvious.

Chapter 6. Copolymerization Kinetics and Copolymer Microstructure/Property Relationships

6.1 Introduction

The objective of the research described in this chapter is to carry out a systematic investigation on the effects of AAm/AAc copolymerization kinetics on various important microstructure/property responses of the copolymer, such as monomer reactivity ratios, copolymerization rate, copolymer composition, sequence length distribution, triad fractions, molecular weight, and shear viscosity. The study reported in this chapter was conducted to establish a general framework between copolymerization kinetics and copolymer microstructure/property relationships. This framework will help us to design copolymers with tailor-made properties for EOR applications. To the author's best knowledge, this type of information does not exist in the literature.

6.2 Experimental design

A D-optimal factorial design was applied to investigate the effects of total monomer concentration, shown as [M] with unit of mol/L, and pH (see Table 6-1). For each of these factors, three levels were considered. The total monomer concentration levels were 0.5, 1.0, and 1.5 M, while the pH was set at 3, 5, and 7. All runs in Table 6-1 were initially conducted

at f_{0AAm}=0.10 and 0.46 (f_{0AAm} denotes initial AAm fraction in the feed). Additional feed fractions were used later, based on optimal feed fractions calculated via optimal values of the reactivity ratios using an iterative sequential scheme.[9,87] All of the experimental runs were independently replicated at least once.

Table 6-1: Experimental design for AAm/AAc copolymerization

Run #	[M]	pH	Run #	[M]	pH	Run #	[M]	pH
1	0.5	3	4	1.0	3	7	1.5	3
2	0.5	5	5	1.0	5	8	1.5	5
3	0.5	7	6	1.0	7	9	1.5	7

The other factors in the experimental trials including initiator type and concentration, and reaction temperature were kept constant (see Section 3.2). It should be noted that ionic strength levels were different among the various feed fractions for a given condition (monomer concentration and pH), based on the amount of AAc in the feed. Therefore, sodium chloride salt was added to the solutions with lower AAc fraction in the feed to compensate for the lower concentrations of ions in the reaction solution and thus keep the ionic strength constant among runs. Considering run 7 ([M]=1.5, pH=3), for example, the experiment was done at three different f_{0AAm} (0.1, 0.46, and 0.8). Table 6-2 summarizes the ionic strength values and the amount of added salt at each feed fraction.

Table 6-2: Ionic strength calculations for run 7

f_{0AAm}	AAc (M)	Degree of ionization	Ionized AAc (M)	Ionic strength (M)	Salt (M)
0.1	1.35	0.059	0.079	0.079	0
0.46	0.80		0.047	0.047	0.032
0.8	0.30		0.018	0.018	0.062

6.3 Results and discussion

6.3.1 Monomer reactivity ratios

The AAm feed mole fractions of 0.10 and 0.46 were used as initial points. Using these initial feed fractions, experiments were carried out to high conversion with at least one independent replicate for each run. Reactivity ratios were estimated by applying the EVM algorithm combined with the DNI approach, which is based on cumulative copolymer composition values and is applicable over the whole conversion trajectory. As explained in Chapter 4, EVM methodology is a sequential and iterative procedure; after estimating reactivity ratios, one can resort to additional sequential optimal designs, in order to improve the estimates. Therefore, based on the estimated reactivity ratios, an optimal feed mole fraction for the specific reaction conditions was determined and the experiment was replicated for each run at the new feed fraction. The reactivity ratios were once again estimated including the information for all three feed fractions (0.10, 0.46, and the new optimal one). Table 6-3 summarizes results from all the experimental runs and the corresponding reactivity ratios.

Figure 6-1 shows the overall map for the effects of total monomer concentration and pH obtained from the experimental work on monomer reactivity ratios. The joint confidence regions (JCRs) at a 95% confidence level reflect the level of uncertainty in reactivity ratio estimation. The plot clearly shows that by changing pH and monomer concentration, the reactivity ratios shift noticeably.

Table 6-3: Estimated reactivity ratios from the experimental runs

Run	[M]	pH	f_{0AAm}	Initially estimated reactivity ratios		New optimal f_{0AAm}	Optimal reactivity ratios	
				r_{AAm}	r_{AAc}		r_{AAm}	r_{AAc}
1	0.5	3	0.10 0.46	0.16	0.83	0.88	0.38	1.11
2	0.5	5	0.10 0.46	0.88	0.90	0.58	1.18	0.95
3	0.5	7	0.10 0.46	1.80	0.17	0.45	1.77	0.16
4	1.0	3	0.10 0.46	0.51	1.32	0.68	0.61	1.34
5	1.0	5	0.10 0.46	0.71	0.74	0.62	1.07	0.77
6	1.0	7	0.10 0.46	1.33	0.23	0.51	1.06	0.22
7	1.5	3	0.10 0.46	0.29	0.77	0.80	0.48	1.09
8	1.5	5	0.10 0.46	0.56	0.82	0.67	0.87	0.87
9	1.5	7	0.10 0.46	0.74	0.33	0.63	1.04	0.34

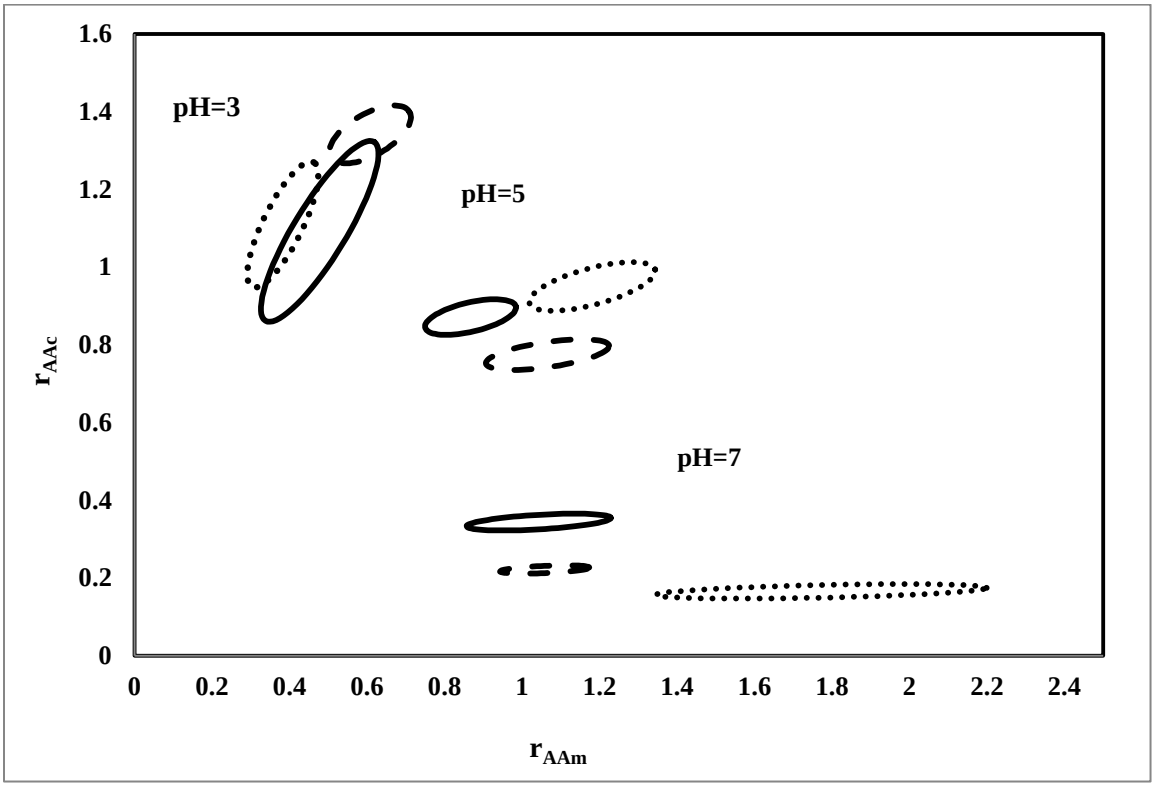

Figure 6-1: Effect of monomer concentration and pH on r_{AAm} and r_{AAc}; total monomer concentration: 0.5 M (dotted line), 1.0 M (dashed line), and 1.5 M (solid line); pH values as indicated in the plot

Figure 6-2 shows the behavior of r_{AAm} and r_{AAc} with respect to pH. The plot shows that with increasing pH from 3 to 7, r_{AAm} increased, while r_{AAc} decreased. At pH=3, $r_{AAc} > r_{AAm}$, while at pH=7, $r_{AAm} > r_{AAc}$. In addition, at pH=5, both reactivity ratios are close to each other showing the so-called semi-crossover point, which has been reported in the literature in the range of 3.6-4.2.[10] The trends in reactivity ratio values with respect to pH are in agreement with those reported in the literature. However, in terms of the actual values (point estimates), there are some deviations. The JCRs of Figure 6-1 allow one to place reactivity ratio values

from the literature at similar conditions and make relative comparisons. Values inside or very close to the JCRs of Figure 6-1 become likely values, in agreement with the general trends, barring of course typical fluctuations due to slight differences in experimental conditions. For example, in a recent study on AAm/AAc copolymerization at low monomer concentrations, reactivity ratios were estimated as r_{AAm}=0.69 and r_{AAc}=1.34 at pH=2.7, and r_{AAm}=1.83 and r_{AAc}=0.51 at pH=5.3.[17] Reported reactivity ratio values at pH=2.7 are in agreement with our estimated values, in contrast to the reported values at pH=5.3, which are not. The differences might stem from the fact that reaction conditions were not exactly the same (e.g., monomer concentration, ionic strength, and initiator). Of course, characterization techniques and the parameter estimation methods themselves can lead to differences, if not performed appropriately. In addition, even larger differences might be expected due to uncontrolled or unreported ionic strength levels. For example, in another recent study, reactivity ratios were estimated as r_{AAm}=1.46 and r_{AAc}=2.06 at pH=3.6.[11] However, these values seem to suffer from parameter estimation issues, and can be disregarded, since both reactivity ratios greater than 1 is not reasonable for a free radical copolymerization.

Based on the data in Figure 6-2, the trends have been confirmed at low, medium and high monomer concentration values, in that the observed general trend for the effect of pH on reactivity ratios of AAm/AAc is not dependent on monomer concentration.

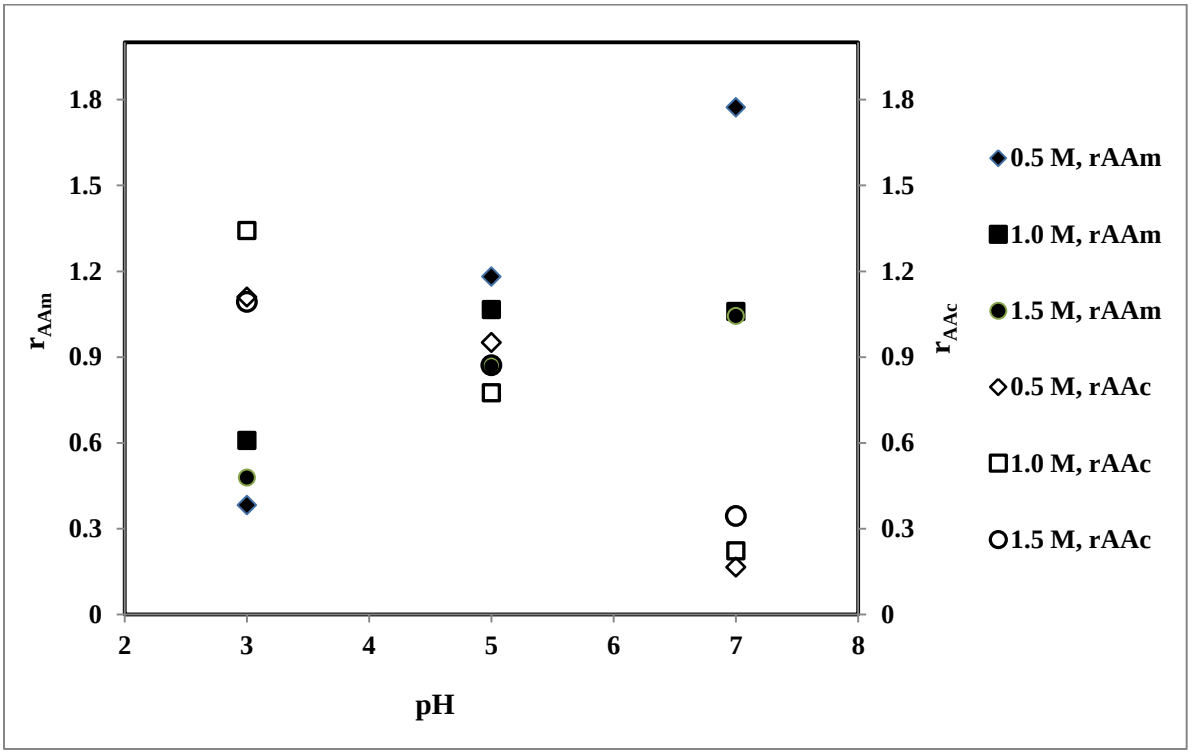

Figure 6-2: Reactivity ratios, r_{AAm} (filled) and r_{AAc} (empty) with respect to pH

Figure 6-3 shows the effect of total monomer concentration on monomer reactivity ratios. An increase in monomer concentration, generally speaking, means having a higher ion concentration in the system (higher concentration of AAc and consequently more NaOH in the reaction mixture to obtain the target pH). Considering Figure 6-1 and Figure 6-3, the results show that the effect of monomer concentration on reactivity ratios is more pronounced at higher pH values. At pH=3, the effect of monomer concentration seems rather negligible (see the almost overlapping JCRs in Figure 6-1), whereas it becomes significant with increasing pH, when AAc is more ionized. At pH=7, one can observe an increase in r_{AAc} and a decrease in r_{AAm} with increasing monomer concentration from 0.5 to 1.0 M, but a much

smaller effect upon increasing monomer concentration to 1.5 M. This is in agreement with Rintoul and Wandrey who studied the effect of monomer concentration on reactivity ratios at elevated pH levels (7 and above).[17] Other specific trends are not easily discernible from the data of Figure 6-3, but one can observe that increasing monomer concentration makes the reactivity ratios less scattered.

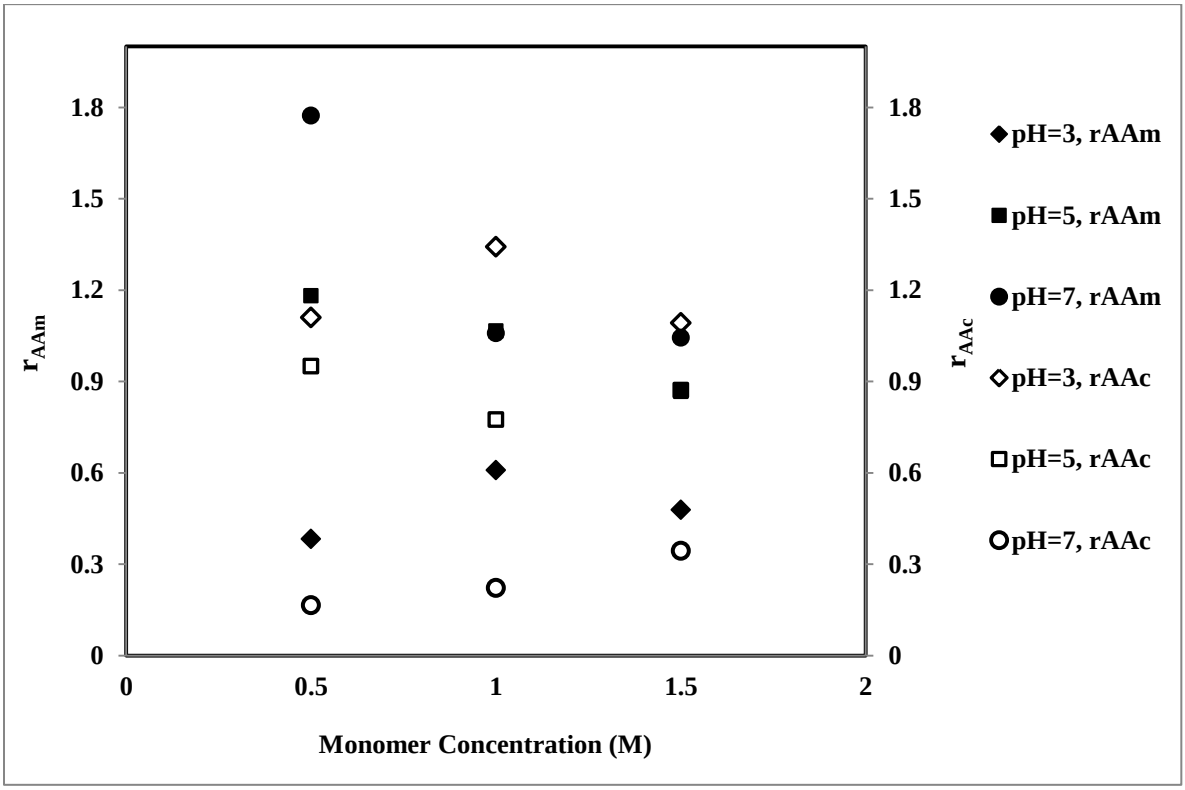

Figure 6-3: Reactivity ratios, r_{AAm} (filled) and r_{AAc} (empty) with respect to total monomer concentration

6.3.2 Copolymerization rate

The behavior of monomer conversion with respect to monomer concentration was also studied (Figure 6-4). It has been noticed that having a concentrated monomer solution makes the reaction go faster (as expected), with shorter retardation time. This is in agreement with what has been reported recently in the literature for the same system.[42]

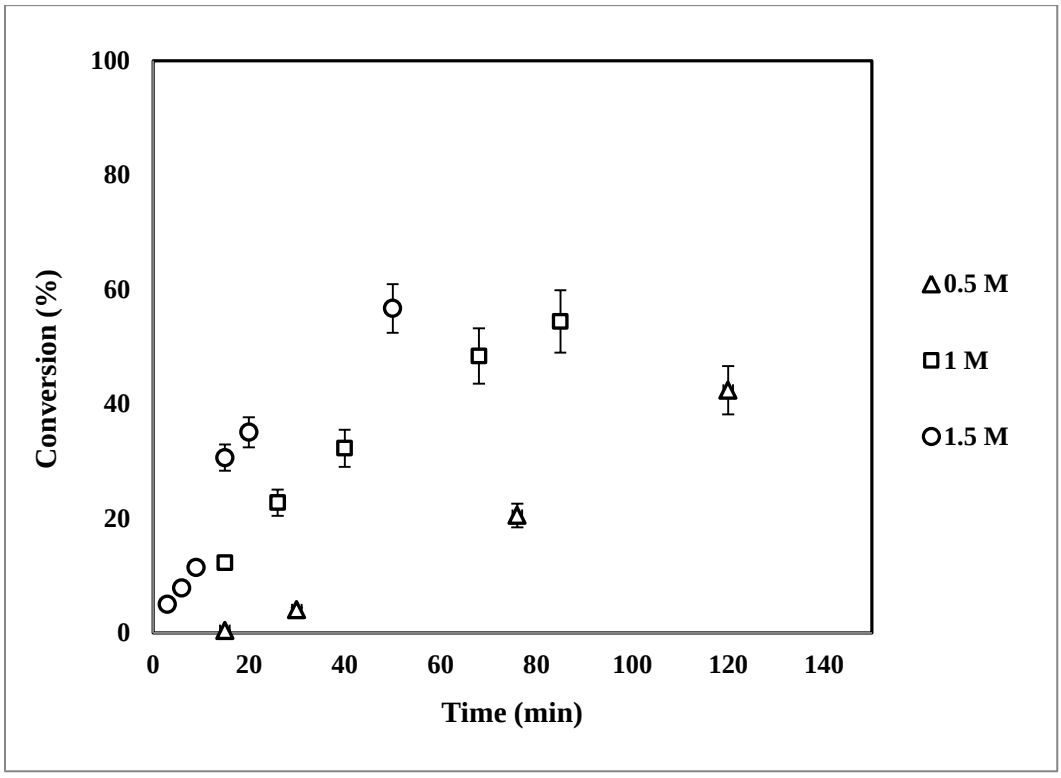

Figure 6-4: Copolymerization at various monomer concentrations, pH=3 and f_{0AAm}=0.46

Monomer feed fraction influences the conversion versus time results as well. Figure 6-5 shows that more AAm in the feed increases the overall rate of polymerization at pH = 5. The

same trend was observed at other pH values. These results are consistent with the results shown in Section 5.3.4 for the effect of monomer composition on copolymerization rate.

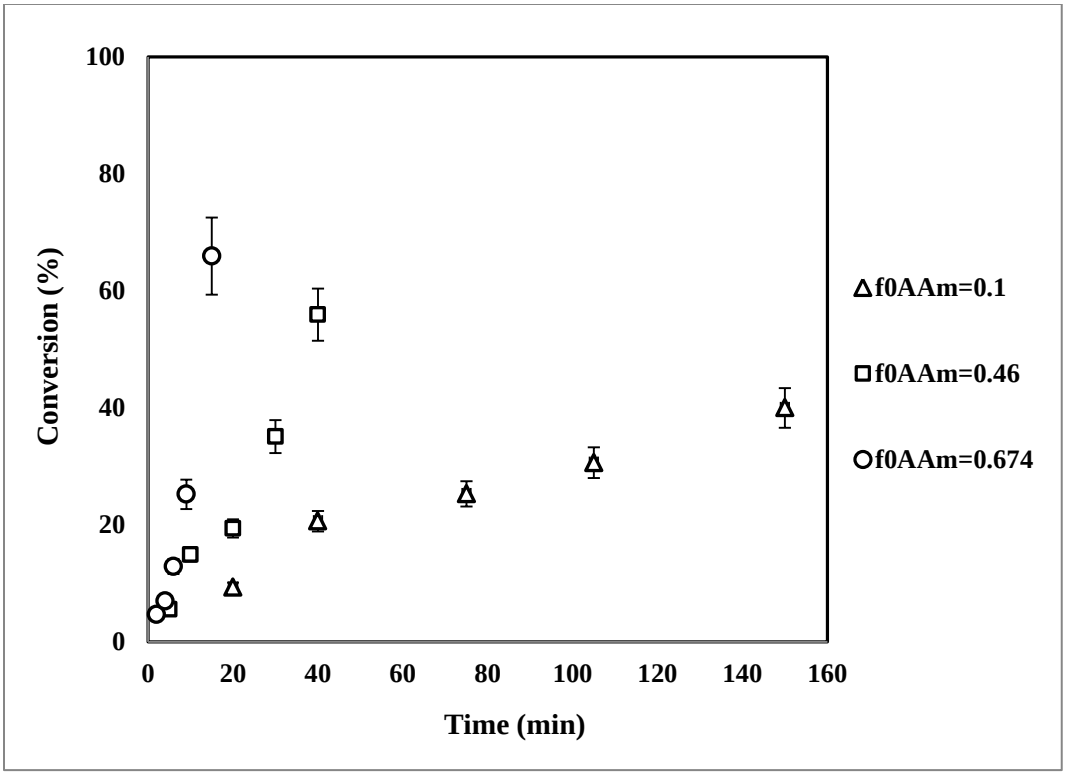

Figure 6-5: Copolymerization at various monomer feed fractions, pH=5 and total monomer concentration=1.5 M

pH level also affects the copolymerization rate, especially at monomer ratios richer in AAc. Figure 6-6 shows a comparison between various pH levels. At pH=3, the AAc is almost completely non-ionized and therefore the electrostatic repulsions are at the minimum level and the copolymerization rate is fastest. However, at pH=5 and 7, most or all of the AAc has been converted to acrylate ions, respectively. As a result, electrostatic repulsions between reacting species are expected, which makes the overall rate of copolymerization slower.

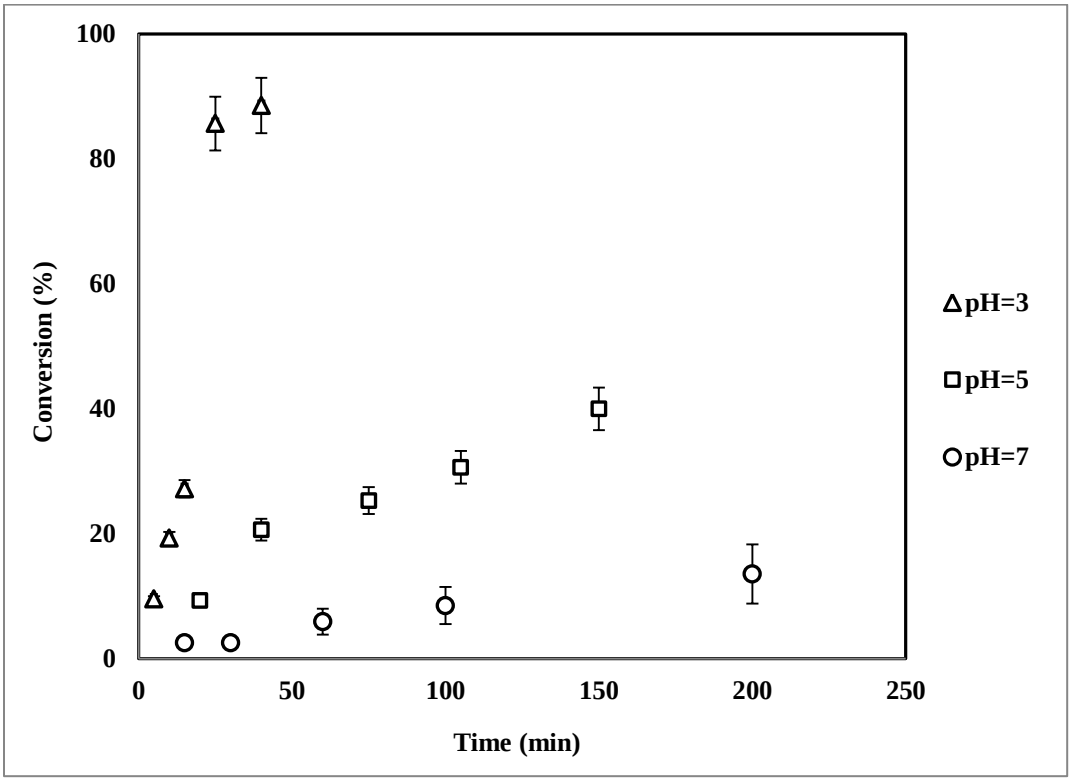

Figure 6-6: Monomer conversion versus time for AAm/AAc copolymerization at various pH levels, f_{0AAm}=0.1, total monomer concentration=1.5 M

6.3.3 Copolymer composition

Instantaneous copolymer composition profiles based on the Mayo-Lewis model and the estimated reactivity ratios for different runs are plotted with respect to feed mole fraction in Figure 6-7. At pH=3, all the curves for the instantaneous copolymer composition of AAm lie below the 45 degree line, while by changing pH to 5, the curves are almost on the 45 degree line and, finally, at pH=7, the curves are above the 45 degree line. Hence, by moving from pH=3 to 7, one can see a reversal in the behavior of the instantaneous copolymer composition with respect to the feed fraction. It is clear that in order to have a high percentage of AAm

units in the copolymer, one can carry out the polymerization at high pH values, since AAm is the more reactive monomer compared to AAc at pH=7 compared to pH=3 and 5. Moreover, these plots can be used to predict the magnitude of composition drift at various feed fractions. For example, at pH=3, it is expected that drift would be less for lower AAm factions in the feed. While, at pH=7, less composition drift can be achieved at higher AAm fractions in the feed.

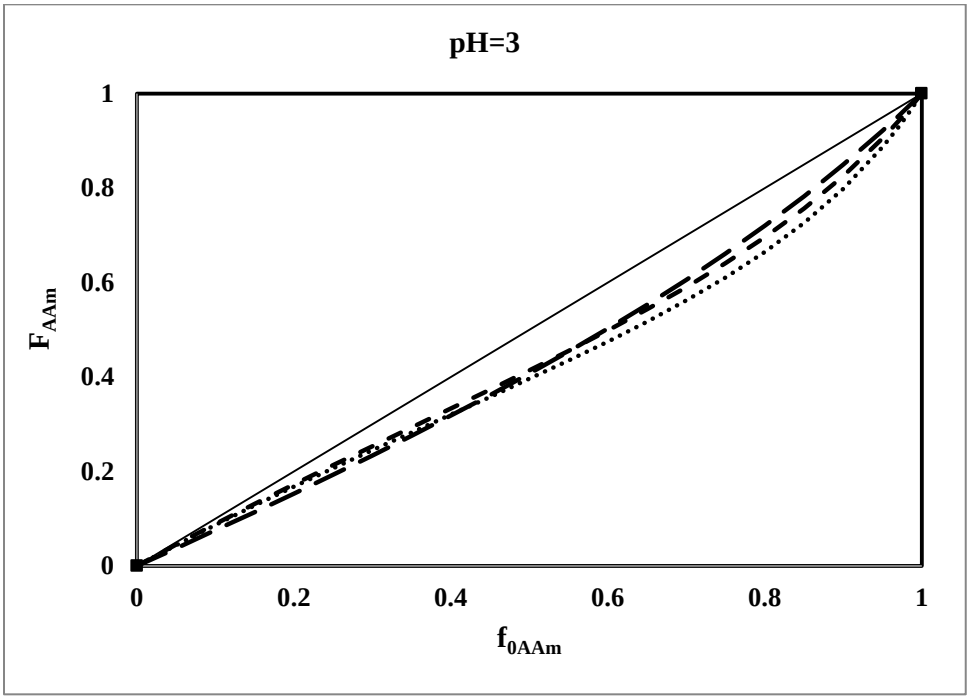

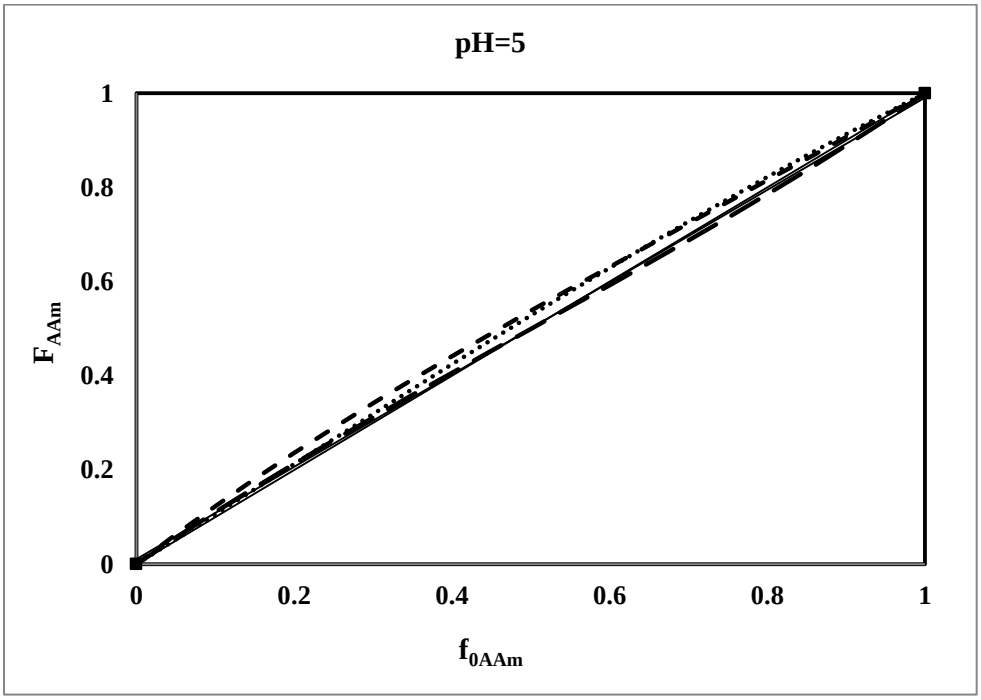

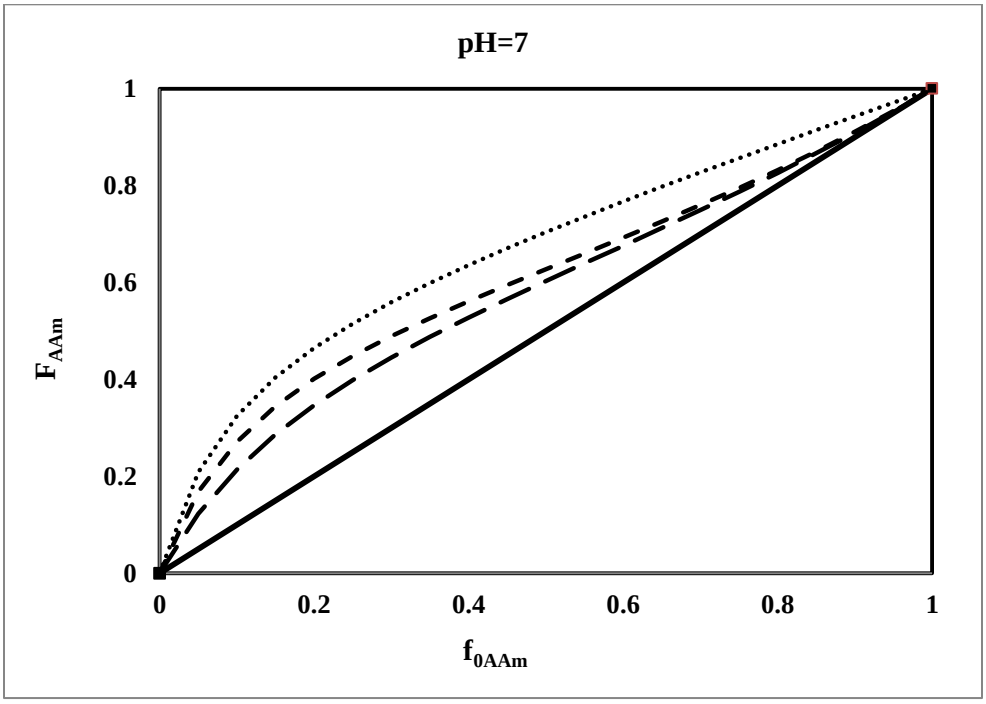

Figure 6-7: Instantaneous copolymer composition versus feed fraction for total monomer concentration: 0.5 M (dotted line), 1.0 M (dashed line), and 1.5 M (long dashed line). pH values are indicated in the plot

The predicted and experimental trends for cumulative copolymer composition of AAm with respect to monomer conversion are shown in Figure 6-8 at different initial feed mole fractions for total monomer concentration of 1.0 M and at the three pH values. The trends for the other two monomer concentrations were very similar to those of Figure 6-8**.** As can be seen from the data in Figure 6-8, there is a variable degree of composition drift during the reaction because of the different reactivities of the monomer species. At pH=3, there is a slight increase in cumulative copolymer composition of AAm as the reaction proceeds. At pH=5, on the other hand, one can observe almost a flat line, while by increasing the pH to 7, there is a noticeable downward drift in the cumulative copolymer composition of AAm with respect to conversion. The trends in composition drift are in agreement with the instantaneous compositions shown in Figure 6-7.

These trends can be explained by the electrostatic nature of this polyelectrolyte system. Considering the low pH level first, there are units of AAm and non-ionized AAc in the reaction system. AAc is the monomer that incorporates relatively faster in the copolymer chain (see Figure 6-7) and as the reaction proceeds, there is less AAc left and therefore progressively more AAm incorporates in the copolymer chain (see Figure 6-8). That is the reason for the increase in the cumulative copolymer composition of AAm with respect to conversion. The same reasoning can be used for the cumulative copolymer composition at pH=7, but this time the nature of the trajectory is due to the electrostatic repulsions between AAc reacting species, and hence the descending trajectory. At pH=5, on the other hand, the reactivities of the two monomers are similar with both reactivity ratios being close to 1 (see Figure 6-7). This results in the trend for cumulative copolymer composition being almost flat

with respect to monomer conversion. In other words, at this pH, the copolymer composition remains relatively constant during the course of the reaction (see Figure 6-8). This is very important from a practical point of view for targeting high conversion copolymerizations for commercial production, when minimal copolymer composition drift is desirable in the reaction to maintain product consistency.

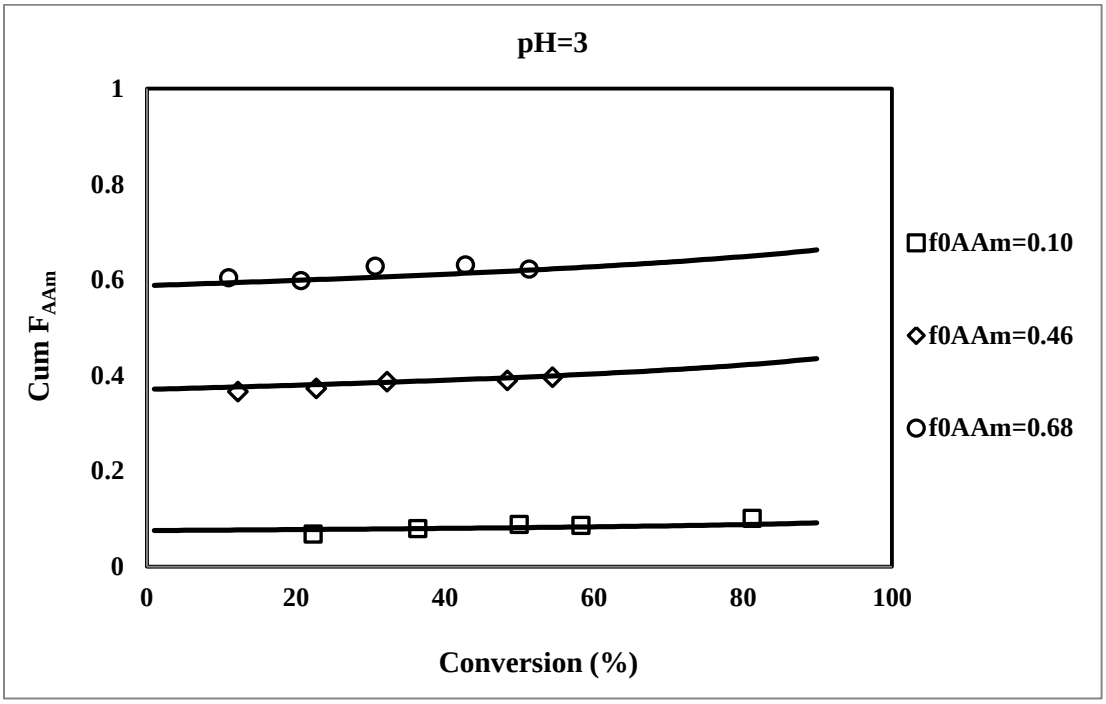

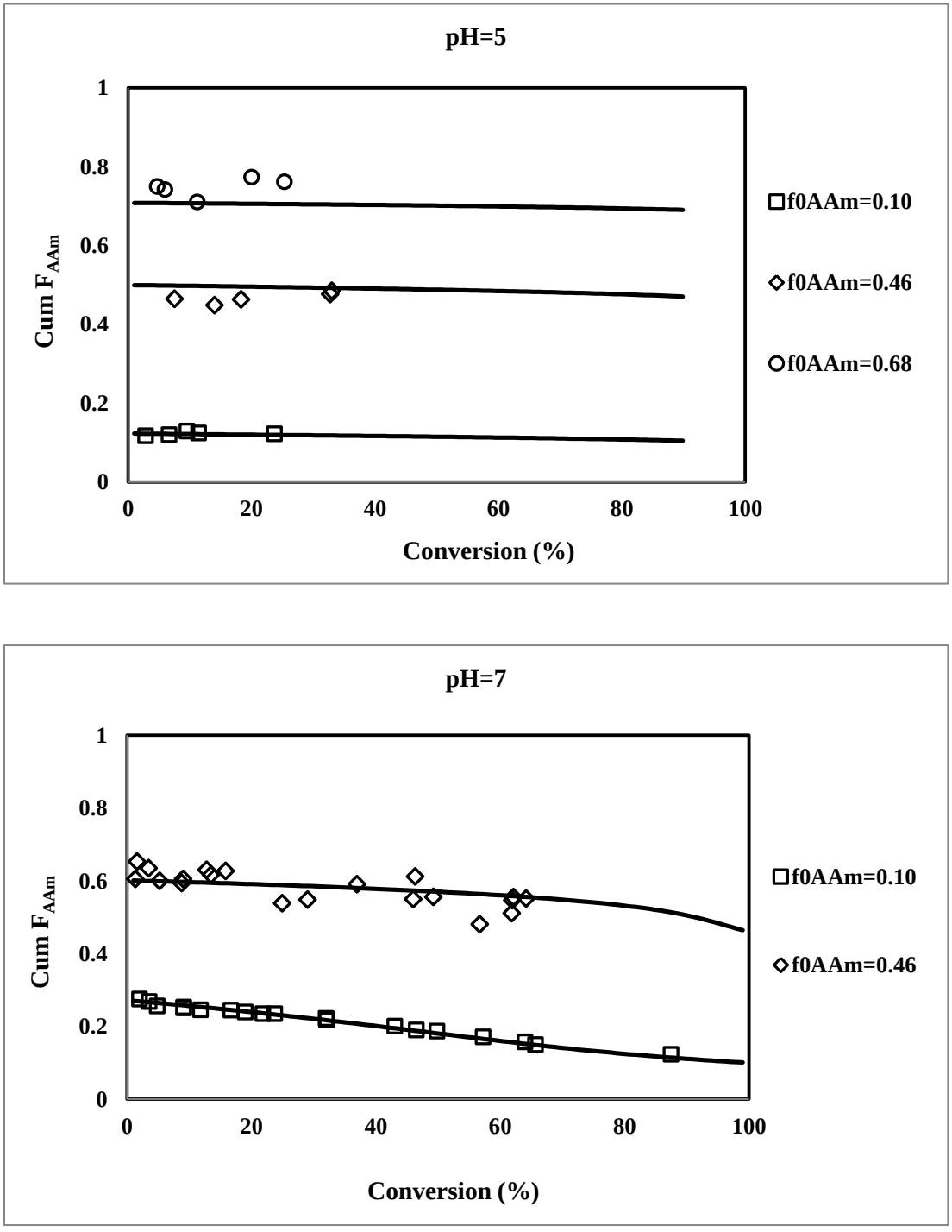

Figure 6-8: Cumulative copolymer composition of AAm versus monomer conversion at constant monomer concentration of 1.0 M but different initial feed fractions and pH levels. (Symbols correspond to experimental data; solid lines are model predictions)

6.3.4 Sequence length distribution and triad fractions

Solution properties of polyelectrolytes are not only affected by copolymer composition and molecular weights, but also are influenced by the microstructure of the chains, as described by such indicators as sequence length distribution and/or triad fractions of the monomers. Reactivity ratios can be used to predict trends in microstructure and in turn microstructure analysis can be used to confirm the reactivity ratio values.

Sequence length distribution gives information about how monomer units are distributed along the polymer chain.[88] The mole fraction N_i of monomer i (M_i) sequences of length l, is defined by a probability function as Equation 6-1:

$$(N_i)_l = (p_{ii})^{(l-1)} p_{ij} \qquad \textbf{Equation 6-1}$$

where p_{ii} is the probability of formation of monomer i dyads (M_iM_i), given by Equation 6-2:

$$p_{ii} = \frac{r_i f_i}{r_i f_i + f_j} \qquad \textbf{Equation 6-2}$$

and p_{ij} is the probability of formation of monomer ij dyads (M_iM_j) as Equation 6-3:

$$p_{ij} = \frac{f_j}{r_i f_i + f_j} \qquad \textbf{Equation 6-3}$$

where f_i and f_j represent the corresponding mole fractions of unreacted monomer i and j, respectively. One should immediately observe the appearance of, and hence the dependence on, reactivity ratio values. Figure 6-9 shows the sequence length distribution of AAm in the AAm/AAc copolymer chain (Equation 6-1) at different initial mole fractions of AAm in the feed and pH levels. It is observed that increasing the sequence length (l) resulted in a decrease in the probabilities in general. More specifically, the probability values are different based on the initial feed mole fractions. By increasing the AAm feed mole fraction, it is more probable for AAm monomer to be incorporated in the chain and therefore this makes the probability distribution broader. In other words, considering different feed fractions shows that having less AAm in the feed fraction, e.g. for f_{0AAm}=0.10, makes the sequence length distribution narrower, while having AAm present in larger amounts makes the distribution broader. This can be explained by the fact that having more AAm in the feed increases the probability of propagating centers reacting with AAm, and as a result the sequence distribution becomes broader.

For the data shown in Figure 6-9-a, r_{AAc} is greater than r_{AAm} (r_{AAm} and r_{AAc} are smaller and greater than unity, respectively, as per Table 6-3). Considering the almost equimolar feed fraction, f_{0AAm}=0.46, p_{11}=p_{21}≈0.06 and p_{12}=p_{22}≈0.92 (subscript 1 denotes AAm and 2 is for AAc). This shows that both radicals have a 15 to 1 tendency to react with monomer 2 (here AAc) rather than monomer 1 (AAm). To be more specific, AAm sequences are at 75.4% for l=1, 18.5% for l=2 (dyads), 4.5% for l=3 (triads), 1.1% for tetrads, and 0.27% for pentads. For AAc, the sequences are at 43.4% for l=1, 24.5% for l=2 (dyads), 13.9% for l=3 (triads),

7.8% for tetrads, and 4.44% for pentads. Therefore, the sequence length distribution is narrower for AAm, which is the less reactive monomer.

In Figure 6-9-b, both reactivity ratios are close to one with r_{AAm} slightly larger than r_{AAc} (see Table 6-3). Considering again the same feed fraction, $f_{0AAm}=0.46$, $p_{11}=p_{12}=p_{21}=p_{22}\approx 0.5$, so the sequence distribution of AAc units is similar to that of AAm units. In this case, AAm sequences are 50% for l=1, and the percentages of dyads, triads, tetrads and pentads are 25%, 12.5%, 6.3% and 3.1%, respectively.

Finally, for the data in Figure 6-9-c, r_{AAm} is noticeably greater than r_{AAc} (see Table 6-3). For the almost equimolar feed, AAm sequences are at 39.8% for l=1, 23.9% for l=2 (dyads), 14.4% for l=3 (triads), 8.7% for tetrads, and 5.2% for pentads. AAc sequences, on the other hand, are at 83.7% for l=1, 13.6% for l=2 (dyads), 2.2% for l=3 (triads), 0.36% for tetrads, and 0.06% for pentads. Hence, this time the sequence length distribution is broader for the AAm monomer, which is the more reactive in the copolymerization.

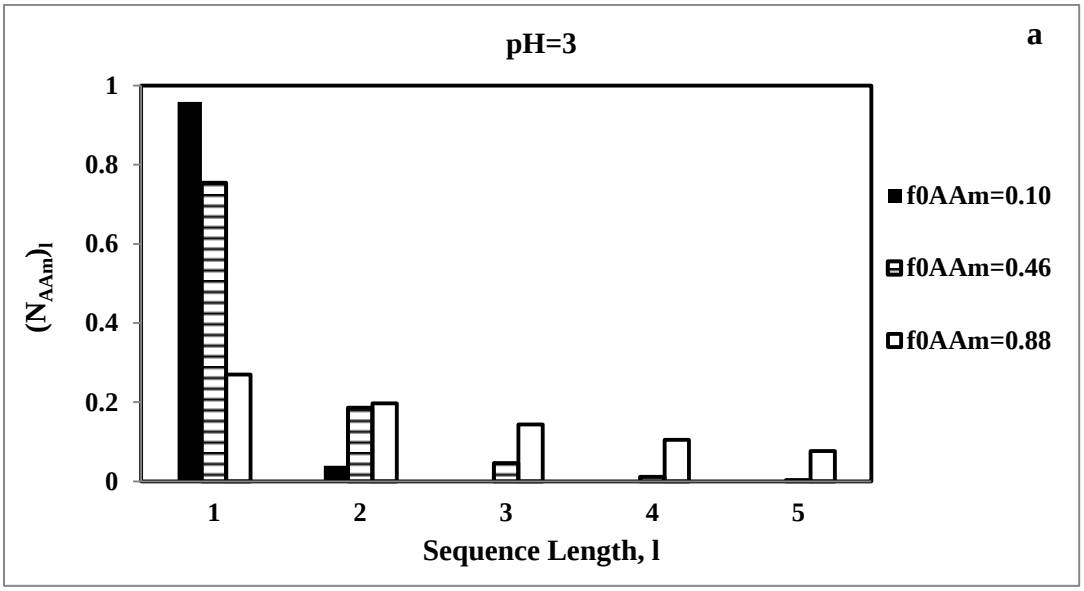

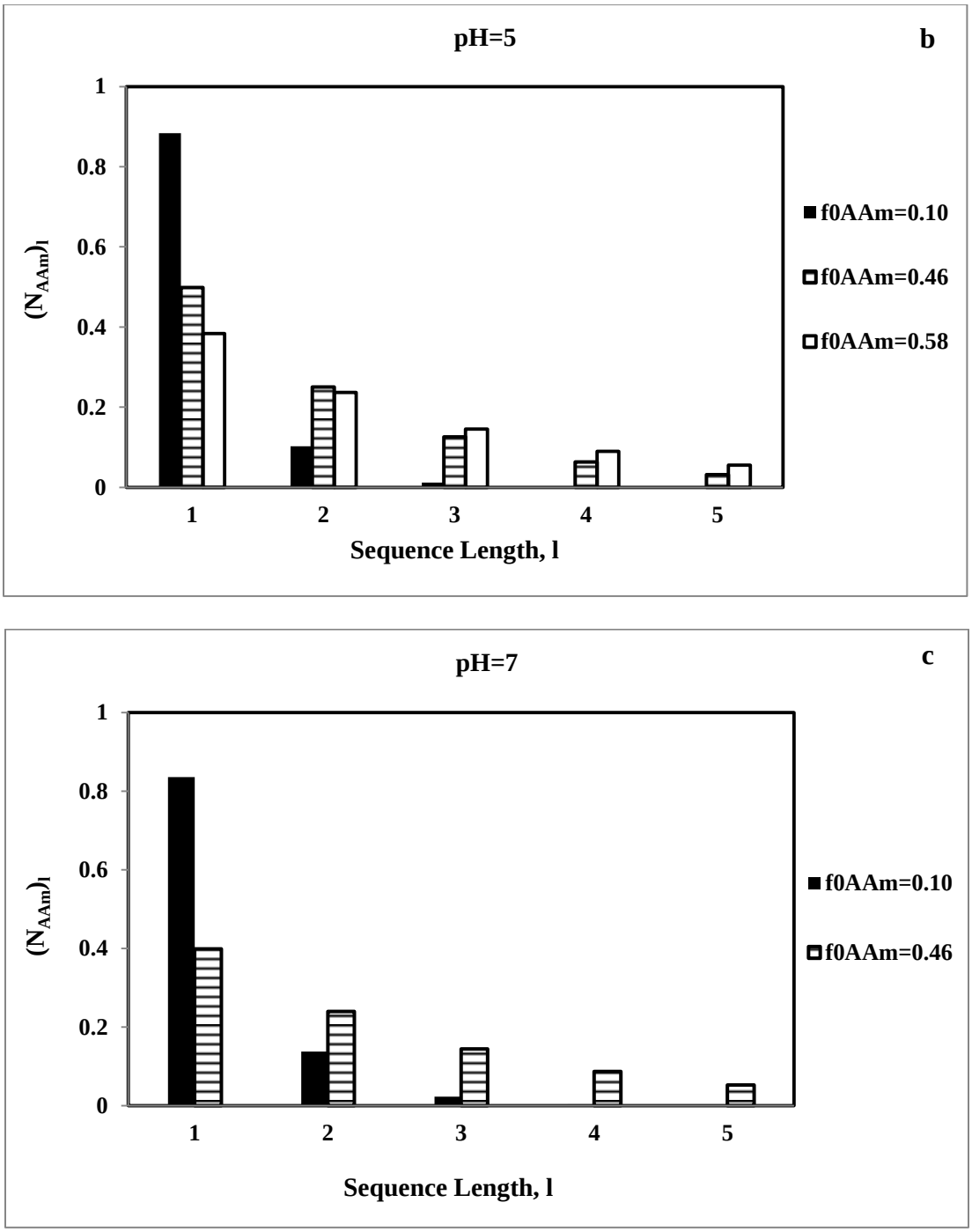

Figure 6-9: Snapshots of the sequence length distribution of AAm in the copolymer for total monomer concentration of 0.5 M at different pH and f_{0AAm} levels.

It should be mentioned that the trends for other monomer concentrations were similar. These data are useful in giving an indication of how pH can influence the sequence length distribution of monomers along the chain.

An additional indicator of sequence length characteristics is the instantaneous number average sequence length of monomer i, $\bar{n}_i$, which gives the average number of monomer i units, M_i, connected together consecutively.[88] $\bar{n}_i$ can be calculated based on the probability of having n consecutive units of monomer i in a growing chain. In a copolymer system, $\bar{n}_i$ can again be expressed in terms of reactivity ratios and monomer feed fractions (Equation 6-4):

$$\bar{n}_i = 1 + r_{ij}\frac{f_i}{f_j}$$ **Equation 6-4**

For any high conversion polymerization the instantaneous distributions are of limited quality control value and cumulative compositions have to be considered. The cumulative number average sequence length, $\bar{N}_i$, can be calculated by integrating the instantaneous equation, as shown in Equation 6-5:[89]

$$\bar{N}_i = \frac{\int_0^x F_i dx}{\int_0^x (1-p_{ii})F_i dx}$$ **Equation 6-5**

In Equation 6-5, F_i and x denote instantaneous copolymer composition of species i and overall monomer conversion, respectively.

Figure 6-10 shows the cumulative number average sequence length (Equation 6-5) of AAm in AAm/AAc copolymerization at constant monomer concentration of 1.0 M and various initial AAm feed fraction (f_{0AAm}) and pH values. The cumulative number average sequence length trends are in agreement with cumulative copolymer composition results presented in Figure 6-8. As can be seen from Figure 6-10, there is an increase in cumulative sequence length of AAm during the course of the reaction at pH=3, while the trend is the opposite at pH=7. There is almost a flat line for AAm cumulative sequence length versus conversion at pH=5.

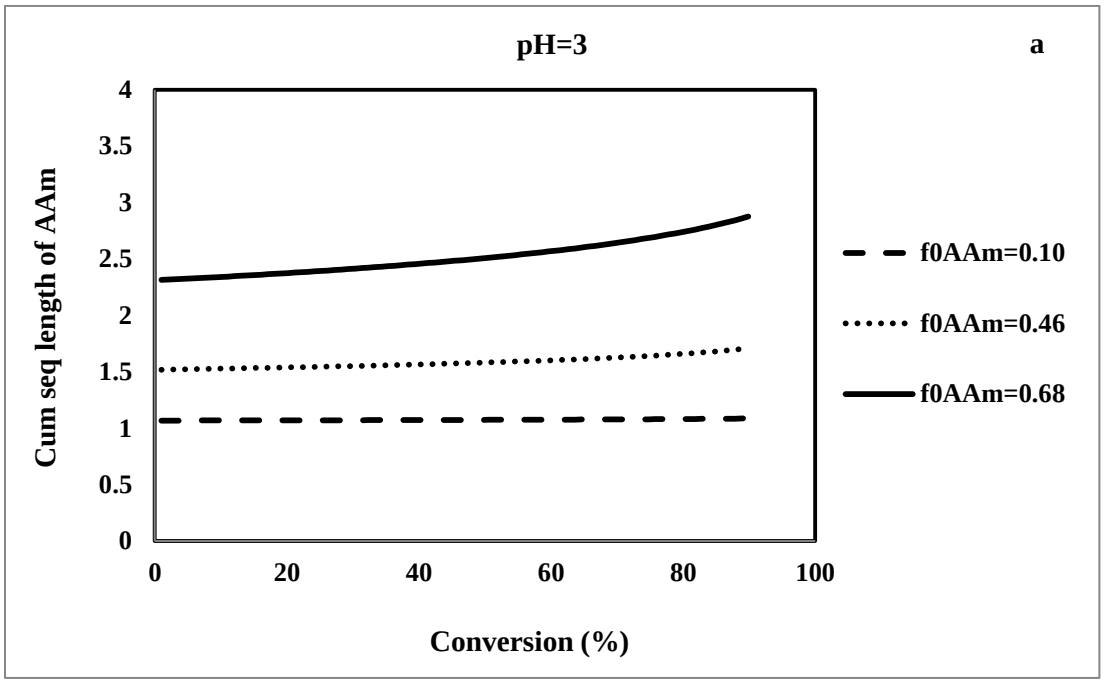

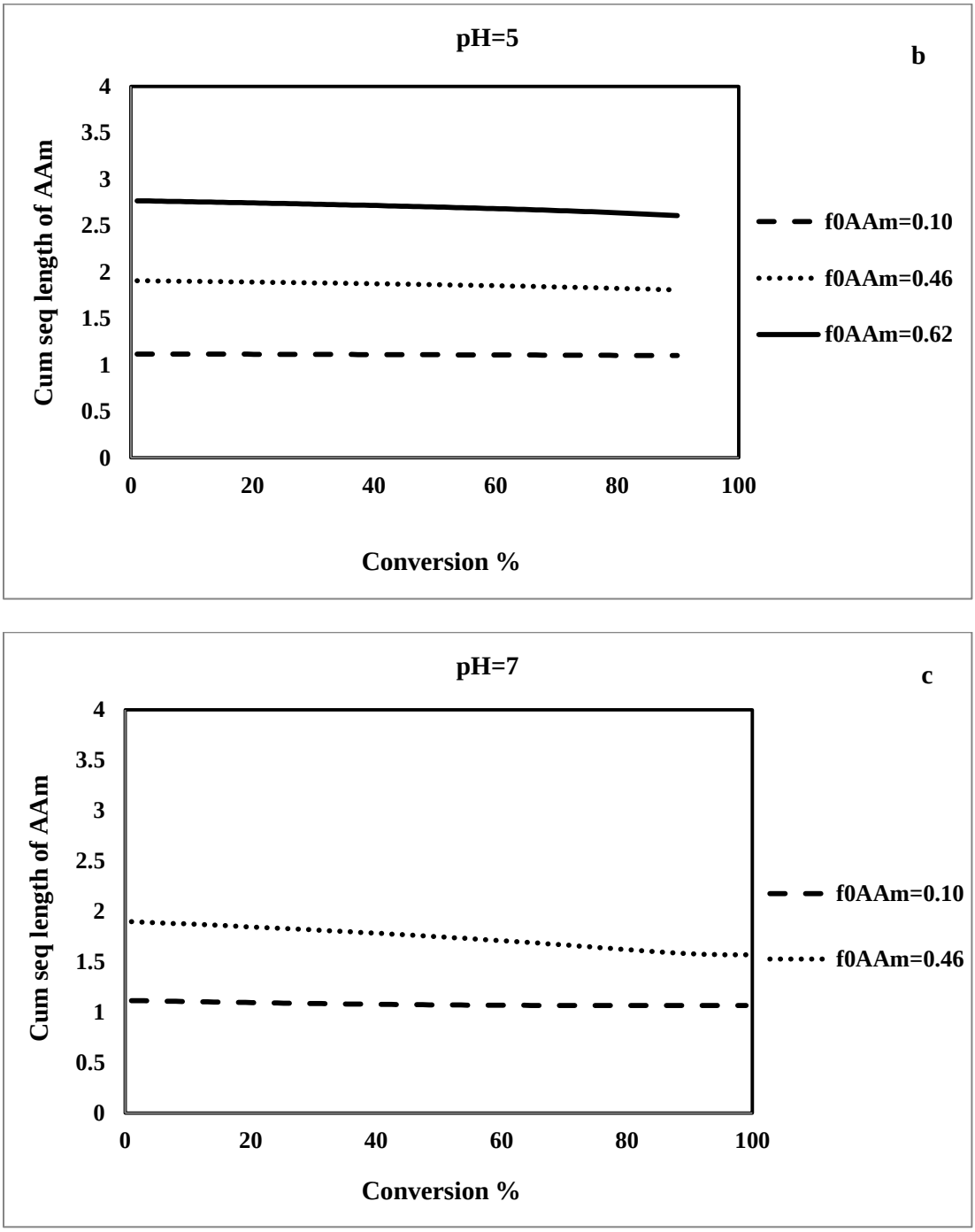

Figure 6-10: AAm cumulative number average sequence length of AAm/AAc copolymer versus monomer conversion at constant monomer concentration of 1.0 M but different initial feed mole fractions and pH levels

Yet another way of studying the microstructure of a copolymer is the calculation of its instantaneous triad fractions as Equation 6-6, Equation 6-7, and Equation 6-8:

$$A_{iii} = \left(\frac{r_{ij}f_i}{f_j + r_{ij}f_i}\right)^2$$ **Equation 6-6**

$$A_{jij} = \left(\frac{f_j}{f_j + r_{ij}f_i}\right)^2$$ **Equation 6-7**

$$A_{iij} = A_{jii} = \frac{r_{ij}f_i f_j}{(f_j + r_{ij}f_i)^2}$$ **Equation 6-8**

Cumulative triad fractions, $\bar{A}_{ijk}$, are expressed as in Equation 6-9. Therefore, by integrating the instantaneous triad fractions with respect to conversion, cumulative triad fractions can be calculated.

$$\frac{d(x\bar{A}_{ijk})}{dx} = A_{ijk}$$ **Equation 6-9**

Instantaneous triad fractions evaluated for a total monomer concentration of 0.5 M at different pH levels were calculated based on Equation 6-6, Equation 6-7, and Equation 6-8. The results are shown in Table 6-4 (for tested feed compositions) and Figure 6-11 (for the whole range of feed compositions). It can be seen that as the AAm content in the polymerizing mixture increases, regardless of the pH levels, the AAm-rich fraction, A_{111}, becomes dominant in the copolymer, whereas the AAc-rich fraction, A_{212}, decreases.

Table 6-4: Instantaneous AAm-centered and AAc-centered triad fractions for AAm/AAc copolymer at monomer concentration of 0.5 M

pH	f_{0AAm}	AAm-centered			AAc-centered		
		A111	A112+A211	A212	A121	A221+A122	A222
3	0.1	0.0017	0.0782	0.9201	0.0083	0.1655	0.8262
3	0.46	0.0604	0.3708	0.5687	0.1886	0.4914	0.3199
3	0.88	0.5329	0.3942	0.0729	0.7469	0.2346	0.0184
5	0.1	0.0135	0.2051	0.7814	0.0109	0.1874	0.8016
5	0.46	0.2516	0.4999	0.2484	0.2234	0.4985	0.2780
5	0.58	0.3796	0.4731	0.1473	0.3462	0.4843	0.1694
7	0.1	0.0271	0.2749	0.6979	0.1615	0.4807	0.3578
7	0.46	0.3619	0.4793	0.1587	0.7012	0.2723	0.0264

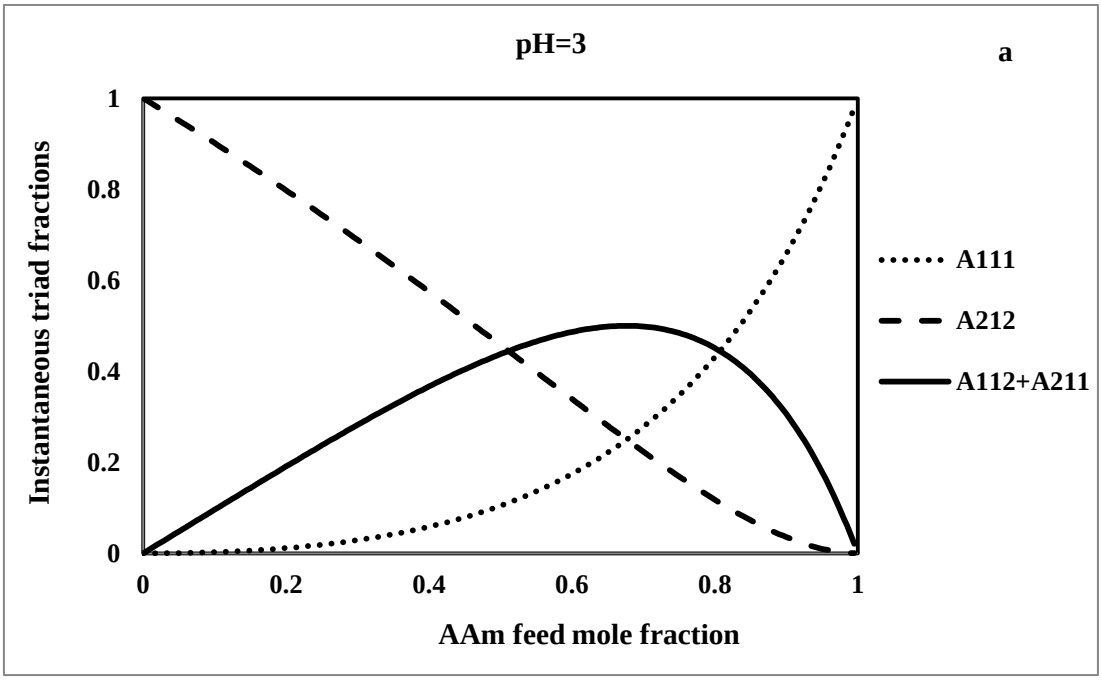

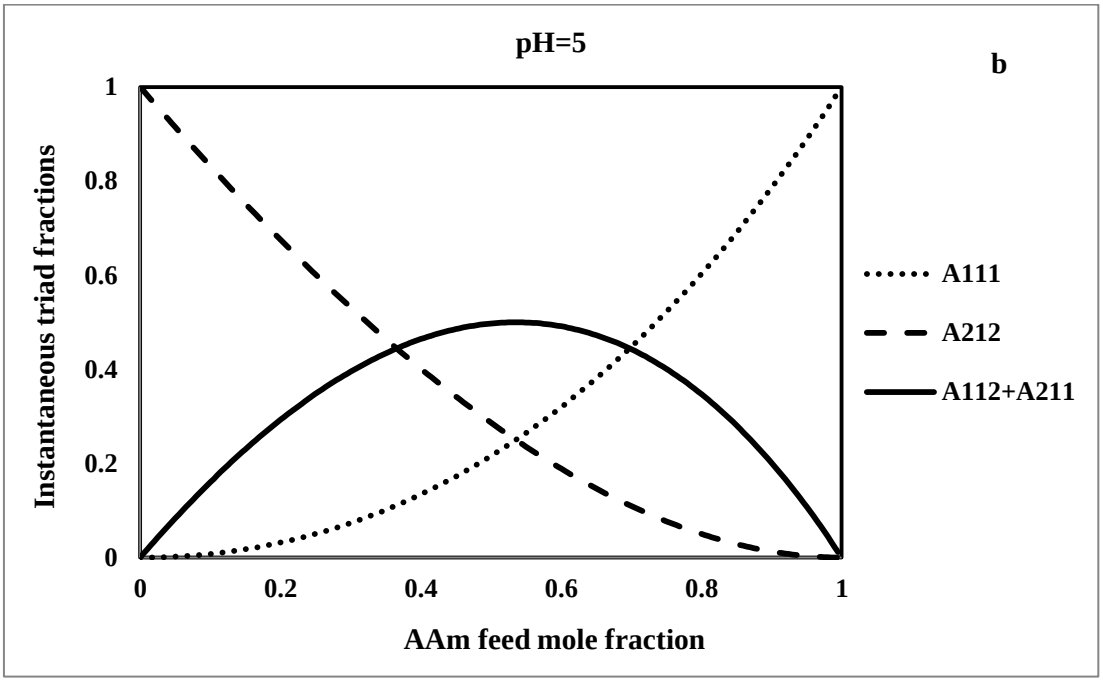

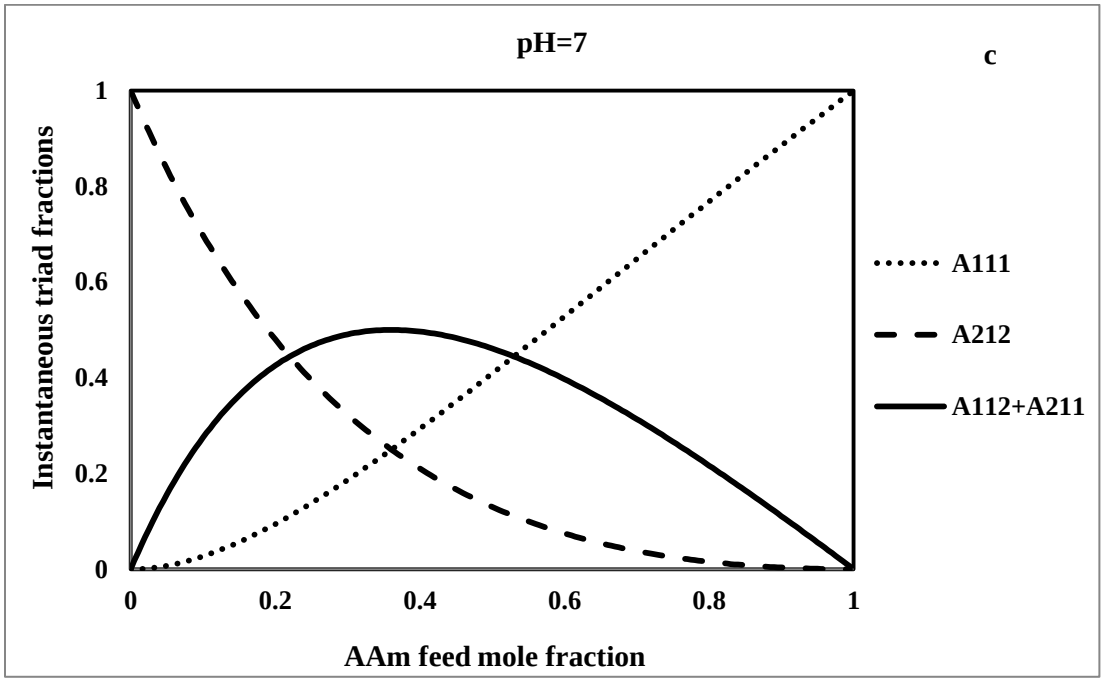

Figure 6-11: AAm-centered (monomer 1) instantaneous triad fractions versus AAm feed mole fraction for AAm/AAc copolymer at monomer concentration of 0.5 M and different pH levels

Cumulative triad fractions with respect to monomer conversion were found by applying Equation 6-9 along with the estimated reactivity ratios for the different conditions. Representative results are shown for run 3 of Table 6-3 at f_{0AAm}=0.46 in Figure 6-12. The overall picture offered by Figure 6-12 is essential for fine-tuning the microstructure of the copolymer for target applications (above and beyond the usual information offered by average measures such as copolymer composition).

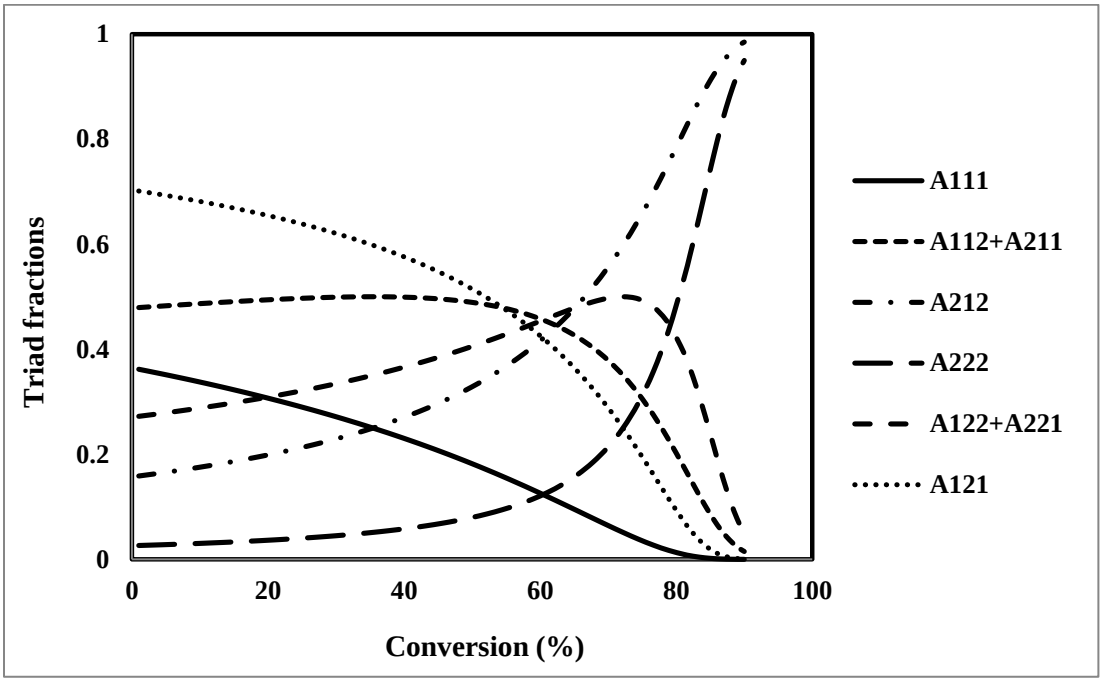

Figure 6-12: AAm-centered (monomer 1) cumulative triad fractions for AAm/AAc copolymer versus conversion, run 3 with f_{0AAm}=0.46

^{13}C NMR analysis was conducted in order to gain more insight into the microstructure of the copolymer chains and also to compare experimentally determined triad fractions with their

theoretical values. In AAm/AAc copolymer, there are three types of carbon atoms with different substituents: methylene, methine, and carbonyl.[19] Therefore, three distinct sets of signals can be distinguished in the ^{13}C NMR spectrum. Figure 6-13 shows these signals in the ^{13}C $\{^{1}H\}$ NMR spectrum of run 3 with f_{0AAm}=0.46. Carbonyl resonance patterns were used to study the triad fractions of the AAm/AAc copolymer because of the less overlapping nature of the obtained peaks. The chemical shifts of the carbonyl resonances corresponding to AAc and AAm are about 183.34 ppm and 180.25 ppm, respectively. From low to high chemical shifts, the resonances are assigned to AAm-centered triads (A_{111}, A_{112}+A_{211}, A_{212}) and AAc-centered triads (A_{121}, A_{221}+A_{122}, and A_{222}). The area under each peak was determined and then the ratios of the areas were calculated to find the corresponding triad fractions.

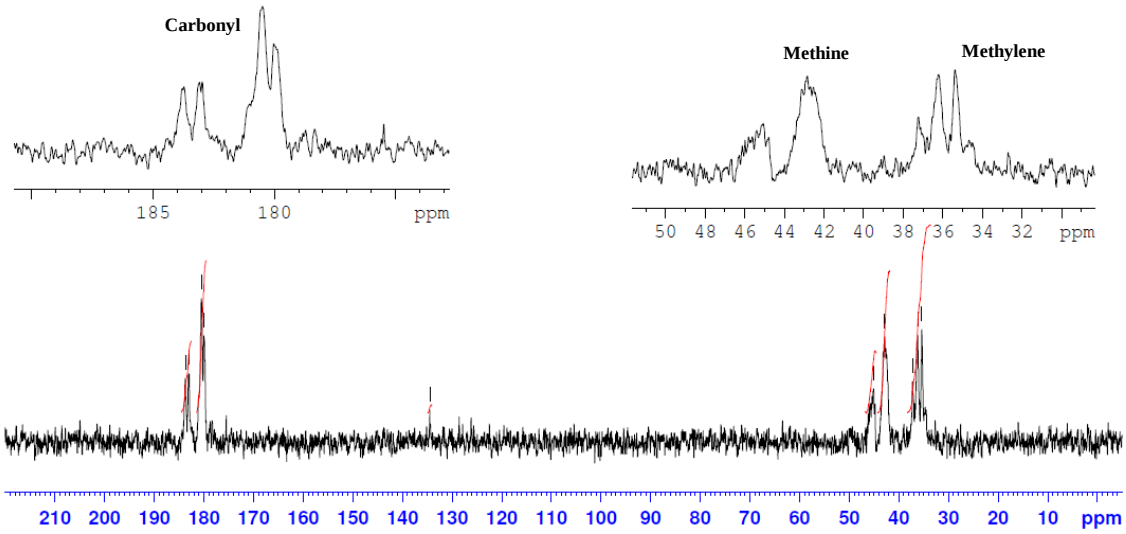

Figure 6-13: ^{13}C $\{^{1}H\}$ NMR spectrum for AAm/AAc copolymer; f_{0AAm}=0.46, cumulative F_{AAm}=0.66

Table 6-5 presents the experimental triad fractions from the ^{13}C NMR results (Figure 6-13) and those from the theoretical results (Figure 6-12). Comparing theses values suggests that the predicted triad fractions are quite reliable and can be used to study copolymer microstructure.

Table 6-5: Comparison of experimental (^{13}C NMR) and theoretical triad fractions for AAm/AAc copolymer, run 3

	AAm-centered (M_1)			AAc-centered (M_2)		
	A_{111}	$A_{112}+A_{211}$	A_{212}	A_{222}	$A_{221}+A_{122}$	A_{121}
NMR	0.27	0.58	0.15	0.02	0.36	0.62
Theory	0.31	0.49	0.19	0.03	0.30	0.66

6.3.5 Molecular weight

Molecular weights for AAm/AAc copolymer samples were estimated by GPC. Aqueous GPC test conditions, such as pH and type of the mobile phase, flow rate, polymer solution concentration and data analysis algorithms were selected after an extensive fine-tuning period to come up with an optimal sample analysis protocol. The test conditions are cited in Section 3.3. Typical chromatograms with detector responses (concentration, viscometer, and dual angle light scattering) along with the molecular weight response versus retention time are shown in Figure 6-14. The peak average molecular weight for the copolymer sample in this figure was estimated at 5 million.

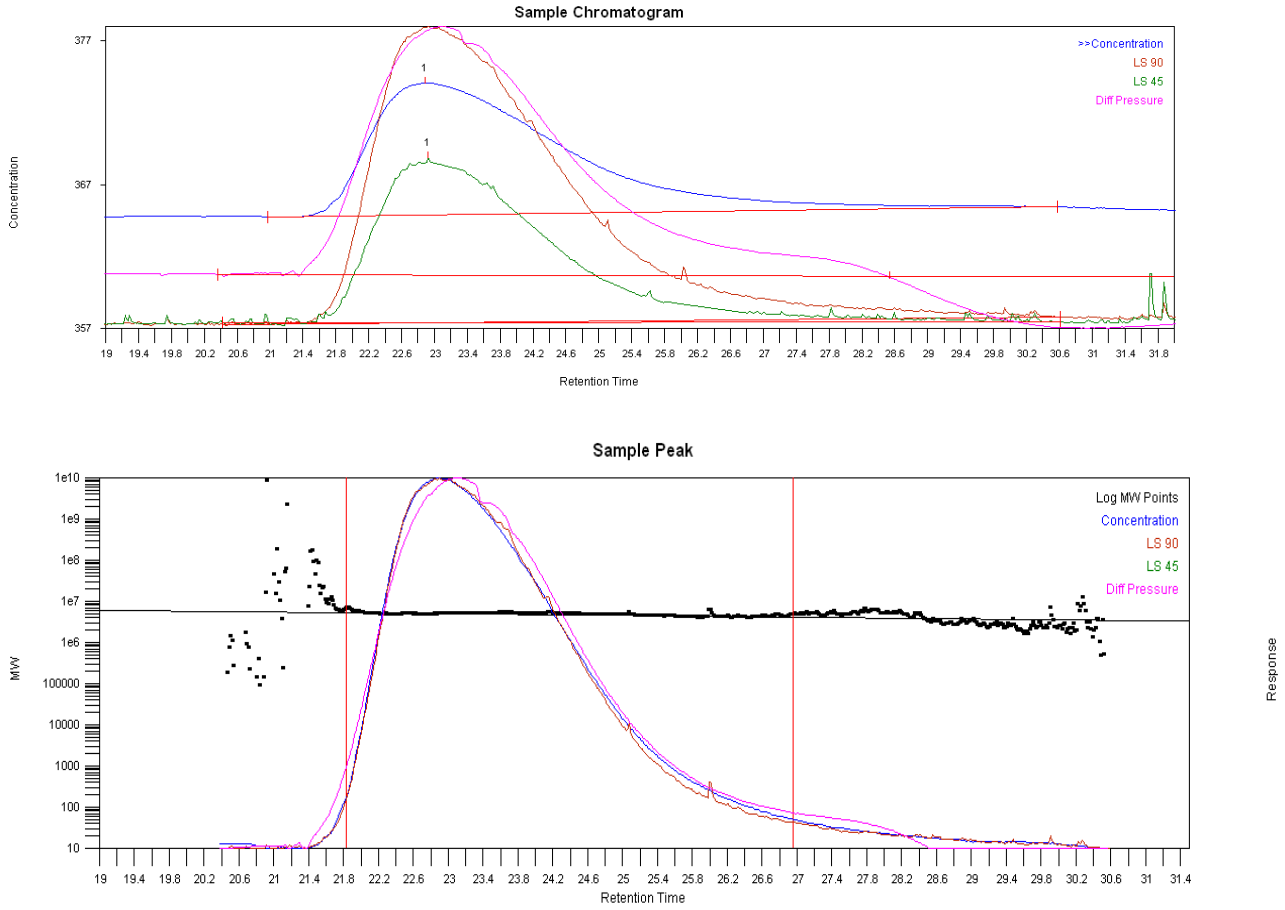

Figure 6-14: Typical detector responses from multi-detector aqueous GPC (upper panel) and molecular weight trend with retention volume (lower panel).

In multi-detector GPC, the radius of gyration is estimated from the hydrodynamic volume (determined from intrinsic viscosity and molecular weight obtained by the viscometer and light scattering detectors, respectively). Hydrodynamic volume is then used to calculate a particle scattering factor (a measure of the angular dissymmetry for large molecules) from the Debye expression and then used in the Zimm equation. Therefore, the value determined for molecular weight is affected by the hydrodynamic volume of the copolymer chain, and

any factor that influences hydrodynamic volume can change the molecular weight. In polyelectrolytes, variations in copolymer composition and sequence length distribution define the electrostatic environment of the copolymer chain and, as a result, alter the hydrodynamic volume. In addition, high molecular weights and subsequently high viscosities (especially for the AAm/AAc copolymer solutions) make it very difficult to obtain a perfectly homogeneous solution. Mendichi and Schieroni have stated that for polyelectrolytes and ultra-high molecular weight hyaluronic acid polymers, simple equilibrium between permeation and exclusion of the macromolecules in the column pores is not the only important mechanism for size exclusion.[90] Another important mechanism, that of "retardation" or entrapment also plays an important role in the fractionation of the polymer chains with high hydrodynamic volumes. This means that high molecular weight polymer chains elute from the column at longer times, because of the electrostatic interactions between the polyelectrolyte and the GPC column that introduces additional delay or retardation in the elution time. This can explain the marginal variation of the molecular weight curves with respect to retention time shown in Figure 6-14. This retardation effect causes an underestimation of the polymer molecular weights and polydispersity index (PDI) and is likely the reason for getting PDI values around 1 for almost all of the samples. This is not reasonable for a free radical polymerization and is not expected looking at the range of elution volumes for the peak. The overall implication is that the assumption of monodisperse slices for molecular weight analysis is not met and so slices at high retention volumes in the GPC elution profile contain portions of high molecular weight polymer which is indicated by the results from light scattering.

The molecular weight versus retention volume result in Figure 6-14 is clearly unreasonable as there is no decreasing trend in molecular weight with respect to the retention volume. It is expected to see a line with negative slope as high molecular weight species exit at lower retention volume, while low molecular weight chains leave the column at higher retention volume. This phenomenon has been observed previously for polymers in aqueous GPC by Mendichi and Schieroni.[90]

Typical evolution of weight-average molecular weight, $\bar{M}_w$, with conversion for copolymerization at low AAm feed mole fraction is given in Figure 6-15. There is a decrease of weight-average molecular weight with respect to monomer conversion, which is as expected for solution polymerization when there is no gel effect. This trend was observed for all copolymerizations at the other conditions.

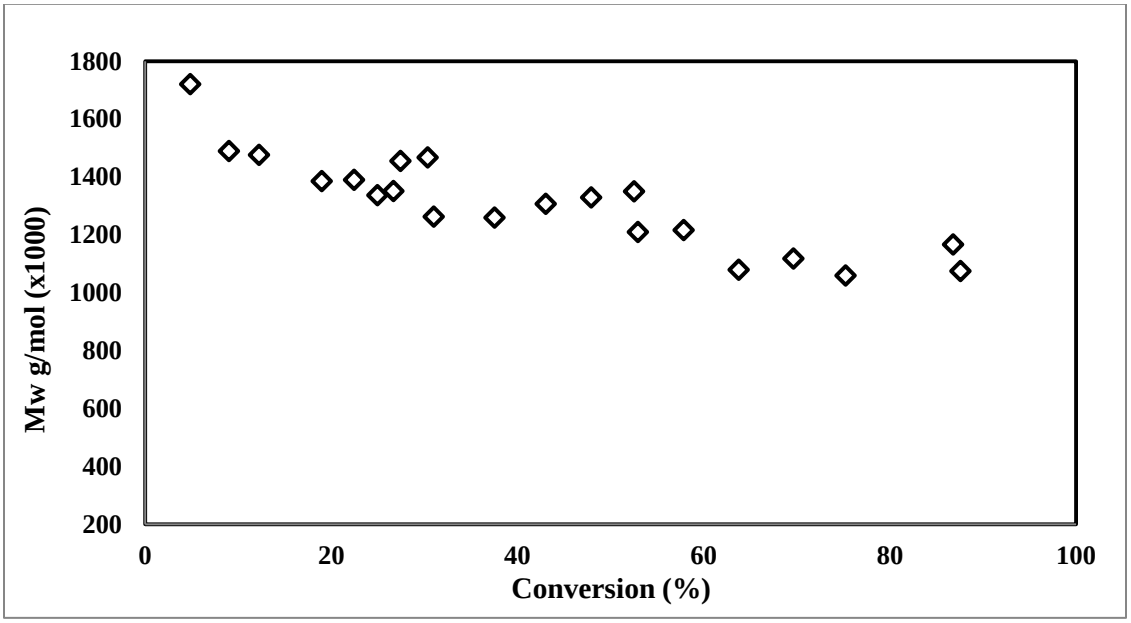

Figure 6-15: Weight average molecular weight at pH=7, [M]=1, f_{0AAm}=0.1 vs. conversion

Peak average molecular weights for the runs at different monomer concentrations but constant pH=3 and 20-30% conversion are shown in Figure 6-16. Considering each monomer concentration, it can be seen that increasing the AAm mole fractions in the feed increases the molecular weight of the copolymer. For example, at monomer concentration of 1.0 M, increasing the feed fraction from 0.1 to 0.46, and then to 0.68, causes an increase in the average molecular weight values from 1.7 to 2.4, and then to 4.3 million. It can also be noted from the data in Figure 6-16 that by increasing monomer concentration, the molecular weight values increase, which is expected for typical free radical polymerizations. Considering f_{0AAm}=0.10, by increasing monomer concentration from 0.5 to 1.0 and then to 1.5 M, the average molecular weights have changed from 1.2 to 1.8, and then to 2.6 million. It should also be mentioned that no specific trend was observed for the effect of pH on copolymer molecular weights.

Since the molecular weight of the copolymer plays an important role in determining its rheological properties and therefore application performance, the usual aim for AAm/AAc copolymers for EOR applications is to deliver a high average molecular weight in the range of 4 to 30 million g/mol (most commonly around 9 million g/mol).[45] By running the copolymerization at high monomer concentration with a high fraction of AAm in the monomer feed, for example, one could reach higher molecular weight values, as the trends of Figure 6-16 indicate.

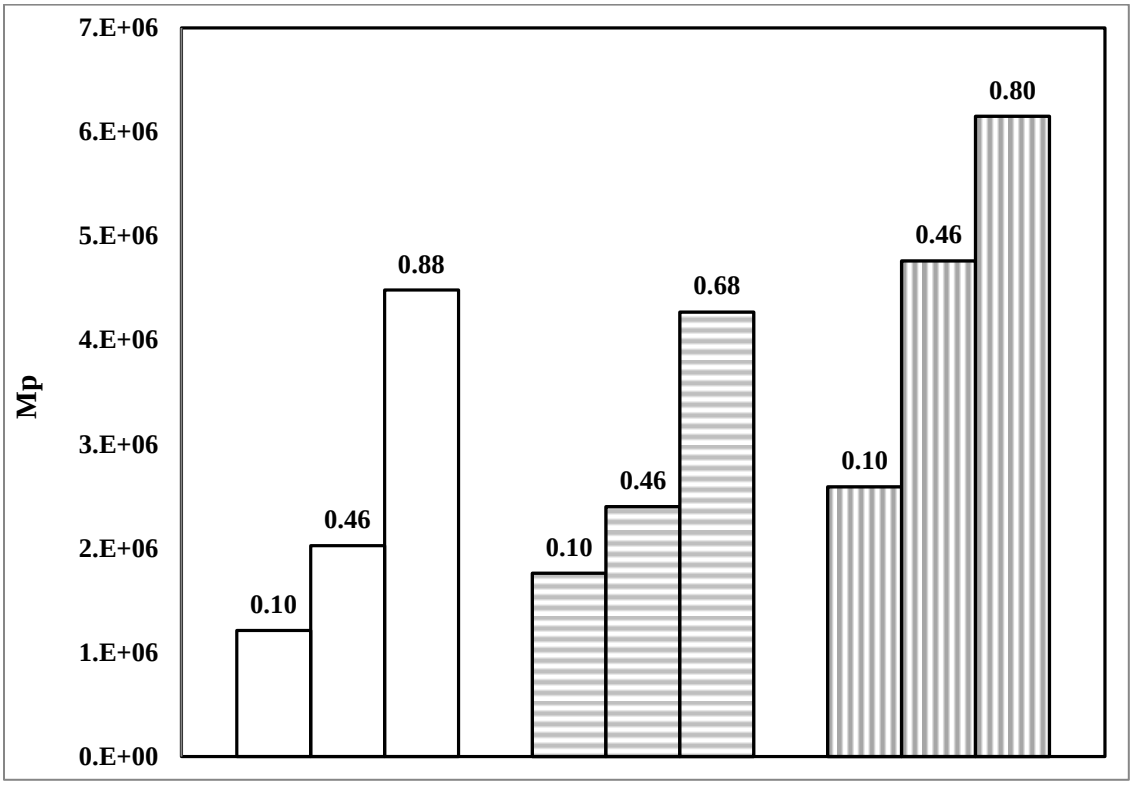

Figure 6-16: Peak average molecular weights at pH=3 for [M]=0.5 M (no-fill), [M]=1.0 M (horizontal fill), and [M]=1.5 M (vertical fill). Numbers on the bars represent the feed mole fraction of AAm (f_{0AAm})

6.3.6 Shear viscosity

The shear viscosity of a copolymer solution is extremely important in determining the performance properties of AAm/AAc copolymers. Copolymers with selected properties were prepared in order to study the effect of polymer concentration, copolymer composition, and salinity on the shear viscosity of the copolymer solutions. These preliminary rheology tests were done in order to understand the shear viscosity behavior of AAm/AAc solutions. Copolymers were dissolved in high purity water or an aqueous solution of sodium nitrate,

$NaNO_3$ (0.2 M), and sodium phosphate, NaH_2PO_4/Na_2HPO_4 (0.01 M), with pH adjusted to 7. This was done to evaluate the effect of salts on the shear viscosity of polymers as opposed to pure water. It was crucial to grind the polymer into a fine powder before dissolving it in water or brine and also add the powder gradually with some agitation; since the viscosity of polymer solutions is very high (otherwise, homogeneous polymer solutions cannot be obtained). The polymer solution concentration was varied between 0.01 and 0.005 g/ml to check the effect of polymer concentration on shear viscosity.

All shear viscosity measurements were replicated independently and average values are reported herein. For example, in Figure 6-17, the shear viscosity of AAm/AAc copolymer with cumulative copolymer composition of AAm equal to 0.44, cum F_{AAm}=0.44, is shown for two independent replicates. As one can easily see, the shear viscosity profiles are very close and as a result the average of the two runs is reported further in this section.

The effect of polymer concentration on the shear thinning behavior of copolymer solutions was studied first. Figure 6-18 shows the shear viscosity of two AAm/AAc copolymer solutions of different polymer concentrations versus shear rate at 25 ºC. Both polymer solutions exhibit shear thinning (pseudo-plastic) behavior, because of uncoiling, chain alignments, and dissociation of chain entanglement with increasing shear rate, with an obvious increase of shear viscosity at higher copolymer concentration.

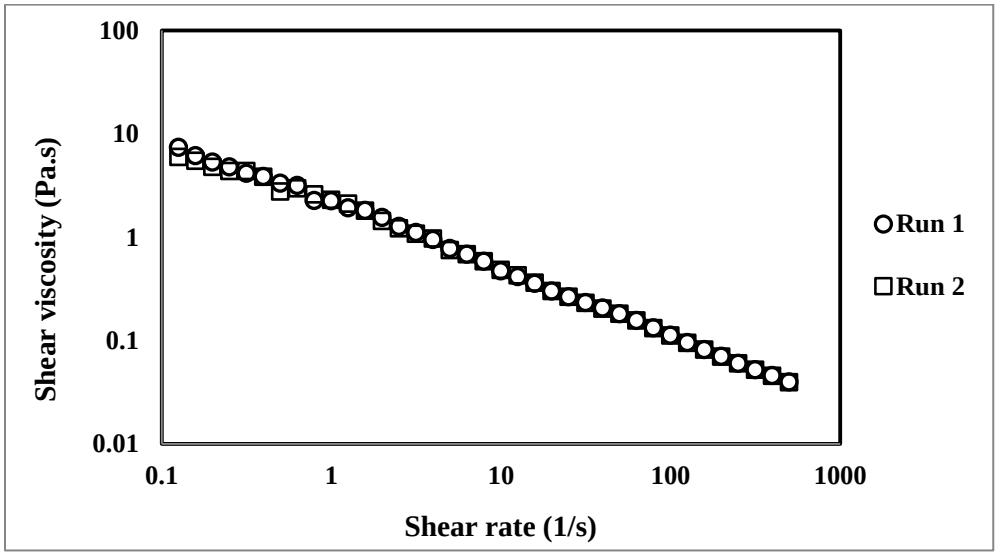

Figure 6-17: Shear viscosity of AAm/AAc copolymer aqueous solutions with cum F_{AAm}=0.44 and polymer solution concentration of 0.01 g/ml, versus shear rate at 25 ºC; two independent replicates

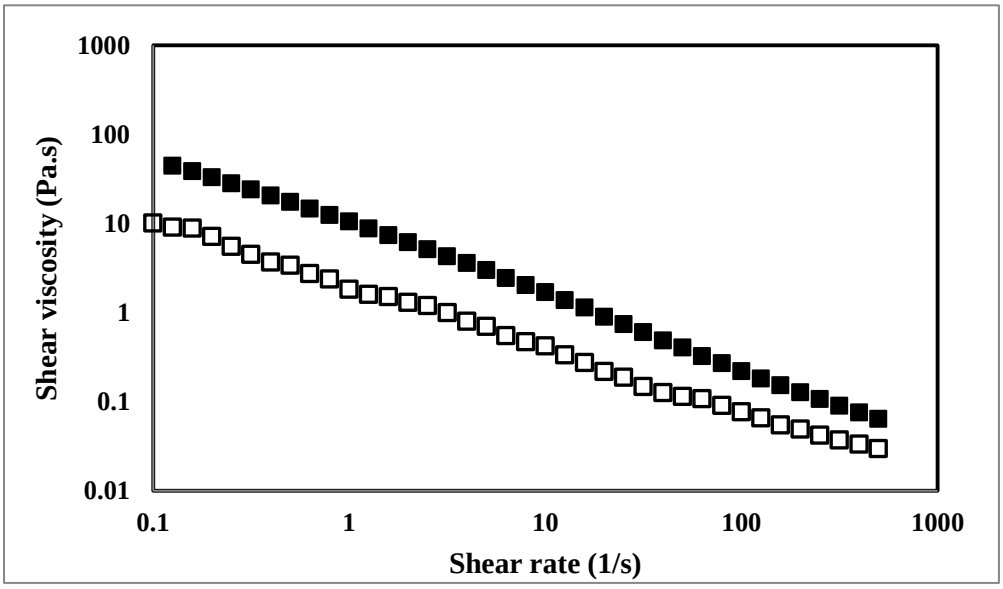

Figure 6-18: Shear viscosity of AAm/AAc copolymer aqueous solutions with cum F_{AAm}=0.77, versus shear rate, at two polymer solution concentrations: 0.01 g/ml (filled squares) and 0.005 g/ml (open squares) at 25 ºC

In order to check the effect of salinity on solution viscosity, two sets of polymer solutions were prepared in high purity water and buffer solution. The buffer solution was an aqueous solution of $NaNO_3$ (0.2 M) and NaH_2PO_4/Na_2HPO_4 (0.01 M) with pH=7. Representative results of shear viscosity versus shear rate are shown in Figure 6-19 to highlight the effect of the presence of salts in the solutions on shear viscosity.

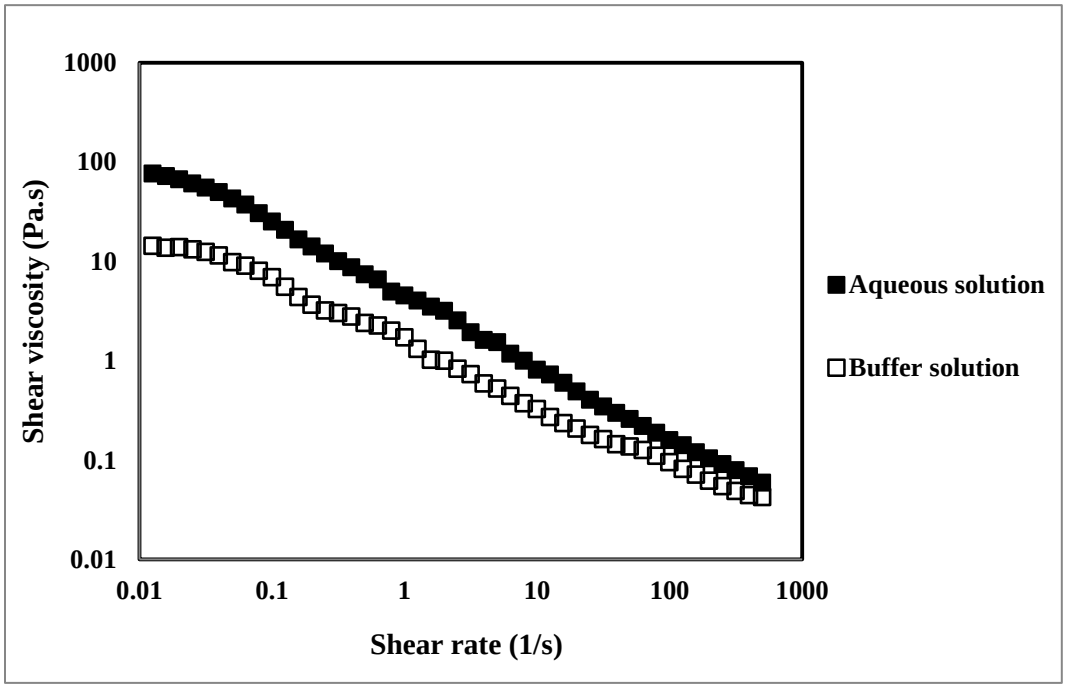

Figure 6-19: Shear viscosity of AAm/AAc copolymer solutions with cum F_{AAm}=0.64 and polymer solution concentration of 0.01 g/ml; aqueous solution with high purity water (filled squares) and buffer solution with added salts (open squares) versus shear rate at 25 ºC

The polymer in buffer solution exhibited a noticeable reduction in shear viscosity compared to the polymer dissolved in pure water. In the presence of sodium nitrate and sodium phosphate salts, the negative charges on the copolymer chain and, consequently, the electrostatic repulsions within the polyelectrolyte solution are neutralized (collapse of the electrostatic fields surrounding the copolymer). Therefore, the polymer chain conformation changes from a stretched chain to a random coil structure. Hence, it can be concluded that by adding salts in the solution, the polymer coil dimensions and, subsequently, solution viscosity decrease. This is in agreement with what has been reported in the literature for this copolymer.[55,55]

The other important factor that affects the solution viscosity is copolymer composition. The shear thinning behavior of AAm/AAc copolymers with various copolymer compositions is shown in Figure 6-20. As can be seen from Figure 6-20, depending on the AAm fraction in the copolymer chains, different solution viscosity profiles arise.

At first glance, the shear viscosity profiles of Figure 6-20 look puzzling. As cum F_{AAm} increases from 0.2 to 0.72, shear viscosity values increase as well. But then an interesting reversal takes place at cum F_{AAm} of 0.77. Although the copolymer composition is lower than 0.87, the shear viscosity is higher. Furthermore, the polymer with 0.96 AAm cumulative copolymer composition exhibits viscosity values almost as low as the ones for cum F_{AAm}=0.2.

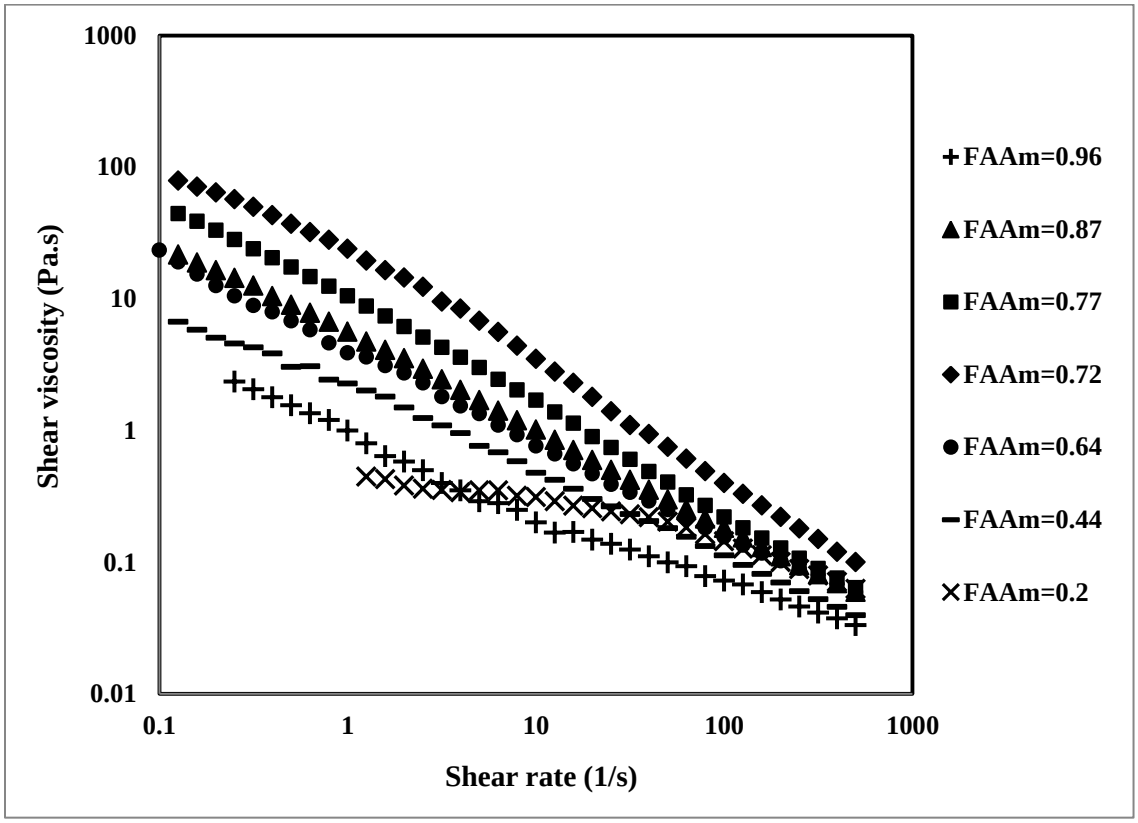

Figure 6-20: Shear viscosity of AAm/AAc copolymer aqueous solutions with polymer solution concentration 0.01 g/ml versus shear rate at 25 ºC; effect of copolymer composition

Since the target application of this copolymer is in EOR, the shear viscosity of these copolymers can more meaningfully be compared at a shear rate equal to 7 (1/s), which is a typical shear rate in oil fields. The results of this comparison are presented in Figure 6-21, and the behavior can explain the observations in Figure 6-20 discussed above. Based on Figure 6-21, it can be seen that the copolymer with AAm cumulative fraction of 0.72 has the highest shear viscosity among the copolymers. Therefore, AAm/AAc copolymers with around 30% AAc content provide the highest shear viscosity and are thus favorable in EOR

because of their viscosity enhancement capability, which is one of the main desirable characteristics for polymer flooding.

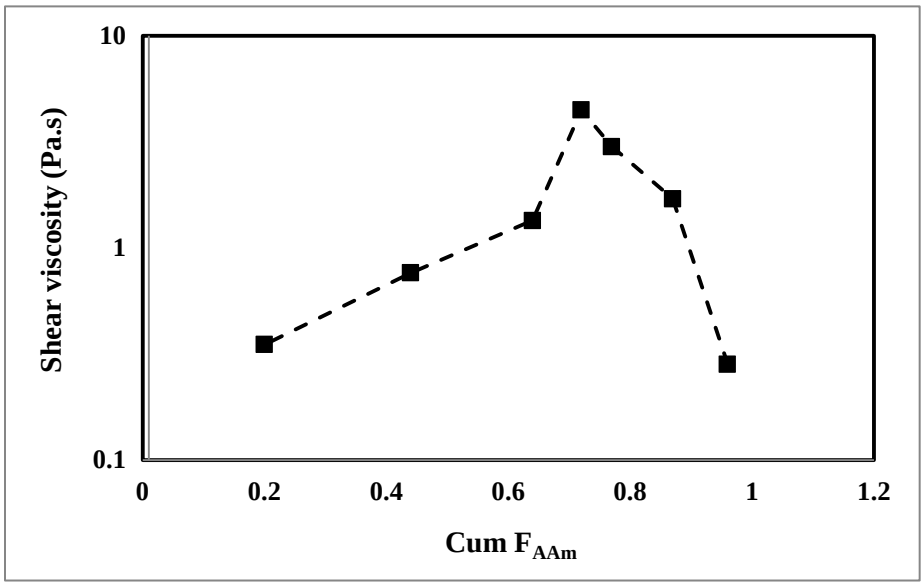

Figure 6-21: Shear viscosity at a shear rate of 7 (1/s) for AAm/AAc copolymer aqueous solutions versus cumulative copolymer composition at fixed polymer solution concentration of 0.01 g/ml and 25 ºC.

The copolymer composition changes the electrostatic environment of the copolymer, and as a result the copolymer chain size and solution properties will be different for given molecular weights. By having more AAc (or less AAm) in the copolymer, more electrostatic interactions will be involved. These interactions extend the polymer chains and this increases the shear viscosity. In the presence of salts in the solution, these electrostatic repulsions are screened and therefore the polyelectrolyte nature does not play such a dominant role in the

shear viscosity behavior of the solution. Instead, having more AAc enhances the chance of intramolecular hydrogen bonding and chain stiffness, and therefore increases shear viscosity of the polymer solution. On the other hand, having more AAm in the copolymer increases the copolymer molecular weight based on results from Section 6.3.5. These observations show the occurrence of a maximum effect with regards the copolymer composition on the shear thinning behavior of copolymer solutions. In other words, there is a specific copolymer composition at which the shear viscosity of the solution is maximum for a given molecular weight (see Figure 6-21), and the region of the maximum should be used in order to obtain the highest viscosity enhancement, as needed for EOR applications.

6.4 Concluding remarks

Effects of two important factors, total monomer concentration and solution pH, on various responses including reactivity ratios and copolymer microstructure/property characteristics for AAm/AAc copolymerization were studied. Changing monomer concentration and pH was able to shift monomer reactivity ratios to different regions. Instantaneous and cumulative copolymer compositions also changed based on reaction pH. By increasing pH from 3 to 7, one could observe a reversal in the behavior of copolymer composition trends. Peak average molecular weights of the copolymer were found to be dependent on monomer concentration and feed fractions. Having more AAm in the feed and making a more concentrated monomer solution could increase the peak average molecular weight of the copolymer. AAm/AAc copolymer sequence length distribution and triad fractions were also affected by pH. Solution

pH dictated the instantaneous and cumulative sequence length distribution characteristics along with the triad fractions of monomer units in the copolymer chain. Theoretical results were confirmed by ^{13}C NMR. Regarding the shear viscosity of the copolymer, it was observed that having concentrated copolymer solutions enhanced the shear viscosity. In addition, shear viscosity decreased in the presence of salts in the polymer solution because of neutralizing the electrostatic repulsions between the chains. Moreover, the shear viscosity of AAm/AAc copolymer solutions exhibited a maximum around 30% AAc (70% AAm) in the copolymer. Hence, in order to achieve higher solution viscosity, which is required in EOR applications, one can make concentrated polymer solutions with copolymer composition around 30% AAc. In other words, by adjusting the copolymer composition and solution concentration, the shear viscosity of AAm/AAc copolymers can be maximized.

Chapter 7. Application Performance of AAm/AAc Copolymers in EOR

7.1 Introduction

Chapter 2 has described several factors that should be considered when designing a polymer for EOR applications. One should aim for maximum viscosity enhancement, water solubility, low polymer retention in the reservoir, and high mechanical, chemical, and thermal stability.[48] Taking into account all these important factors in polymer flooding, it is crucial to design and fine-tune the polymer for the application. In previous chapters, we established a structure-property framework for AAm/AAc copolymers which can be used for designing tailor-made polymers for polymer flooding applications. The work described in this chapter applies the previous knowledge to tailor-make AAm/AAc copolymers with high molecular weight, high AAm levels in the copolymer chain, limited composition drift for consistency, random distribution of AAc monomer along the chain, and also produced by reasonably fast polymerizations that go to high conversion.

In order to evaluate copolymer performance as in real oil reservoirs, it is crucial to determine polymer viscosity enhancement and polymer retention carefully. Polymer flooding tests in the sand-pack provide this valuable information for better understanding of the polymer

behavior in porous media. Subsequent heavy oil displacement tests also give information about the efficiency of oil recovery in a sand-pack designed to mimic real conditions.

7.2 Designing copolymers for EOR applications

7.2.1 Polymerization conditions

Copolymerizations were conducted at specific conditions to design tailor-made copolymers for EOR performance evaluation. A summary of the copolymerization conditions is given in Table 7-1. Other copolymerization conditions were as previously described in Chapter 3.

Table 7-1: Copolymerization conditions for designing copolymers for EOR

Polymer #	f_{0AAm}	pH	Monomer concentration (M)	Ionic strength (M)	NaCl (M)
1	0.65	5	1.5	0.45	0
2	0.75			0.33	0.12
3	0.85			0.19	0.26
4	0.95			0.07	0.39

All polymerization conditions were chosen based on the knowledge from Chapters 4 to 6 and additional justifications will be given below:

- The AAm monomer feed (mole) fractions were chosen between 0.65-0.95. This was done because a higher percentage of AAc in the copolymer makes the copolymer too sensitive towards brine salinity and this is not desirable for EOR. At the same time, a lower percentage of AAc in the copolymer increases the molecular weight and subsequently the

viscosity of the solutions for a given polymer concentration. Hence, the percentage target of AAc in the copolymer was chosen between 5 to 35%.

- Polymerization pH was selected at 5, because the minimum composition drift at all monomer feed ratios was observed only at this pH.
- Total monomer concentration of 1.5 M was selected to make the chains longer, which is desirable for EOR. Moreover, using high monomer concentration naturally means a larger amount of polymer could be obtained for characterization and the subsequent EOR tests.
- The ionic strength among the four runs of Table 7-1 varied based on the fraction of AAc monomer in the feed. Therefore, pre-calculated amounts of NaCl were added to adjust the ionic strength among the runs to a similar value (as described in Chapter 5).

7.2.2 Tailor-made AAm/AAc copolymer properties

Copolymer composition was determined by elemental analysis and the results for all four runs along with monomer conversions are given in Appendix D. Average cumulative copolymer compositions are presented in Table 7-2. As can be seen, the cumulative copolymer composition of AAm was very close to the initial fraction of AAm in the feed, as expected from the trends described in Chapter 6. The copolymer composition of the reference polymer that is commercially available is also presented in Table 7-2.

Table 7-2: Cumulative copolymer composition of AAm in tailor-made AAm/AAc copolymer

Polymer #	f_{0AAm}	Cum F_{AAm}
1	0.65	0.675
2	0.75	0.768
3	0.85	0.862
4	0.95	0.931
Reference	N/A	0.920

In summary, the cumulative copolymer composition range was selected at cum F_{AAm}=0.65-0.95, with more AAm monomer units in the copolymer compared to AAc monomer. Based on copolymer composition results and conversion values (see Appendix D), reactivity ratios were re-estimated by EVM and the DNI approach (same methodology as described earlier in Chapter 4). The reactivity ratio point estimates are given in Table 7-3. The results are consistent with the reactivity ratios estimated for similar conditions (pH=5, total monomer concentration=1.5 M) discussed in Chapter 6.

Table 7-3: Reactivity ratios for tailor-made AAm/AAc copolymers

r_{AAm}	r_{AAc}
0.86	0.87

Since the reactivity ratios of two monomers are equal and close to 1, it was expected to observe no composition drift in the resulting copolymer. The AAm monomer feed fraction and copolymer composition, including instantaneous copolymer composition (F_{AAm}) and

cumulative copolymer composition (cum F_{AAm}), for all runs are shown in Figure 7-1. As expected, there was almost no composition drift in cumulative copolymer composition at all monomer feed ratios.

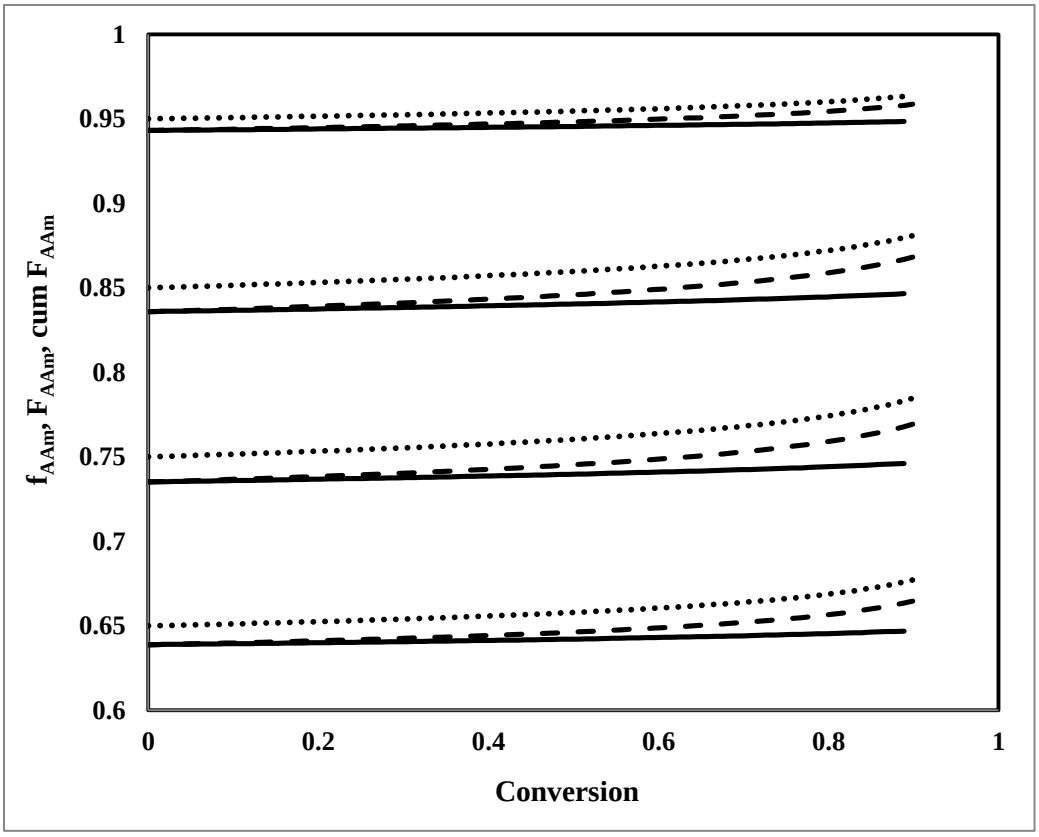

Figure 7-1: AAm monomer feed fraction (dotted line); F_{AAm} (dashed line); cum F_{AAm} (solid line) for tailor-made AAm/AAc copolymers

Since $r_{AAm} \times r_{AAc}$ is equal to 0.75, it is expected to obtain an alternate-random copolymer with higher probability of random distribution of monomer units along the chain. A random

distribution of anionic charges separated along the chain is more favorable compared to polymers with uneven and possibly clustered distribution of charges on the chain.[45]

To achieve a better insight into the copolymer microstructure, the sequence length distributions of the tailor-made AAm/AAc copolymers were calculated (Equation 6-1). Figure 7-2 shows the probability of sequence length distribution of AAm (top plot) and AAc (bottom plot) in the copolymer chains at various monomer mole fractions in the feed. In general, as sequence length (l) increased, a decrease was observed in the probabilities of AAm and AAc sequences in the copolymer. Moreover, the sequence length distribution of AAm was broader compared to that for AAc, because the initial feed solutions were all richer in AAm monomer and as a result it was more probable for AAm monomer to be incorporated in the chain. Therefore, overall, it was expected to get a random distribution of the two monomers along the copolymer chain with a higher probability of having longer AAm sequences.

The cumulative number average sequence length of monomers with conversion was also calculated (Equation 6-5) in order to determine the average number of monomer units connected together consecutively with respect to conversion. Figure 7-3 shows the cumulative number average sequence length of AAm in the tailor-made AAm/AAc copolymers. As can be seen from Figure 7-3, there was almost a flat profile for AAm cumulative sequence length versus conversion. This means that the cumulative number average sequence of AAm units in the copolymer did not change with conversion and was higher when the initial fraction of AAm in the feed was higher.

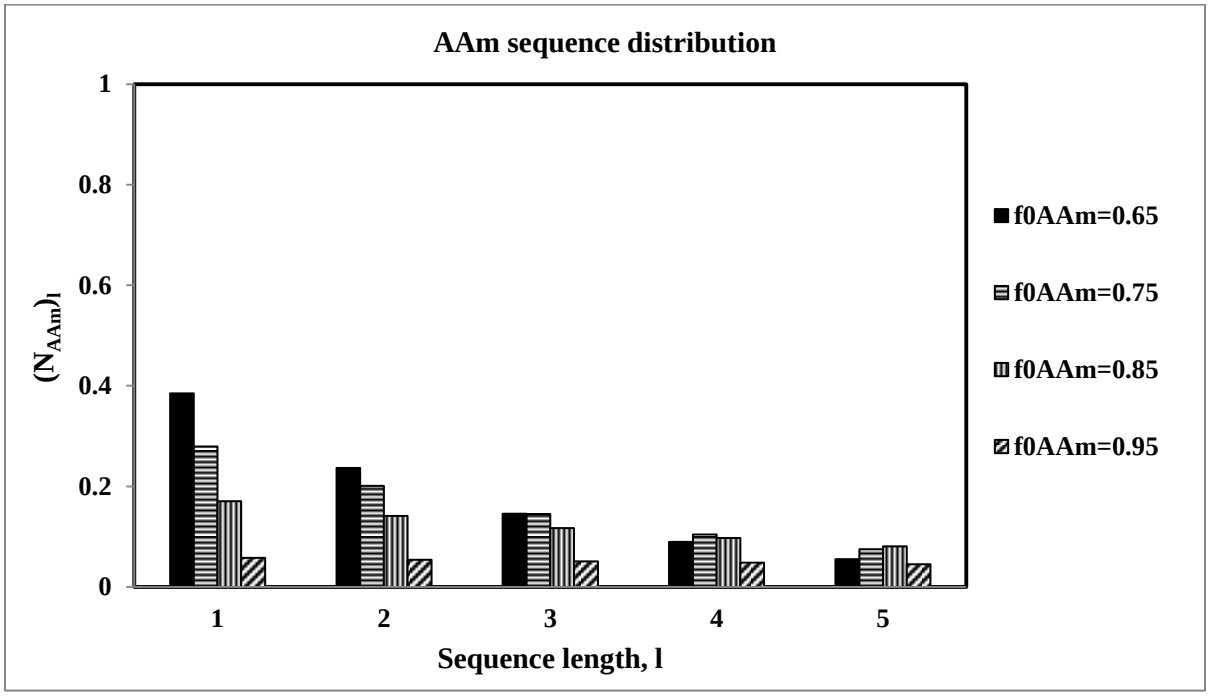

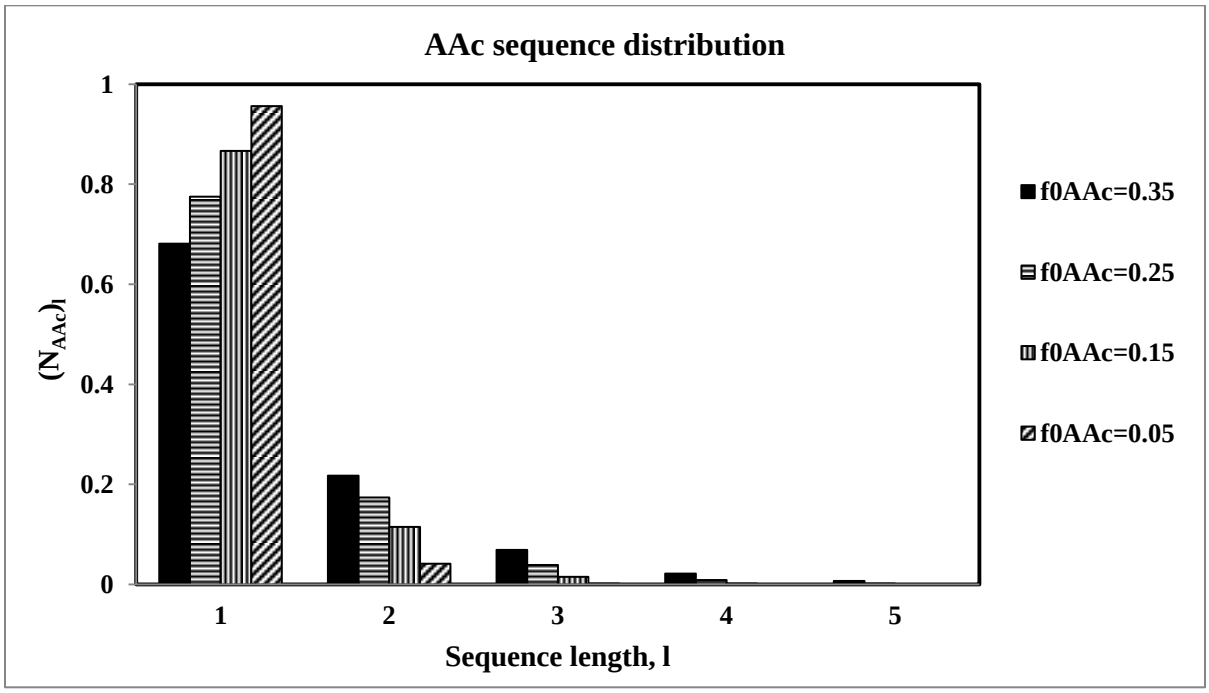

Figure 7-2: Sequence length distributions of AAm/AAc copolymer at various monomer feed compositions

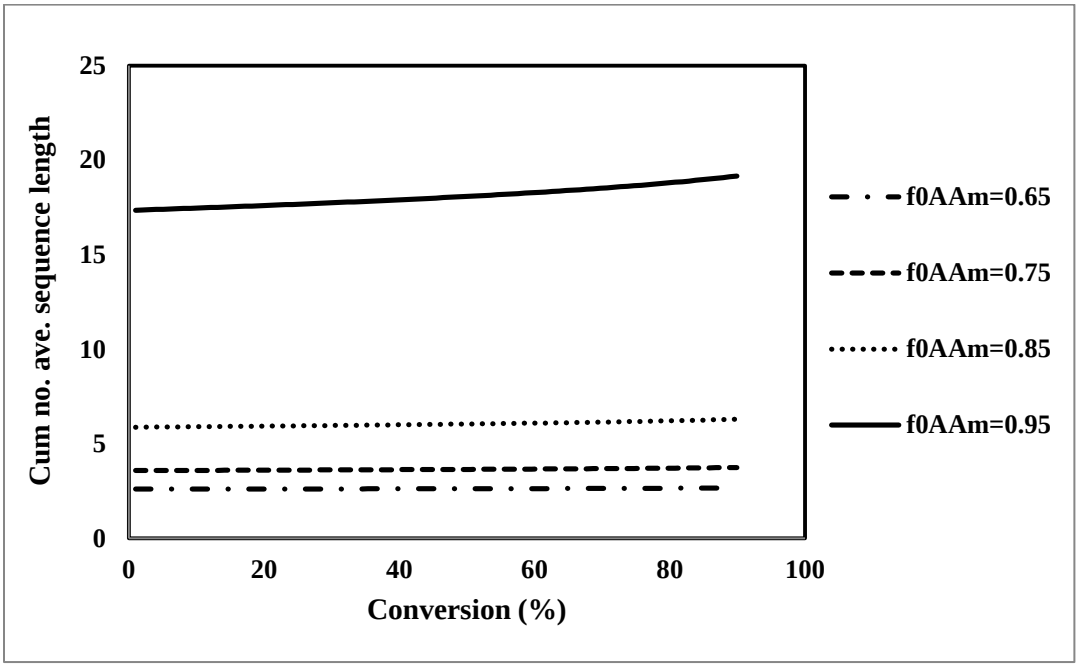

Figure 7-3: Cumulative number average sequence length of AAm in the copolymer versus conversion

In order to achieve better performance of the AAm/AAc copolymers in EOR applications, the aim was a high molecular weight copolymer. High molecular weight polymer has a high level of chain entanglements, and as a result, this increases the solution viscosity further. At the same time, if the molecular weight of the polymer is too high, the polymer chain becomes too sensitive to shear degradation and injectivity issues can be observed. Therefore, we aimed at a 'happy medium' molecular weight between 4-9 million to have the benefit of high molecular weight polymers and at the same time avoid issues with overly high molecular weight chains. Molecular weights of the tailor-made and the reference polymer were measured by GPC. A typical GPC chromatogram for polymer 3 is depicted in Figure 7-4.

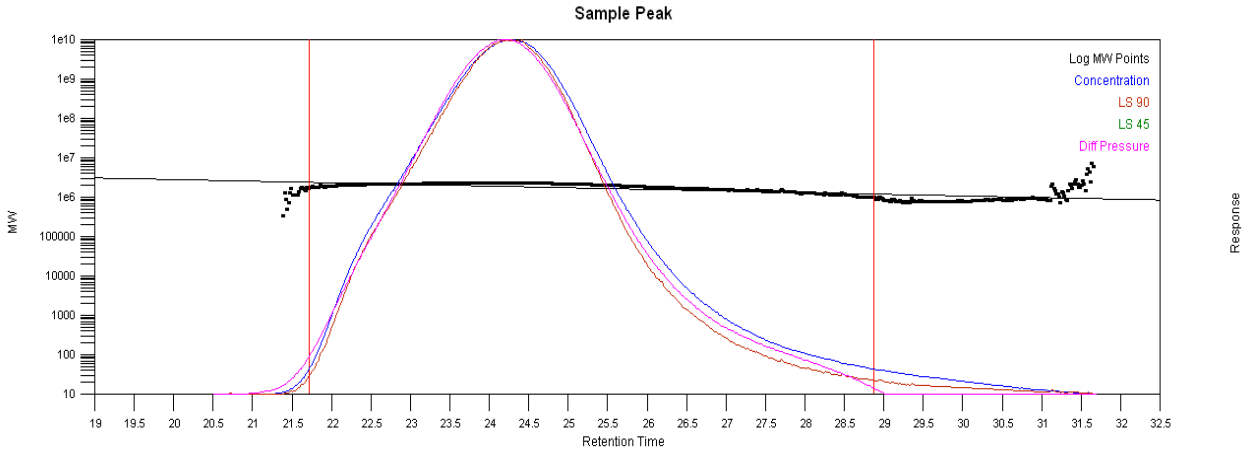

Figure 7-4: Molecular weight profile with retention time from multi-detector aqueous GPC for polymer 3

The peak average molecular weights are presented in Table 7-4. The molecular weights of designed copolymers varied between 4 to 10 million, as expected for the selected polymerization conditions. The peak average molecular weights, showed a maximum behavior with respect to the copolymer composition, with the highest molecular weight observed for polymer 2 with cum F_{AAm}=0.768.

Table 7-4: Peak average molecular weight for AAm/AAc copolymers

Polymer #	Mp (g/mol)
1	6.0 E+06
2	9.0 E+06
3	7.8 E+06
4	4.5 E+06
Reference	4.0 E+06

Shear viscosity tests were conducted by parallel plate rheometer to investigate the effect of shear rate on polymer solution shear viscosity (Table 7-5). It should be mentioned that the shear viscosity tests were conducted at 1 and 7 (1/s) shear rates, which was similar to the average shear rates encountered during actual conditions far from the injection port in oil reservoirs.[74]

Table 7-5: Shear viscosity tests of polymer solutions (1 wt% concentration in brine) with parallel plate rheometer

Polymer #	Shear viscosity (Pa.s)	
	$\dot{\gamma}$=1 1/s	$\dot{\gamma}$=7 1/s
1	3.41	0.89
2	3.90	1.00
3	1.92	0.68
4	1.35	0.55
Reference	0.96	0.37

The results from shear viscosity tests revealed that having more AAc in the copolymer increases the shear viscosity up to the expected limiting composition. Considering the polyelectrolyte nature of AAm/AAc copolymers because of having ionizable AAc monomer units, this trend is reasonable. These results are also in agreement with molecular weight results presented in Table 7-4.

Frequency sweep tests were subsequently conducted to study the viscoelastic behavior of the polymer solutions. A strain sweep test is the prerequisite for a frequency sweep test to detect

the linear viscoelastic region. Figure 7-5 shows a sample of such a strain sweep test (at a fixed frequency of 1 rad/s) that was done for the reference polymer sample. As can be seen from Figure 7-5, both storage (elastic) modulus, G', and loss (viscous) modulus, G", exhibited linear behavior with respect to strain up to 40%. A 10% strain was selected for all subsequent tests to make sure that the tests were all within the linear viscoelastic region.

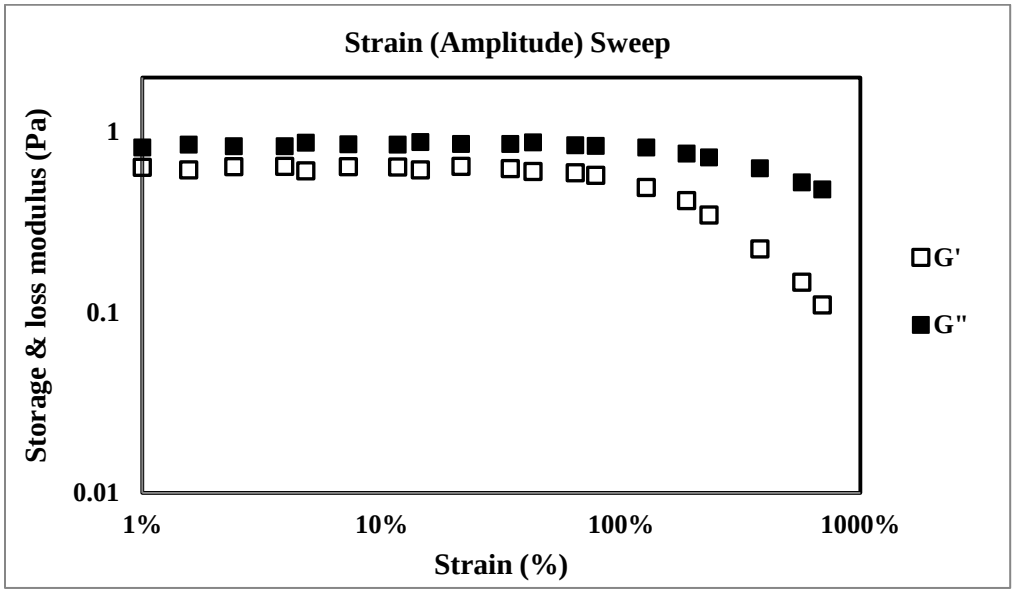

Figure 7-5: Strain sweep test; Storage modulus, G', and loss modulus, G', versus strain for reference polymer (1wt% concentration in brine solution)

Figure 7-6 presents the results from the frequency sweep tests, 0.01-100 rad/s, at fixed strain (10%) for all polymer solutions. All polymer solutions showed the same trend in terms of the storage and loss modulus. It can be seen that by having more AAc in the copolymer, higher storage and loss modulus values for polymer solutions could be obtained. This enhancement was more pronounced at lower frequencies.

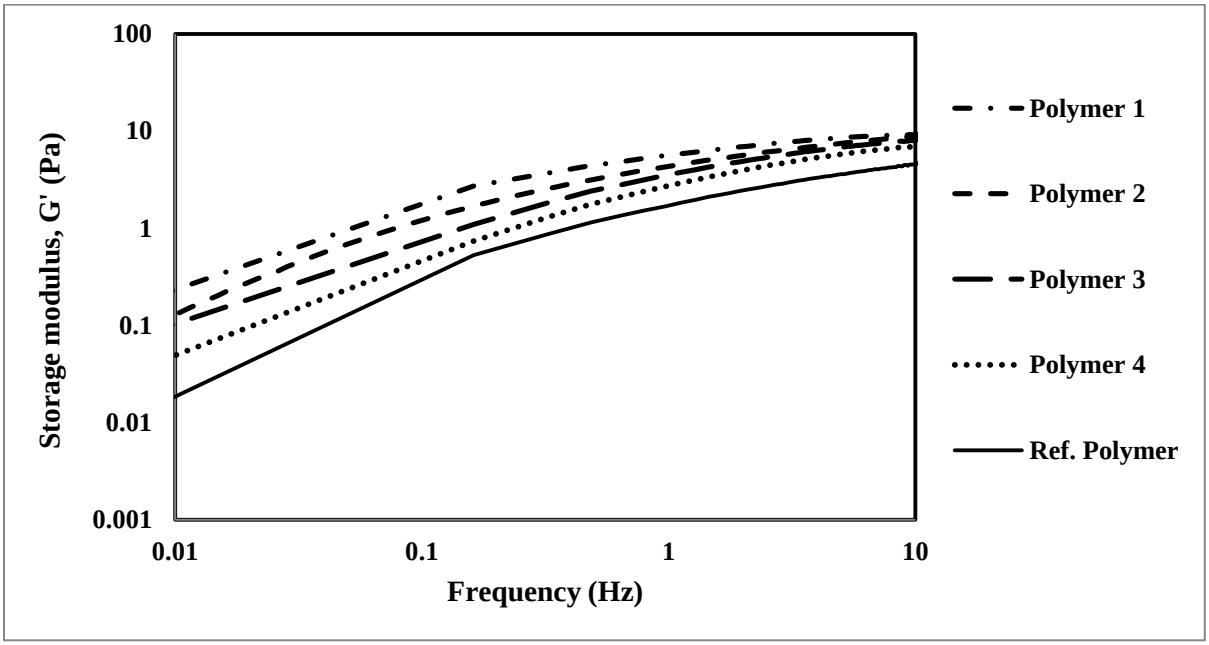

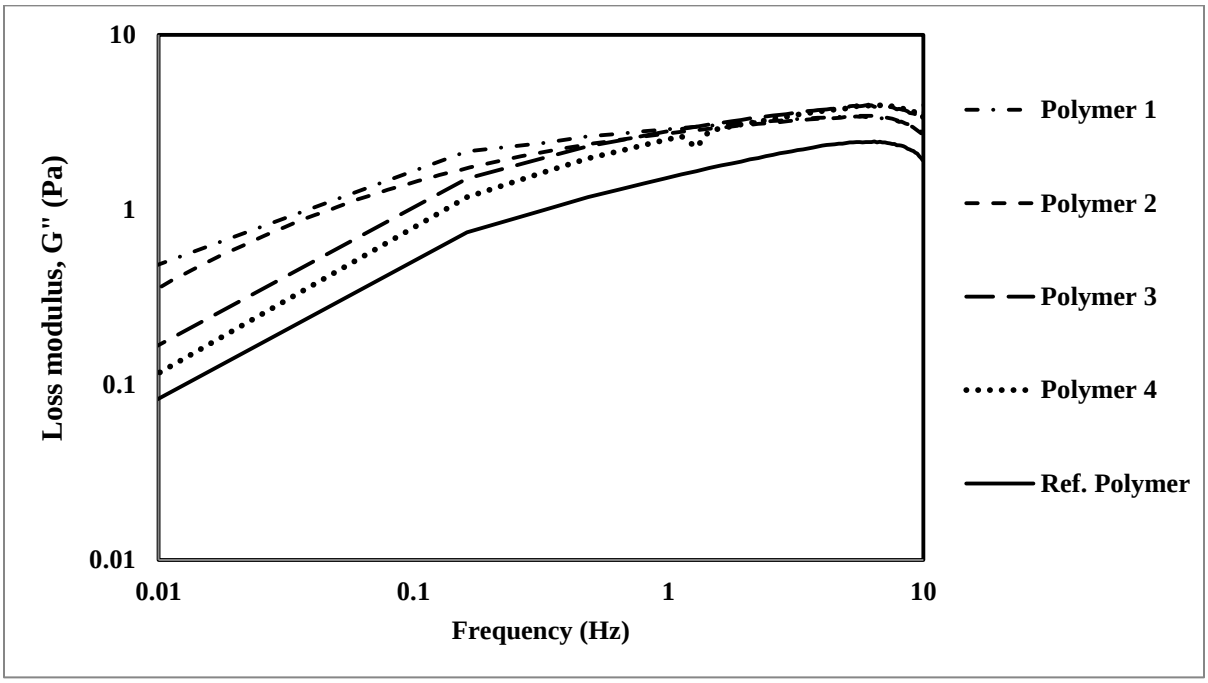

Figure 7-6: Frequency sweep tests (10% strain); storage (G') & loss (G") modulus versus frequency for polymer solutions (1 wt% concentration in brine)

Another criterion to evaluate the elastic nature of the polymer is the intersection of the two moduli (G' and G"). At this intersection (crossover) point, the values of both moduli are equal. In the G'<G" region, the polymer solution behavior is considered more viscous and less elastic, whereas in the G'>G" region, the polymer solution is considered less viscous and more elastic. The crossover frequency values are given in Table 7-6. Results showed that having more AAc units in the copolymer reduced the crossover point frequency and therefore enhanced the elasticity of the polymer solution. In other words, copolymers with a higher AAc content exhibited less viscous behavior over the studied range of frequencies. That means that the elastic response of the copolymer was stronger than the viscous response in the frequency range studied.

Table 7-6: Crossover frequency for AAm/AAc copolymer solutions in frequency sweep

Polymer #	Cross-over frequency (Hz)
1	0.03
2	0.17
3	0.42
4	0.73
Reference	0.55

Another way to evaluate the elasticity of polymers is by looking at the viscous to elastic modulus ratio (G"/G'). Figure 7-7 presents the G"/G' trends of AAm/AAc polymer solutions. The results suggested that polymer 4 and the reference polymer showed a similar behavior. Polymer 1 had the lowest G"/G' ratio, indicating this copolymer should have the highest

elasticity. It is important to know about the elasticity of the polymer solution, because it has been claimed in the literature that polymer solutions showing higher elasticity enhances the efficiency of oil recovery.[62]

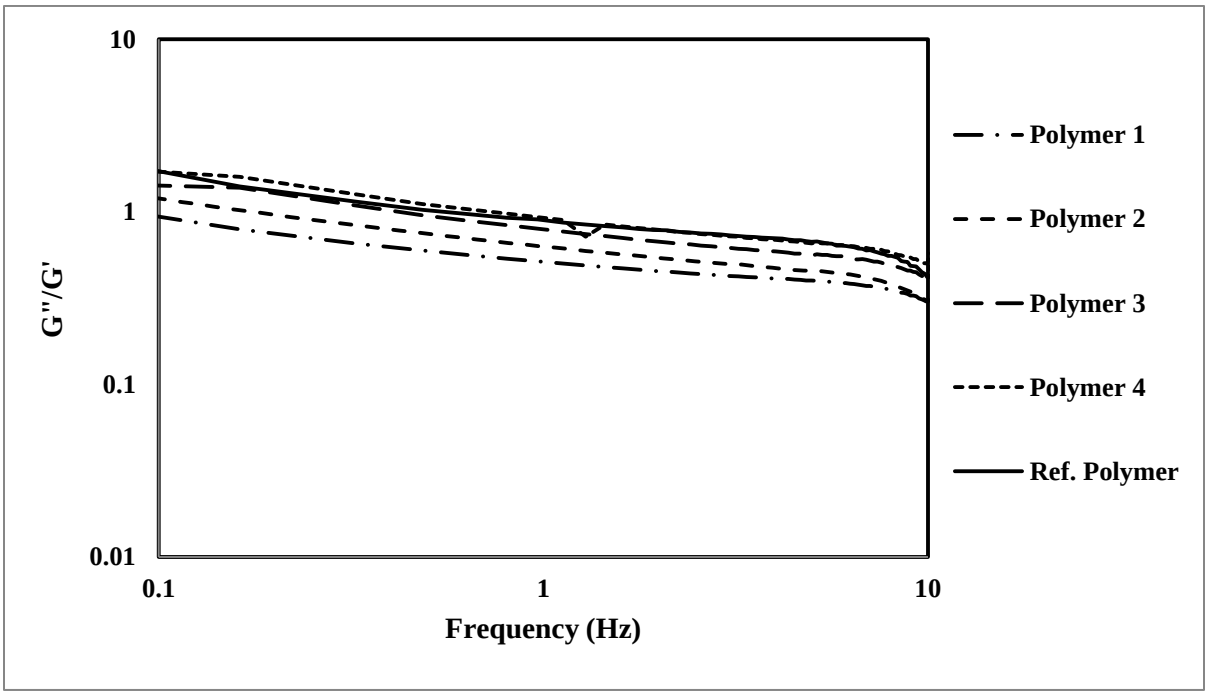

Figure 7-7: Loss over storage modulus ratio (G"/G') versus frequency for polymer solutions (1 wt% concentration in brine)

7.3 Results and discussion

7.3.1 Flow behavior characteristics

In the polymer flooding tests, a sand-pack was flooded with brine and polymer solution at fixed flow rate (the test procedure was described in Section 3.4.1). The sand-pack characteristics (including porosity, permeability, and pore volume) were similar to typical oil

reservoirs. The flow behavior of the polymer solutions in sand-pack porous media can be evaluated by the Resistance Factor (RF or Fr) and the Residual Resistance Factor (RRF or Frr).

The resistance factor, RF, is defined in Equation 7-1, where λ_w and λ_p are the mobility of the water and polymer solution, respectively.[48] It should be mentioned that λ_w can be replaced by λ_b (with subscript b denoting brine), if the water contains salt or if it is a brine solution.

$$RF = \frac{\lambda_w}{\lambda_p} = \frac{k_w/\mu_w}{k_p/\mu_p} \qquad \textbf{Equation 7-1}$$

μ in Equation 7-1 denotes the viscosity of either water or polymer solution. Permeability k of the porous media (in millidarcy, mD), can be determined from Equation 7-2.

$$k = 1000 \, \frac{L}{A} \, \mu \, Q \, \frac{1}{(P_0 - P_i)} \qquad \textbf{Equation 7-2}$$

where Q is the volumetric flow rate (ml/s), P_o and P_i are the outlet and inlet fluid pressures (atm), μ is the fluid dynamic viscosity (centipoise, cP), L is the length of the sand-pack (cm), and A is the cross-sectional area of the sand-pack (cm^2).

By inserting Equation 7-2 in Equation 7-1, at fixed flow rate, the resistance factor can be rewritten as Equation 7-3, where ΔP is the pressure difference across the sand-pack at steady state conditions:

$$RF = \frac{\Delta P_{(Polymer\ flooding)}}{\Delta P_{(Brine\ before\ polymer\ flooding)}}$$ **Equation 7-3**

The residual resistance factor, RRF, is defined by Equation 7-4, as the ratio of the mobility of water (or brine) before polymer injection over the mobility of water (or brine) after polymer flooding:

$$RRF = \frac{\lambda_b(Before\ polymer\ injection)}{\lambda_b(After\ polymer\ injection)}$$ **Equation 7-4**

RRF can also be rewritten with respect to the pressure difference across the sand-pack before and after polymer solution injection (Equation 7-5):

$$RRF = \frac{\Delta P_{(Brine\ after\ polymer\ flooding)}}{\Delta P_{(Brine\ before\ polymer\ flooding)}}$$ **Equation 7-5**

Sample calculations for RF and RRF values are given in Appendix E.

The permeability and porosity of the sand-pack were determined before each polymer flooding. The procedure was to inject brine at various flow rates and record the pressures

along the sand-pack. Representative data for one of the runs (polymer 1, run 2) are presented in Table 7-7.

Table 7-7: Pressure gauge readings before and after sand-pack at various brine flow rates for polymer 1

	Pressure gauge #1, before sand-pack						**Pressure gauge #6, after sand-pack**					
Flow rate (ml/min)	**25.0**	**30.0**	**35.0**	**40.0**	**45.0**	**47.5**	**25.0**	**30.0**	**35.0**	**40.0**	**45.0**	**47.5**
Pressure readings (psi)	6.2	8.0	7.5	8.6	9.1	9.5	0.0	0.0	0.0	0.0	0.0	0.0
	6.3	8.2	8.2	8.7	9.4	9.3	0.0	0.0	0.0	0.0	0.0	0.0
	5.9	8.0	9.0	9.0	9.6	9.5	0.0	0.0	0.0	0.0	0.0	0.0
	7.6	8.0	9.8	9.3	10.9	12.1	0.0	0.0	0.0	0.0	0.0	0.0
	6.1	7.2	8.2	9.8	10.7	10.9	0.0	0.0	0.0	0.0	0.0	0.0
	5.4	6.9	8.2	9.9	10.6	10.8	0.0	0.0	0.0	0.0	0.0	0.0
	5.3	6.8	8.3	9.7	10.6	10.6	0.0	0.0	0.0	0.0	0.0	0.0
	5.4	6.7	8.1	9.6	10.4	11.0	0.0	0.0	0.0	0.0	0.0	0.0
	5.2	6.7	8.3	9.6	10.5	10.7	0.0	0.0	0.0	0.0	0.0	0.0
	5.9	7.4	8.4	9.4	10.2	10.5	0.0	0.0	0.0	0.0	0.0	0.0

After recording pressures, the pressure drop across the sand-pack (difference between inlet and outlet pressures) was calculated at various flow rates (Table 7-8).

Table 7-8: Pressure difference before and after sand-pack at various flow rates for polymer 1

ΔP (psi)	ΔP (atm)	Flow rate (ml/min)	Flow rate (ml/s)
5.9	0.42	25.0	0.42
7.4	0.52	30.0	0.50
8.4	0.59	35.0	0.58
9.4	0.66	40.0	0.67
10.2	0.72	45.0	0.75
10.5	0.74	47.5	0.79

The permeability equation (Equation 7-2) can be rearranged and rewritten as Equation 7-6:

$$\Delta P = 1000 \, \frac{A}{L} \, \mu \, \frac{1}{k} \, Q = slope \times \Delta Q \qquad \textbf{Equation 7-6}$$

Pressure differences with respect to various flow rates for polymer 1 (run 2) are plotted in Figure 7-8. There is a direct relationship between ΔP and flow rate: as flow rate increases, the pressure difference across the sand-pack goes up. By applying linear regression, the slope of the ΔP versus flow rate line could be used in order to calculate permeability. It should be mentioned that the procedure of recording pressures at different flow rates should be replicated several times in order to obtain a reliable slope and its associated error.

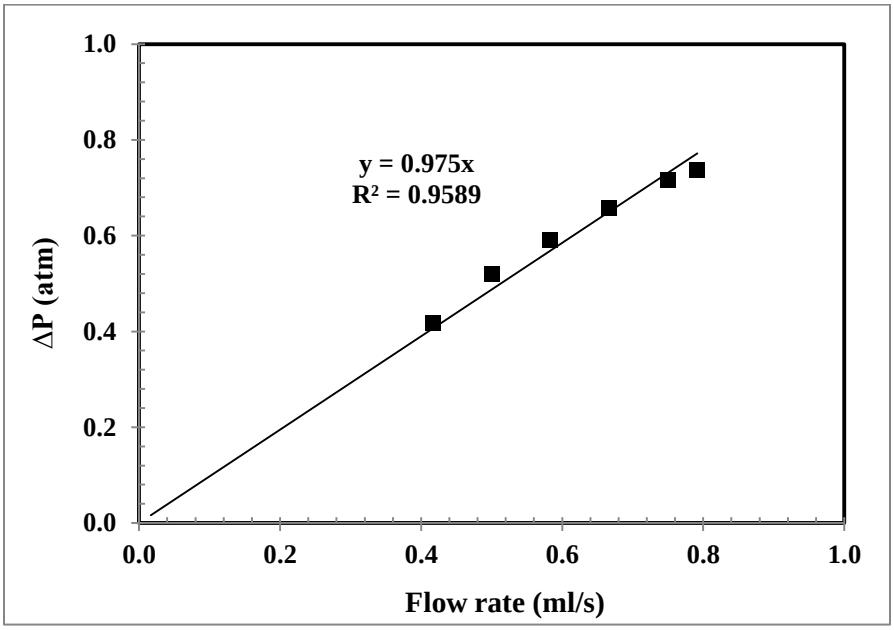

Figure 7-8: Pressure difference across the sand-pack versus flow rate for polymer 1, run 2

Based on Equation 7-6 and the slope of the line from Figure 7-8, the permeability of the sand-pack can be calculated according to the values for parameters given in Table 7-9.

Table 7-9: Sand-pack permeability calculations

Sand-pack length, L	46.10 (cm)
Sand-pack cross sectional area, A	12.25 (cm^2)
Brine dynamic viscosity, μ	1 (cP)
Slope	0.97 (atm.s/ml)
Permeability, k	**3858.44 mD**

Sand-pack porosity was calculated by the ratio of pore volume and the sand-pack volume (Section 3.4.1). Table 7-10 presents pore volume, porosity, and permeability values of each run for the five polymer solutions used in polymer flooding tests.

Table 7-10: Sand-pack properties at each run for five polymer solutions

Polymer #		Pore volume (ml)	Porosity	Permeability (mD)
1	Run 1	160.65	0.28	4397.92
	Run 2	160.65	0.28	3858.00
2	Run 1	160.65	0.28	6954.00
	Run 2	160.65	0.28	1229.00
3	Run 1	80.00	0.14	6468.33
	Run 2	80.00	0.14	5729.00
4	Run 1	139.00	0.25	13493.50
	Run 2	145.00	0.26	17155.00
Reference	Run 1	160.65	0.28	3180.60
	Run 2	160.65	0.28	3976.00

Figure 7-9 contains several plots that show how pressure changes along the sand-pack during polymer solution injection (polymer flooding). P1 and P6 are the pressure gauges before and after the sand-pack, respectively. P2, P3, P4, and P5 show the pressures along the sand-pack from the beginning to the end.

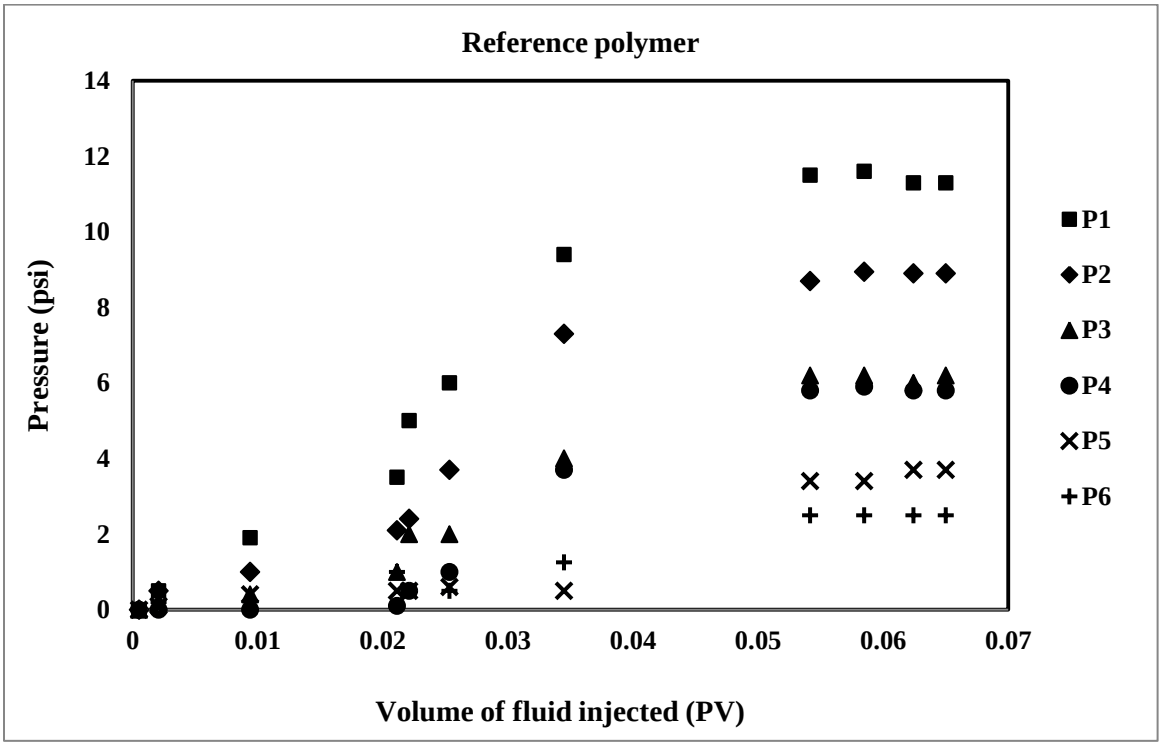
Reference polymer
Pressure (psi)
14
12
10
8
6
4
2
0
0
0.01
0.02
0.03
0.04
0.05
0.06
0.07
Volume of fluid injected (PV)
P1
P2
P3
P4
P5
P6

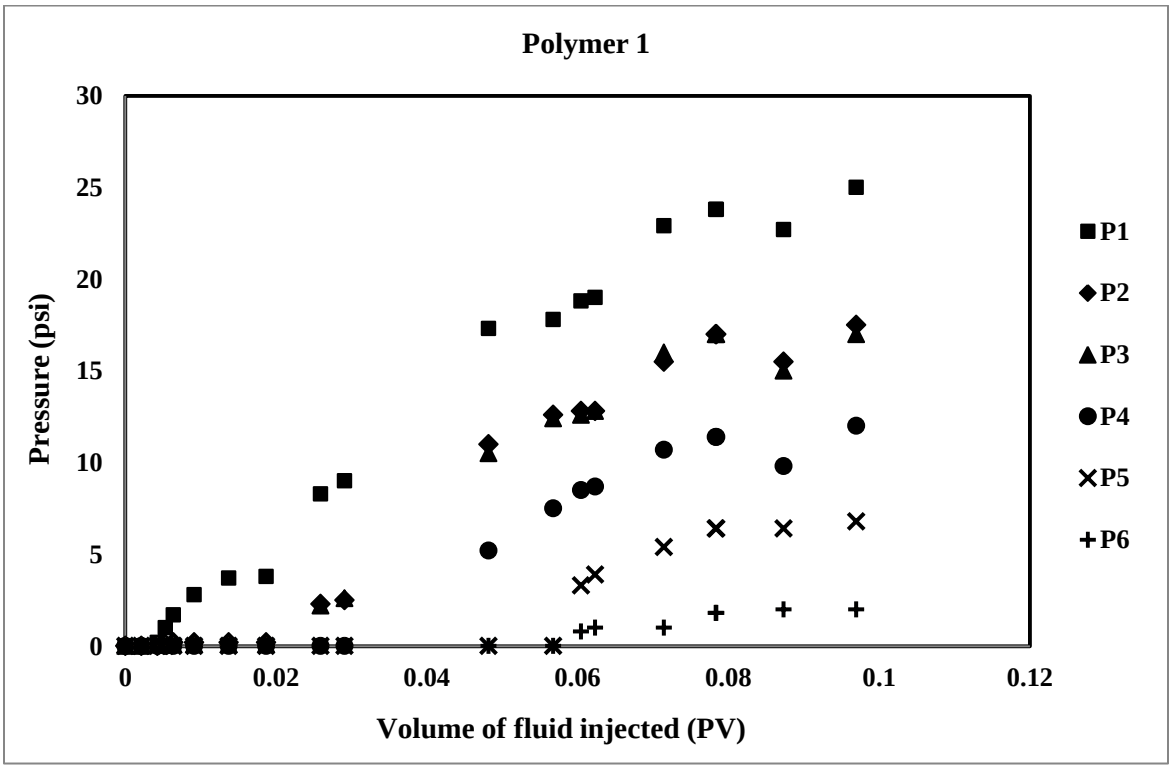
Polymer 1
Pressure (psi)
30
25
20
15
10
5
0
0
0.02
0.04
0.06
0.08
0.1
0.12
Volume of fluid injected (PV)
P1
P2
P3
P4
P5
P6

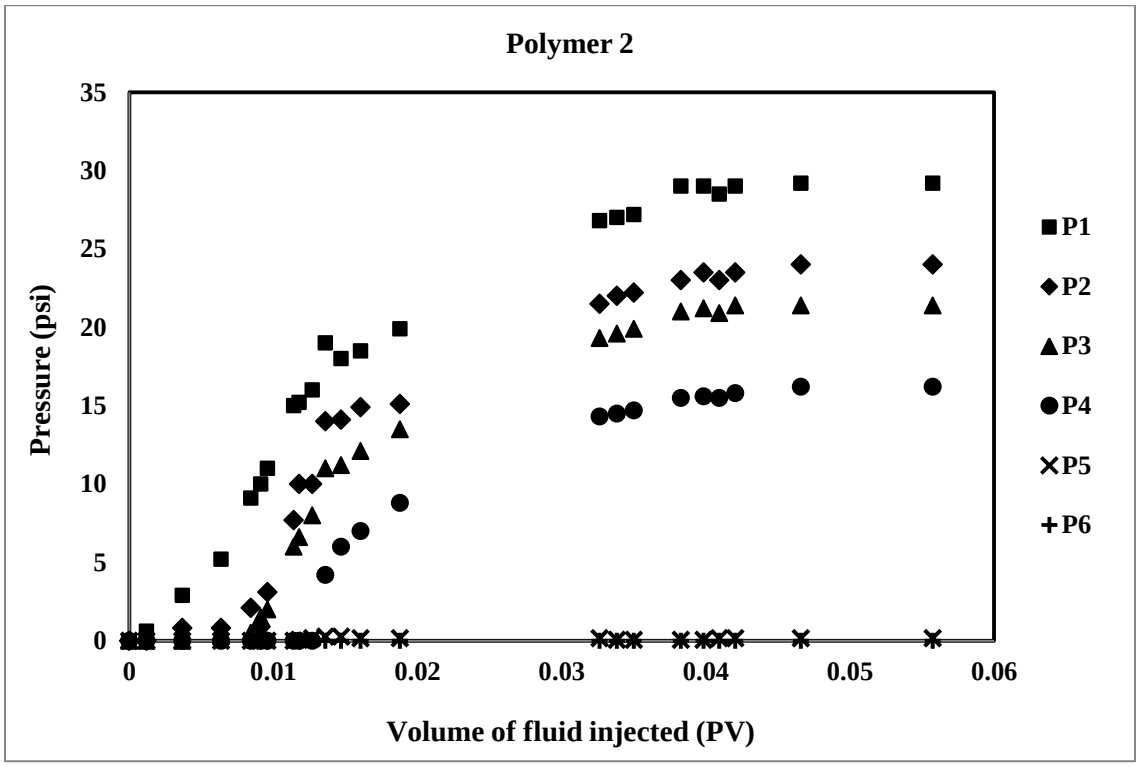
Polymer 2
Pressure (psi)
35
30
25
20
15
10
5
0
0
0.01
0.02
0.03
0.04
0.05
0.06
Volume of fluid injected (PV)
P1
P2
P3
P4
P5
P6

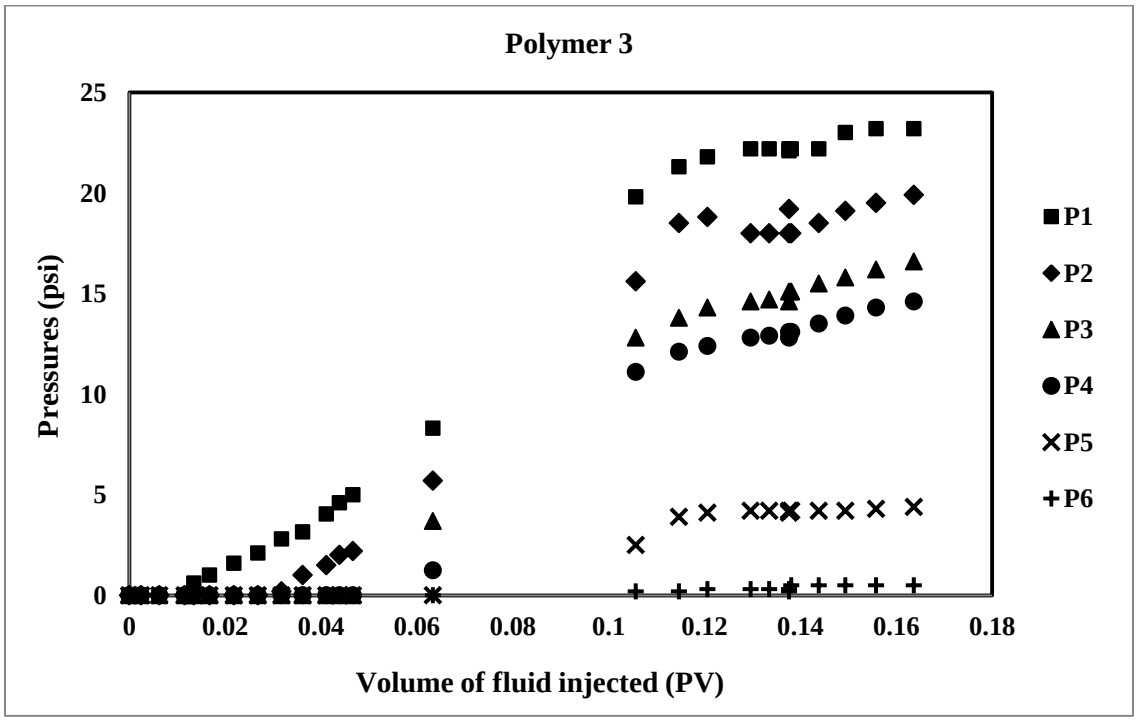
Polymer 3
Pressures (psi)
25
20
15
10
5
0
0
0.02
0.04
0.06
0.08
0.1
0.12
0.14
0.16
0.18
Volume of fluid injected (PV)
P1
P2
P3
P4
P5
P6

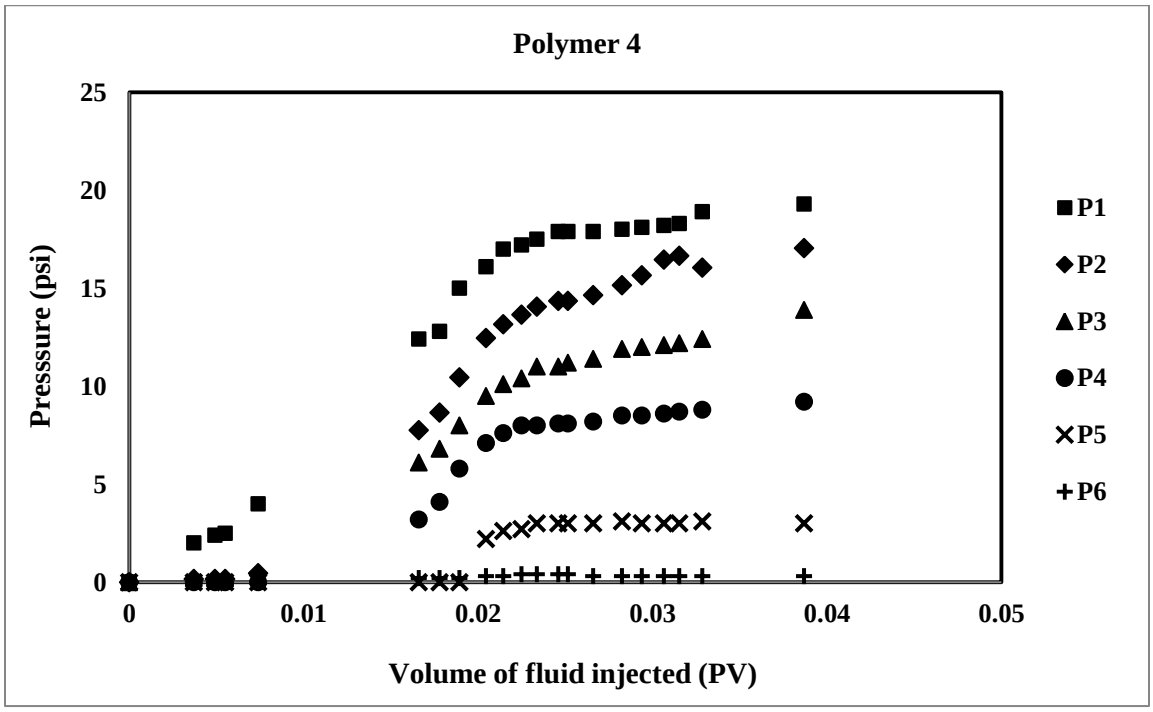

Figure 7-9: Pressure profiles in the sand-pack during polymer flooding for all polymer solutions

When a polymer solution has minimal retention, the pressure profile increases with the volume of the fluid injected (PV on x axis) and there is no large difference between the pressure values. The pressure profiles of polymer solutions 1, 4 and the reference showed a sign of good propagation in the sand-pack. Polymers 2 and 3, on the other hand, showed a sign of retention during the flow in the porous media; there is a noticeable discontinuity between their pressure profiles. This shows that the polymer solution was retained in the porous media and could not propagate till the end of the sand-pack and, as a result, there is no increase in P5 and P6 pressures (P5 and P6 are almost zero in the pressure profiles of polymers 2 and 3). These trends were confirmed visually during the experiments as well;

polymers 2 and 3 clogged the sand-pack in such a way that normal cleaning of the sand-pack with bleach after polymer flooding was not successful.

As mentioned earlier in this section, the resistance factor, RF, reflects the effective viscosity of the polymer solution, while the residual resistance factor, RRF, indicates polymer solution retention as the polymer solution travels through the porous medium. These two important factors can be determined from Equation 7-3 and Equation 7-5.

RF as a function of injected fluid volume (PV) is shown in Figure 7-10. It should be mentioned that the presented results of RF are the average of two independent replicates. The effects of sand-pack permeability and porosity differences between various runs have been normalized by using the concept of a capillary bundle parameter. The capillary bundle parameter (with unit of mD^{-1}) is defined by Equation 7-7:

$$Capillary\ bundle\ parameter = \frac{F \times t \times (1-\emptyset) \times A}{(\emptyset \times k)^{0.5} \times PV} \qquad \textbf{Equation 7-7}$$

In Equation 7-7, F is flux (cm/min), t is injection time (min), Φ is porosity (dimensionless), k is permeability (mD), A is sand-pack cross sectional area (cm^2), and PV is sand-pack pore volume (cm^3), which is the x-axis of Figure 7-9. Values for the different factors in Equation 7-7 were given in Table 3-2 in Section 3.4.1 and Table 7-10 in Section 7.3.1. Since sand-pack conditions can vary between runs and samples, it is necessary to normalize the volume of the fluid injected for the comparisons to make sense.

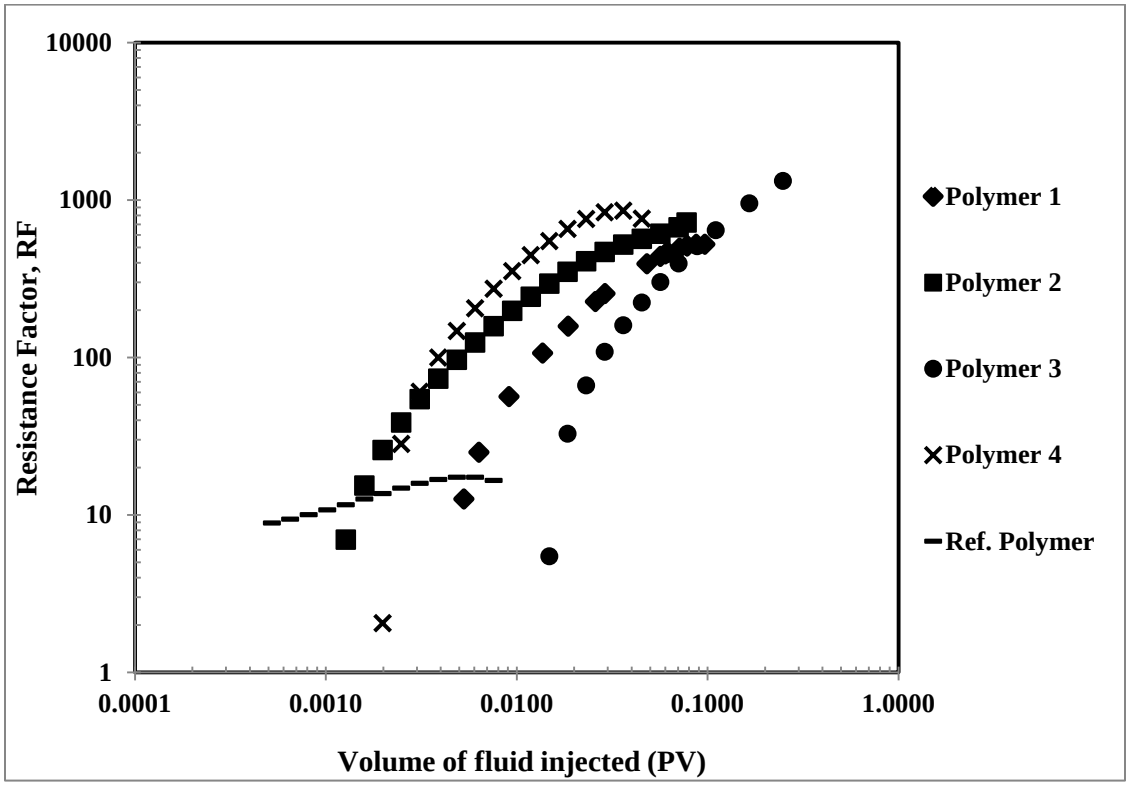

Figure 7-10: Sand-pack flooding test for polymer solutions; RF versus pore volume of injected fluid.

Figure 7-10 clearly shows that the tailor-made copolymers presented significantly higher RF and, consequently, higher effective viscosity during flow through the sand-pack compared to the reference polymer. The results in the figure show that the designed polymers had better mobility control capability compared to that of the commercial polymer.

At a fixed volume of fluid injected, such as 0.01 PV, polymers 2 and 4 achieved higher RF values compared to polymers 1 and 3. Moreover, in order to achieve a specific RF value, say, 100, lower volumes of fluid are required for polymers 2 and 4. The reason for the better performance of polymer 2 compared to polymers 1, 3, and the reference polymer can be

attributed to its higher molecular weight and shear viscosity. However, the performance of polymer 4 in terms of the highest RF compared to the other tailor-made polymers is not very clear at this point.

As indicated in Figure 7-10, the RF values increased with the volume of the injected fluid until a plateau was reached. However, the RF values of polymer 3 did not level off and showed no sign of stabilization during flow through the sand-pack. This behavior may be due to the high retention of polymer 3 in the porous medium, which will be discussed later in this section.

The RF plateau values (steady state) are presented in Table 7-11. Polymer 4 showed the highest RF value (RF_{Steady}=808.5) as compared to the other polymer solutions. On the other hand, the reference polymer presented the lowest RF value (RF_{Steady}=16.9).

Table 7-11: Steady state RF values for polymer solutions in sand-pack flooding test

Sample	**RF @ steady state conditions**
Polymer 1	522.7
Polymer 2	696.0
Polymer 3	No plateau exhibited
Polymer 4	808.5
Ref. Polymer	16.9

The plot of residual resistance factor (RRF) as a function of volume of fluid injected normalized for permeability and porosity using the capillary bundle parameter is shown in Figure 7-11. The RRF values presented are the averages of two independent replicates.

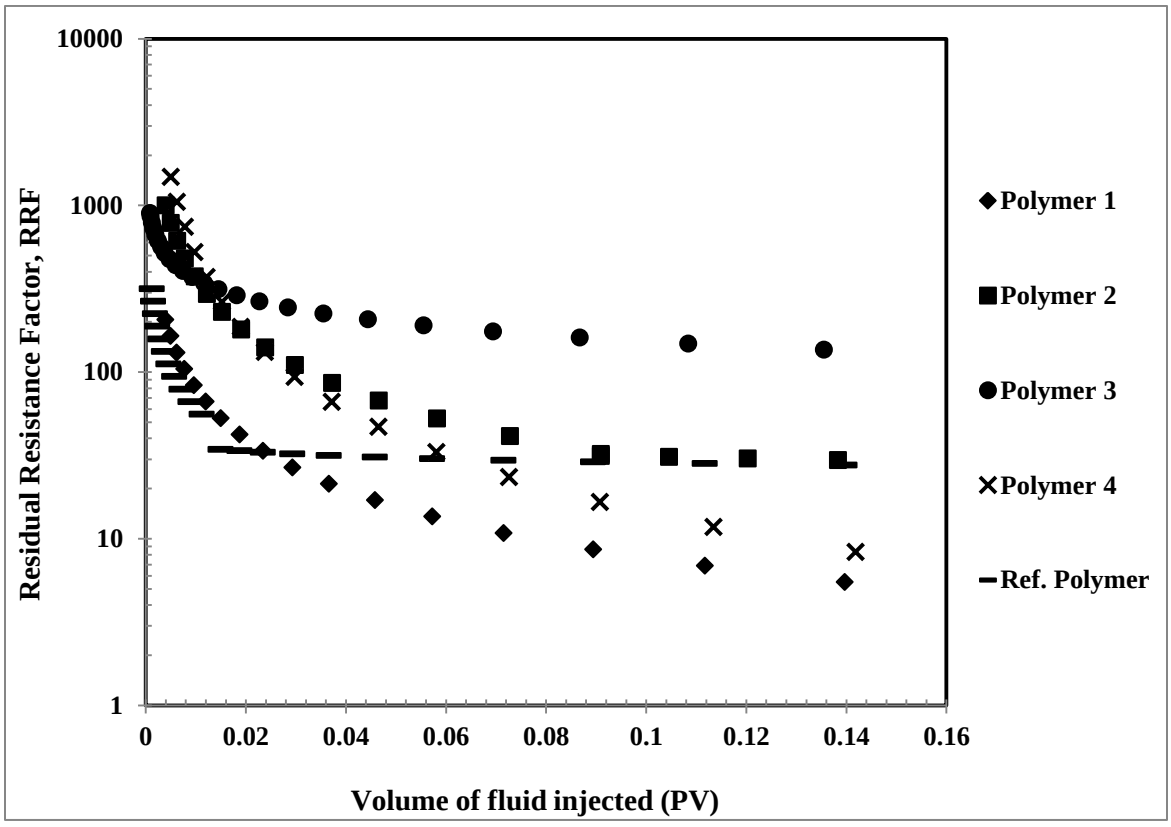

Figure 7-11: Sand-pack flooding test for polymer solutions; RRF versus pore volume of injected fluid

Figure 7-11 suggests that all polymer solutions exhibited similar trends with a decreasing RRF as more pore volume of the brine was injected into the sand-pack. Moreover, polymers 1 and 4 had the lowest retention in the sand-pack, while polymers 2 and 3 had the highest

retention. The RRF results of Polymers 2 and 3 are consistent with their pressure profiles during polymer flooding (see Figure 7-9). The behavior of the reference polymer in terms of retention lay somewhere in the middle of designed polymers. Table 7-12 presents the steady state values of RRF for all polymers tested.

Table 7-12: Steady state RRF values for polymer solutions in sand-pack flooding test

Sample	RRF @ steady state conditions
Polymer 1	5.5
Polymer 2	29.6
Polymer 3	136.2
Polymer 4	8.3
Ref. Polymer	27.6

The RRF behavior of polymer 3 was perfectly consistent with its RF result (no plateau in the RF curve). This polymer solution showed the highest retention with a steady state RRF value of 136. This meant that the initial permeability of the sand-pack was reduced by 136 times due to retention of polymer 3, which is a sign of poor propagation of the polymer solution through the sand-pack. This confirmed the pressure profile of Polymer 3 in Figure 7-9, where there was no increase in pressure at the end of the sand-pack due to poor propagation of the polymer solution. High retention in porous media is a result of either mechanical retention (due to the high molecular weight of the polymer) or adsorption (electrostatic interaction with the sand-pack). If we consider mechanical retention only, polymers 2 and 3 are the ideal candidates for polymer retention in the sand-pack, since these two polymers had the highest

molecular weights (see Table 7-4). But if we consider electrostatic interactions between sandstones and copolymers only, polymers 3 and 4 are candidates for poor propagation (high retention) in the sand-pack, since they have less AAc monomer units in the copolymer chain and there are fewer chances for electrostatic repulsions between polymers and negatively charged sandstones. By considering the two factors at the same time, both mechanical retention and adsorption, it can be concluded that polymer 3 had the highest RRF and retention in the porous media.

On the other hand, polymer 1 showed the least retention in the sand-pack. This can be explained by the fact that this polymer had the highest amount of AAc in the backbone. Since the sandstones of the sand-pack are negatively charged, having a higher fraction of AAc increases the repulsion between the polymer and the porous media and, as a result, decreases polymer retention. Moreover, polymer 1 had relatively lower molecular weight, which reduces its chance for mechanical retention. This also explains why most of the commercial AAm-based polymers used in EOR applications have around 5% AAc in the backbone.

The ideal polymer for mobility control in EOR should provide high effective viscosity (high RF) and low retention/good propagation across the sand-pack (low RRF). Therefore, Polymer 4 is the ideal polymer for polymer flooding, since it showed the highest effective viscosity and it decreased the initial sand-pack permeability by only 8.32 times, which is quite good. The next candidate would be polymer 1, which showed the third highest viscosity efficiency and the lowest retention among all the polymer solutions. On the other hand, polymers 2 and 3 had high RRF (high retention/low propagation) in the sand-pack, which

made them unsuitable candidates for heavy oil displacement tests. Therefore, polymers 1 and 4 were selected for the subsequent heavy oil displacement tests (this which will be discussed in Section 7.3.4).

It should be mentioned herein that polymer 2 is suitable for water shutoff applications, where both high effective viscosity and retention (poor propagation) are needed. In water shutoff applications, water-soluble polymers decrease the permeability of water in oil reservoirs with little effect on oil permeability.[48] This can be very valuable in production wells for water flow blocking and consequently water permeability reduction.

7.3.2 Heavy oil displacement

Heavy oil displacement tests were conducted in the same experimental set-up used for polymer flooding tests with the characteristics described in Section 3.4.1. A typical heavy oil displacement test can be divided into 4 main stages: oil injection, brine injection, polymer injection, and again brine injection. First, the sand-pack was flooded with brine in order to measure the sand-pack characteristics (pore volume, permeability, and porosity). Then, the sand-pack was saturated with oil. After oil injection, brine injection (referred to here as water flooding) took place. This was followed by polymer flooding and another extended water flooding (post-polymer water flooding). The detailed procedure is explained in Section 3.4.2.

Sand-pack permeability was measured for each run based on the procedure explained in Section 7.3.1. Then, sand-pack porosity was calculated (see Section 3.4.1). Flux was measured by dividing fluid flow rate by sand-pack cross-sectional area. Initial oil saturation

was the amount of oil in the sand-pack relative to the pore volume of the sand-pack. Table 7-13 presents pore volume, porosity, and permeability along with the initial test conditions for the reference polymer, polymer 1, and polymer 4 used in the heavy oil displacement tests.

Table 7-13: Sand-pack properties and initial test conditions two polymer samples

Sample	Pore volume (ml)	Porosity	Permeability (mD)	Flux (cm/min)	Initial oil saturation S_{oi} (%)
Reference Polymer	121.0	0.214	4907	0.020	72.34
Polymer 1	136.6	0.242	6875	0.017	81.60
Polymer 4	151.6	0.268	5967	0.019	90.96

Figure 7-12 presents pressure profiles along the sand-pack with respect to the volume of the fluid injected (PV on x axis) during polymer flooding. As mentioned in Section 7.3.1, P1 and P6 are the pressure gauges before and after the sand-pack, respectively. P2, P3, P4, and P5 show the pressures along the sand-pack from the beginning to the end. Pressure profiles showed a similar behavior, with slightly better propagation (less discontinuity between pressure profiles) for polymer 1 and polymer 4 compared to the reference polymer. The better propagation for polymer 1 and polymer 4 is in agreement with the RRF results of Figure 7-11, which indicated a lower retention of polymer 1 and polymer 4 in comparison to that of the reference polymer.

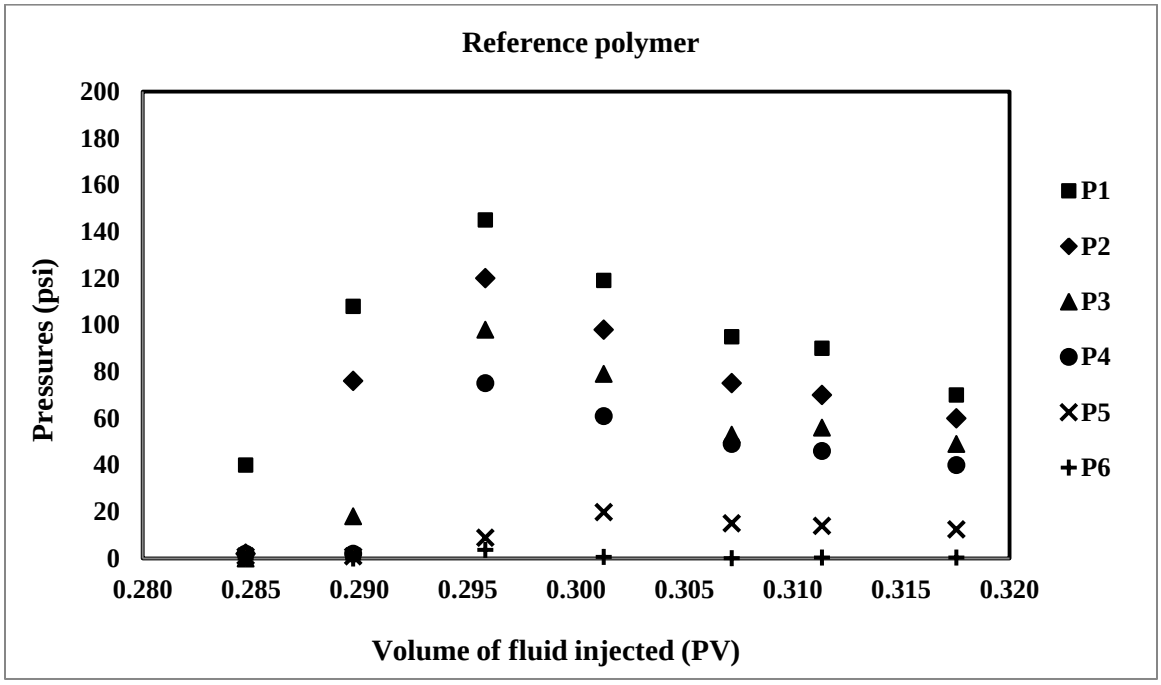
Reference polymer
Pressures (psi)
200
180
160
140
120
100
80
60
40
20
0
0.280
0.285
0.290
0.295
0.300
0.305
0.310
0.315
0.320
Volume of fluid injected (PV)
P1
P2
P3
P4
P5
P6

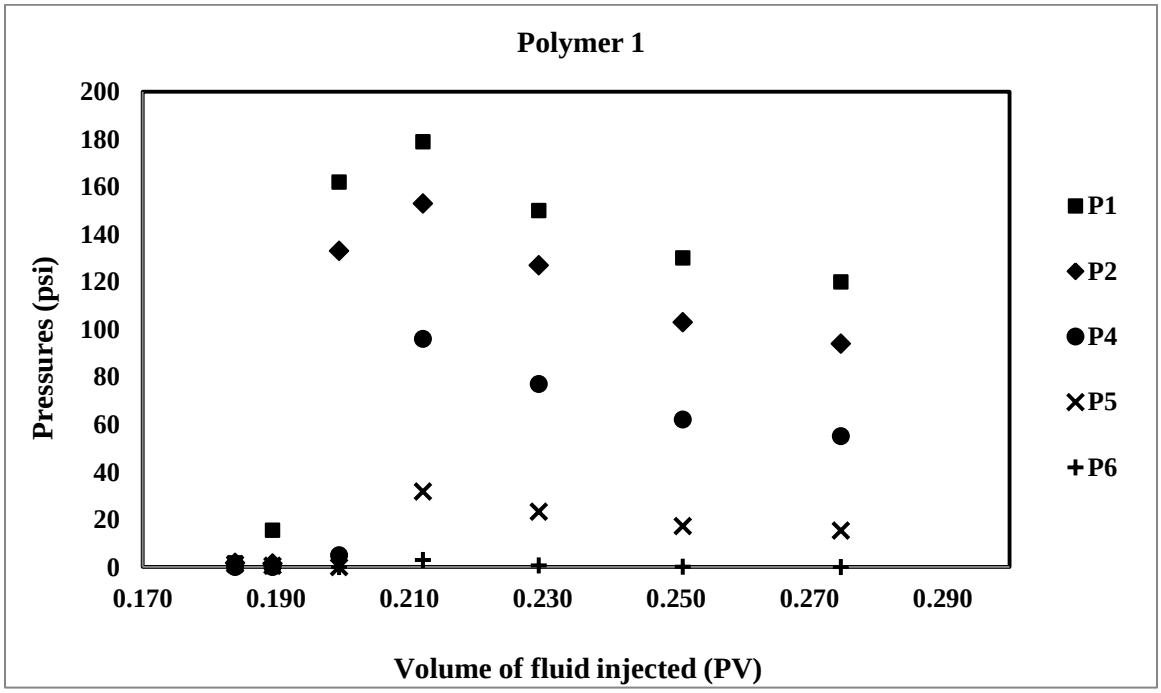
Polymer 1
Pressures (psi)
200
180
160
140
120
100
80
60
40
20
0
0.170
0.190
0.210
0.230
0.250
0.270
0.290
Volume of fluid injected (PV)
P1
P2
P4
P5
P6

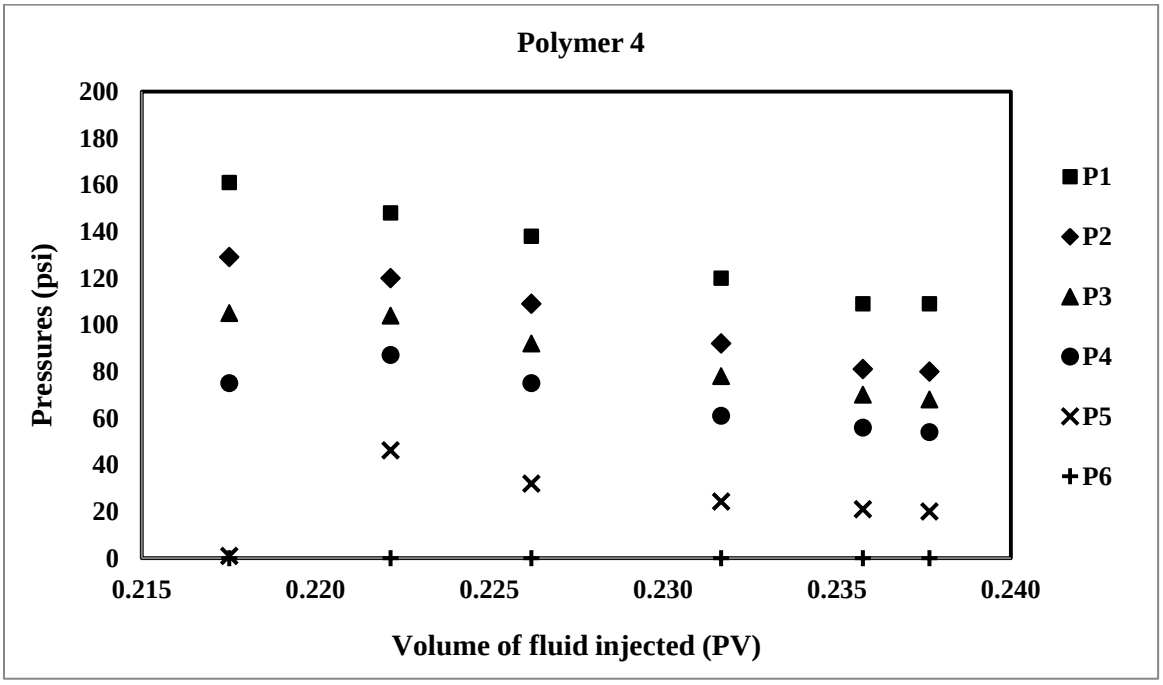

Figure 7-12: Pressure profiles in the sand-pack during polymer flooding for polymer solutions

Figure 7-13 compares pressure difference during polymer flooding, $\Delta P_{polymer}$, over the pressure difference during water flooding, ΔP_{brine}, with respect to the volume of the fluid injected for the polymers in the heavy oil displacement tests. The ratio of $\Delta P_{polymer}$ / ΔP_{brine} represents the mobility control of the polymer. Figure 7-13 shows polymer 1 has better mobility control compared to the reference polymer, because of its higher pressure ratio values, which was also reflected in Figure 7-12. This is consistent with the RF results shown in Figure 7-10, which showed better RF behavior for polymer 1 compared to the reference polymer. In addition, polymer 1 showed better stability compared to the reference polymer, as more fluid was injected to the sand-pack.

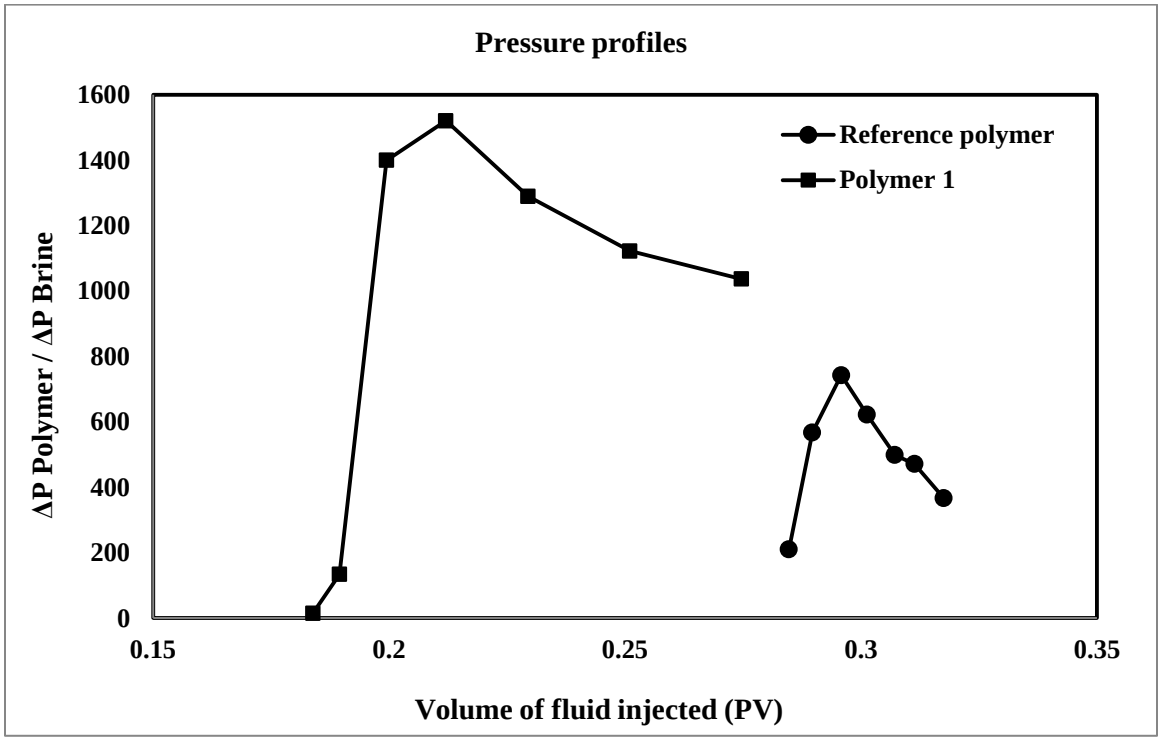

Figure 7-13: Pressure difference during polymer flooding over brine flooding versus the volume of fluid injected in heavy oil displacement tests

The efficiency of oil recovery can be evaluated by oil saturation in the sand-pack and original oil in place (OOIP) recovered by polymer flooding. The oil saturation is defined as the amount of oil in the sand-pack at each stage relative to the pore volume of the sand-pack. OOIP recovered by polymer flooding is defined as the volume of the oil that has been recovered over the original amount of the oil in the sand-pack.

A summary of the results for the different stages during the heavy oil displacement tests for reference polymer and polymer 1 is presented in Table 7-14 and Table 7-15 and Table 7-16.

Table 7-14: Summary of heavy oil displacement test for reference polymer

Reference Polymer					
Oil injection	**Flow rate (ml/min)**	**Total oil injected (ml)**	**Oil in sand pack (ml)**	**Oil saturation (%)**	**OOIP (%)**
	0.18	181.47	87.53	72.34	72.34
Water injection	**Flow rate (ml/min)**	**Total brine injected (ml)**	**Oil in sand pack (ml)**	**Oil saturation (%)**	**OOIP recovered by water flooding (%)**
	0.26	1491.06	23.80	19.67	72.81
Polymer injection	**Flow rate (ml/min)**	**Total polymer injected (ml)**	**Oil in sand pack (ml)**	**Oil saturation (%)**	**OOIP recovered by polymer flooding (%)**
	0.23	169.92	8.82	7.29	17.11
Post-polymer water injection	**Flow rate (ml/min)**	**Total brine injected (ml)**	**Oil in sand pack (ml)**	**Oil saturation (%)**	**OOIP recovered by extended water flooding (%)**
	0.25	397.50	5.52	4.56	3.77
Overall	**Average flow rate (ml/min) =** 0.25				
	Overall OOIP recovered (%) = 93.69				

Table 7-15: Summary of heavy oil displacement test for polymer 1

Polymer 1					
Oil injection	**Flow rate (ml/min)**	**Total oil injected (ml)**	**Oil in sand pack (ml)**	**Heavy oil saturation (%)**	**OOIP (%)**
	0.18	227.54	111.46	81.59	81.60
Water injection	**Flow rate (ml/min)**	**Total brine injected (ml)**	**Oil in sand pack (ml)**	**Heavy oil saturation (%)**	**OOIP recovered by water flooding (%)**
	0.21	1326.27	68.75	50.33	38.31
Polymer injection	**Flow rate (ml/min)**	**Total polymer injected (ml)**	**Oil in sand pack (ml)**	**Heavy oil saturation (%)**	**OOIP recovered by polymer flooding (%)**
	0.22	181.25	64.00	46.85	4.26
Post-polymer water injection	**Flow rate (ml/min)**	**Total brine injected (ml)**	**Oil in sand pack (ml)**	**Heavy oil saturation (%)**	**OOIP recovered by extended water flooding (%)**
	0.20	345.84	41.28	30.22	20.38
Overall	**Average flow rate (ml/min) =** 0.21				
	Overall OOIP recovered (%) = 62.96				

Table 7-16: Summary of heavy oil displacement test for polymer 4

Polymer 4					
Oil injection	**Flow rate (ml/min)**	**Total oil injected (ml)**	**Oil in sand pack (ml)**	**Heavy oil saturation (%)**	**OOIP (%)**
	0.18	242.50	137.90	90.96	90.96
Water injection	**Flow rate (ml/min)**	**Total brine injected (ml)**	**Oil in sand pack (ml)**	**Heavy oil saturation (%)**	**OOIP recovered by water flooding (%)**
	0.24	1865.30	66.10	43.60	60.33
Polymer injection	**Flow rate (ml/min)**	**Total polymer injected (ml)**	**Oil in sand pack (ml)**	**Heavy oil saturation (%)**	**OOIP recovered by polymer flooding (%)**
	0.23	232.00	31.60	20.84	25.02
Post-polymer water injection	**Flow rate (ml/min)**	**Total brine injected (ml)**	**Oil in sand pack (ml)**	**Heavy oil saturation (%)**	**OOIP recovered by extended water flooding (%)**
	0.26	482.60	21.10	13.92	7.61
Overall	**Average flow rate (ml/min) =** 0.24				
	Overall OOIP recovered (%) = 92.96				

The amounts of oil recovered by polymer flooding and extended water flooding (shown in tables as OOIP recovered by polymer flooding and OOIP recovered by extended water flooding, respectively) for the reference polymer, polymer 1, and polymer 4 are equal to 20.88%, 24.65%, and 32.63%, respectively. By comparing these values, it is clear that the oil recovery as a result of polymer flooding was better for polymer 4 among three polymer solutions. In general, tailor-made polymers had better performance in terms of oil recovery.

Since only 1 PV of the polymer was injected into the sand-pack (pore volume is equivalent to the volume available for fluids storage in the porous media) during polymer flooding, oil recovery by polymer continued even during the extended water flooding. This was because there were still polymer residues in the sand-pack and as a result, extended water flooding also included polymer flooding that should be considered.

It should be noted that the reference polymer had the best oil recovery as a result of water flooding (shown in tables as OOIP recovered by water flooding) compared to tailor-made polymers. This can be explained by the different permeability of the sand-pack for these three polymers (see Table 7-13). Permeability of the sand-pack was higher for polymer 1 compared to the polymer 4 and the reference polymer. Higher permeability increased the chance of water channeling in the sand-pack and therefore, the oil recovery by water flooding decreased significantly. So, there is a reversal relationship between sand-pack permeability and oil recovery by water flooding. This phenomenon actually happens in real oil reservoirs too. Since the target of this research was to compare the performance of the designed

copolymers with the reference polymer, water flooding was not considered further in the comparisons.

Figure 7-14 displays the performance of the three polymers in displacing oil as OOIP recovered by polymer flooding and extended water flooding with respect to the volume of the fluid injected. It can be seen that there was a rapid increase in oil recovery by injecting the polymer into the sand-pack. After this stage, extended water flooding happened, where the oil recovery started to level off gradually and came to a plateau. Tailor-made polymers, polymer 1 and polymer 4, showed considerably better performance in terms of oil recovery.

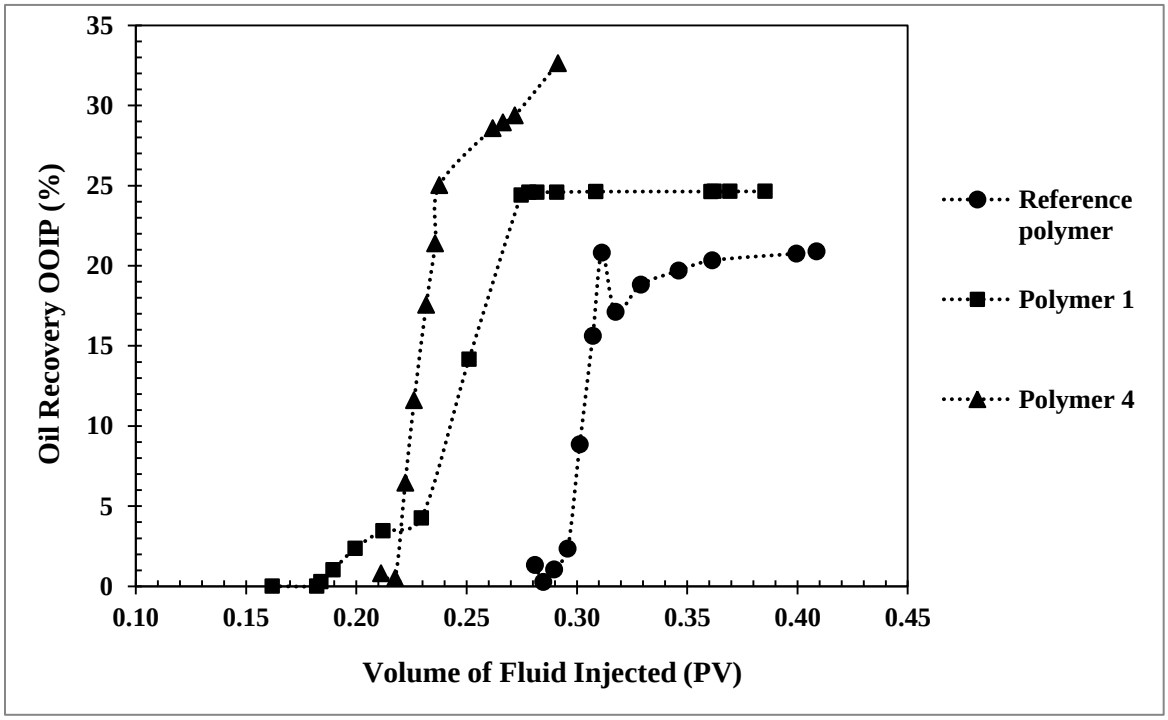

Figure 7-14: OOIP recovered by polymer flooding and post-polymer water flooding versus volume of fluid injected.

Figure 7-15 shows the ratio of final oil saturation, S_{of}, to initial oil saturation, S_{oi}, in the sand-pack with respect to the volume of injected fluid for polymer 1. The different stages during the oil displacement test can be seen in this figure. After the oil injection stage, the ratio of S_{of} / S_{oi} was equal to 1, since no oil had been extracted yet. With water flooding, there is a decline in the ratio of S_{of} / S_{oi}, showing the amount of oil recovery by water flooding. By injecting more water, no more oil could be recovered and the oil saturation curve in the sand-pack showed a plateau. This could represent the end of oil recovery if no polymer flooding was involved. At the start of polymer flooding, there is another decline in the ratio, representing the amount of oil recovered by polymer flooding. This amount of recovered oil could not have been achieved without polymer injection and thus shows the importance of polymer flooding in EOR.

Figure 7-16 shows the ratio of produced water to oil for the three polymers in the heavy oil displacement tests. This ratio can be calculated based on the amount of water (brine) and oil that were produced from the sand-pack during the test. The procedure to measure the volume of produced water and oil was mentioned in Section 3.4.2.

Figure 7-16 shows again the different stages of the heavy oil displacement tests. The maximum for the water to oil ratio occurred at the end of the water flooding stage. After that, there was a decrease in the ratio, due to polymer flooding. Upon starting the extended water flooding, the water to oil ratio continued to increase steadily till the end of the test. Overall, it can be inferred from this figure that polymer 1 and polymer 4 exhibited better performance in controlling the produced water to oil ratio compared to that of the reference polymer

(indicated by the significant decrease in the ratio after polymer flooding). This is another confirmation that heavy oil displacement efficiency was improved by use of tailor-made polymers as compared to the results for the reference polymer, due to the lower amount of produced water to oil. In general, in oil reservoirs, a lower water to oil ratio is favorable, because of the costs of water handling, disposal, and recycling according to environmental regulations.

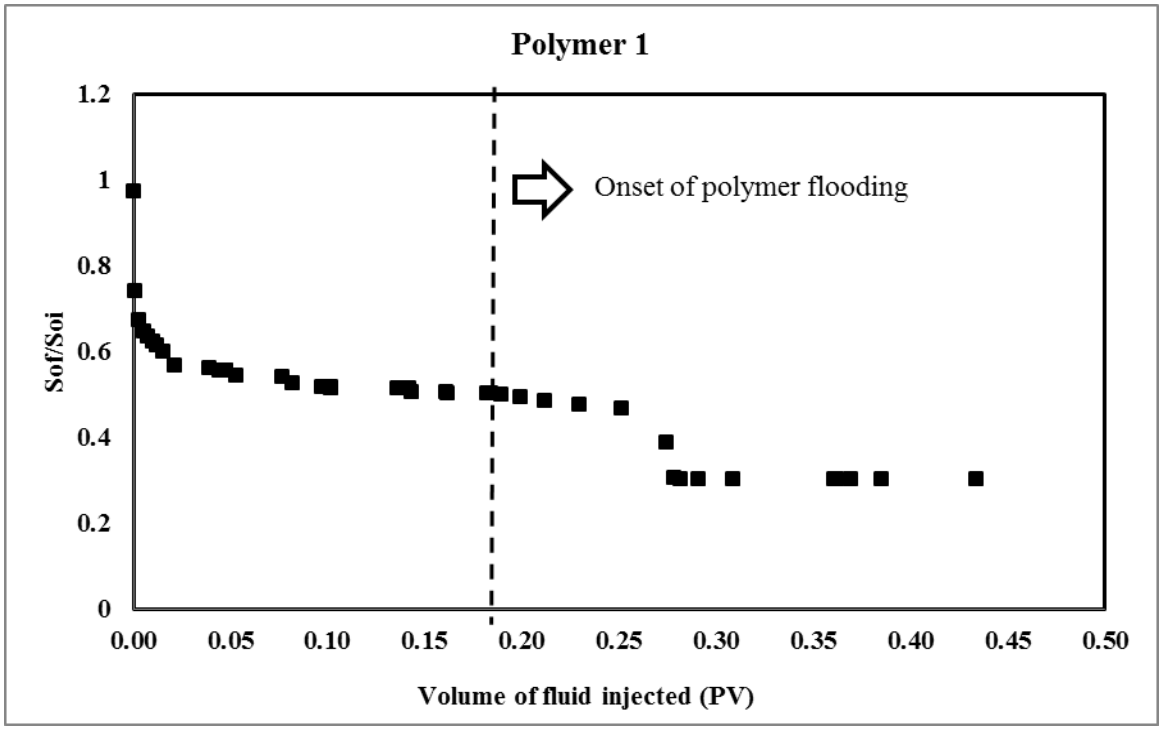

Figure 7-15: Ratio of final oil saturation, S_{of}, to initial oil saturation, S_{oi}, in the sand-pack versus volume of injected fluid.

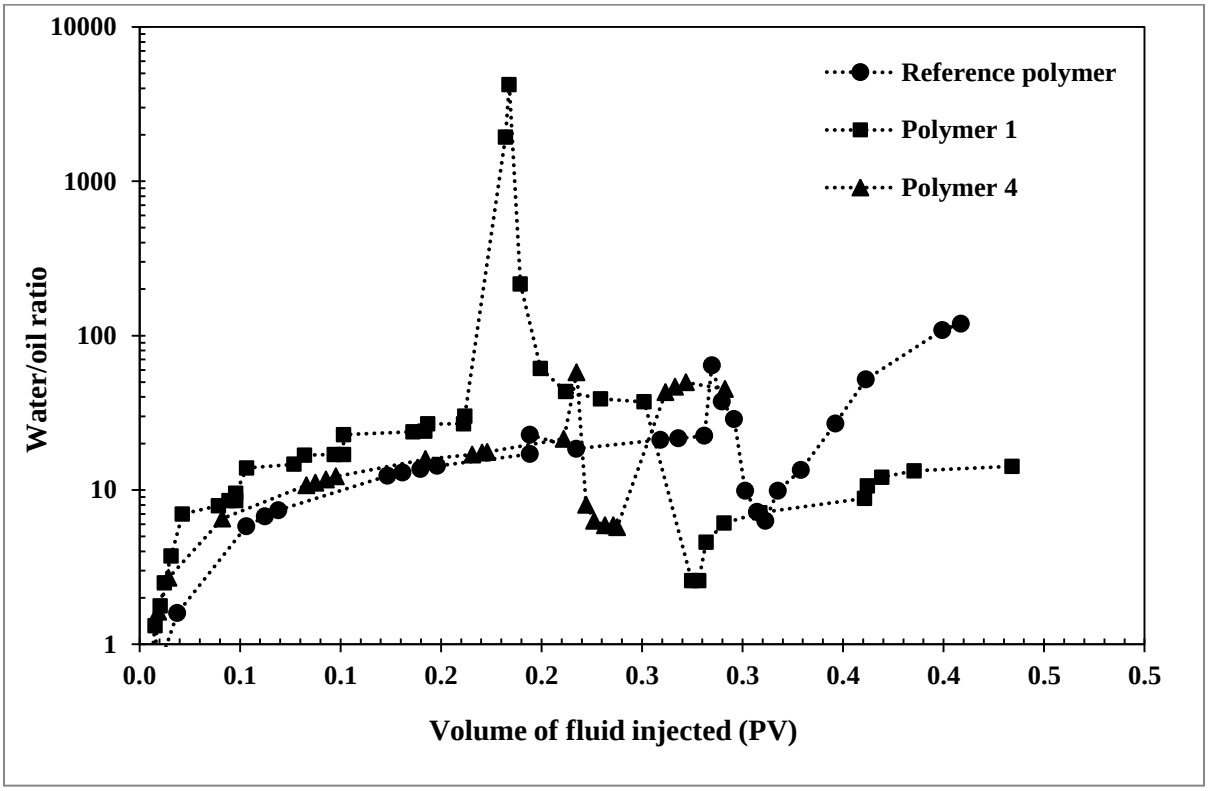

Figure 7-16: Produced water to oil ratio as a function of volume of injected fluid

The excellent EOR performance of the designed AAm/AAc copolymers can be attributed to the higher molecular weight, shear viscosity, and elasticity of the tailor-made polymers compared to the reference polymer.

7.3.3 Concluding remarks

Tailor-made AAm/AAc copolymers were prepared in order to evaluate their performance in EOR application. Copolymerizations were conducted at selected conditions (pH=5, high AAm monomer fractions in the feed, total monomer concentration of 1.5 M) to synthesize

copolymers with desirable properties. Designed AAm/AAc copolymers had high AAm content in the copolymer composition (cum F_{AAm} = 0.67-0.93), high average molecular weights (M_p = 4.5-9 million), and a random distribution of anionic charges along the copolymer chain. Solution shear viscosity measurements showed that copolymers with higher AAc content had higher shear viscosity up to a certain limiting copolymer composition. Moreover, having higher AAc units in the copolymer, caused higher elasticity of the copolymer solution.

The results of polymer flooding tests showed that the designed copolymers exhibited significantly better performance in terms of the resistance factor (effective viscosity) compared to the commercially available copolymer. In other words, the designed AAm/AAc copolymers showed better mobility control in comparison to the reference copolymer. Residual resistance factor trends of tailor-made copolymers and reference copolymer were similar, showing that all the copolymers behaved in a more or less similar way in terms of retention in the sand-pack. The tailor-made copolymers with the highest effective viscosity and lowest retention in the sand-pack were selected for the final heavy oil displacement tests. The results showed that the amounts of original oil in place recovered by the tailor-made copolymers were higher than those with the commercial copolymer, thus representing higher oil recovery efficiency for the designed copolymers. Moreover, less volume of water was required and produced in the heavy oil displacement tests for the tailor-made copolymers compared to the reference copolymer. This can decrease the operational costs for water handling and disposal in real oil reservoirs.

Chapter 8. Conclusions, Main Thesis Contributions, and Recommendations

8.1 Summary and conclusions

The topic of clarifying copolymerization kinetics for tailoring properties of AAm/AAc copolymers for ehnahnced oil recovery (EOR) applications was extensively studied in this thesis. A systematic approach was applied in order to study the full circle involving copolymerization kinetics, copolymer properties, and application performance of this copolymer.

First, optimal reactivity ratios were estimated for the AAm/AAc system at low, medium, and high conversions. Moreover, we ascertained the reasons for the highly scattered reactivity ratios in the literature. We implemented the EVM parameter estimation method for the numerically integrated form of the cumulative composition model by using direct numerical integration (DNI) approach.

Following the establishment of the methodology to obtain reliable reactivity ratios, we looked at the effect of main factors in the copolymerization kinetics of AAm/AAc. We started with the effect of ionic strength, which is critically important in polyelectrolyte systems. It was observed that incorporating salt in the reaction solution affects the monomer reactivity ratios as well as the copolymerization rate, by decreasing the electrostatic

repulsions between the charged ions. The effect of ionic strength on reactivity ratios was so significant that the AAm/AAc copolymerization could be shifted into a system with an azeotropic behavior. Therefore, changing the ionic strength can be used as a powerful tool in order to fine-tune copolymer microstructure as well as reaction kinetics.

Having established the effect of ionic strength, the effects of other main factors such as monomer concentration, monomer feed composition, and pH were studied by targeting various responses (copolymer microstructure/property characteristics) while the ionic strength of the polymerization was kept constant. It was observed that changing monomer concentration and pH could shift monomer reactivity ratios significantly. As a result, one could control copolymer composition, sequence length of monomer units and triad fractions along the chain, molecular weight, and polymer shear viscosity by changing copolymerization factors/conditions. Based on the results from this study, a general framework for copolymerization kinetics and copolymer structure/property was established.

Our ultimate goal in this thesis was to shed light on the ambiguous procedure of making AAm/AAc copolymers for EOR applications. To the author's best knowledge, despite the extensive use of these copolymers in polymer flooding applications, a well-established recipe for required properties of AAm/AAc copolymer does not exist in the literature. Therefore, we applied the knowledge from copolymerization kinetics and copolymer structure/property relationships to tailor-make copolymers for polymer flooding applications. Having a detailed knowledge of the copolymerization kinetics enabled us to design copolymers with desirable properties such as high molecular weight, high AAm content in the copolymer and random

distribution of anionic charges along the copolymer chain. Moreover, rheological properties showed that copolymers with higher AAc content in the copolymer had higher solution viscosity and elasticity, which both were desirable for EOR application.

In order to further pursue our ultimate goal, we subsequently evaluated the performance properties of our tailor-made copolymers and compared them with a commercially available copolymer as a reference. We tested flow behavior characteristics and heavy oil displacement efficiency of our designed copolymers in a sand-pack with simulated real reservoir conditions. It was observed that the tailor-made copolymers had better effective viscosity and mobility control capability compared to the reference copolymer. Moreover, the efficiency of heavy oil recovery was higher for the designed copolymers compared to the commercial copolymer. These results emphasized the importance of having a systematic approach in designing appropriate copolymers for polymer flooding applications (or any other application, for that matter).

8.2 Main thesis contributions

The research in this thesis has made the following original contributions:

- Fundamental aspects:

    1. Reactivity ratios for AAm/AAc copolymerization have been reported by several research groups in the literature. A detailed study of monomer reactivity ratios in the literature showed a significant diversity of reported values. We established a

methodology to estimate reactivity ratios for this system by using data from monomer conversion levels and the respective cumulative copolymer compositions. This methodology was applicable at all conversion levels (low, medium, and high) without introducing any restrictions. This allowed us to include all the information regarding composition drift over the polymerization trajectory in the analysis. This work has been discussed in Chapter 4 and published in the Journal of Polymer Science Part A: Polymer Chemistry in 2013 (see reference 9).

2. The effect of ionic strength is critically important in AAm/AAc polymerization kinetics (a polyelectrolyte system). However, proper investigation of this factor has been neglected widely in the literature. In this research, the importance of ionic strength and its effect on copolymer compositions, reactivity ratios, and polymerization rate have been clarified. This work has been discussed in Chapter 5 and published in the Journal of Applied Polymer Science in 2014 (see reference 88).
3. Copolymerization kinetics and copolymer microstructure for the AAm/AAc system have been tackled in a fragmented way in the literature. In this research, a rigorous design of experiments was applied in order to establish a general framework for the relationships between reaction medium factors (monomer concentration, monomer feed fraction, and pH) and copolymer microstructure (reactivity ratios, copolymer composition, molecular weight, sequence length), and solution viscosity. This systematic study provided the required knowledge for designing copolymers with specific structure that would be useful for EOR applications at the next step. This work has been discussed in Chapter 6. The major part of these results has been

published in the Macromolecular Reaction Engineering Journal in 2015 (see reference 12). The rest of the results with pertinent analysis (on shear viscosity) are to appear in Macromolecular Symposia (recently accepted).

- Applied aspects:

1. The ultimate target in EOR is to make water-soluble polymers that are efficient for polymer flooding applications. Studying the literature clearly shows that there is a large gap between understanding the AAm/AAc copolymerization kinetics with resulting associated (synthesized) copolymer microstructure and then applying this knowledge for designing macromolecules to be used for efficient polymer flooding applications. Therefore, we applied the information we gathered in the fundamental aspects of this research to design AAm/AAc copolymers for polymer flooding. This work has been discussed in Chapter 7 (publications in preparation).
2. Finally, the performance of AAm/AAc copolymers in EOR applications was studied. Polymer flooding and heavy oil displacement tests were performed in order to evaluate the flow behavior and oil recovery efficiency of our tailor-made copolymers. The results showed a noticeable improvement in the behavior of the designed copolymers compared to a commercially available polymer that is currently being used in polymer flooding. This work has been also discussed in Chapter 7, with publications in preparation.

8.3 Recommendations for future steps

8.3.1 Short-term recommendations

- Solution viscosity measurements provide valuable information such as shear viscosity, shear stress, power-law constants, etc. In this study, only shear viscosity was measured and reported (see Chapter 6). One could also determine power-law models for describing polymer solution behavior.
- It is important to know about normal stresses and elongation viscosity of AAm/AAc copolymer solutions in EOR applications. This is because there are elongation stresses that are applied on the polymer solution in porous media and at the injection port of the oil reservoirs. It is recommended to utilize capillary rheometer to estimate elongation viscosity profiles of AAm/AAc copolymer solution.

8.3.2 Long-term recommendations

- Thermal stability of water-soluble polymers in oil reservoirs with high temperatures is very important. Thermal gravimetric analysis (TGA) tests are recommended in order to study the thermal stability of AAm/AAc copolymers for EOR applications.
- It is claimed in the literature that the stability of AAm/AAc copolymer can be improved by adding another monomer and thus consider a terpolymer system. The effect of adding a third monomer, such as sodium-2-acrylamido-2-methyl propane sulfonate (AMPS), can be studied in order to evaluate the thermal and mechanical stability of the

AAm/AAc/AMPS terpolymer and compare with AAm/AAc copolymers. This avenue has already been initiated as a side project which is an offspring of this PhD research.

- Molecular weight of AAm/AAc copolymer was evaluated by GPC (see Chapters 6 and 7). It is recommended to measure intrinsic viscosity of the copolymers and determine the viscosity average molecular weight. This can be an alternative way to characterize the molecular weight for this system and it seems to be the prevalent way described in the literature due to its simplicity.

- The effect of copolymer composition as a single variable on polymer flooding performance can be studied. It is recommended to make copolymers with similar molecular weights but various copolymer compositions in order to evaluate the performance of these polymers in more detail in EOR.

- Preliminary results of a flocculation application of AAm/AAc copolymers were promising (see Appendix A). It is recommended to synthesize copolymers with lower molecular weights (e.g. by using transfer agents and reducing monomer concentration) for pursuing flocculation applications as well.

Appendix A

Testing Copolymer Performance in Flocculation

This appendix presents supplementary information for flocculation application performance of AAm/AAc copolymer presented in Chapter 2, Section 2.7.2.

Polymer-enhanced ultrafiltration was used in order to remove the heavy metal Cu^{2+} from waste-water. The schematic of the ultrafiltration set-up is shown in Figure A.1.

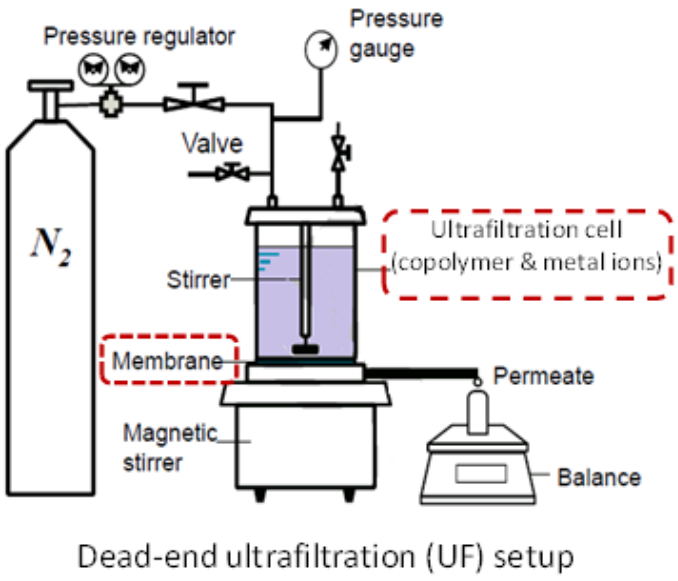

Figure A.1: Dead-end ultrafiltration set-up [membrane group in the Department of Chemical Engineering, University of Waterloo]

The AAm/AAc copolymer with the cumulative copolymer composition of cum F_{AAm}=0.6 and peak average molecular weight of M_p=3.5E6 was used. The experiment conditions of the ultrafiltration test to evaluate the flocculation performance of the copolymer are summarized in Table A.1.

Table A.1: Experimental conditions for flocculation application

Cu^{2+} concentration in feed (ppm)	**Copolymer concentration (ppm)**	**Feed volume (ml)**	**Pressure (psi)**
17.53	615	200	30

AAm/AAc has negative charges on the polymer chain and therefore there is an electrostatic attraction between the copolymer chains and heavy metals. This helps to adsorb copper ions on the copolymer chain and since the size of the macromolecule is larger than the membrane porosity (or molecular weight cut-off of the membrane), the copolymer chains with adsorbed copper ions filter out from the water.

A rejection factor is defined as Equation A.1:

$$R = \frac{C_0 - C_i}{C_0} \qquad \textbf{Equation A.1}$$

where C_0 and C_i are the concentration of heavy metals in feed and permeate, respectively. The test was replicated 6 times and the average values are reported in Table A.2. Test results showed a 99.98% rejection of copper ions which was very good. However, because of the high polymer solution viscosity, the flux was reduced by almost 10 times compared to the

regular situation at the same pressure. This issue can be fixed by making lower molecular weight polymers or using more diluted polymer concentrations.

Table A.2: Flocculation application results

Cu^{2+} concentration (ppm)		**Rejection %**	**Flux after 1 hr ($kg/h \cdot m^2$)**
Feed	**Permeate**		
3.5064	0.0026	99.98%	6.4

Appendix B

Sample Calculation for Monomer Mass in Copolymerization

This appendix shows a sample calculation for monomer mass in the copolymerization mixture, related to Chapter 3, Section 3.3.1.

Considering a copolymerization of AAm/AAc at pH=5 and total monomer concentration of 1.5 M, the amount of each monomer in 250 ml solution is given in Table B.1.

Table B.1- Monomer amounts in 250 ml solution

AAm (g)	AAm (mol)	AAc + NaAc (mol)
50.58	0.71	0.04

In order to find the total monomer mass, we have to find the mass of AAc and NaAc separately. Since the pH=5, the degree of ionization is 0.863 (see Equation 2-5). So, the mass of each monomer is calculated as follows:

Mass of NaAc (g) = 0.04 × 94.04 (molar mass of NaAc) × 0.863 = 3.24

Mass of AAc (g) = 0.04 × 72.06 (molar mass of NaAc) × 0.137 = 0.39

The total monomer mass in copolymerization can be found as follows:

Total monomers mass (g) = 50.58 + 3.24 + 0.39 = 54.21

Appendix C

Typical Calculation for Elemental Analysis Based on C and N Atoms

This appendix presents elemental analysis calculations for determining copolymer composition, related to Chapter 3, Section 3.3.3.

Table C.1 shows sample results from elemental analysis of an AAm/AAc copolymer.

Table C.1: Elemental analysis for a sample AAm/AAc copolymer

Element	Wt %	Moles
C	40.83	3.399
H	5.99	5.95
N	10.76	0.77

If we consider the moles of AAc = n, and the moles of AAm = m, then, the total moles of carbon are: C = 3n + 3m ➔ 3n + 3m = 3.399. On the other hand, the total moles of nitrogen are: N = m = 0.77. Considering 1 mole for N (m = 1); then moles of H = 7.743 and moles of C = 4.4251. So, we can rewrite the previous equation as 3n + 3 = 4.4251 ➔ n = 0.475.

The cumulative copolymer compositions can be calculated as:

$F_{AAc} = 0.475/1.475 = 0.322$ and $F_{AAm} = 0.678$

Appendix D

Experimental Data of Monomer Conversion and Cumulative Copolymer Composition for Tailor-made Copolymer for EOR

This appendix shows monomer conversion data along with cumulative copolymer composition for tailor-made AAm/AAc copolymers for EOR application, as given in Chapter 7, Section 7.2.2. The data are presented at various monomer feed fractions in Table D.1.

Table D.1: Monomer conversion and AAm cumulative copolymer composition

f_{0AAm}=0.65		f_{0AAm}=0.85	
Conversion (%)	**Cum F_{AAm}**	**Conversion (%)**	**Cum F_{AAm}**
78.67	0.66	67.66	0.86
76.84	0.67	70.83	0.87
78.65	0.685	72.48	0.86
76.45	0.685	72.42	0.87
76.39	0.67	72.82	0.85
78.97	0.68	71.43	0.88
f_{0AAm}=0.75		f_{0AAm}=0.95	
Conversion (%)	**Cum F_{AAm}**	**Conversion (%)**	**Cum F_{AAm}**
68.84	0.76	88.01	0.92
68.28	0.79	85.78	0.94
69.99	0.76	89.64	0.91
69.66	0.77	88.29	0.93
71.05	0.78	91.91	0.94
71.66	0.76	91.85	0.94

Appendix E

Sample Calculations for RF and RRF

This appendix presents sample calculations for the Resistance Factor (RF) and the Residual Resistance Factor (RRF), related to Chapter 7, Section 7.3.1.

By having $(\Delta P_{brine})_{before\ polymer\ flooding}$=0.05 (from permeability measurements) and knowing that RF= $\Delta P_{polymer} / \Delta P_{brine}$, the pressure, pressure difference, and corresponding RF values are presented in Table E.1.

Table E.1: Pressure readings during polymer flooding and corresponding RF values

Time running (min)	Pressure (psi)							RF
	P1	P2	P3	P4	P5	P6	ΔP=P1-P6	
0	0	0	0	0	0	0	0	0.00
148	1.4	0	0	0	0	0	1.4	26.62
191	2.4	0	0	0	0	0	2.4	45.63
251	3.4	0	0	0	0	0	3.4	64.64
418	4.3	0	0	0	0	0	4.3	81.75
575	6.9	0	0	0	0	0	6.9	131.19
693	8.9	0.9	0	0	0	0	8.9	169.21
805	11.4	2.9	0.5	0	0	0	11.4	216.74
1123	26.0	17.2	15.9	10.9	6.9	0.2	25.8	490.53
1195	29.5	20.0	18.2	13.4	8.7	1.7	27.8	528.55
1397	32.5	22.2	20.5	15.4	10.5	1.9	30.6	581.79

1418	32.0	20.5	19.0	0	9.2	1.8	30.2	574.18
1436	32.0	22.2	21.6	15.0	10.5	1.9	30.1	572.28
1556	32.0	22.2	20.1	15.0	10.5	1.9	30.1	572.28
1754	32.0	22.9	20.6	15.4	10.8	1.9	30.1	572.28
1782	32.0	22.9	20.6	15.4	10.8	1.9	30.1	572.28
2067	32.0	22.2	19.0	14.3	9.2	1.8	30.2	574.18

By having $(\Delta P_{brine})_{before\ polymer\ flooding}$=0.05 (from permeability measurements) and knowing that RRF= $(\Delta P_{brine})_{after\ polymer\ flooding}$ / $(\Delta P_{brine})_{before\ polymer\ flooding}$, the pressure, pressure difference, and corresponding RRF values are presented in Table E.2.

Table E.2: Pressure readings after polymer flooding and corresponding RRF values

Time running (min)	**Pressure (psi)**							**RRF**
	P1	**P2**	**P3**	**P4**	**P5**	**P6**	**ΔP=P1-P6**	
0	32.0	20.5	20.4	14	5.5	1.8	30.2	574.18
23	22.5	14.7	15.4	10.2	3.6	1.6	20.9	397.37
50	25.1	20.5	20.5	14.3	5.4	1.8	23.3	443.00
126	11.0	10.5	11	7.8	0.1	0.1	10.9	207.24
170	7.0	5.2	6	2.7	0.1	0	7.0	133.09
226	4.0	3.9	4.4	2.1	0.1	0	4.0	76.05
286	2.3	1.9	2.5	0.9	0.1	0	2.3	43.73
346	1.3	0.1	0.6	0	0.1	0	1.3	24.72
406	0.10	0	0.4	0	0.1	0	0.1	1.98
474	0.10	0	0.2	0	0	0	0.1	1.98
1215	0.09	0	0	0	0	0	0.09	1.84
2669	0.08	0	0	0	0	0	0.08	1.58
2856	0.08	0	0	0	0	0	0.08	1.58

References

1. Finch, C. A., “Chemistry and Technology of Water-soluble Polymers”, Plenum Press, New York, US (1983).

2. Ebeling, J. M., Rishel, K. L., Sibrell, P. L., “Screening and evaluation of polymers as flocculation aids for the treatment of aquacultural effluents”, Aquacultural Engineering, 33 (4), 235-249 (2005).

3. Myagchenkov, V. A., Kurenkov, V. F., “Applications of acrylamide polymers and copolymers: a review”, Polymer-Plastics Technology and Engineering**,** 30 (2), 109-135 (1991).

4. Maerker, J. M. “Shear degradation of partially hydrolyzed polyacrylamide solutions”, Society of Petroleum Engineers, 15 (4), 311-322 (2012).

5. Wever, D. A. Z., Picchioni, F., Broekhuis, A. A., “Polymers for enhanced oil recovery: a paradigm for structure-property relationship in aqueous solution”, Progress in Polymer Science, 36 (11), 1558-1628 (2011).

6. Abdel-Alim, A. H., Hamielec, A. E., “Shear degradation of water-soluble polymers. I. Degradation of polyacrylamide in a high-shear couette viscometer”, Journal of Applied Polymer Science, 17 (12), 3769-3778 (1973).

7. Zaitoun, A., Makakou, P., Blin, N., Al-Maamari, R. S., Al-Hashmi A. R., Abdel-Goad, M., "Shear stability of EOR polymers", Society of Petroleum Engineers, 17 (2), 335-339 (2012).

8. Kurenkov, V. F., Myagchenkov, V. A., "Effect of reaction medium on the radical polymerization and copolymerization of potassium and sodium p-styrenesulphonate", European Polymer Journal, 15 (9), 849-862 (1979).

9. Riahinezhad, M., Kazemi, N., McManus, N., Penlidis, A., "Optimal estimation of reactivity ratios for acrylamide/acrylic acid copolymerization", Journal of Polymer Science, Part A: Polymer Chemistry, 51 (22), 4819-4827 (2013).

10. Cabaness, W. R., Lin, T. Y. C., Párkányi, C., "Effect of pH on the reactivity ratios in the copolymerization of acrylic acid and acrylamide", Journal of Polymer Science, Part A: Polymer Chemistry, 9 (8), 2155-2170 (1971).

11. Paril, A., Giz, A., Catalgil-Giz, H., "Composition control through pH and ionic strength during acrylic acid/acrylamide copolymerization", Journal of Applied Polymer Science, 127 (5), 3530-3536 (2013).

12. Riahinezhad, M., McManus, N., Penlidis, A., "Effect of monomer concentration and pH on reaction kinetics and copolymer microstructure of acrylamide/acrylic acid copolymer", Macromolecular Reaction Engineering, 9 (2), 100-113 (2015).

13. Sheng, J. J., Leonhardt, B., Azri, N., “Status of polymer-flooding technology”, Journal of Canadian Petroleum Technology, 54 (2), 116-126 (2015).

14. Mayo, F. R., Lewis, F. M., “Copolymerization. I. A basis for comparing the behavior of monomers in copolymerization; the copolymerization of styrene and methyl methacrylate.”, Journal of the American Chemical Society, 66 (9), 1594-1601 (1944).

15. Ponratnam, S., Kapur, S. L., “Reactivity ratios of ionizing monomers in aqueous solution. Copolymerization of acrylic and methacrylic acids with acrylamide”, Macromolecualr Chemistry and Physics, 178 (4), 1029-1038 (1977).

16. Paril, A., Alb, A. M., Giz, A. T., Çatalgil-Giz, H., “Effect of medium pH on the reactivity ratios in acrylamide acrylic acid copolymerization”, Journal of Applied Polymer Science, 103 (2), 968-974 (2007).

17. Rintoul, I., Wandrey, C., “Polymerization of ionic monomers in polar solvents: Kinetics and mechanism of the free radical copolymerization of acrylamide/acrylic acid”, Polymer, 46 (13), 4525-4532 (2005).

18. Shawki, S. M., Hamielec, A. E., “Estimation of the reactivity ratios in the copolymerization of acrylic acid and acrylamide from composition-conversion measurements by an improved nonlinear least-squares method”, Journal of Applied Polymer Science, 23 (11), 3155-3166 (1979).

19. Truong, N. D., Galin, J. C., François, J., Pham, Q. T., "Microstructure of acrylamide-acrylic acid copolymers: 2. as obtained by direct copolymerization", Polymer, 27 (3), 467-475 (1986).

20. Bourdais, J., "Reactivity of acrylic acid in copolymerization". Bulletin de la Societe Chimique de France, 485-489 (1955).

21. Chapiro, A., Dulieu, J., Mankowski, Z., Schmitt, N., "Effect of solvents on the copolymerization of acrylic acid with acrylonitrile and acrylamide", European Polymer Journal, 25 (9), 879-884 (1989).

22. Vinu, R., Madras, G., "Photocatalytic degradation of poly (acrylamide-co-acrylic acid)", Journal of Physical Chemistry, 112 (30), 8928-8935 (2008).

23. Kurenkov, V. F., Gubanova, T. A., Kurenkov, A. V., Lobanov, F. I., "Copolymerization of acrylamide with sodium acrylate in aqueous salt solutions", Russian Journal of Applied Chemistry, 81 (8), 1414-1418 (2008).

24. Plochocka, K., Wojnarowski, T. J., "The effect of Li, Na, K cations on the reactivities of acrylic acid salts and acrylamide in copolymerization in aqueous medium", European Polymer Journal, 7 (7), 797-804 (1971).

25. Reilly, P. M., Patino-Leal, H., "A Bayesian Study of the Error-in-Variables Model", Technometrics, 23 (3), 221-231 (1981).

26. Dube, M., Sanayei, R. A., Penlidis, A., O'Driscoll, K. F., Reilly, P. M., "Microcomputer program for estimation of copolymerization reactivity ratios", Journal of Polymer Science, Part A: Polymer Chemistry, 29 (5), 703-708 (1991).

27. Polic, A. L., Duever, T. A., Penlidis, A., "Case studies and literature review on the estimation of copolymerization reactivity ratios", Journal of Polymer Science, Part A: Polymer Chemistry, 36 (5), 813-822 (1998).

28. Meyer, V. E., Lowry, G. G., "Integral and differential binary copolymerization equations", Journal of Polymer Science Part A: General Papers, 3 (8), 2843-2851 (1965).

29. Kazemi, N., Duever, T. A., Penlidis, A., "Reactivity ratio estimation from cumulative copolymer composition data", Macromolecular Reaction Engineering, 5 (9-10), 385-403 (2011).

30. Dobrynin, A. V., Rubinstein, M., "Theory of polyelectrolytes in solutions and at surfaces", Progress in Polymer Science, 30 (11), 1049-1118 (2005).

31. Scott, R. A., Peppas, N. A., "Kinetic study of acrylic acid solution polymerization", American Institute of Chemical Engineers Journal, 43 (1), 135-144 (1997).

32. Sorbie, K. S., "Polymer-improved Oil Recovery", Blackie and Son Ltd (1991).

33. Ikegami, A., "Hydration and ion binding of polyelectrolytes". Journal of Polymer Science Part A: General Papers, 2 (2), 907-921 (1964).

34. Kurenkov, V. F., Nadezhdin, I. N., Antonovich, O. A., Lobanov, F. I., “Phase separation in aqueous solutions of binary copolymers of acrylamide with sodium 2-acrylamido-2-methylpropanesulfonate and sodium acrylate”, Russian Journal of Applied Chemistry, 77 (5), 804-808 (2004).

35. McCormick, C. L., Salazar, L. C., “Water-soluble copolymers. XLI. copolymers of acrylamide and sodium 3-acrylamido-3-methylbutanoate”, Journal of Macromolecular Science, Part A: Pure and Applied Chemistry, 29 (3), 193-205 (1992).

36. Kurenkov, V. F., Myagchenkov, V. A., “Effects of reaction medium on the radical polymerization and copolymerization of acrylamide”, European Polymer Journal, 16 (12), 1229-1239 (1980).

37. Mast, C. J., Cabaness, W. R., “The effect of zinc chloride on the copolymerization of acrylic acid and acrylamide”. Journal of Polymer Science: Polymer Letters Edition, 11 (3), 161-163 (1973).

38. Rintoul, I., Wandrey, C., “Approach to predict copolymer compositions in case of variable monomer reactivity”, Macromolecules, 38 (19), 8108-8115 (2005).

39. Lacik, I., Beuermann, S., Buback, M., “PLP-SEC study into the free-radical propagation rate coefficients of partially and fully ionized acrylic acid in aqueous solution”, Macromolecular Chemistry and Physics, 205 (8), 1080-1087 (2004).

40. Kurenkov, V. F., Nadezhdin, I. N., Antonovich, O. A., Lobanov, F. I., “Phase separation in aqueous solutions of binary copolymers of acrylamide with sodium 2-acrylamido-2-methylpropanesulfonate and sodium acrylate”, Russian Journal of Applied Chemistry, 77 (5), 804-808 (2004).

41. Kabanov, V. A., Topchiev, D. A., Karaputadze, T. M., “Some features of radical polymerization of acrylic and methacrylic acid salts in aqueous solutions”, Journal of Polymer Science: Polymer Symposia, 42 (1), 173-183 (1973).

42. Preusser, C., Hutchinson, R. A., “An in-situ NMR study of radical copolymerization kinetics of acrylamide and non-ionized acrylic acid in aqueous solution”, Macromolecular Symposium, 333 (1), 122-137 (2013).

43. Chapiro, A., “Influence of solvents on apparent reactivity ratios in the free radical copolymerization of polar monomers”, European Polymer Journal, 25 (7-8), 713-717 (1989).

44. Smets, G., Hesbain, A. M., “Hydrolysis of polyacrylamide and acrylic acid-acrylamide copolymers”, Journal of Polymer Science, 40, 217-226 (1959).

45. Thomas, A., Gaillard, N., Favero, C., “Some key features to consider when studying acrylamide-based polymers for chemical enhanced oil recovery”, Oil and Gas Science and Technology, 67 (6), 887-902 (2012).

46. Klein, J., Conrad, K. D., “Molecular weight determination of poly (acrylamide) and poly(acrylamide-co-sodium acrylate)”, Makromolecular Chemistry, 179 (6), 1635-1638 (1978).

47. Candau, F., Zekhnini, Z., Heatley, F., Franta, E., “Characterization of poly (acrylamide-co-acrylates) obtained by inverse microemulsion polymerization”, Colloid & Polymer Science, 264 (8), 676-682 (1986).

48. Lake, L. W., Holstein, E. D., “Petroleum engineering handbook: Volume V reservoir engineering and petrophysics, Society of Petroleum Engineers (2007).

49. Seright, R. S., Seheult, J. M., Talashek, T., “Injectivity Characteristics of EOR Polymers”, Society of Petroleum Engineers, Reservoir Evaluation & Engineering, 12 (5), 783-792 (2009).

50. Wu, X. Y., Hunkeler, D., Hamielec, A. E., Pelton, R. H., Woods, D. R., “Molecular weight characterization of poly(acrylamide-co-sodium acrylate). I. Viscometry”, Journal of Applied Polymer Science, 42 (7), 2081-2093 (1991).

51. Kurenkov, V. F., Trofimov, P. V., Kurenkov, A. V., Khartan, K., Lobanov, F. I., “Kinetics of thermal degradation of copolymers of acrylamide with sodium acrylate in aqueous solutions”, Russian Journal of Applied Chemistry, 78 (6), 995-999 (2005).

52. Hunkeler, D., Wu, X. Y., Hamielec, A. E., "Molecular weight characterization of polyacrylamide-co-sodium acrylate. II. Light scattering", Journal of Applied Polymer Science, 46 (4), 649-657 (1992).

53. Kulicke, W. M., Hörl, H. H., "Preparation and characterization of a series of poly (acrylamide-co-acrylates), with a copolymer composition between 0-96.3 mol-% acrylate units with the same degree and distribution of polymerization", Colloid and Polymer Science, 263 (7), 530-540 (1985).

54. Myagchenkov, V. A., Vagapova, A. K., Kurenkov, V. F., Nagel, M. A., "Effect of the chemical heterogeneity of acrylamide-acrylic acid copolymers of varying degree of neutralization on the viscosity of diluted aqueous solutions", Polymer Science U. S. S. R., 30 (4), 759-764 (1988).

55. Jung, J. C., Zhang, K., Chon, B. H., Choi, H. J., "Rheology and polymer flooding characteristics of partially hydrolyzed polyacrylamide for enhanced heavy oil recovery", Journal of Applied Polymer Science, 127 (6), 4833-4839 (2013).

56. Klein, J., Heitzmann, R., "Preparation and characterization of poly (acrylamide-co-acrylic acid)", Makromolecuar Chemistry, 179 (8), 1895-1904 (1978).

57. Buchgraber, M., Clemens, T., Castanier, L. M., Kovscek, A., "A Micro visual Study of the Displacement of Viscous Oil by Polymer Solutions", Society of Petroleum Engineers, Reservoir Evaluation & Engineering, 14 (3), 269-280 (2011).

58. Muller, G., Laine, J. P., Fenyo, J. C., “High-molecular-weight hydrolyzed polyacrylamides. I. Characterization. Effect of salts on the conformational properties”, Journal of Polymer Science: Polymer Chemistry Edition, 17 (3), 659-672 (1979).

59. Will, R. K., Pearson, J., Yokose, K., Löchner, U., Fink, U., “Synthetic water-soluble polymers” (2011).

60. Wei, B., Romero-Zerón, L., Rodrigue, D., “Novel self-assembling polymeric system based on a hydrophobic modified copolymer: formulation, rheological characterization, and performance in enhanced heavy oil recovery”, Polymers for Advanced Technologies, 25 (7), 732-741 (2014).

61. Finch, C. A. “Polymer-improved oil recovery”, Polymer International, 28 (3), 256 (1992).

62. Wei, B., Romero-Zerón, L., Rodrigue, D., “Oil displacement mechanisms of viscoelastic polymers in enhanced oil recovery (EOR): a review”, Journal of Petroleum Exploration and Production Technology, 4 (2), 113-121 (2014).

63. Romero-Zerón, L., “Introduction to enhanced oil recovery (EOR) processes and bioremediation of oil-contaminated sites”, InTech (2012).

64. Taylor, K. C., Nasr-El-Din, H. A., “Water-soluble hydrophobically associating polymers for improved oil recovery: A literature review”, Journal of Petroleum Science and Engineering, 19 (3-4), 265-280 (1998).

65. Finch, C. A., “Chemistry and technology of water-soluble polymers”, Journal of the American Oil Chemists’ Society, 60 (11) 1919-1935 (1983).

66. Al-Hashmi, A. A., Al-Maamari, R., Al-Shabibi, I., Mansoor, A., Al-Sharji, H., Zaitoun, A., “Mechanical stability of high-molecular-weight polyacrylamides and an (acrylamido tert-butyl sulfonic acid)-acrylamide copolymer used in enhanced oil recovery”, Journal of Applied Polymer Science, 131 (20), DOI: 10.1002/app.40921(2014).

67. Tolstikh, L. I., Akimov, N. I., Golubeva, I. A., Shvetsov, I. A., “Degradation and stabilization of polyacrylamide in polymer flooding conditions”, International Journal of Polymeric Materials, 17 (3-4), 177-193 (1992).

68. Kheradmand, H., François, J., Plazanet, V., “Hydrolysis of polyacrylamide and acrylic acid-acrylamide copolymers at neutral pH and high temperature”, Polymer, 29 (5), 860-870 (1988).

69. Taylor, K. C., Nasr-El-Din, H. A., “Acrylamide copolymers: A review of methods for the determination of concentration and degree of hydrolysis”, Journal of Petroleum Science and Engineering, 12 (1), 9-23 (1994).

70. Sabhapondit, A., Borthakur, A., Haque, I., “Characterization of acrylamide polymers for enhanced oil recovery”, Journal of Applied Polymer Science, 87 (12), 1869-1878 (2003).

71. Seright, R. S., Fan, T., Wavrik, K., Wan, H., Gaillard, N., Favéro, C., "Rheology of a new sulfonic associative polymer in porous media, Society of Petroleum Engineers, Reservoir Evaluation & Engineering, 14 (6), 726-734 (2011).

72. http://www.oilfield-solutions.basf.com (2015)

73. Seright, R. S., Zhang, G., Akanni, O. O., Wang, D. A, "Comparison of polymer flooding with in-depth profile modification", Society of Petroleum Engineers, Canadian Unconventional Resources Conference, Alberta, Canada (2011).

74. Wei, B., Romero-Zerón, L., Rodrigue, D., "Mechanical properties and flow behavior of polymers for enhanced oil recovery", Journal of Macromolecular Science, Part B**:** Physics, *53* (4), 625-644. (2013).

75. Wei, B., Romero-Zerón, L., "The evaluation of a technological trend in polymer flooding for heavy oil recovery", Petroleum Science and Technology, 32 (19), 2396-2404 (2014).

76. Wang, D., Cheng, J., Yang, Q., Wenchao, G., Qun, L., Chen, F., "Viscous-elastic polymer can increase microscale displacement efficiency in cores", Society of Petroleum Engineers Annual Technical Conference and Exhibition, Texas, US (2000).

77. Wang, D., Xia, H., Liu, Z., Yang, Q., "Study of the mechanism of polymer solution with visco-elastic behavior increasing microscopic oil displacement efficiency and the forming of steady "oil thread" flow channels, Society of Petroleum Engineers, Asia Pacific Oil and Gas Conference and Exhibition, Jakarta, Indonesia (2001).

78. Wampler, F. M., “Formation of diacrylic acid during acrylic acid storage”. Plant/Operations Progress, 7 (3), 183-189 (1988).

79. Zurimendi, J. A., Guerrero, S. J., Leon, V., “The determination of the degree of hydrolysis in poly (acrylamides): simple methods using C13 NMR, and elementary analysis”, Polymer, 25 (9), 1314-1316 (1984).

80. Wei, B.; Romero-Zerón, L., Rodrigue, D., “Improved viscoelasticity of xanthan gum through self-association with surfactant: β-cyclodextrin inclusion complexes for applications in enhanced oil recovery”, Polymer Engineering and Science, 55 (3), 523-532 (2015).

81. Kazemi, N., Duever, T. A., Penlidis, A., “A powerful estimation scheme with the error-in-variables-model for nonlinear cases: Reactivity ratio estimation examples”, Computers & Chemical Engineering 48 (0), 200-208 (2013).

82. Keeler, S. E., Reilly, P. M., “The error-in-variables model applied to parameter estimation when the error covariance matrix is unknown”, Canadian Journal of Chemical Engineering, 69 (1), 27-34 (1991).

83. Kazemi, N., Duever, T. A., Penlidis, A., “Design of experiments for reactivity ratio estimation in multicomponent polymerizations using the error-in-variables approach”, Macromolecular Theory and Simulations, 22 (5), 261-272 (2013).

84. Tidwell, P. W., Mortimer, G. A., “Improved method of calculating copolymerization reactivity ratios”, Journal of Polymer Science Part A: General Papers, 3 (1), 369-387 (1965).

85. Mortimer, D. A., “Synthetic polyelectrolytes: a review”, Polymer International, 25 (1), 29-41 (1991).

86. Kabanov, V. A., Topchiev, D. A., Karaputadze, T. M., “Some features of radical polymerization of acrylic and methacrylic acid salts in aqueous solutions”, Journal of Polymer Science: Polymer Symposia, 42 (1), 173-183 (1973).

87. Riahinezhad, M., Kazemi, N., McManus, N., Penlidis, A., “Effect of ionic strength on the reactivity ratios of acrylamide/acrylic acid (sodium acrylate) copolymerization”, Journal of Applied Polymer Science, 131 (20), DOI: 10.1002/app.40949 (2014).

88. Odian, G., “Principles of Polymerization”, 4th edition, Wiley-Interscience, Hoboken, NJ, (2004).

89. Hamielec, A.E., MacGregor, J. F., Penlidis, A., “Encyclopedia of Comprehensive Polymer Science”, Pergamon Press, (1987).

90. Mendichi, R., Giacometti-Schieroni, A., “Fractionation and characterization of ultra-high molar mass hyaluronan: 2. On-line size exclusion chromatography methods”, Polymer, 43 (23), 6115-6121 (2002).